Supplementary information

Electrochemical Hydrogenation of Alkenes over a Nickel Foam Guided by Life Cycle, Safety and Toxicological Assessments

Pedro Jesus Tortajada Palmero,[a] Therese Kärnman,[b] Pablo Martínez-Pardo,[a] Charlotte Nilsson,[c] Hanna Holmquist,[b] Magnus J. Johansson[a,d] and Belén Martín-Matute*[a]

Belen.martin.matute@su.se

[a] Department of Organic Chemistry, Stockholm University, 106 91 Stockholm, Sweden.
[b] IVL Swedish Environmental Research Institute, 411 33 Gothenburg, Sweden.
[c] RISE Research Institutes of Sweden, 151 36 Södertälje, Sweden.
[d] Medicinal Chemistry, Research and Early Development, Cardiovascular, Renal and Metabolism (CVRM) Biopharmaceuticals R&D AstraZeneca, 431 50 Mölndal, Sweden.

Table of Contents

S1. General Experimental Details

All solvents and reagents were purchased from commercial sources and used without further purification. ^{1}H NMR measurements were performed at 400 MHz and ^{13}C NMR at 100 MHz on a Bruker Advance spectrometer. ^{1}H and ^{13}C NMR chemical shifts (δ) were reported in ppm from tetramethylsilane with the solvent resonance as the internal standard ($CDCl_3$: δH 7.26 ppm and δC 77.00 ppm). Coupling constants (J) were given in Hz. Gas chromatography experiments (GC–FID) were performed on a Shimazu GC system (GC-2010 Plus) equipped with a mass selective detector (QP 2020) and flame ionization detector and two parallel HP-5MS columns (30 m × 0.25 mm × 0.25 μm) with helium as a carrier gas and on a Agilent 8860 GC equipped with an FID, TCD detectors and a CP-Sil 5 CB column (30m x 0.25mm x 0.25um) with hydrogen as carrier gas All compounds were purified by flash column chromatography with silica gel. Product yields were determined by isolation and by ^{1}H and ^{13}C NMR spectroscopy using 1,3,5-trimethoxybenzene as internal standard. Compounds **2k**, **2l**, **2m** and **2q** were not isolated due to low yields. Compounds **2x**, **2x'** and **2ab** were not isolated since they had the same retention time during purification. Their characterization has been described elsewhere.[1-8]

S1.2 Electrochemical methodology

Electrochemical experiments were performed using a GAMRY potentiostat (Interface 1010E) or a Biologic VSP-3e potentiostat. The set up consisted of a divided cell, separated by a porous glass frit (G4). Septa with a glass tube were placed in the openings to minimize solvent evaporation while keeping the system open to air. Potentials were measured *vs* Ag/AgCl/KCl (3M) reference electrode, using a nickel foam as working electrode (1.6 x 10 x 20 mm, 95% porosity, with 1 cm^2 geometrical area submerged into the solution) and a platinum wire as counter electrode (13 cm^2) (Figure S1). All reported potentials were referenced against the Fc/Fc^+ redox couple.[9] The distance between anode and cathode was approximately of 5.4 cm (Figure S2). Each cell contained 25 mL of solution. Stirring was set at least at 1200 rpm during electrolysis.

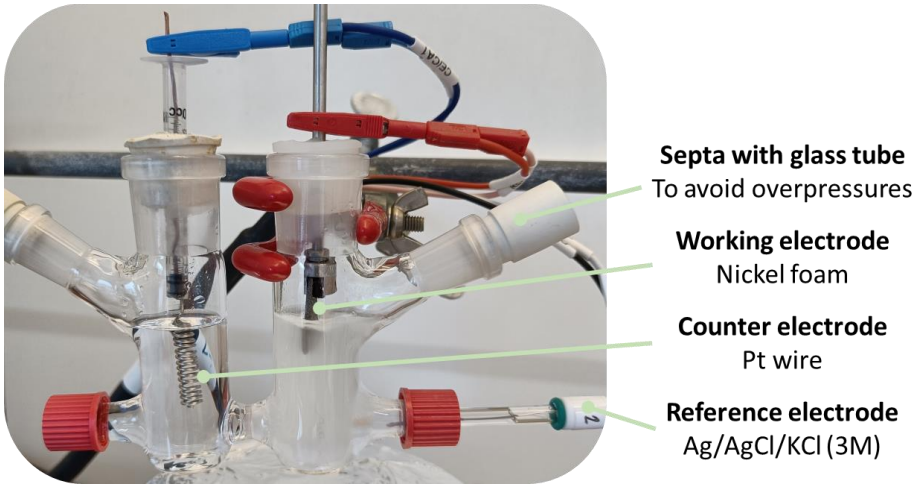

Figure S1. H-cell used in this study.

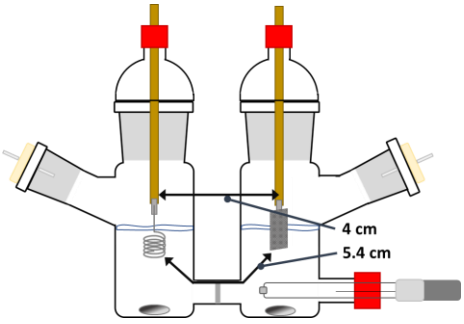

Figure S2. Representation of the divided cell employed in this study.

S2. SUPPLEMENTARY FIGURES

S2.1 Reaction optimization

Table S1 Optimization with 4-hydroxybenzylidene acetone

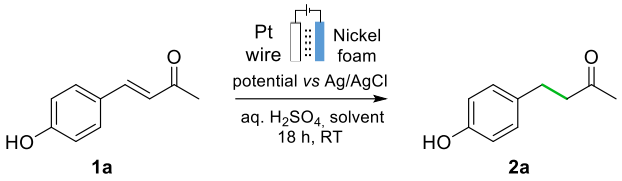

1a **2a**

Entry	Solvent	Solv. Ratio	[H_2SO_4] (M)	Potential (V)	Time (h)	Conversion (%)	Yield (%)	FE (%)
1	Acetone	1:1	0.13	– 2.5	18	> 95	56	3
2	Acetone	1:1	0.25	– 2.5	18	87	56	1
3	MeOH	1:1	0.25	– 2.5	18	87	73	< 1
4	MeOH	1:1	0.25	– 0.9	18	60	35	3
5	MeOH	3:1	0.38	– 0.9	20	> 95	78	4
6	MeOH	3:1	0.38	– 0.9	6	63	45	7
7	MeOH	3:1	0.38	– 0.9	12	72	49	4
8	MeOH	3:1	0.19	– 0.9	18	> 95	77	6
9	MeOH	3:1	0.10	– 0.9	18	61	47	8
10	MeOH	3:1	0.19	– 0.7	18	68	63	9
11	EtOH	3:1	0.19	– 0.9	18	> 95	89	10
12[a]	EtOH	3:1	0.19	– 0.9	18	> 95	88	10
13[b]	EtOH	3:1	0.19	– 0.9	18	53	47	7
14[a,c]	EtOH	3:1	0.19	– 0.9	18	83	31	2
15[a]	Ethylene Glycol	3:1	0.19	– 0.9	18	85	67	7
16[a]	Acetone	3:1	0.19	– 0.9	18	50	50	3
17[a]	MeCN	3:1	0.19	– 0.9	18	25	15	1
18[a,d]	EtOH	3:1	0.19	– 5 mA	18	30	22	< 1
19[a,d]	EtOH	3:1	0.19	– 10 mA	18	45	25	< 1
20[a,d]	EtOH	3:1	0.19	– 15 mA	18	> 95	42	< 1
21[a,d]	EtOH	3:1	0.19	– 20 mA	18	> 95	35	< 1
22	EtOH	3:1	0.19	– 0.5	18	25	5	< 1
23[a]	EtOH	3:1	0.19	0.0	18	0	0	–
24[a,e]	EtOH	3:1	0.19	0.0	18	0	0	–
25[a,f]	EtOH	3:1	–	– 0.9	18	30	0	–
26[a,g]	EtOH	3:1	–	– 0.9	18	33	8	< 1
27[a,h]	EtOH	3:1	0.19	– 0.9	18	87	11	< 1
28[a,i]	EtOH	3:1	0.19	– 0.9	18	> 95	73	4
29[a,j]	EtOH	3:1	0.19	– 0.9	18	55	55	3

1a (0.4 mmol, 0.016 M). Yields were determined via ^{1}H NMR spectroscopy using 1,3,5-trimethoxybenzene as internal standard. (a) Nickel foam activated with aqueous H_2SO_4 3 M. (b) Using a nickel foam half the thickness (0.8 x 10 x 20 mm). (c) Using a flat nickel piece as working electrode. (d) Galvanostatic conditions. (e) With a H_2 balloon. (f) Using NaOH 1 M as electrolyte. (g) Using NaCl 0.5 M as electrolyte. (h) Undivided cell. (i) Using 1 equiv. of 1,1-diphenylethylene. (j) Using 10 equiv. of *tert*-butanol.

Table S2 Optimization with 2-cyclohexenone

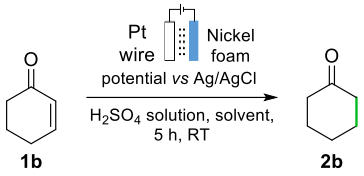

Entry	Solvent	Solv. Ratio	[H_2SO_4] (M)	Potential (V)	Conversion (%)	Yield (%)	FE (%)
1	Acetone	1:1	0.25	– 2.5	> 99	94	6
2	MeOH	1:1	0.25	– 0.9	95	78	20
3	MeOH	3:1	0.38	– 0.9	92	82	10
4	MeOH	3:1	0.19	– 0.9	98	84	22
5	EtOH	3:1	0.19	– 0.9	97	90	24

1b (0.4 mmol, 0.016 M). Yields were determined via GC- FID using a calibration curve.

S2.2 Counter-electrode optimization

Table S3 Counter electrode screening

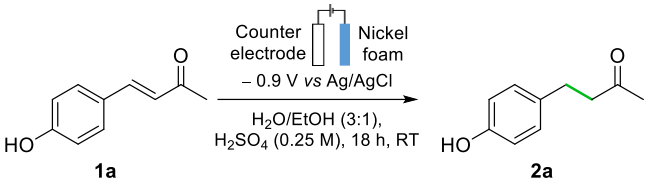

Entry	Counter electrode	Surface (cm^2)[a]	Yield (%)[b]	FE (%)
1	Carbon paper	16	45	3
2	Carbon cloth	16	40	3
3	Carbon cloth	40	48	5
4	Pt wire	13	89	10
5	Graphite	16	77	7

1a (0.4 mmol, 0.016 M). (a) Yield determined *via* ^{1}H NMR spectroscopy using an internal standard. (b) Bulk electrode configuration was considered for surface calculation.

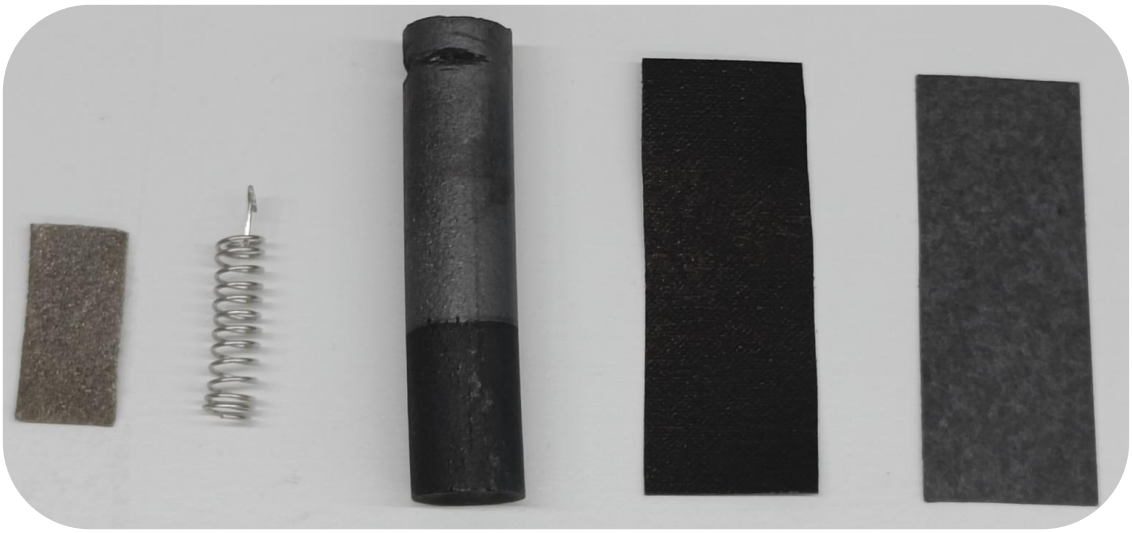

Figure S3. Different counter electrodes employed in the electrochemical hydrogenation of alkenes. From left to right: nickel foam, platinum wire, graphite bar, carbon cloth and carbon paper.

S2.3 Scale up

Table S4 Scale up study for 2-cyclohexenone.

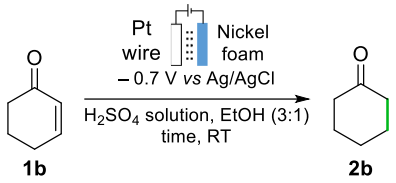

Entry	Scale	Time	[H_2SO_4] (M)	Conversion (%)	Yield (%)
1	0.4	18	0.19	97	79
2	1.6	6	0.19	47	28
4	1.6	18	0.19	58	52
3	1.6	18	0.38	96	95

1b (0.4 mmol, 0.016 M). Yields were determined via GC- FID using a calibration curve.

S2.4 Second solvent optimization

Table S5. Additional solvent screening for low-solubility substrates.

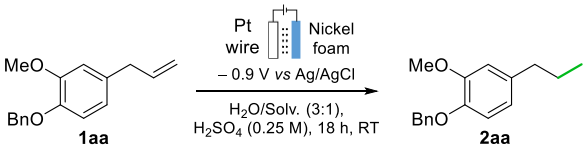

Entry	Solvent	Yield (%)
1	EtOH	26
2	Methyl ethyl ketone	31
3	Isopropanol	30
4	*n*-Propanol	59
5	*n*-BuOH[a]	75

S2.5 Recyclability of graphite rod as counter electrode

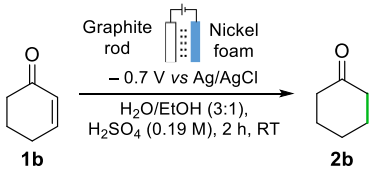

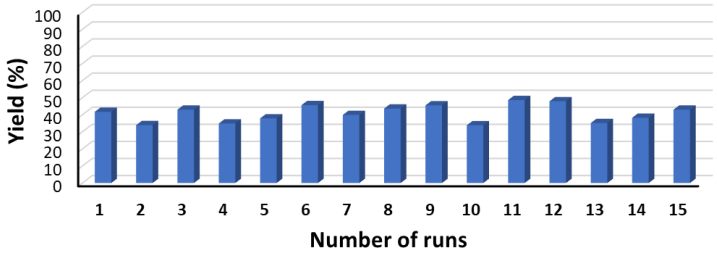

Scheme S1. Recyclability performance of the graphite anode in the nickel foam method at low conversions, after reaction times of 2 h. **1b** (0.4 mmol, 0.016 M). Graphite electrode surface of 23 cm^2. Yields were determined by GC-FID using a calibration curve.

S2.6 Limitations

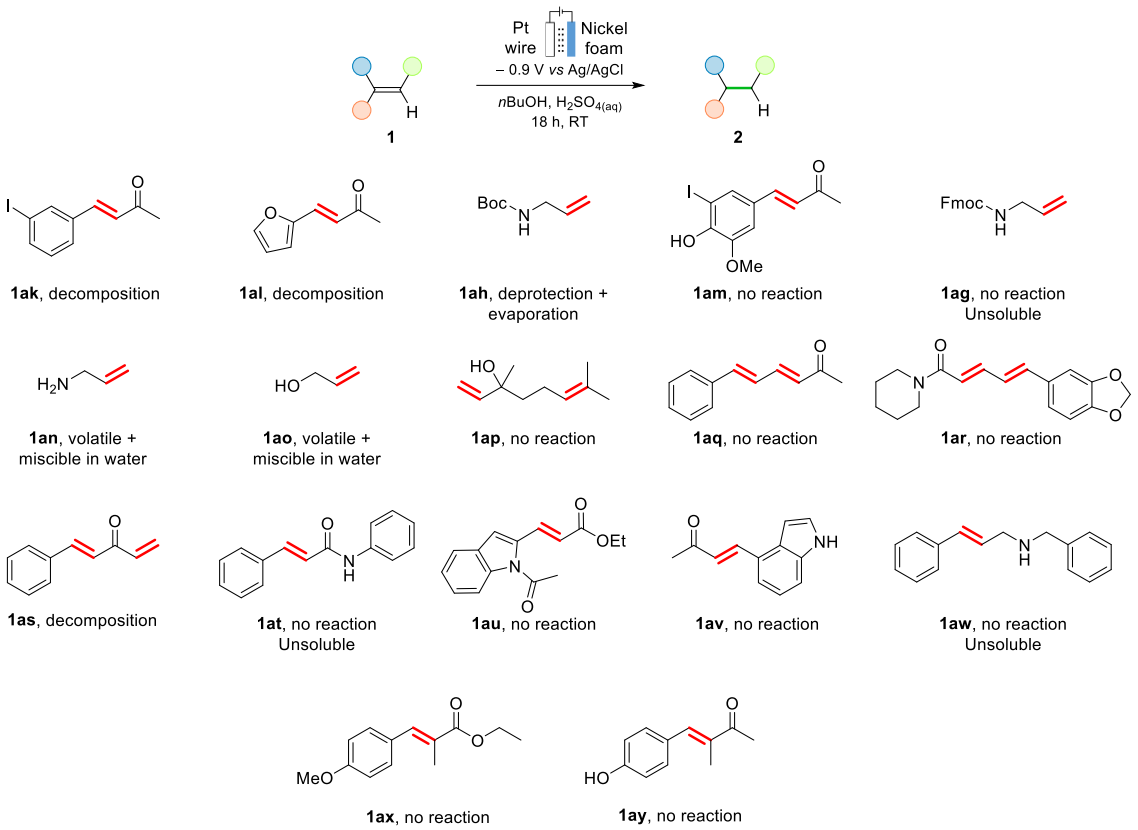

Scheme S2 Limitations of the scope. Substrates **1an** and **1ao** were difficult to characterize due to their low boiling point (48 °C and 97 °C respectively) and complete solubility in water, which prevented an effective extraction.

S2.7 Faradaic Efficiencies

Table S6 Faradaic efficiencies of the products of the scope.

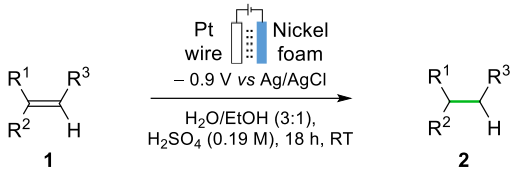

Entry	Product	Faradaic Efficiency (%)
1	**2a**	9.6
2	**2b**[a]	24.2
3	**2c**	7.6
4	**2d**	4.9
5	**2e**	11.2
6	**2f**	5.7
7	**2g**	6.2
8	**2g**[b]	7.0
9	**2h**	6.2
10	**2i**	6.6
11	**2i**[b]	2.9
12	**2j**	5.9
13	**2j**[b]	3.1
14	**2k**	4.9
15	**2l**	4.1
16	**2m**	2.5
17	**2n**	4.7
18	**2o**	11.6
19	**2p**	7.6
20	**2q**	2.4
21	**2r**	4.1
22	**2s**	6
23	**2t (*E*)**	7.8
24	**2t (*Z*)**	7.1
25	**2u**	3.3
26	**2v**	7
27	**2w**	4.7
28	**2x**	2
29	**2x´**	2
30	**2y**	8.6
21	**2z**	6.4
22	**2aa**	2.8
23	**2aa**[b]	4.4
24	**2ab**	2
25	**2ab**[b]	3
26	**2ac**	3
27	**2ad**	5
28	**2ae**	2
29	**2ae´**	3
30	**2af**	7
31	**2ai**	6

Alkene (0.4 mmol, 0.016 M). (a) − 0.7 V, 5 h. (b) *n*-BuOH as cosolvent (7%)

S2.8 Cyclic voltammetry

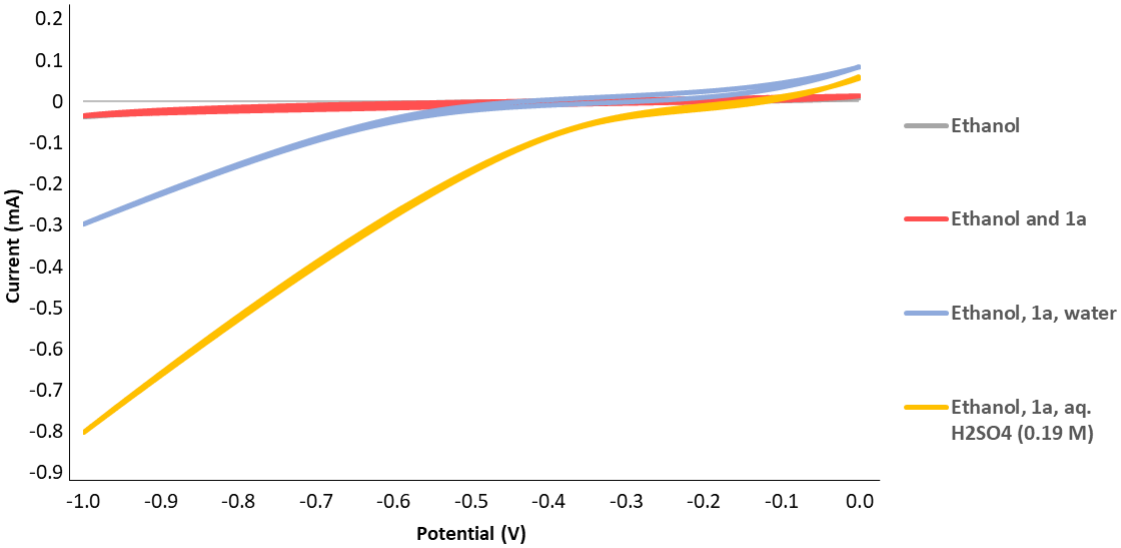

Figure S4. Cyclic voltammetry of the reaction components using $TBAPF_6$ (0.1M) as electrolyte. In the case that Ni-H species would be formed from nickel and EtOH, an increase in current due to HER or ECH would have been observed by cyclic voltammetry in the absence of sulfuric acid and of aqueous media. Instead, the CV depicts a very small current when only EtOH is used, without water nor acid (Figure S4). Therefore, EtOH in its own cannot provide the active Ni-H.

S2.9 Kinetic profile

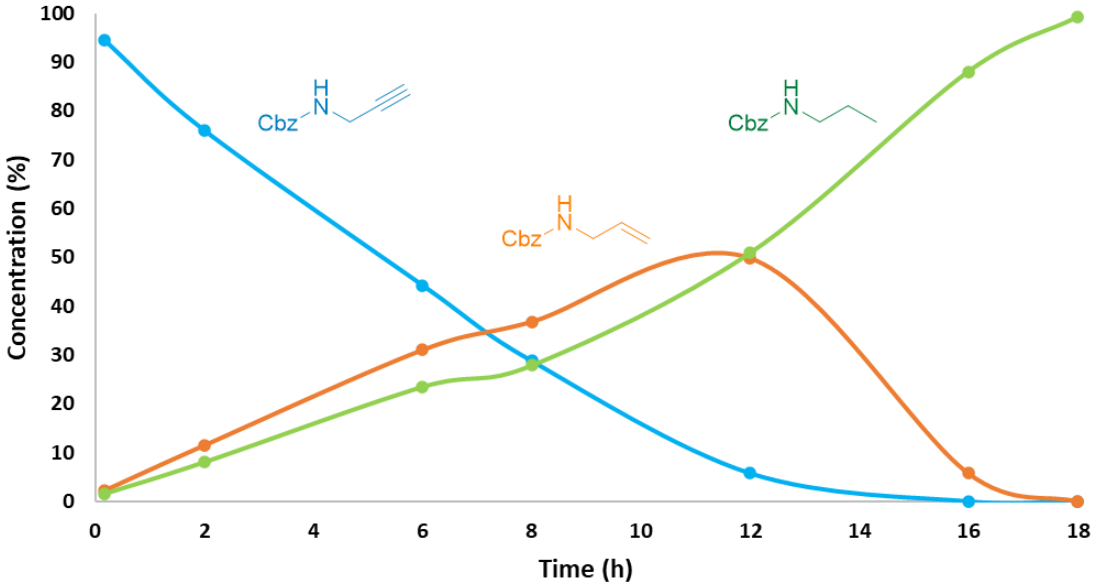

Figure S5. Kinetic profile for the ECH of alkyne **1aj** to fully saturated **2ae** *via* the formation of **1ae**. Values were determined *via* ^{1}H NMR spectroscopy using an internal standard.

S3. TOXICOLOGICAL ASSESSMENT DATA

S3.1 Pd/C system description

The conventional catalytic system used in the hydrogenation process involves the use of a palladium on charcoal (Pd/C) catalyst, in powder form, and hydrogen gas (Scheme S3). It consists of a batch process, which frequently uses solvents such as MeOH or EtOH.[10,11] The catalyst and solvent used in this system can be separated and reused with an almost complete recovery of the substances (only evaporation losses would occur).[12,13] Additionally, filtration is used to separate Pd/C from the solvent.[14]

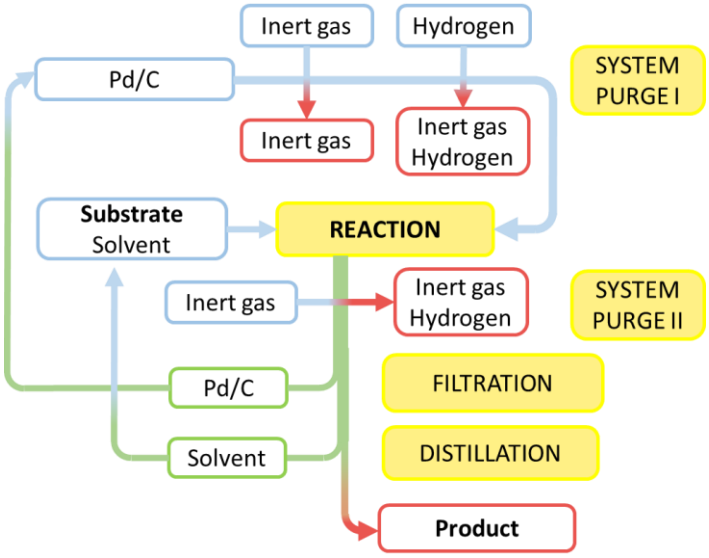

Scheme S3 Pd/C catalyzed hydrogenation process.

S3.2 Nickel foam system description

The new alternative system used for the hydrogenation is based on an electrocatalytic process that requires the use of a nickel foam catalyst, platinum (Pt) electrodes and an aqueous acid solution. Initially, MeOH was employed as cosolvent, but was replaced by EtOH during the method development due to its toxicological hazard. A similar process took place for the acid employed, being hydrochloric acid discarded in favor of sulfuric acid.

The reaction is performed in a batch process, which starts with the activation of nickel foam by acidic washing (Scheme S4). This process removes the layer of nickel oxide that was present on the surface, which in turn enhances the catalytic performance. In theory, the catalyst wash produces a discharge solution containing nickel sulfate ($NiSO_4$) dissolved in water, which is disposed of in compliance with lab waste management rules (no measurement has detected such a small flow of $NiSO_4$ in wastewater). As the presence of nickel oxide is significantly reduced during operation, this substance was not considered for the risk assessment.

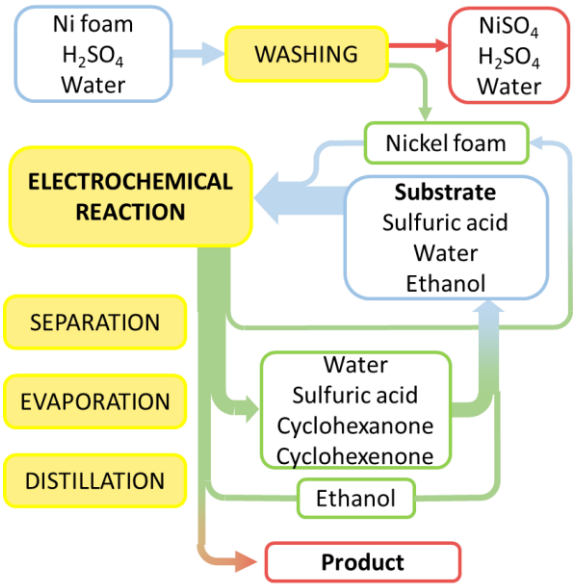

Scheme S4 Nickel foam electrocatalyzed hydrogenation process.

To produce the nickel foam used as catalyst (pure Ni 99,9%, not in nanoform), an open-cell foam structure of thermally decomposable material (polymers) is placed in an atmosphere containing nickel carbonyl gas. The foam structure is heated to a temperature at which the nickel carbonyl gas decomposes to form a nickel-plated structure which is then sintered to remove the decomposable polymeric structure leaving an isotropic, open-cell network of interconnected nickel wires to form the nickel foam.[15]

S3.3 Substrate and product

Due to the wide scope of the method, no substrate and product were selected for the toxicological assessment.

S3.4 Hazards information

The purpose of the Classification, Labelling and Packaging (CLP) Regulation ((EC) No 1272/2008) is to ensure a high level of protection of health and the environment within the EU, as well as the free movement of substances and mixtures. The CLP regulation is based on the United Nations' Globally Harmonized System (GHS). Classification is the starting point for hazard communication and the identified hazards must be communicated to other actors in the supply chain, including consumers and users. A safety data sheet and labelling of a substance/mixture are both necessary and are important tools to communicate with the user of a substance/mixture and to alert them about the presence of a hazard and the need to manage the associated risks.

This section provides an overview of the health and environmental hazardous properties of the chemicals involved in both catalytic processes under comparison in the case study. It provides a short description, from a regulatory context, of the hazard classification of the assessed compound and a table including CAS number, the list of the main hazard codes and related hazard phrases.

The **CLP (1272/2008)** regulatory processes identified in the Tables are:

- **Harmonised C&L**: Indicates if a European Union harmonised **classifications and labelling** has been assigned to the substance according to Annex VI to CLP.
- **CLP notification**: Indicates that notified C&L's have been submitted to ECHA for a substance by companies that manufacture or import the substance.

The following sub-sections indicate the substance classifications (hazard codes and hazard statements) provided by manufacturers and importers under REACH and CLP notifications, as well as whether the substance is defined under harmonised classification and labelling (CLH) (Scheme S5).[16] Furthermore, for some of the chemicals, an occupational exposure limit value and/or a specific concentration limit, where available, are reported in this section as well.

S3.4.1 Conventional system hazard assessment

Palladium on activated charcoal (Pd/C)
The catalyst of the conventional system consists of palladium on activated charcoal (Pd/C) 10 wt% Pd. Palladium on activated charcoal has same ID (CAS and EC numbers) and same hazardous properties as elemental palladium (Pd).

According to the notifications provided by companies in REACH registrations, no hazards have been classified. This substance is registered under the REACH Regulation and is manufactured in and/or imported to the European Economic Area, at ≥ 100 to < 1 000 tonnes per annum. In relation to this tonnage, less information about hazards is required.

Hydrogen gas
There are no health or environmental hazard classifications provided by companies in CLP notifications for this substance. Physical hazards have been notified, being hydrogen gas a very flammable gas, which often is transported in pressurized containers.

Methanol
According to the harmonised classification and labelling, this substance is toxic if swallowed, in contact with skin or inhaled, and causes damage to organs. Furthermore, it is a flammable liquid.

Ethanol
The classification provided by companies to ECHA in REACH registrations identifies that this substance is a flammable solvent.

Nitrogen gas
There are no physical, health or environmental hazard classifications provided by companies in CLP notifications for this substance.

S3.4.2 Nickel foam system hazard assessment

Nickel foam
According to the classification provided by companies to ECHA in REACH registrations, nickel metal is a skin sensitizer, suspected of causing cancer and causes damage to organs through either prolonged or repeated exposure.

This substance is registered under the REACH Regulation and is manufactured in and/or imported to the European Economic Area, at ≥ 100.000 tonnes per annum. The high tonnage range requires higher requirements providing numerous hazards information.

Moreover, the production of the nickel foam implies different hazardous chemicals such as nickel carbonyl gas.

Tetracarbonyl nickel (nickel carbonyl)
According to the harmonized classification and labelling approved by the European Union, this substance is highly flammable, fatal if inhaled, suspected of causing cancer, is very toxic to aquatic life, is very toxic to aquatic life with long lasting effects, and may damage fertility.

Graphite

According to the notifications provided by companies to ECHA in REACH registrations no hazards have been classified.

Hydrogen chloride
According to the harmonised classification and labelling, this substance causes severe skin burns and eye damage and may cause respiratory irritation.

Sulfuric acid
According to the harmonised classification and labelling, this substance causes severe skin burns and eye damage.

Nickel chloride
According to the harmonised classification and labelling approved by the European Union, this substance is toxic if swallowed, is toxic if inhaled, causes skin irritation, can cause an allergic skin reaction and may cause allergy or asthma symptoms or breathing difficulties if inhaled, causes damage to organs through prolonged or repeated exposure, is very toxic to aquatic life with long lasting effects, is suspected of causing genetic defects, and can damage fertility.

Nickel sulfate
According to the harmonised classification and labelling, this substance is harmful if swallowed, is harmful if inhaled, can cause skin irritation and sensitization, may cause asthma symptoms or breathing difficulties if inhaled, causes damage to organs through prolonged or repeated exposure, is very toxic to aquatic life with long lasting effects, is suspected of causing genetic defects, and can damage fertility.

Platinum (Pt)
According to the notifications provided by companies to ECHA in REACH registrations no hazards have been classified.

	CAS	Not class.	H220	H225	H226	H227	H270	H280	H301	H302	H311	H314	H315	H317	H318	H319	H330	H331	H332	H334	H335	H336	H341	H351	H370	H372	H400	H410	H412	H350i	H360D
EtOH	**64-17-5**			2																											
MeOH	**67-56-1**			2					3		3							3							1						
Nickel	**7440-02-0**													1										2		1					
Platinum	**7440-06-4**																														
Graphite	**7782-42-5**																														
Sulfuric acid	**7664-93-9**											1																			
HCl	**7647-01-0**											1									3										
Cl_2	**7782-50-5**						1						2			2		3			3						1				
n-BuOH	**71-36-3**				3					4			2		1						3	3									
$NiCl_2$	**7718-54-9**								3				2	1				γ		1			2			1	1	1		1	1
$NiSO_4$	**7786-81-4**									4			2	1					4	1			2			1	1	1		1	1
$Ni(CO)_4$	**13463-39-3**			2													1							2			1	1			1
Palladium	**7440-03-5**																														
Hydrogen gas	**1333-74-0**		1					1																							
Nitrogen gas	**7727-37-9**							1																							
Cyclohexanol	**108-93-0**									4			2						4		3										
1,1-diethoxycyclohexane	**1670-47-9**																												3		
3-ethoxycyclohexanone	**13619-73-3**					4							2			2					3										

Hazard category	1A, 1B, 1C	2	3	4
Color				

H220	Extremely flammable gas	**H311**	Toxic in contact with skin	**H332**	Harmful if inhaled	**H400**	Very toxic to aquatic life
H225	Highly flammable liquid and vapour	**H314**	Causes severe skin burns and eye damage	**H334**	May cause allergy or asthma symptoms or breathing difficulties if inhaled	**H410**	Very toxic to aquatic life with long lasting effects
H226	Flammable liquid and vapour	**H315**	Causes skin irritation	**H335**	May cause respiratory irritation	**H412**	Harmful to aquatic life with long lasting effects
H227	Combustible liquid	**H317**	May cause an allergic skin reaction	**H336**	May cause drowsiness or dizziness	**H350i**	May cause cancer by inhalation
H270	May cause or intensify fire: oxidizer	**H318**	Causes serious eye damage	**H341**	Suspected of causing genetic defects	**H360F**	May damage fertility
H280	Contains gas under pressure: may explode if heated	**H319**	Causes serious eye irritation	**H351**	Suspected of causing cancer		
H301	Toxic if swallowed	**H330**	Fatal if inhaled	**H370**	Causes damage to organs		
H302	Harmful if swallowed	**H331**	Toxic if inhaled	**H372**	Causes damage to organs through prolonged or repeated exposure		

Scheme S5 Toxicological classification of the different substances according to CLP and notified CLP.

S4. Screening Life Cycle Assessment

S4.1 Life cycle inventory

S4.1.1 Nickel foam method

For the electrochemical hydrogenation of 2-cyclohexenone using nickel foam as catalyst, modifications from the standard conditions were required for the comparison with a well-stablished protocol. The use of extraction procedures for the purification were substituted by more industrially applied methods such as evaporations and distillations. Moreover, halogenated solvents were substituted by EtOH.

The electrochemical method is represented in Scheme S6. It started with the activation of the nickel foam *via* acid treatment and ultrasounds, which removed the layer of nickel oxide (Scheme S6, flows 1–3). The activated nickel foam was placed in the H-cell as working electrode, followed by the rest of the components, reagents, and solvents (Scheme S6, flows 4–5) After a determined time, the electrodes were removed from the set up and nickel foam washed with EtOH (Scheme S6, flows 6–8). The mother liquor was purified by evaporation and distillation processes, leading to a fraction comprised by cyclohexanone as major component (Scheme S6, flows 9–13).

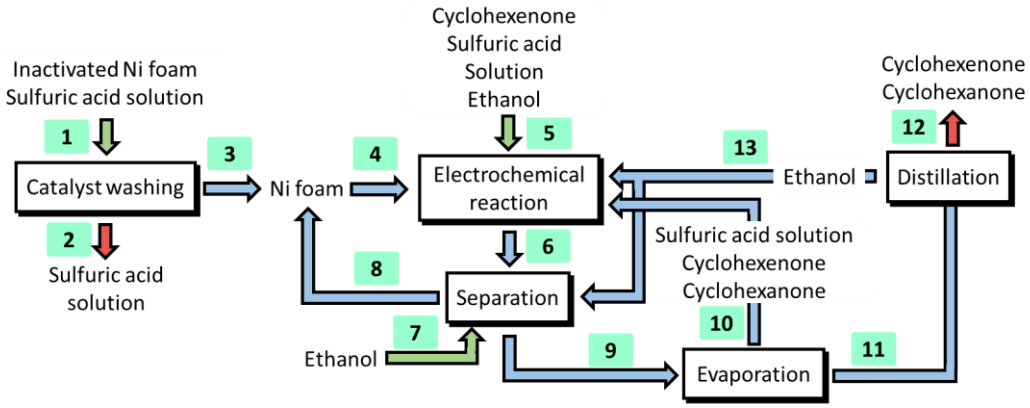

Scheme S6 Flow diagram for the hydrogenation of 2-cyclohexenone using nickel foam as electrocatalyst. By-products and other losses were excluded from the diagram.

During the evaporation step, 72.1 % of cyclohexanone and 2-cyclohexenone were collected at the rotary evaporator trap (Scheme S6, flow 11), while the remaining 27,9 % was recirculated together with the aqueous solution (Scheme S6, flow 10).

Data was collected from the scaled-up reaction (Table 2, entry 5) and extrapolated to 1 g scale with a 6.5 factor (Table S7). A yield of 98% was assumed, which was in line with the ratio between starting material and product.

Table S7 Values for the scale-up reaction and the assumed values at 1 g scale

Entry	Component	Value 0.156 g scale	Value 1 g scale
1	Cyclohexenone	0.154 g	1.02 g
2	Cyclohexanone	0.154 g	1.00g
3	Sulfuric acid	1.04 mL	6.76 mL
4	Water	36.46 mL	237 mL
5	Sulfuric acid	0.33 mL	2.16 mL
6	Water	1.67 mL	10.9 mL
7	Nickel foam	0.2540 g	1.65 g
8	EtOH	14.5 mL	94 mL
9	Platinum wire	1.3494 g	8.77 g

Entries 5 and 6 are considered only at the system set up and employed for catalyst activation.

The first evaporation stage shows a moderate performance for the component's separation. Nevertheless, recirculation of the aqueous solution enables an efficient recovery (Scheme S7). Therefore, we could consider a value of 1.001 g of cyclohexenone per cycle as input for the reaction, with the exception of the first cycle which would employ 1.386 g.

A loss of 8.5% and 4% were observed for EtOH at the evaporation and distillation steps respectively.

The method did not present a measurable consumption of H_2SO_4. Its quantification *via* titration only indicated an uneven distribution. After the reaction, the anodic cell showed an 8% increase in H_2SO_4 content, which matched with the amount missing at the cathodic cell. For the subsequent cycles, the uneven distribution could be circumvented by the combination of solutions before the next reaction.

Previous studies also informed a loss of 6% of the aqueous sulfuric acid solution due to water evaporation. The fraction used for catalyst washing can be employed (*via* dilution) as electrolyte in the reaction.

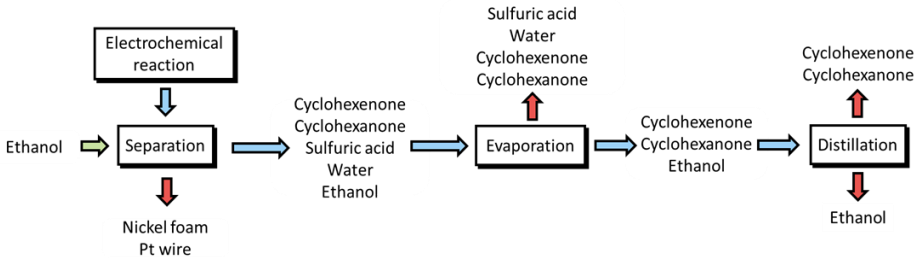

Efficiency separation	0.721			
RUN 1	Input	Output	Remains at aqueous	Remains at organic
Cyclohexenone (g)	1.386	0.028	0.008	0.020
Cyclohexanone (g)	1.387	1.000	0.387	1.000
Sulfuric acid (mL)	6.760	6.760	6.760	0.000
Water	236.990	236.990	236.990	0.000
Ethanol	94.250	82.789	0.000	82.789
RUN 2	Input	Output	Remains at aqueous	Remains at organic
Cyclohexenone (g)	0.992	0.020	0.006	0.014
Cyclohexanone (g)	1.379	1.000	0.379	1.000
Sulfuric acid (mL)	6.760	6.760	6.760	0.000
Water	236.990	236.990	236.990	0.000
Ethanol	94.250	82.789	0.000	82.789
RUN 3	Input	Output	Remains at aqueous	Remains at organic
Cyclohexenone (g)	1.001	0.020	0.006	0.014
Cyclohexanone (g)	1.381	1.000	0.381	1.000
Sulfuric acid (mL)	6.760	6.760	6.760	0.000
Water	236.990	236.990	236.990	0.000
Ethanol	94.250	82.789	0.000	82.789
RUN 4	Input	Output	Remains at aqueous	Remains at organic
Cyclohexenone (g)	0.999	0.020	0.006	0.014
Cyclohexanone (g)	1.381	1.000	0.381	1.000
Sulfuric acid (mL)	6.760	6.760	6.760	0.000
Water	236.990	236.990	236.990	0.000
Ethanol	94.250	82.789	0.000	82.789

Scheme S7 Evaluation of the separation efficiency over the first cycles. Values from the first activation with H_2SO_4 3 M have not been included in this table.

The final fraction was comprised by a mixture of cyclohexanone and cyclohexenone in a 98:2 ratio. A fractional distillation would be the reasonable stage in purification. Nevertheless, data could not be collected as this equipment was not present in our laboratory.

The amount of H_2 produced via HER is estimated to be 429 mL on the 1 g scale reaction according to the 37% FE.

However, both approaches (nickel foam and palladium on carbon) presented a final fraction comprised of a mixture of volatile compounds, and in both cases a similar procedure would have taken place. This similarity allows us not to consider this stage at the study but still have a meaningful comparison.

Final values can be consulted in Tables S8 and S9.

Table S8 Life cycle inventory (LCI) values for the nickel foam method for the use of the nickel foam in 52 runs. Note that in the LCI model all flows are scaled to an output of 1 g of isolated product. Water consumption was disregarded in the LCI model.

Flow	Concept	Value	Unit	Comment	Link to Scheme 6
1	"Fresh" nickel foam	1.651	g	Only at the start of the method, 52 runs modelled.	Input to catalyst washing
	Sulphuric acid	2.145	mL		
	Water	10.855	mL		
2	Sulphuric acid	2.145	mL	No mass loss of nickel was observed. Only at the start of the method.	Output from catalyst washing
	Water	10.855	mL		
3	Nickel foam	1.651	g	Activated nickel foam ready to be used. Only at the start of the method.	Output from catalyst washing
4	Nickel foam	1.651	g		Input to ECH reaction (3+8)
	Pt wire	8.771	g	Pt wire (new or recycled). 1500 runs modelled.	
5	Cyclohexenone	1.001	g	Starting material	Input to ECH reaction
	Sulfuric acid	6.76	mL	Per both cells	
	Water	240.37	mL		
	EtOH	81.25	mL	Cosolvent, per both cells	
6	Nickel foam	1.651	g	99.5% recycling rate, nickel losses to water included.	Output from ECH reaction
	Cyclohexenone	0.02	g	Starting material	
	Cyclohexanone	1.381	g	Product	
	Pt wire	8.771	g		
	EtOH	81.25	mL	Cosolvent, per both cells	
	Water	240.37	mL	Per both cells	
	Sulfuric acid	6.76	mL		
7	EtOH	13	mL	Cosolvent, per both cells	Input to separation
8	Nickel foam	1.651	g	99.5% recycling rate	Output from separation
	Pt wire	8.771	g		
9	Cyclohexenone	0.02	g	Starting material	Output from separation and input to evaporation
	Cyclohexanone	1.381	g	Product	
	EtOH	94.25	mL	Cosolvent, per both cells	
	Water	240.37	mL	Per both cells	
	Sulfuric acid	6.76	mL	Per both cells	
10	Cyclohexenone	0.006	g	Starting material	Output from evaporation and input to ECH reaction
	Cyclohexanone	0.381	g	Product	
	Water	225.95	mL	Per both cells	
	Sulfuric acid	6.76	mL		
11	Cyclohexenone	0.014	g	Starting material	Output from evaporation and input to distillation
	Cyclohexanone	1.000	g	Product	
	EtOH	86.23	mL	Cosolvent, per both cells	
12	Cyclohexenone	0.014	g	Starting material	Output from distillation – isolated product
	Cyclohexanone	1.000	g	Product	
13	EtOH	82.789	mL	Cosolvent, per both cells	Output from distillation and input to ECH reaction

Table S9 Electricity consumption for the nickel foam method. Values in kJ/1g isolated product

Process	Value
Reaction	668
Separation	–
Activation	54
Evaporation	4320
Distillation	2532

S4.1.2 Palladium on carbon and hydrogen gas method

The same transformation was studied using the Pd/C catalyzed strategy, as a representation of the conventional method. The flow diagram of the method is represented in Scheme S8. It starts with the addition of Pd/C in a round-bottom flask and dispersed in EtOH (Scheme S8, flow 1). The system was sealed and purged 3 times with nitrogen and 3 times with hydrogen (Scheme S8, flows 2–3). A hydrogen balloon (1 L) was then attached to the set up. The substrate, dissolved in EtOH, was added for over 210 minutes. 30 minutes later, the flask was purged with nitrogen (Scheme S8, flows 4–8). The suspension was then filtered over a phase separator (Scheme S8, flows 9–12). The product could be isolated from the mother liquor *via* fractional distillation (Scheme S8, flows 12–14).

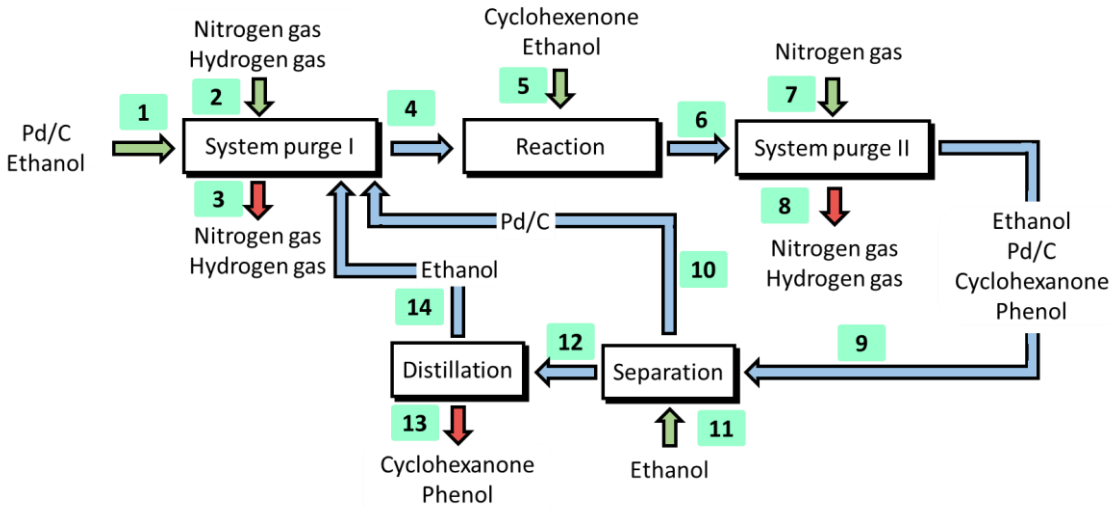

Scheme S8 Hydrogenation Flow diagram for the hydrogenation of 2-cyclohexenone using Pd/C and hydrogen gas.

Values were obtained from a 1.00 g scale reaction (Scheme S9 and Table S10). The recyclability properties of Pd/C were studied using **1a** as substrate, as the slow addition required for **1b** hampered the evaluation at low conversions. Several techniques were explored to recover the Pd/C after the reaction, being the filtration *via* phase separator the one that gave better performance (Scheme S10). The method showed a good but fluctuating performance for at least 10 runs, obtaining the desired hydrogenated product 2a in 29±6.8% yields after 20 min (Scheme S11). The mass loss of palladium was not evaluated due to its pyrophoric nature. We assumed a similar performance regarding its recyclability, and a value of 52 cycles will be used. Moreover, 4% of EtOH was lost during the distillation step. Gases were not recovered and released to the atmosphere. H_2 gas released after the reaction was not measured but estimated to be 1190 mL according to the reaction yield. Its applicability was also tested for a variety of enones at shorter reaction times, but showed lower chemoselectivity, as ketone reduction was also accessed (Scheme S12). Formation of alcohol **3a** as over hydrogenation by-product takes place in parallel to the desired hydrogenation from **1a** to **2a** (Scheme S13).

The final values can be consulted in Tables S11 and S12.

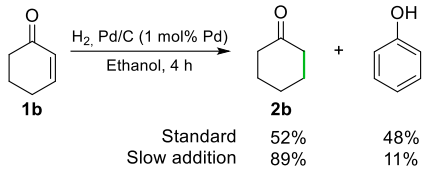

Scheme S9 Hydrogenation of 2-cyclohexenone **1b** using Pd/C and hydrogen gas. Slow addition of substrate **1b** over 3.5 h at a rate of 48μL/min using a 10 mL syringe containing 1.00 g of **1b** in EtOH.

Table S10 Values for the scale-up reaction and the assumed values at 1 g scale

Entry	Component	Values
1	Cyclohexenone	1.126 g
2	Cyclohexanone	1.000 g
3	Phenol	0.111 g
4	EtOH	40 mL
5	Palladium on Carbon	0.100 g
6	Hydrogen gas	1.75 L
7	Nitrogen gas	1.5 L

Entries 5 and 6 are considered only at the system set up and employed for catalyst activation.

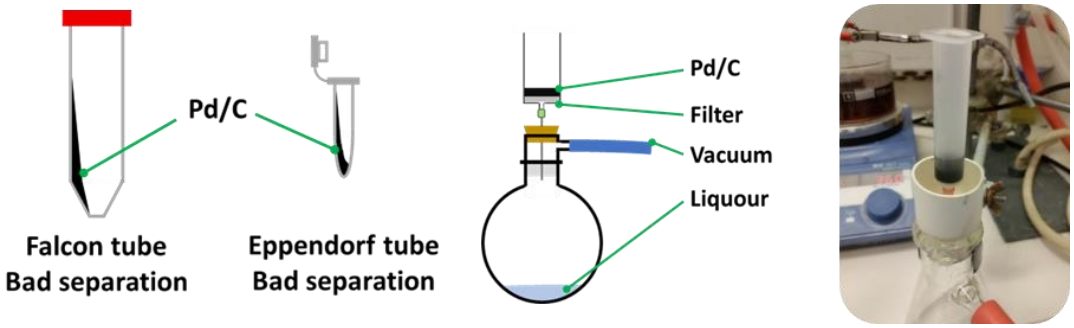

Scheme S10. Pd/C recovery strategies. From left to right: centrifugation *via* Falcon or Eppendorf tube, with bad results due to resuspension. A filtration using a phase separator (TELOS) enabled high recovery of the catalyst.

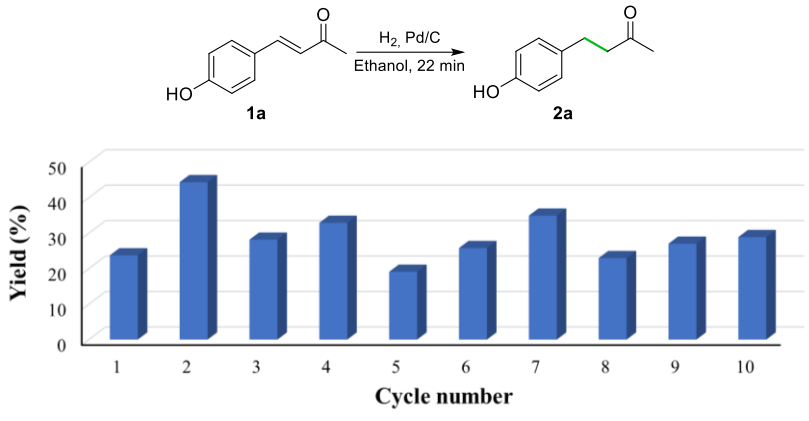

Scheme S11. Recyclability performance of the Pd/C and hydrogen gas method at low conversions. Yields were determined *via* ^{1}H NMR spectroscopy using an internal standard.

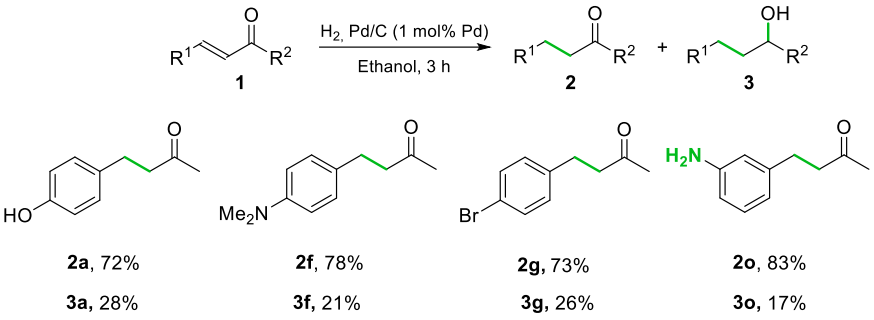

Scheme S12. Scope of alkene hydrogenation using hydrogen gas and Pd/C as catalyst. Yields were determined *via* ^{1}H NMR spectroscopy using an internal standard.

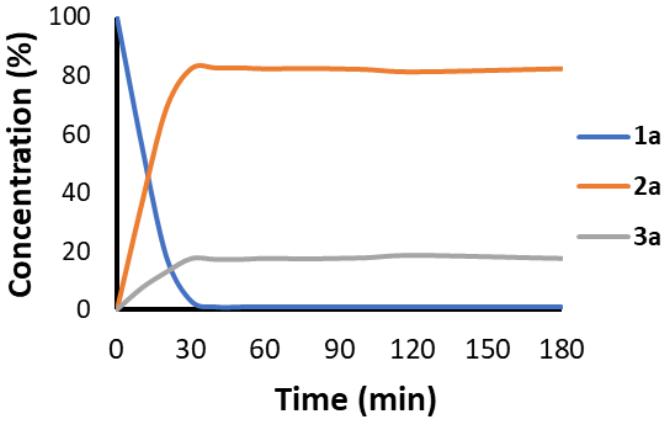

	Concentration (%)		
Time (min)	**1a**	**2a**	**3a**
10	56	36	7
20	18	69	13
30	0	83	17
40	0	83	17
50	0	83	17
60	0	82	18
80	0	83	17
100	0	82	18
120	0	81	19
180	0	83	18

Scheme S13. Kinetic profile for the hydrogenation of **1a** using hydrogen gas and Pd/C as catalyst. Values were determined *via* ^{1}H NMR spectroscopy using an internal standard.

Table S11 Life cycle inventory values for the palladium on carbon and hydrogen gas method in 52 runs. Note that in the LCI model all flows are scaled to an output of 1 g of isolated product. Water consumption was disregarded in the LCI model.

Flow	Concept	Value	Unit	Comment	Link to Scheme 8
1	Palladium on carbon EtOH	0.1 20	g mL	Catalyst. Only at the start of the method.	Input to system purge I
2	Nitrogen gas Hydrogen gas	0.75 1.75	L L	Inert gas	Input to system purge I
3	Nitrogen gas Hydrogen gas	0.75 0.75	L L	Inert gas	Output from system purge I
4	Palladium on carbon EtOH Hydrogen gas	0.1 20 1.0	g mL L	Catalyst Solvent	Output from system purge I and input to reaction
5	Cyclohexenone EtOH	1.126 10	g mL	Substrate Solvent	Input to reaction
6	Cyclohexanone Phenol Palladium on carbon EtOH Hydrogen gas	1.0 0.111 0.1 30 0.44	g g g mL L	Product By-product Catalyst Solvent	Output from reaction and input to system purge II
7	Nitrogen gas	0.75	L	Inert gas	Input to system purge II
8	Nitrogen gas Hydrogen gas	0.75 0.44	L L	Inert gas	Output from system purge II
9	Cyclohexanone Phenol Palladium on carbon EtOH	1.0 0.111 0.1 30	g g g mL	Product By-product Catalyst Solvent	Output from system purge II and input to separation
10	Palladium on carbon	0.1	g	Catalyst	Output from separation and input to system purge I
11	EtOH	10	mL	Solvent	Input to separation
12	Cyclohexanone Phenol EtOH	1.0 0.111 40	g g mL	Product By-product Solvent	Output from separation and input to distillation
13	Cyclohexanone Phenol	1.0 0.111	g g	Product By-product	Output from distillation – isolated product
14	EtOH	38.4	mL	Solvent	Output from distillation and input to system purge I

Table S12 Electricity consumption for the Pd/C catalyzed method. Values in kJ/1g isolated product

Process	Value
Reaction	64.8
Separation	–
Slow addition	151
Evaporation	4320

The handling of solid and liquid waste was not included in the Pd/C and hydrogen gas method, except for a pyrolysis step to recover Pd. In an extension of the LCA, beyond this screening assessment, scenarios for allocation, re-use and waste handling are recommended. In this

screening LCA the disregard of further waste handling of Pd and liquid waste was not expected to affect conclusions compared to an inclusion of generic waste handling.

S4.1.3 Other details

A reported LCA study on the production of different metals compared, among others, the impacts of nickel, palladium, and platinum production (Table S13).[17] Nickel presented a lower contribution for all impact categories, while platinum has the largest contribution.

A study from P. Engels *et al*. assessed the environmental impact of graphite production for batteries, pointing to a Global Warming Potential (GWP) of 9.6 Kg CO_2eq/kg graphite.[18] Another work, from M. Cossutta *et al*. informs that depending on the graphite production technology, the GWP can be between 46 to 284 Kg CO_2eq/kg graphite on a commercial scale.[19]**Table S13** Environmental impacts in the production of nickel, palladium, and platinum.[17-19]

Concept	Nickel	Palladium	Platinum	Graphite
Global warming potential (kg CO2 -eq/kg)	6.5	3880	12500	9.6-284
Cumulative energy demand (MJ -eq/kg)	111	72700	243000	ND
Terrestrial acidification (kg SO2 -eq/kg)	1.5	1700	2200	ND
Freshwater eutrophication (kg P -eq/kg)	0.014	10	51	ND

ND stands for not determined.

Nickel production is diversified, being Indonesia, Philippines and Russia the largest producers. For palladium, most production takes place at Russia and South Africa, while South Africa was the responsible for most platinum production.[20] Differences arise between Russian and South African production because for the Russian production, noble metal extraction uses the waste of nickel production, whereas the South African extraction is highly efficient for a variety of noble metals.

S4.1.4 Assumptions

Not all processes were available as datasets in GaBi database, which means that a priority of data and assumptions had to be made (Table S14). The following priority order were applied:

1. Data from professional database GaBi
2. ecoinvent (version 3.7.1)
3. Assumptions based on structural similarities and availability of datasets

At all production processes in the background system for which we do not have good quality data, we have assumed 20% losses. All quantitative assumptions are listed in Table S15 with an argumentation for applying a certain value.

No loss of platinum has been considered during the electrochemical reaction, as the operational potentials of the method (– 0.7 to – 0.9 V) were smaller than the potential required for Pt dissolution (from – 1.05 V).[21] A lifetime of 1500 cycles has been considered for the calculations.

A proxy characterization factor (CF) for palladium was calculated. All the parameters descripting the exposure and fate were assumed to be equal as those of Ag(I), being the closest substance (in the periodic table), using data from the USEtox 2.12 database. Furthermore, ecotoxicological data from only one species was included (*Hyalella Azteca*). For quality control, in a second stage, the CF of palladium was recalculated using Cr(VI) as proxy because of its high (eco)toxicological impact. The only difference was observed for human toxicity (cancer).

The amount of $NiSO_4$ formed after each reaction was calculated from the mass loss of nickel observed during the recyclability study.

Table S14 Summary of all processes in the models including those which were used as proxy.

Entry	Real process	Process in GaBi/dataset	Source
1[a]	Cyclohexenone production	GLO: chemical production, organic	ecoinvent
2	Sulphuric acid	EU-28: sulphuric acid (96%)	Sphera
3	Polyurethane foam	Polyurethane flexible foam (PU) (EU-27)	Europur
4	Carbon black	Carbon black (EU-28)	Thinkstep
5	Carbon monoxide	Carbon monoxide (DE)	Thinkstep
6	Nickel	Nickel (Nickel institute 2013, GLO)	Nickel institute
7	EtOH	EtOH (96%) from ethylene hydration	Sphera
8	Pt electrodes	GLO: platinum mix	Sphera
9	Waste management of nickel and platinum	EU-28: Municipal solid waste on landfill	Sphera
10	Wastewater treatment	EU-28: municipal waste water	Sphera
11	Electricity	SE: Electricity production	Sphera
12[b]	Transport (truck)	T32_Dist_E6	Sphera
13[c]	Transport (ferry)	Bulk_Ocean_Dist	Sphera
14	Hydrogen	EU-28: Hydrogen (europipeline)	Sphera
15	Nitrogen	EU-28: Nitrogen (gaseous)	Thinkstep
16[d]	District heat	SE: Thermal energy [X[d]]	Sphera
17	Chlorine	EU-28: Chlorine (Cl2)	Thinkstep
18	Palladium	GLO: palladium mix	Sphera
19	Activated carbon	Activated carbon	ecoinvent
20	Hydrochloric acid	DE: Hydrochloric acid (32%)	Sphera
21	Nitric acid	DE: Nitric acid (98% HNO3)	Thinkstep
22	Formaldehyde	EU-28: Formaldehyde (HCHO, 37%)	Sphera
23	Sodium hydroxide	EU-28: Sodium hydroxide mix	Sphera
24	Potassium hydroxide	RER: Potassium hydroxide production	Sphera
25[e]	Catalyst washing	Manually modelled processes according to the lab set-up for the nickel foam system	
26[e]	ECH reaction		
27[e]	Separation		
28[e]	Evaporation		
29[e]	Distillation		
30[f]	System purge I	Manually modelled processes according to the lab set-up for the Pd/C and H_2 system	
31[f]	Reaction		
32[f]	System purge II		
33[f]	Separation		
34[f]	Distillation		

(a) No dataset available for cyclohexanone in databases used herein. (b) 28-32 tot weight Euro 6 Loading factor: 0.85 Fuel sulphur content: 6. (c) Bulk transport. (d) Mixture of multiple datasets; solid biomass (83%), peat (5%), hard coal (5%), natural gas (4%) and heavy fuel oil (3%). (e) Input/output flows as indicated in Schema S6 and Table S8.

Table S15 Summary of all assumptions made and an argumentation of the reasoning behind it. Each assumption has been assigned with a level of uncertainty.

Entry	Process	Assumption	Level of uncertainty
1	Open-cell foam (PU foam + carbon black)	1.79g required to produce 1.49g Nickel foam.	High
2	Nickel carbonyl gas	5.21g required to produce 1.49g Nickel foam.[15]	High
3	Polyurethane foam (PU)	2.08g required to produce 1.79g open-cell foam.[15]	High
4	Carbon black	0.064g required to produce 1.79g open-cell foam.[15]	High
5	Electricity (prod of Nickel foam)	259.4kJ.[22]	Moderate
6	CO	4.11g required to produce 5.21g $Ni(CO)_4$.	Moderate
7	Ni	2.15g required to produce 5.21g $Ni(CO)_4$.	Moderate
8	Pt electrodes	The electrode production was approximated as the production of Pt.	High
9	Cyclohexenone production	The cyclohexenone production was approximated as a generic process for organic chemical production.	High
10	Waste management of Ni and Pt	Municipal solid waste on landfill.	High
11	Activated carbon	102.6g used to produce 95g Pd/C catalyst.[23]	Moderate
12	Hydrochloric acid	28.32g used to produce 95g Pd/C catalyst.[23]	Moderate
13	Nitric acid	111.6g used to produce 95g Pd/C catalyst.[23]	Moderate
14	Formaldehyde	10.392g used to produce 95g Pd/C catalyst.[23]	Moderate
15	Sodium hydroxide	28.32g used to produce 95g Pd/C catalyst.[23]	High
16	Potassium hydroxide	28.32g used to produce 95g Pd/C catalyst.[23]	High
17	Electricity	2592kJ.[24]	Moderate
18	Palladium chloride	8.2g to produce 95g Pd/C catalyst.	Moderate
19	Chlorine	3.912g to produce 8.2g palladium chloride	Low
20	Palladium	5.88g to produce 8.2g palladium chloride	Low

S4.2 Impact Assessment

The hot spots in each impact category have been identified as those processes that contributes to ≥75% of the total impact in the specific impact category. Those processes are the ones included in Figure S6-14 in the following sub-sections.

A contribution analysis has also been performed, identifying which substances in each hot spot that contributes the most to the total impact. Those substances, and its share of the total emission, are also explained in the following sub-sections as well.

S4.2.1 Baseline scenario

Acidification

The acidification potential of the nickel foam system was approximately 15 times larger than the Pd/C system, as can be seen in Figure S6. In the nickel foam system, the platinum electrode production was responsible for 92% of the total impact in this category even though a lifetime of 1500 runs had been applied in the calculations. Electricity production from downstream (DS) processes and the catalyst production represented the hotspots in the Pd/C system, corresponding to 52% and 42% each.

In the nickel foam system, the substance that contributed the most was an emission of sulphur dioxide to air, which represents approximately 88% of the total acidification potential from the Pt electrode production.

For the Pd/C system, nitrogen oxides (45%) and Sulphur dioxide to air (41%) represented the major emissions from the electricity production. For the Pd/C production, sulphur dioxide was responsible for 93% of its acidification potential.

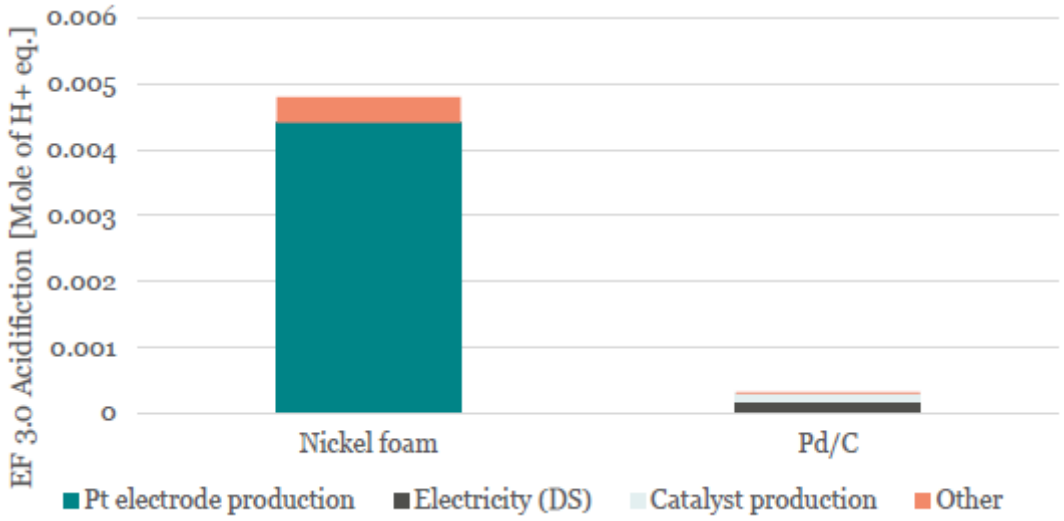

Figure S6 Illustration of the Acidification potential of the two systems including the identified hotspots contributing to ≥75% of the total impact in this category.

Climate change

The global warming potential of the nickel foam system was approximately 5 times larger than the Pd/C system, as can be seen in Figure S7. Platinum electrode production (62%) and electricity production DS (29%) were the identified hotspots in the nickel foam system. The electricity production DS was the sole hotspot in the Pd/C system, responsible for 83% of the total impact in this impact category.

In the nickel foam system, carbon dioxide to air contributed the most, which represented approximately 94% of the total GWP from the electricity production and 88% for the Pt electrode production.

For the Pd/C system, carbon dioxide emissions to air (94%) represented the major emissions from the electricity production.

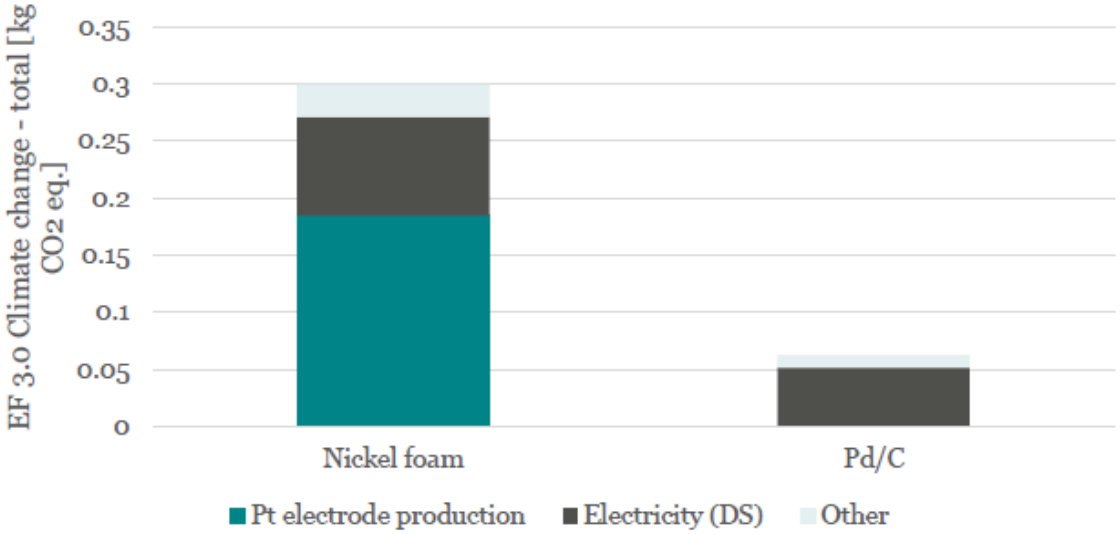

Figure S7 Illustration of the Global warming potential of the two systems including the identified hotspots contributing to ≥75% of the total impact in this category.

Eutrophication potential – freshwater

The eutrophication potential (freshwater) of the nickel foam system was almost 1.5 times larger than the Pd/C system, as can be seen in Figure S8. Electricity production DS (77%) was the identified hotspot in the nickel foam system. The same processes were identified in the Pd/C system, with shares of 66% and 33% respectively.

In the nickel foam system, emissions of phosphate to freshwater represented the major eutrophication potential from the electricity production and substrate production, corresponding to 95% and 88% respectively.

For the Pd/C system, an inorganic emission to fresh water of phosphate represented 94% of the major eutrophication potential in the electricity production and 88% for the substrate production.

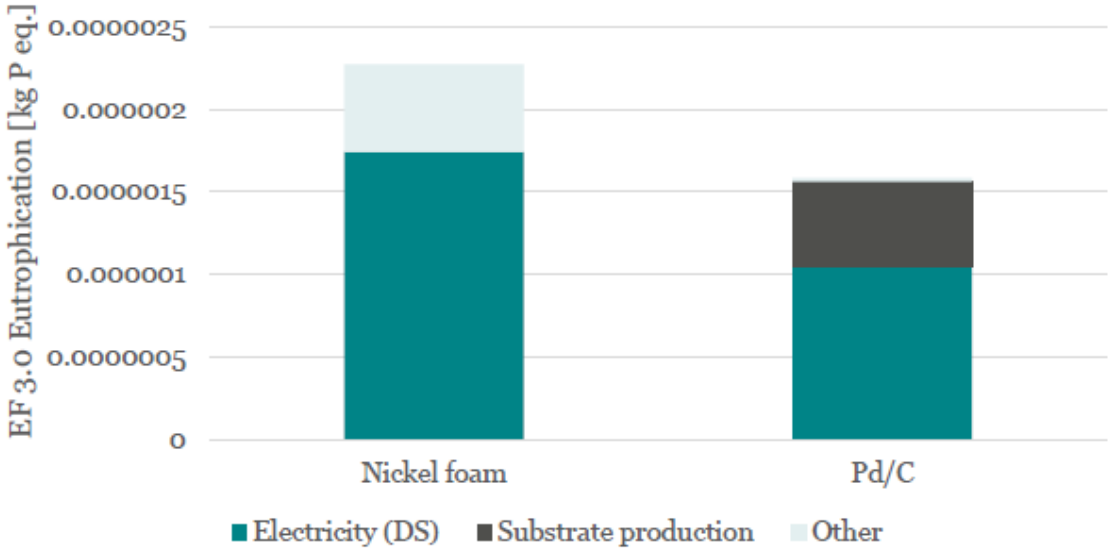

Figure S8 Illustration of the Eutrophication (freshwater) potential of the two systems including the identified hotspots contributing to ≥75% of the total impact in this category.

Eutrophication potential – marine

The eutrophication potential (marine) of the nickel foam system was almost 6 times larger than the Pd/C system, as can be seen in Figure S9. The identified hotspots in the nickel foam system were the platinum electrode production (72%) and the electricity production DS (25%). The latter was the sole hotspot in the Pd/C, responsible for 86% of the total impact in this impact category.

In the nickel foam system, emissions of nitrogen oxide to air represented the major eutrophication potential from the electricity production and platinum electrode production, corresponding to 64% and 97% respectively.

For the Pd/C system, inorganic emissions to fresh water of nitrogen oxides (64%) and nitrate (28%) represented the major eutrophication potential in the electricity production.

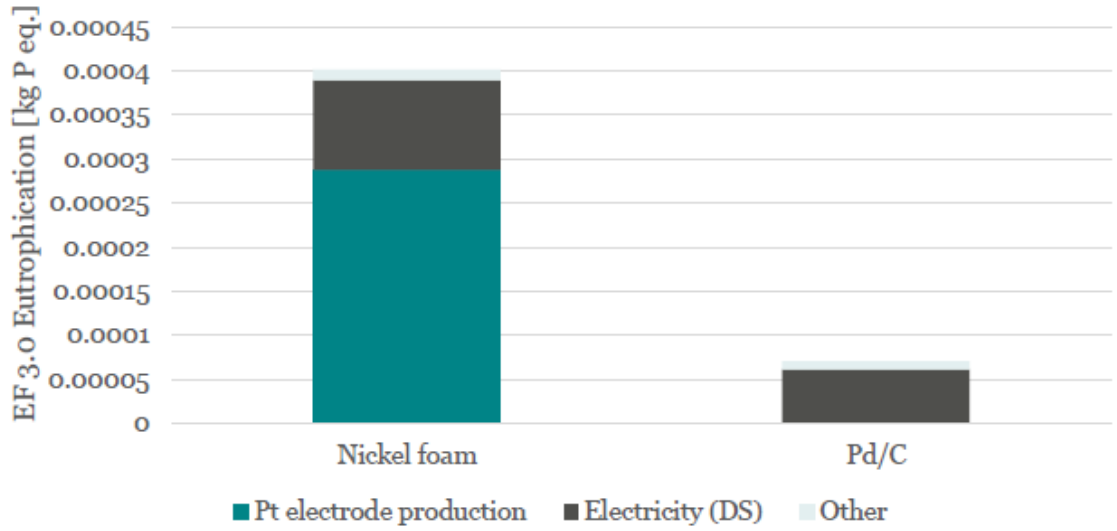

Figure S9 Illustration of the Eutrophication (marine) potential of the two systems including the identified hotspots contributing to ≥75% of the total impact in this category.

Resource use, minerals and metals

The resource use in the nickel foam system was more than 50 times larger than in the Pd/C system, as can be seen in Figure S10. 99% of the total resource use in the nickel foam system came from the platinum electrode production. The hotspots in the Pd/C system (not visible in the Figure due to large differences) were the catalyst production (71%) and the electricity production DS (21%).

In the nickel foam system, the platinum electrode production corresponded to the main impact in this category. The use of platinum (63%) and chromium (31%) were the major contributors from this process.

For the Pd/C system, the use of copper (21%), gold (18%), lead (16%), chromium (14%) and sulphur (10%) represented the resource use from the electricity production. In the catalyst production, it was gold (47%) and platinum (41%) that represented the major resource use.

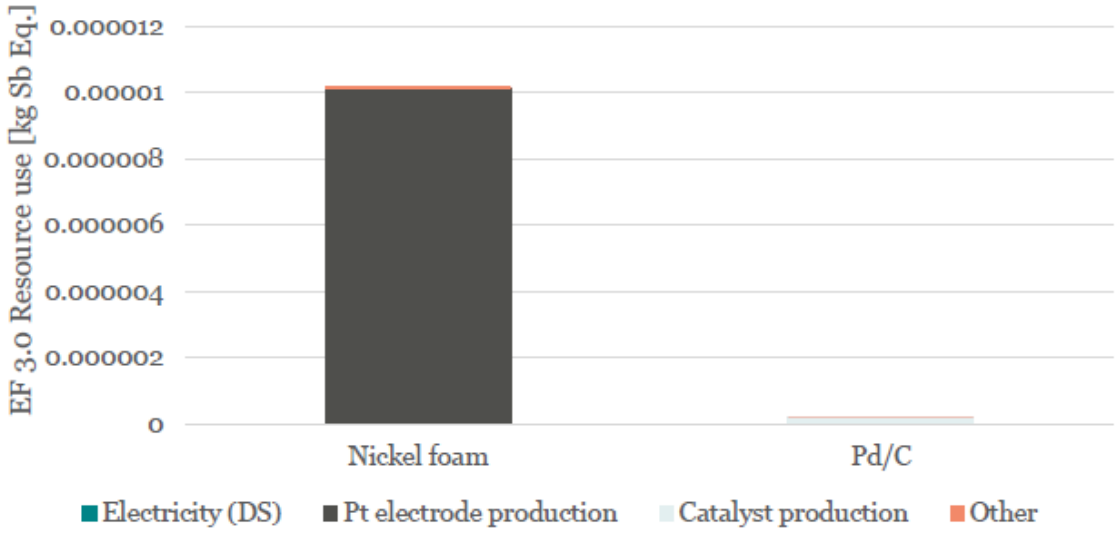

Figure S10 Illustration of the Resource use (minerals and metals) in the two systems including the identified hotspots contributing to ≥75% of the total impact in this category.

Ecotoxicity

The ecotoxicity of the nickel foam system was almost twice as large as the Pd/C system, as can be seen in Figure S11. Electricity production DS (54%), catalyst production (23%) and substrate production (20%) were the identified hotspots in the nickel foam system. In the Pd/C system, it were the electricity production DS (58%) and the substrate production (41%) which contributed the most in this impact category.

In the nickel foam system, an emission of aluminum to freshwater represented the main contribution to the total impact from electricity production (89%), catalyst production (97%) and substrate production (89%).

For the Pd/C system, an emission to fresh water of aluminum (87%) represented the major ecotoxicity potential from the substrate production. The same substance represents 89% of total ecotoxicity potential from the electricity production.

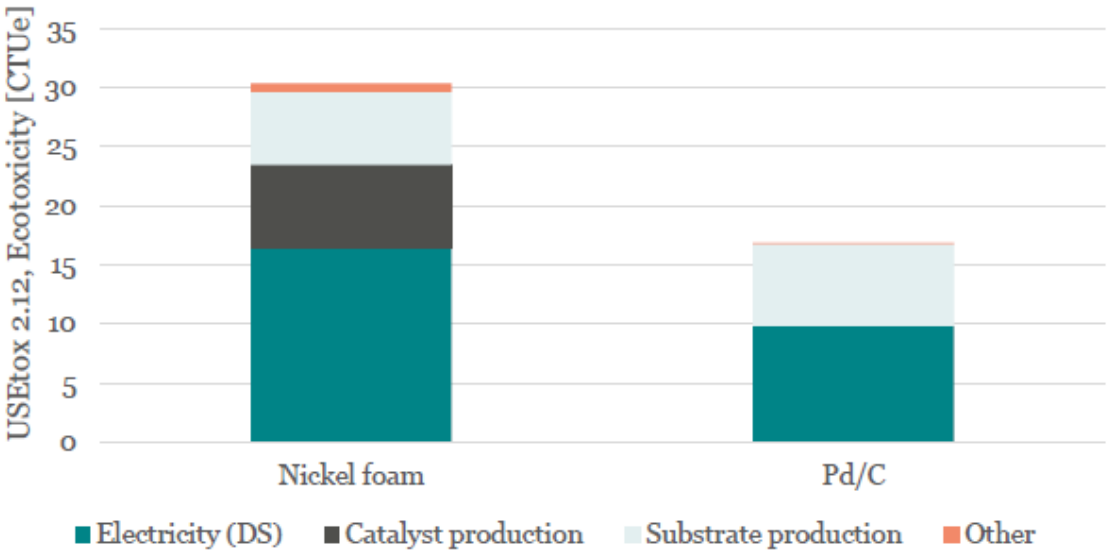

Figure S11 Illustration of the Ecotoxicity potential of the two systems including the identified hotspots contributing to ≥75% of the total impact in this category.

Human toxicity – cancer

The human toxicity (cancer) of the nickel foam system was almost 3 times larger than the Pd/C system, as can be seen in Figure S12. The hotspots in the nickel foam system were the platinum electrode production (31%), electricity production DS (29%) and EtOH production (16%). The electricity production DS (48%) and the substrate production (38%) were the hotspots in the Pd/C system.

In the nickel foam system, the electricity production contributed significantly to the total impact of the system. From this process, emissions of mercury to air (23%), Polychlorinated dibenzo-p-furans to air (35%), chromium to freshwater (18%) constituted the main flows. The production of the platinum electrodes was also an important process for the systems human toxicity (cancer), in which the emissions of mercury (33%), nickel (26%) to air and chromium (18%) to freshwater contributed the most. Emission of chromium (76%) to freshwater from the EtOH production was also significant for the systems human toxicity potential.

For the Pd/C system, an emission to fresh water of chromium (88%) represented the major human toxicity (cancer) potential from the substrate production. Emissions of mercury (23%) and polychlorinated dibenzo-p-furans (35%) to air, and chromium (18%) to freshwater represented the flows contributing the most to the ecotoxicity from the electricity production.

A characterization factor for Pd was calculated using USEtox 2.12 and the procedures in the corresponding manuals. There were a lot of assumptions and simplifications made in the data gathering as explained previously. To check whether these assumptions and simplifications affected the final result, a sensitivity analysis was performed by assigning CFs for Cr(VI) to Pd. Cr(VI) was chosen because of its high ecotoxicological impact.

The only changes observed were in the Pd/C system for the impact category Human toxicity (cancer). Figure S13 illustrates the new hotspots and the reduced difference between the systems. It was clear that the CF for Pd affected the results significantly, but the Nickel foam system still indicated to cause higher impact.

The new hotspots (and shares) for the Pd/C system were catalyst production (47%), electricity production DS (26%) and substrate production (21%).

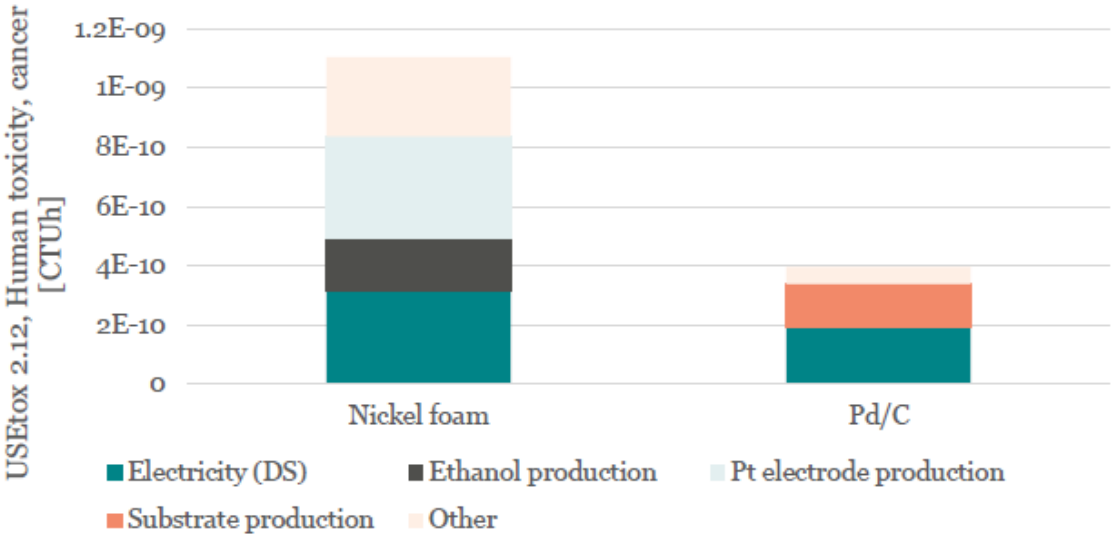

Figure S12 Illustration of the Human toxicity (cancer) potential of the two systems including the identified hotspots contributing to ≥75% of the total impact in this category.

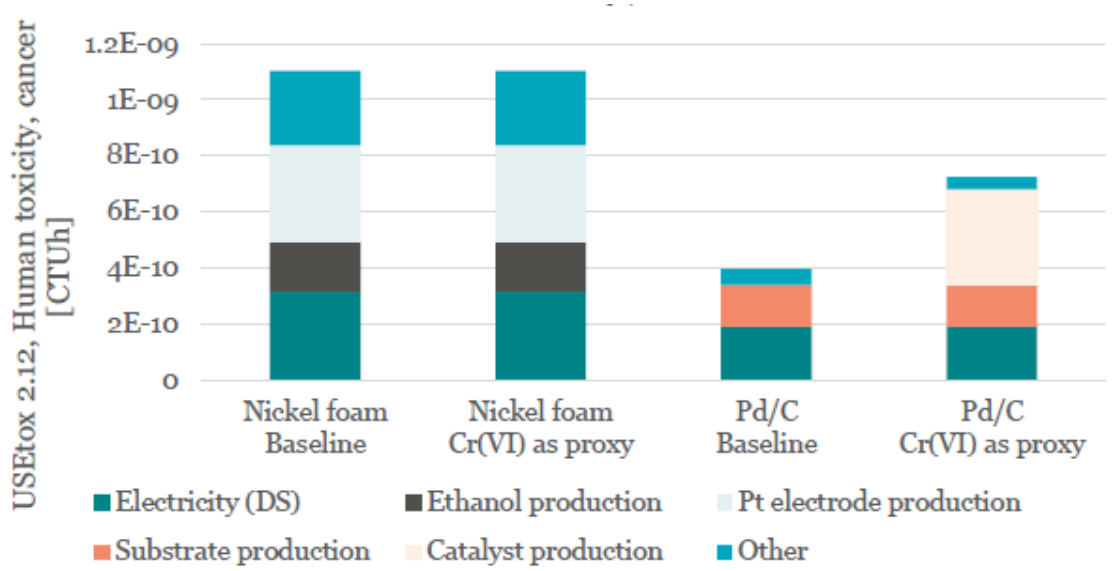

Figure S13 Illustration of the Human toxicity potential of the two systems including the identified hotspots contributing to ≥75% of the total impact in this category for the case when CFs for Cr(VI) was used for Pd.

Human toxicity – non-cancer

The human toxicity (non-cancer) of the nickel foam system was almost 3 times larger than the Pd/C system, as can be seen in Figure S14. Electricity production DS (57%) and platinum electrode production (28%) were the processed identified as hotspots in the nickel foam system. In the Pd/C system, the electricity production DS (89%) was the sole hotspot.

In the nickel foam system, electricity production was important for the human toxicity (non-cancer) from which emissions of mercury (54%) to air, lead (16%) and mercury (10%) to agricultural soil were the main contributors. Mercury to air was the main contributor from the platinum electrode production as well, responsible for 86% of its total human toxicity.

For the Pd/C system, an emission to air of mercury (54%) and emissions of lead (16%) and mercury (10%) to agricultural soil represented the major human toxicity (non-cancer) potential from the electricity production.

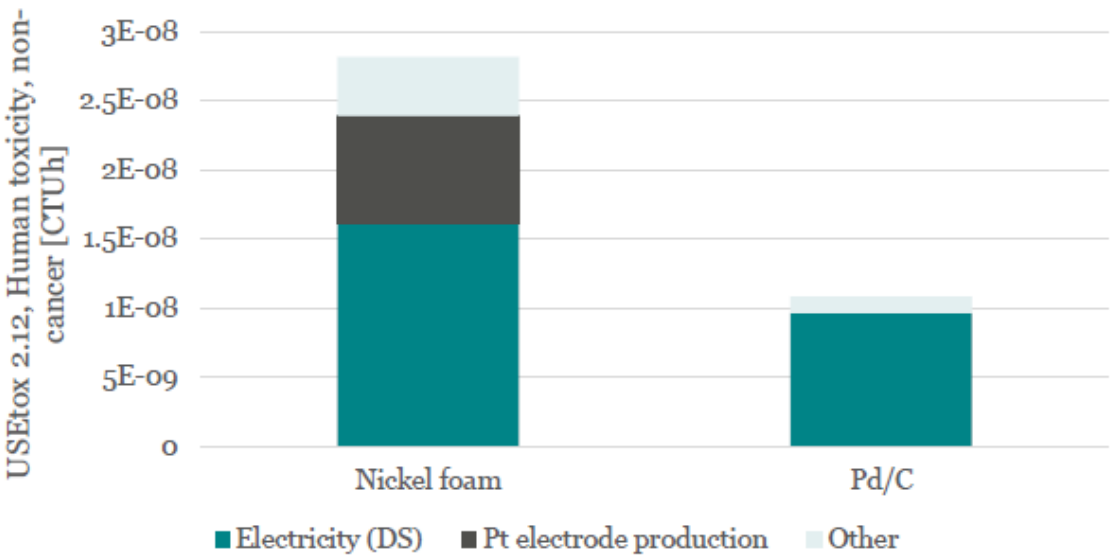

Figure S14 Illustration of the Human toxicity (non-cancer) potential of the two systems including the identified hotspots contributing to ≥75% of the total impact in this category.

Table S16 Summary of the contributions of the nickel foam and Pd/C systems for various impact categories. The impact categories of nickel foam method were set to 100% for internal normalization with the Pd/C system.

Impact category	**System under study**	**Electricity**	**Auxiliary material**	**Lab equipment**	**Catalyst**	**Pt electrode**	**Substrate**	**Transport**	**Waste management**	TOTAL
Acidification	Nickel foam	5.7%	0.6%	0.0%	1.4%	92.1%	0.2%	0.0%	0.0%	100.0%
	Pd/C	3.4%	0.1%	0.0%	2.8%	0.0%	0.2%	0.1%	0.0%	6.6%
Climate change	Nickel foam	28.8%	8.2%	0.0%	0.3%	61.7%	0.7%	0.3%	0.0%	100.0%
	Pd/C	17.2%	1.7%	0.0%	1.1%	0.0%	0.8%	0.1%	0.0%	20.8%
Eutrophication (fw)	Nickel foam	76.7%	1.6%	0.0%	0.2%	0.8%	20.6%	0.1%	0.0%	100.0%
	Pd/C	45.9%	0.3%	0.0%	0.4%	0.0%	23.0%	0.0%	0.0%	69.7%
Eutrophication (mw)	Nickel foam	25.3%	2.4%	0.0%	0.2%	71.7%	0.4%	0.1%	0.0%	100.0%
	Pd/C	17.5%	15.1%	0.5%	0.0%	1.3%	0.0%	0.5%	0.2%	35.1%
Resource use	Nickel foam	0.7%	0.0%	0.0%	0.1%	99.1%	0.1%	0.0%	0.0%	100.0%
	Pd/C	0.4%	0.0%	0.0%	1.4%	0.0%	0.2%	0.0%	0.0%	2.0%
Ecotoxicity	Nickel foam	54.2%	0.6%	0.1%	23.2%	1.6%	20.4%	0.0%	0.0%	100.0%
	Pd/C	32.4%	0.1%	0.0%	0.2%	0.0%	22.7%	0.0%	0.0%	55.5%
Human toxicity (canc.)	Nickel foam	28.7%	16.0%	3.5%	7.9%	31.3%	12.1%	0.5%	0.0%	100.0%
	Pd/C	17.2%	3.7%	0.2%	1.2%	0.0%	13.5%	0.1%	0.0%	35.9%
Human toxicity (non-canc.)	Nickel foam	57.3%	13.0%	0.0%	0.9%	27.7%	0.8%	0.3%	0.0%	100.0%
	Pd/C	34.3%	2.7%	0.0%	0.6%	0.0%	0.8%	0.1%	0.0%	38.5%

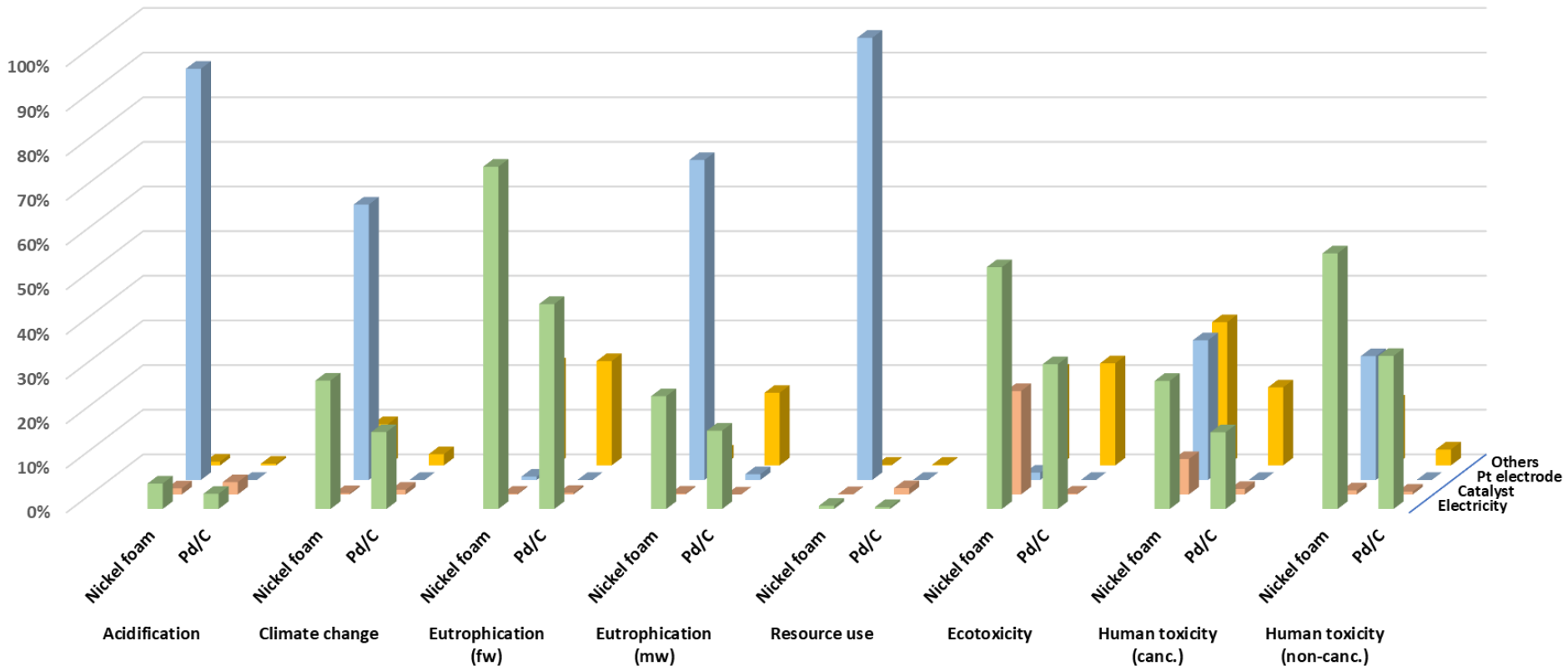

Figure S15. 3D representation of the normalized contributions for the different impact categories.

S4.2.2 2030 Electricity grid scenario

For the baseline scenario, the electricity grid mix of Sweden was used. The reference year for the electricity production based on GaBi/Sphera is 2018 (this dataset was from Sphera with Professional database version 2021.2). In the baseline scenario the electricity generation was a hot spot in several of the impact categories. Due to its prevalence, a sensitivity analysis scenario was considered, changing the electricity production grid mix to a reasonable future electricity grid mix in year 2030. This scenario was based on the IEA statics from 2022.[23] Shares for each electricity source can be seen in Table S17. The data were linearized between two data points, 1990 and 2020, disregarding any trend there between. Acknowledging the high uncertainty in such a simplistic approach, this gave Scenario 2030, which values are presented in Table S17.[23] Negative shared were implemented as 0% in GaBi. As a result, the contribution from electricity decreased in magnitude for all impact categories (Table S18).

Table S17 Share of each electricity source in 1990, 2022 and 2030, as implemented in the LCA model in a simplified future scenario (all values are given in %).

Year	Coal	Oil	Natural gas	Biofuel	Waste	Nuclear	Hydro	Wind	Solar
1990	1.08	0.89	0.27	1.3	0.07	46.54	49.85	0.0	0.0
2020	1.1	0.21	0.06	4.7	2.1	30.06	44.13	17	0.64
2030	1.1	0	0	5.9	2.8	24.83	41.62	22.91	0.84

Table S18 Changes in the values for the different impact categories for future energy mix scenario

Impact category	Nickel foam			Pd/C		
	Baseline scenario	2030 grid scenario	**Change (%)**	Baseline scenario	2030 grid scenario	**Change (%)**
Acidification	4.8E-03	4.6E-03	-4%	3.1E-04	2.0E-04	-37%
Climate change	3.0E-01	2.4E-01	-20%	6.2E-02	2.7E-02	-57%
Eutrophication (freshwater)	2.3E-06	1.0E-06	-55%	1.6E-06	8.3E-07	-48%
Eutrophication (marine)	4.0E-04	3.3E-04	-18%	7.0E-05	2.8E-05	-61%
Resource use	1.0E-05	1.0E-05	0%	2.0E-07	1.9E-07	-9%
Ecotoxicity	3.0E+01	1.7E+01	-44%	1.7E+01	8.8E+00	-47%
Human toxicity (cancer)	1.1E-09	9.0E-10	-18%	4.0E-10	2.8E-10	-31%
Human toxicity (non-cancer)	2.8E-08	1.8E-08	-36%	1.1E-08	4.8E-09	-55%

S4.3 Usability of the results

The results obtained from a screening LCA are to be seen as indicative. The reason for this is that it comes with high uncertainty, assumptions, simplifications, and a lot of data gaps. The purpose of a life cycle-based assessment early on in a process innovation is to steer the decisions towards more sustainable alternatives avoiding the lack of unsustainable choices and burden shifting. Consequently, the results obtained in the screening LCA are to be used for guidance and identification of possible improvements. For example, the Pt electrode was identified as a hotspot in several impact categories for the nickel foam system. Although the quantified results are uncertain, it is clear that there is a need for further research in regard to the selection of electrodes, which is one of the main outcomes of the screening LCA.

To further discuss usability of the results it is important to highlight that database data was used during the modelling of upstream processes, Table S14. With that comes uncertainty and data gaps. For example, a process may be well studied in regard to its carbon footprint, meaning that the process inventory may cover emissions related to climate change in a reasonable way, while the emissions relevant for ecotoxicity may be lacking. Such data gaps are not only difficult to identify, but also difficult to reduce if observed. Additionally, some datasets may include emissions relevant for ecotoxicity, but those flows may be uncharacterized, meaning they are empty and do not contribute to the actual impact.

S5. GENERAL PROCEDURES FOR THE SYNTHESIS OF STARTING MATERIALS

S5.1 Synthesis of α,β-unsaturated carbonyl compound

Acetone (20.0 equiv.) was added to a suspension of aldehyde (10.0 g, 81.9 mmol, 1.0 equiv.) in NaOH 1% (0.25 M). The reaction was stirred at 50 °C until full conversion was achieved, frequently in 2 h. Reaction was followed via TLC. Septa was placed to minimize acetone evaporation. The reaction mixture was quenched *via* addition of 1 M HCl(aq) solution and subsequently extracted with EtOAc (3 x 50 mL). The combined organic layers were dried over $MgSO_4$, filtered and solvent removed via rotary evaporator to yield the corresponding α,β-unsaturated carbonyl compound.

(*E*)-4-(*p*-Hydroxyphenyl)-3-buten-2-one (**1a**)

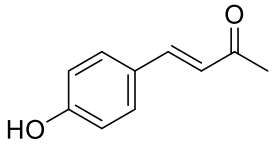

The method was applied using *p*-hydroxybenzaldehyde (10.0 g, 81.9 mmol, 1.0 equiv.) and acetone (120 mL, 1.6 mol, 20 equiv.). Product **1a** (12.0 g, 74 mmol, 90% yield) was purified by recrystallization in toluene. ^{1}H and ^{13}C NMR spectroscopy data is in accordance with previously reported literature.[25]

^{1}H NMR (400 MHz, $CDCl_3$) δ 7.64 (s, 1H), 7.54 (d, J = 16.2 Hz, 1H), 7.47 (d, J = 8.6 Hz, 2H), 6.94 (d, J = 8.6 Hz, 1H), 6.63 (d, J = 16.3 Hz, 1H), 2.42 (s, 3H) ^{13}C NMR (101 MHz, $CDCl_3$) δ 200.32, 159.15, 145.03, 130.52, 126.38, 124.28, 116.26, 27.21

(*E*)-4-(*p*-Tolyl)-3-buten-2-one (**1d**)

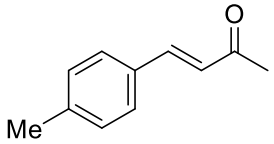

The method was applied using *p*-tolualdehyde (0.5 g, 4.2 mmol, 1.0 equiv.) and acetone (6.2 mL, 83.2 mmol, 20 equiv.). Product **1d** (0.65 g, 4.0 mmol, > 95% yield) was purified by column chromatography using pentane/Et_2O (9:1) as eluent. ^{1}H and ^{13}C NMR spectroscopy data is in accordance with previously reported literature.[26]

^{1}H NMR (400 MHz, $CDCl_3$) δ 7.51 (d, *J* = 16.3 Hz, 1H), 7.45 (d, *J* = 8.1 Hz, 2H), 7.21 (d, *J* = 8.0 Hz, 2H), 6.69 (d, *J* = 16.3 Hz, 1H), 2.38 (s, 3H), 2.37 (s, 3H). ^{13}C NMR (101 MHz, $CDCl_3$) δ 198.85, 143.80, 141.10, 131.64, 129.74, 128.33, 126.19, 27.35, 21.49.

(*E*)-4-(*p*-Methoxyphenyl)-3-buten-2-one (**1e**)

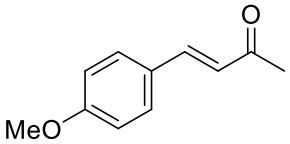

The method was applied using *p*-anisaldehyde (0.5 g, 3.7 mmol, 1.0 equiv.) and acetone (5.4 mL, 73.4 mmol, 20 equiv.). Product **1e** (0.65 g, 3.7 mmol, > 95% yield) was purified by column chromatography using pentane/EtOAc (95:5) as eluent. ^{1}H and ^{13}C NMR spectroscopy data is in accordance with previously reported literature.[26]

^{1}H NMR (400 MHz, $CDCl_3$) δ 7.56 – 7.44 (m, 3H), 6.93 (d, *J* = 8.4 Hz, 2H), 6.62 (d, *J* = 16.2 Hz, 1H), 3.85 (s, 3H), 2.37 (s, 3H). ^{13}C NMR (101 MHz, $CDCl_3$) δ 198.40, 161.63, 143.25, 129.97, 127.07, 125.03, 114.45, 55.40, 27.40.

(*E*)-4-(4-(Dimethylamino)phenyl)-3-buten-2-one (**1f**)

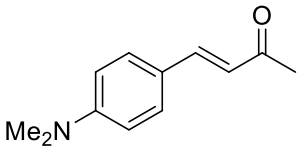

The method was applied using *p*-dimethylaminobenzaldehyde (0.5 g, 3.3 mmol, 1.0 equiv.) and acetone (4.9 mL, 67.0 mmol, 20 equiv.). Acidification was not carried out during work up. Product **1f** (0.65 g, 3.3 mmol, > 95% yield) was purified by column chromatography using pentane/EtOAc (9:1 + 3% Et_3N) as eluent. ^1H and ^{13}C NMR spectroscopy data is in accordance with previously reported literature.[27]

^1H NMR (400 MHz, $CDCl_3$) δ 7.52 – 7.43 (m, 3H), 6.72 (d, J = 8.6 Hz, 2H), 6.57 (d, J = 16.1 Hz, 1H), 3.06 (s, 6H), 2.37 (s, 3H). ^{13}C NMR (101 MHz, $CDCl_3$) δ 198.50, 151.93, 144.36, 130.07, 122.47, 111.92, 111.01, 40.16, 27.18.

(*E*)-4-(*p*-Bromophenyl)-3-buten-2-one (**1g**)

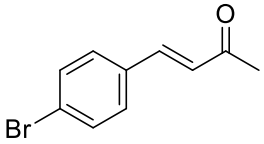

The method was applied using *p*-bromobenzaldehyde (0.5 g, 2.7 mmol, 1.0 equiv.) and acetone (4 mL, 54 mmol, 20 equiv.). Product **1g** (0.317 g, 1.4 mmol, 52% yield) was purified by column chromatography using pentane/Et_2O (9:1) as eluent. ^1H and ^{13}C NMR spectroscopy data is in accordance with previously reported literature.[28]

^1H NMR (400 MHz, $CDCl_3$) δ 7.55 (d, *J* = 8.5 Hz, 2H), 7.50 – 7.40 (m, 3H), 6.72 (d, *J* = 16.2 Hz, 1H), 2.40 (s, 3H). ^{13}C NMR (101 MHz, $CDCl_3$) δ 198.04, 141.90, 132.22, 129.61, 127.56, 124.77, 27.69.

(*E*)-4-(*m*-Tolyl)-3-buten-2-one (**1h**)

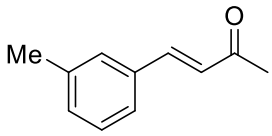

The method was applied using *m*-tolualdehyde (0.5 g, 4.2 mmol, 1.0 equiv.) and acetone (6.2 mL, 83.2 mmol, 20 equiv.). Product **1h** (0.59 g, 4.2 mmol, > 95 yield) was purified by column chromatography using pentane/Et_2O (9:1) as eluent. ^1H and ^{13}C NMR spectroscopy data is in accordance with previously reported literature.[27]

^1H NMR (400 MHz, $CDCl_3$) δ 7.47 (d, *J* = 16.3 Hz, 1H), 7.37 – 7.29 (m, 2H), 7.26 (t, *J* = 7.7 Hz, 1H), 7.18 (d, *J* = 7.5 Hz, 1H), 6.69 (d, *J* = 16.3 Hz, 1H), 2.35 (s, 3H), 2.35 (s, 3H). ^{13}C NMR (101 MHz, $CDCl_3$) δ 143.66, 138.58, 134.36, 131.38, 128.93, 128.85, 126.93, 125.48, 27.42, 21.28.

(*E*)-4-(3-Methoxyphenyl)-3-buten-2-one (**1i**)

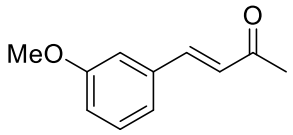

The method was applied using *m*-anisaldehyde (0.5 g, 3.7 mmol, 1.0 equiv.) and acetone (6.2 mL, 83.2 mmol, 20 equiv.). Product **1i** (0.65 g, 3.7 mmol, > 95% yield) was purified by column chromatography using pentane/EtOAc (9:1) as eluent. ^{1}H and ^{13}C NMR spectroscopy data is in accordance with previously reported literature.[29]

^{1}H NMR (400 MHz, $CDCl_3$) δ 7.44 (d, J = 16.3 Hz, 1H), 7.27 (t, J = 7.9 Hz, 1H), 7.09 (dt, J = 8.2, 1.1 Hz, 1H), 7.03 (dd, J = 2.6, 1.6 Hz, 1H), 6.91 (ddd, J = 8.3, 2.6, 1.0 Hz, 1H), 6.66 (d, J = 16.3 Hz, 1H), 3.79 (s, 3H), 2.34 (s, 3H). ^{13}C NMR (101 MHz, $CDCl_3$) δ 198.26, 159.93, 143.29, 135.79, 129.93, 127.37, 120.95, 116.34, 113.05, 55.24, 27.44.

(*E*)-4-(3-Hydroxyphenyl)-3-buten-2-one (**1j**)

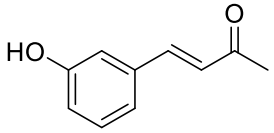

The method was applied using *m*-hydroxybenzaldehyde (0.5 g, 4.0 mmol, 1 equiv.) and acetone (6.0 mL, 82 mmol, 20 equiv.) Product **1j** (0.65 g, 4.0 mmol, > 95% yield) was purified by column chromatography using pentane/EtOAc (9:1) as eluent. ^{1}H and ^{13}C NMR spectroscopy data is in accordance with previously reported literature.[29]

^{1}H NMR (400 MHz, $CDCl_3$) δ 7.50 (d, J = 16.3 Hz, 1H), 7.30 (t, J = 7.8 Hz, 1H), 7.19 – 7.11 (m, 1H), 7.11 – 7.05 (m, 1H), 6.93 (ddd, J = 8.1, 2.6, 1.0 Hz, 1H), 6.72 (d, J = 16.3 Hz, 1H), 5.56 (s, 1H), 2.42 (s, 3H). ^{13}C NMR (101 MHz, $CDCl_3$) δ 198.94, 156.20, 143.52, 135.95, 130.22, 127.38, 121.18, 117.87, 114.54, 27.54.

(*E*)-4-(*m*-Bromophenyl)-3-buten-2-one (**1k**)

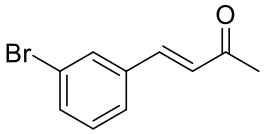

The method was applied using *m*-bromobenzaldehyde (0.5 g, 2.7 mmol, 1.0 equiv.) and acetone (4 mL, 54 mmol, 20 equiv.). Product **1k** (0.60 g, 2.7 mmol, > 95% yield) was purified by column chromatography using pentane/Et_2O (9:1) as eluent. ^{1}H and ^{13}C NMR spectroscopy data is in accordance with previously reported literature.[28]

^{1}H NMR (400 MHz, $CDCl_3$) δ 7.61 (d, J = 1.8 Hz, 1H), 7.48 – 7.42 (m, 1H), 7.41 – 7.32 (m, 2H), 7.21 (t, *J* = 7.8 Hz, 1H), 6.63 (dt, J = 16.3, 1.5 Hz, 1H), 2.32 (s, 3H).^{13}C NMR (101 MHz, $CDCl_3$) δ 197.84, 141.42, 136.54, 133.16, 130.86, 130.44, 128.14, 126.82, 123.02, 27.73.

(*E*)-4-(*o*-Hydroxyphenyl)but-3-en-2-one (**1l**)

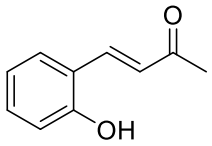

The method was applied using *o*-hydroxybenzaldehyde (0.5 g, 4.0 mmol, 1 equiv.) and acetone (6 mL, 82 mmol, 20 equiv.) Product **1j** (0.64 g, 4.0 mmol, > 95% yield) was purified by column chromatography using pentane/EtOAc (9:1) as eluent. ^{1}H and ^{13}C NMR spectroscopy data is in accordance with previously reported literature.[30]

^{1}H NMR (400 MHz, $CDCl_3$) δ 7.88 (d, J = 16.5 Hz, 1H), 7.50 (dd, J = 7.8, 1.6 Hz, 1H), 7.31 – 7.26 (m, 1H), 7.02 (d, J = 16.4 Hz, 1H), 6.98 – 6.90 (m, 2H), 2.45 (s, 3H). ^{13}C NMR (101 MHz, $CDCl_3$) δ 200.96, 155.89, 140.53, 131.90, 129.57, 127.75, 121.54, 120.76, 116.55, 26.91.

(*E*)-4-(*o*-(trifluoromethyl)phenyl)-3-buten-2-one (**1m**)

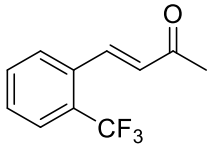

The method was applied using *o*-(trifluoromethyl)benzaldehyde (0.5 g, 2.9 mmol, 1.0 equiv.) and acetone (4.2 mL, 57 mmol, 20 equiv.). Product **1m** (0.59 g, 2.8 mmol, > 95% yield) was purified by column chromatography using pentane/EtOAc (9:1) as eluent. ^{1}H and ^{13}C NMR spectroscopy data is in accordance with previously reported literature.[29]

^{1}H NMR (400 MHz, $CDCl_3$) δ 7.90 (dd, *J* = 16.2, 2.3 Hz, 1H), 7.73 (d, *J* = 7.8 Hz, 2H), 7.65 – 7.56 (m, 1H), 7.51 (t, *J* = 7.7 Hz, 1H), 6.65 (d, *J* = 16.2 Hz, 1H), 2.42 (s, 3H). ^{13}C NMR (101 MHz, $CDCl_3$) δ 198.11, 138.90 (q, *J* = 2.4 Hz), 133.43, 132.21, 131.23, 128.94 (q, *J* = 30.5 Hz), 127.85, 126.24 (q, *J* = 5.6 Hz), 123.99 (q, *J* = 274.0 Hz), 27.12. ^{19}F NMR (377 MHz, $CDCl_3$) δ -58.86.

(*E*)-4,4-Dimethyl-1-phenyl-3-penten-3-one (**1n**)

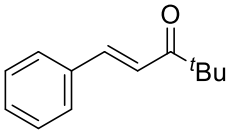

The method was applied using benzaldehyde (1.0 g, 9.4 mmol, 1.0 equiv.) and 3,3-dimethyl-2-butanone (5.9 mL, 47 mmol, 5 equiv.). Product **1n** (0.71 g, 3.8 mmol, 40% yield) was purified by column chromatography using pentane/Et_2O (95:5) as eluent. ^{1}H and ^{13}C NMR spectroscopy data is in accordance with previously reported literature.[31]

^{1}H NMR (400 MHz, $CDCl_3$) δ 7.71 (d, *J* = 15.6 Hz, 1H), 7.59 (dd, *J* = 6.9, 2.8 Hz, 2H), 7.41 (dd, *J* = 5.1, 1.9 Hz, 3H), 7.16 (d, *J* = 15.6 Hz, 1H), 1.26 (s, 9H). ^{13}C NMR (101 MHz, $CDCl_3$) δ 204.21, 142.90, 134.97, 130.21, 128.87, 128.29, 120.75, 43.27, 26.34.

(*E*)-4-(3-nitrophenyl)-3-buten-2-one (**1o**)

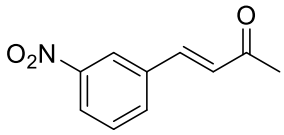

The method was applied using *m*-nitrobenzaldehyde (1.0 g, 6.6 mmol, 1 equiv.) and acetone (9.7 mL, 132 mmol, 20 equiv.) for 15 min. Product **1o** (0.91 g, 4.8 mmol, 72% yield) was purified by column chromatography using pentane/EtOAc (9:1) as eluent. ^{1}H and ^{13}C NMR spectroscopy data is in accordance with previously reported literature.[29]

^{1}H NMR (400 MHz, $CDCl_3$) δ 8.46 – 8.39 (m, 1H), 8.27 (ddd, J = 8.2, 2.2, 1.0 Hz, 1H), 7.87 (dt, J = 7.7, 1.5 Hz, 1H), 7.63 (t, J = 8.0 Hz, 1H), 7.57 (d, J = 16.3 Hz, 1H), 6.86 (d, J = 16.2 Hz, 1H), 2.44 (s, 3H). ^{13}C NMR (101 MHz, $CDCl_3$) δ 197.56, 148.72, 140.18, 136.26, 133.78, 130.07, 129.37, 124.72, 122.61, 28.11.

(*E*)-4-(3-iodophenyl)but-3-en-2-one (**1ak**)

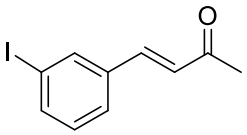

The method was applied using *m*-iodobenzaldehyde (0.5 g, 2.16 mmol, 1 equiv.) and acetone (3.2 mL, 43.1 mmol, 20 equiv.) for 2 h. Product **1ak** (0.11g, 0.4 mmol, 19% yield) was purified by column chromatography using pentane/Et_2O (8:2 towards 1:1) as eluent. ^{1}H and ^{13}C NMR spectroscopy data is in accordance with previously reported literature.[32]

^{1}H NMR (400 MHz, $CDCl_3$) δ 7.91 (d, J = 1.8 Hz, 1H), 7.74 (d, J = 7.9 Hz, 1H), 7.51 (dt, J = 7.7, 1.3 Hz, 1H), 7.41 (d, J = 16.3 Hz, 1H), 7.15 (t, J = 7.8 Hz, 1H), 6.71 (d, J = 16.3 Hz, 1H), 2.40 (s, 3H). ^{13}C NMR (101 MHz, $CDCl_3$) δ 197.96, 141.48, 139.19, 136.95, 136.63, 130.58, 128.07, 127.38, 94.76, 27.78.

(*E*)-4-(furan-2-yl)but-3-en-2-one (**1al**)

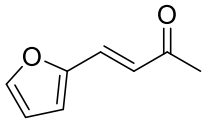

The method was applied using furfural (1.0 g, 6.6 mmol, 1 equiv.) and acetone (15.3 mL, 208 mmol, 20 equiv.) for 2 h. Product **1al** (0.58 g, 4.3 mmol, 41% yield) was purified by column chromatography using pentane/EtOAc (95:5 towards 9:1) as eluent. ^{1}H and ^{13}C NMR spectroscopy data is in accordance with previously reported literature.[32]

^{1}H NMR (400 MHz, $CDCl_3$) δ 7.51 (d, J = 1.8 Hz, 1H), 7.29 (d, J = 16.0 Hz, 1H), 6.68 (d, J = 3.5 Hz, 1H), 6.63 (d, J = 16.0 Hz, 1H), 6.50 (dd, J = 3.4, 1.8 Hz, 1H), 2.34 (s, 3H). ^{13}C NMR (101 MHz, $CDCl_3$) δ 197.87, 150.91, 145.03, 129.44, 124.30, 115.66, 112.55, 27.88.

(*E*)-4-(4-hydroxy-3-iodo-5-methoxyphenyl)but-3-en-2-one (**1am**)

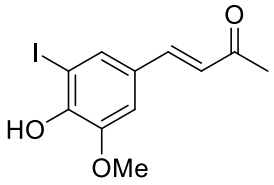

The method was applied using 5-iodovanillin (1.0 g, 3.6 mmol, 1 equiv.) and acetone (5.3 mL, 72 mmol, 20 equiv.) for 2 h. Product **1am** (1.08 g, 3.4 mmol, 94% yield) was obtained without further purification. ^{1}H and ^{13}C NMR spectroscopy data is in accordance with previously reported literature.[33]

^{1}H NMR (400 MHz, $CDCl_3$) δ 7.53 (d, J = 1.9 Hz, 1H), 7.38 (d, J = 16.2 Hz, 1H), 7.03 (d, J = 1.9 Hz, 1H), 6.60 (d, J = 16.2 Hz, 1H), 6.42 (s, 1H), 3.96 (s, 3H), 2.38 (s, 3H). ^{13}C NMR (101 MHz, $CDCl_3$) δ 198.06, 147.99, 146.22, 142.01, 132.06, 128.59, 125.95, 109.27, 81.44, 56.35, 27.49.

(3*E*,5*E*)-6-phenylhexa-3,5-dien-2-one (**1aq**)

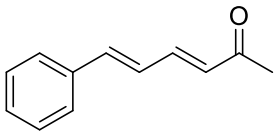

The method was applied using cinnamaldehyde (1.0 g, 7.56 mmol, 1 equiv.) and acetone (11.1 mL, 151 mmol, 20 equiv.) for 2 h. Product **1aq** (1.116 g, 6.5 mmol, 86% yield) ^{1}H and ^{13}C NMR spectroscopy data is in accordance with previously reported literature.[34]

^{1}H NMR (400 MHz, $CDCl_3$) δ 7.55 – 7.44 (m, 2H), 7.42 – 7.25 (m, 4H), 7.06 – 6.82 (m, 2H), 6.27 (d, J = 15.5 Hz, 1H), 2.33 (s, 3H). ^{13}C NMR (101 MHz, $CDCl_3$) δ 198.41, 143.45, 141.28, 135.97, 130.51, 129.25, 128.88, 127.28, 126.67, 27.39.

(*E*)-4-(1H-indol-4-yl)but-3-en-2-one (**1av**)

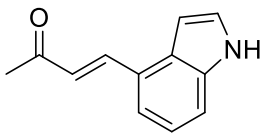

The method was applied using 1*H*-indole-4-carbaldehyde (2.0 g, 13.8 mmol, 1 equiv.) and acetone (20.3 mL, 276 mmol, 20 equiv.) for 2 h. During work up, basification was not required. Product **1av** (2.36 g, 12.7 mmol, 93% yield) was purified by column chromatography using pentane/EtOAc (9:1) as eluent. ^{1}H and ^{13}C NMR spectroscopy data is in accordance with previously reported literature.[35]

^{1}H NMR (400 MHz, $CDCl_3$) δ 8.52 (s, 1H), 7.97 (d, J = 16.3 Hz, 1H), 7.49 (d, J = 8.0 Hz, 1H), 7.43 (d, J = 7.4 Hz, 1H), 7.37 (t, J = 2.9 Hz, 1H), 7.30 – 7.22 (m, 1H), 6.95 (d, J = 16.3 Hz, 1H), 6.87 (ddd, J = 3.2, 2.0, 1.0 Hz, 1H), 2.47 (s, 3H). ^{13}C NMR (101 MHz, $CDCl_3$) δ 198.91, 142.59, 136.32, 127.36, 127.13, 126.55, 125.72, 122.07, 120.81, 113.56, 101.27, 27.57.

S5.2 Wittig reaction

KOH (10 equiv.) and THF (10 mL) were added to a dry round-bottom flask and cooled down to 0 °C. Triethyl phosphonoacetate (1.25 equiv.) in THF (7 mL) was added and the mixture stirred for 30 min. A solution of aldehyde (0.54 g, 5 mmol, 1.0 equiv.) in THF (7 mL) was added and stirred overnight at room temperature. The reaction mixture was diluted in Et_2O and dried over $MgSO_4$, followed by a filtration over Celite®. The solution was concentrated to yield the crude.

Ethyl (*E*)-3-(pyridin-4-yl)acrylate (**1p**)

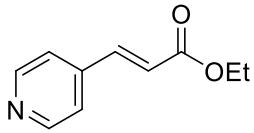

The method was applied using isonicotinaldehyde (0.54 g, 5.0 mmol, 1 equiv.). Product **1p** was purified *via* silica plug with EtOAc as eluent yielded the product (0.29 g, 1.6 mmol, 39% yield). ^1H and ^{13}C NMR spectroscopy data is in accordance with previously reported literature.[36]

^1H NMR (400 MHz, $CDCl_3$) δ 8.65 (d, J = 6.2 Hz, 1H), 7.60 (d, J = 16.0 Hz, 1H), 7.46 – 7.32 (m, 2H), 6.60 (d, J = 16.1 Hz, 1H), 4.29 (q, J = 7.2 Hz, 2H), 1.35 (t, J = 7.1 Hz, 3H). ^{13}C NMR (101 MHz, $CDCl_3$) δ 165.99, 150.53, 141.68, 141.62, 122.94, 121.79, 60.96, 14.24.

Ethyl (*E*)-3-(pyridin-3-yl)acrylate (**1q**)

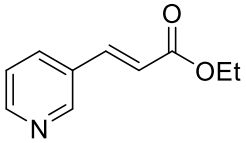

The method was applied using nicotinaldehyde (0.54 g, 5 mmol, 1 equiv.). Product **1q** was purified *via* silica plug with EtOAc as eluent yielded the product (0.24 g, 1.6 mmol, 32% yield). ^1H and ^{13}C NMR spectroscopy data is in accordance with previously reported literature.[37]

^1H NMR (400 MHz, $CDCl_3$) δ 8.77 (d, J = 2.3 Hz, 1H), 8.62 (dd, J = 4.8, 1.6 Hz, 1H), 7.86 (dt, J = 7.9, 2.0 Hz, 1H), 7.69 (d, J = 16.1 Hz, 1H), 7.35 (dd, J = 8.0, 4.8 Hz, 1H), 6.53 (d, J = 16.1 Hz, 1H), 4.30 (q, J = 7.1 Hz, 2H), 1.37 (t, J = 7.1 Hz, 3H). ^{13}C NMR (101 MHz, $CDCl_3$) δ 166.31, 150.92, 149.66, 140.83, 134.24, 130.26, 123.76, 120.54, 60.81, 14.29.

A variation of the method was employed for the synthesis of **1av**. In a round bottom flask, NaH 60% in mineral oil (0.154 g, 3.86 mmol, 1.05 equiv.) was suspended in dry THF (7.8 mL) and cooled down to 0 °C. Triethyl 2-phosphonopropionate (0.962 g, 4.04 mmol, 1.10 equiv.) was added dropwise and kept at 0 °C for 30 min. Then, a solution of the *p*-anisaldehyde (0.500 g, 3.67 mmol, 1.0 equiv.) in dry THF (0.1 M) was added. The mixture was left to react overnight at room temperature. The reaction was quenched with water (20 mL), acidified with sat. NH_4Cl (30 mL) and extracted with EtOAc (3x30 mL). The combined organic phases were dried over $MgSO_4$, filtered and solvent removed via rotary evaporator. The product **1av** (0.755 g, 3.4 mmol, 93% yield) was obtained without further purification. ^1H and ^{13}C NMR spectroscopy data is in accordance with previously reported literature.[37]

Ethyl (*E*)-3-(4-methoxyphenyl)-2-methylacrylate (**1ax**)

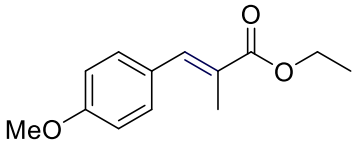

^{1}H NMR (400 MHz, $CDCl_3$) δ 7.66 (d, J = 1.8 Hz, 1H), 7.41 (d, J = 8.8 Hz, 2H), 6.95 (d, J = 8.8 Hz, 2H), 4.29 (q, J = 7.1 Hz, 2H), 3.86 (s, 3H), 2.15 (d, J = 1.4 Hz, 3H), 1.37 (t, J = 7.1 Hz, 3H). ^{13}C NMR (101 MHz, $CDCl_3$) δ 168.96, 159.64, 138.35, 131.41, 128.56, 126.44, 113.85, 60.76, 55.30, 14.37, 14.09.

S5.3 Alcohol esterification

To a solution of mesaconic acid (1.0 g, 8.0 mmol, 1.0 equiv.) in EtOH (45mL), 3 drops of concentrated H_2SO_4 were added and the mixture stirred under reflux for 5 h. The reaction was diluted with saturated aqueous solution of $NaHCO_3$ and extracted 3 times with EtOAc. The combined organic layers were dried over $MgSO_4$, filtered and the solvent was removed *via* rotary evaporator to give product **1u**. Obtained as colorless oil (0.42 g, 2.3 mmol, 29% yield). ^{1}H and ^{13}C NMR spectroscopy data is in accordance with previously reported literature.[38]

Diethyl mesaconate (**1u**)

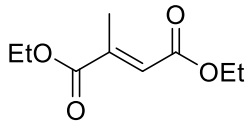

^{1}H NMR (400 MHz, $CDCl_3$) δ 6.75 (s, 1H), 4.21 (dddd, J = 15.5, 8.4, 7.2, 1.3 Hz, 4H), 2.26 (d, J = 1.7 Hz, 3H), 1.29 (tdd, J = 7.0, 4.8, 1.3 Hz, 6H). ^{13}C NMR (101 MHz, $CDCl_3$) δ 167.07, 165.88, 143.70, 126.60, 61.50, 60.54, 14.16, 14.11, 14.05.

S5.4 Grignard addition

To a dry round bottom flask, vinylmagnesium bromide (11.9 mL, 11.9 mmol, 1.6equiv.) solution was added and cooled down to 0ºC. Hydrocinnamaldehyde (1.000 g, 7.4 mmol, 1.0 equiv.) was added dropwise over 15 min and kept 45 min more at 0 ºC. Then, the reaction was allowed to warm to room temperature and kept under stirring for 1 h. The reaction was quenched by the addition of cold MeOH until effervescence ceased. The resulting suspension was treated with aqueous H_2SO_4 (1M) until the suspension became homogeneous. The solution was diluted with CH_2Cl_2 and the layers were separated with a separatory funnel. The aqueous layer was extracted with CH_2Cl_2 (2x20 mL). The combined organic layers were dried over $MgSO_4$, filtered and evaporated to give the product as a colorless oil (1.14 g, 7.0 mmol, 94% yield).[39]

5-Phenyl-1-penten-3-ol (**1w**)

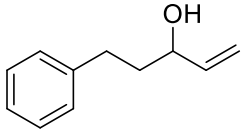

^{1}H NMR (400 MHz, $CDCl_3$) δ 7.32 (dd, J = 8.1, 6.7 Hz, 2H), 7.24 (dt, J = 8.1, 2.0 Hz, 3H), 5.94 (ddd, J = 16.8, 10.4, 6.1 Hz, 1H), 5.28 (dt, J = 17.2, 1.5 Hz, 1H), 5.18 (dt, J = 10.4, 1.4 Hz, 1H), 4.23 – 4.08 (m, 1H), 2.91 – 2.61 (m, 2H), 1.89 (dtd, J = 7.3, 6.3, 5.9, 2.7 Hz, 2H), 1.72 (s, 1H). ^{13}C NMR (101 MHz, $CDCl_3$) δ 141.90, 141.03, 128.49, 128.43, 125.88, 114.97, 72.50, 38.53, 31.65.

S5.5 Alcohol protection with benzyl group

Potassium carbonate (1.26 g, 9.1 mmol, 1.5 equiv.) was added to a solution of eugenol (0.95 mL, 6.1 mmol, 1.0 equiv.) and benzyl bromide (1.1 mL, 9.1 mmol, 1.5 equiv.) in anhydrous acetone (20 mL) under inert atmosphere. The mixture was refluxed overnight. The reaction crude was diluted in water and extracted with EtOAc (3 x 50 mL). The combined organic layers were dried over anhydrous $MgSO_4$, filtered and the solvent was evaporated under reduced pressure. The product was purified by column chromatography (silica, pentane/Et_2O 95:5) to yield the corresponding benzyl protected product **1aa** (1.1 g, 4.3 mmol, 70% yield).[40]

4-Allyl-1-(benzyloxy)-2-methoxybenzene (**1aa**)

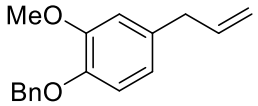

^{1}H NMR (400 MHz, $CDCl_3$) δ 7.49 (d, *J* = 7.3 Hz, 2H), 7.41 (t, *J* = 7.6 Hz, 2H), 7.34 (t, *J* = 7.3 Hz, 1H), 6.85 (d, *J* = 8.2 Hz, 1H), 6.79 (d, *J* = 2.1 Hz, 1H), 6.70 (dd, *J* = 8.1, 2.0 Hz, 1H), 5.99 (ddt, *J* = 16.8, 10.1, 6.7 Hz, 1H), 5.17 (s, 2H), 5.15 – 5.10 (m, 1H), 5.10 – 5.08 (m, 1H), 3.91 (s, 3H), 3.36 (d, *J* = 6.7 Hz, 2H). ^{13}C NMR (101 MHz, $CDCl_3$) δ 149.68, 146.57, 137.65, 137.44, 133.35, 128.52, 127.76, 127.29, 120.45, 115.66, 114.33, 112.48, 71.25, 55.98, 39.85.

S5.6 Alcohol protection with *tert*-butyldimethylsilyl ether (TBS)

Eugenol (0.948 mL, 6.1 mmol, 1.0 equiv.) was dissolved in CH_2Cl_2 (20 mL), followed by the addition of imidazole (0.518 g, 7.6 mmol, 1.25 equiv.). The reaction mixture was cooled down in an ice bath, followed by the slow addition of *tert*-butyldimethylsilyl chloride (1.0 g, 6.7 mmol, 1.1 eq). The reaction mixture was allowed to react at room temperature overnight. The reaction mixture was quenched with a sat. aq. $NaHCO_3$ solution. The phases were separated, and the organic phase was dried over MgSO4, filtered, and solvent was removed by rotary evaporator to yield the corresponding TBS eugenol **1ab** as a yellow oil (1.62 g, 5.8 mmol, 96% yield). ^{1}H and ^{13}C NMR spectroscopy data is in accordance with previously reported literature.[41]

(4-allyl-2-methoxyphenoxy)(tert-butyl)dimethylsilane (**1ab**)

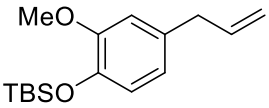

^{1}H NMR (400 MHz, $CDCl_3$) δ 6.81 (d, J = 8.0 Hz, 1H), 6.71 (d, J = 2.1 Hz, 1H), 6.67 (dd, J = 7.9, 2.0 Hz, 1H), 6.00 (ddt, J = 16.9, 10.2, 6.7 Hz, 1H), 5.14 – 5.06 (m, 2H), 3.82 (s, 3H), 3.36 (dd, J = 6.7, 1.6 Hz, 2H), 1.04 (s, 9H), 0.19 (s, 6H). ^{13}C NMR (101 MHz, $CDCl_3$) δ 150.80, 143.28, 137.83, 133.45, 120.73, 120.68, 115.50, 112.62, 55.47, 39.91, 25.77, 18.46, -4.63.

S5.7 Amine protection with Cbz group

Allyl amine (2.6 mL, 35.0 mmol, 1.0 equiv.) and $NaHCO_3$ (4.796 g, 57.1 mmol, 1.63 equiv.) were dissolved in THF (40 mL). Cbz-Cl (5.5 mL, 38.5 mmol, 1.1 equiv.) was added dropwise. The reaction mixture was stirred at room temperature for 4 h. The solution was diluted in water and quenched with aq. HCl 1M. The solution was extracted with EtOAc (3x20 mL). The combined organic layers were washed with water (4x100 mL), and then dried over MgSO4, filtered and the solvent was removed *via* rotary evaporator to give **1ae** as colorless crystals (4.31 g, 22.5 mmol, 64% yield). ^{1}H and ^{13}C NMR spectroscopy data is in accordance with previously reported literature.[42]Benzyl allylcarbamate (**1ae**)

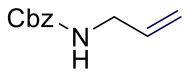

^{1}H NMR (400 MHz, $CDCl_3$) δ 7.41 – 7.31 (m, 5H), 5.87 (ddt, J = 16.1, 10.6, 5.5 Hz, 1H), 5.35 – 5.05 (m, 4H), 4.92 (s, 1H), 3.84 (d, J = 6.1 Hz, 2H). ^{13}C NMR (101 MHz, $CDCl_3$) δ 156.32, 136.57, 134.51, 128.54, 128.15, 116.06, 66.78, 43.51.

Benzyl prop-2-yn-1-ylcarbamate (**1aj**)

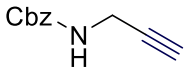

The same protocol was followed using propargyl amine (2.3 mL, 36.3 mmol, 1.0 equiv.). The product was purified *via* column chromatography (silica, pentane/EtOAc 9:1) obtaining the desired product **1aj** as pale yellow crystals (4.59 g, 24.3 mmol, 67% yield). ^{1}H and ^{13}C NMR spectroscopy data is in accordance with previously reported literature.[43]

^{1}H NMR (400 MHz, $CDCl_3$) δ 7.41 – 7.32 (m, 5H), 5.15 (s, 2H), 4.01 (dd, J = 5.8, 2.6 Hz, 2H), 2.27 (t, J = 2.5 Hz, 1H). ^{13}C NMR (101 MHz, $CDCl_3$) δ 155.93, 136.22, 128.57, 128.26, 128.21, 79.70, 71.65, 67.13, 30.87.

S5.8 Amine protection with Fmoc group

Allyl amine (2.6 mL, 35.0 mmol, 1 equiv.), $NaHCO_3$ (4.796 g, 57.1 mmol, 1.6 eq) and 4-dimethylaminopyridine (0.214 g, 1.75 mmol, 0.05 equiv.) were dissolved in THF (40 mL). Fmoc-Cl (9.968 g, 38.5 mmol, 1.1 equiv.) was slowly added. The reaction mixture was stirred at room temperature for 4 h. The solution was diluted in water and quenched with aq. HCl 1M. The solution was extracted with EtOAc (3x20 mL). The combined organic layers were dried over MgSO4, filtered and the solvent was removed *via* rotary evaporator to give **1ag** as colorless crystals (9.3 g, 33.3 mmol, 95% yield). ^{1}H and ^{13}C NMR spectroscopy data is in accordance with previously reported literature.[44]

(9H-Fluoren-9-yl)methyl allylcarbamate (**1ag**)

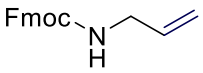

^{1}H NMR (400 MHz, $CDCl_3$) δ 7.80 (dt, J = 7.5, 1.0 Hz, 2H), 7.63 (dd, J = 7.5, 1.0 Hz, 2H), 7.48 – 7.40 (m, 2H), 7.34 (td, J = 7.4, 1.2 Hz, 2H), 5.88 (ddt, J = 16.0, 10.6, 5.5 Hz, 1H), 5.38 – 5.08 (m, 2H), 4.90 (s, 1H), 4.46 (d, J = 6.9 Hz, 2H), 4.26 (t, J = 6.9 Hz, 1H), 3.85 (d, J = 6.0 Hz, 2H). ^{13}C NMR (101 MHz, $CDCl_3$) δ 156.29, 137.52, 136.57, 134.49, 128.76, 128.61, 128.56, 128.42, 128.16, 116.10, 67.99, 66.80, 60.42, 46.29, 43.53, 25.64, 21.07, 14.23.

S5.9 Amine protection with Boc group

Allyl amine (2.6 mL, 35.0 mmol, 1 equiv.), $NaHCO_3$ (4.796 g, 57.1 mmol, 1.63 eq) and 4-dimethylaminopyridine (0.214 g, 1.75 mmol, 0.05 equiv.) were dissolved in THF (40 mL). Boc_2O (8.409 g, 38.5 mmol, 1.1 equiv.) was slowly added. The reaction mixture was stirred at room temperature for 4 h. The solution was diluted in water and quenched with aq. HCl 1M. The solution was extracted with EtOAc (3x20 mL). The combined organic layers were dried over MgSO4, filtered and the solvent was removed *via* rotary evaporator. The crude was purified via flash column chromatography (silica gel, using pentane/EtOAc 9:1 as eluent) to give **1ah** as colorless crystals (3.54 g, 22.5 mmol, 64% yield). ^{1}H and ^{13}C NMR spectroscopy data is in accordance with previously reported literature.[42]

tert-Butyl allylcarbamate (**1ah**)

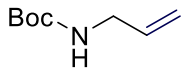

^{1}H NMR (400 MHz, $CDCl_3$) δ 5.83 (ddd, J = 11.7, 10.2, 5.1 Hz, 1H), 5.17 (dq, J = 17.1, 1.5 Hz, 1H), 5.12 – 5.06 (m, 1H), 4.70 (s, 1H), 3.74 (s, 2H), 1.44 (s, 9H). ^{13}C NMR (101 MHz, $CDCl_3$) δ 155.77, 134.93, 115.65, 79.34, 43.06, 28.38.

S5.10 Amine tosylation

To a round bottom flask, allylamine (1.7 mL, 23.12 mmol, 1.2 equiv.), tosyl chloride (3.673 g, 19.27 mmol, 1.0 equiv.) were added and dissolved in THF (55 mL). To this reaction mixture Et3N (2.924 g, 28.9 mmol, 1.5 equiv.) was added and left to react for 4 h. The reaction mixture was quenched by the addition of 20 mL aq. HCl 1M and extracted with EtOAc (3x30 mL). The combined organic fractions were dried over MgSO4, filtered and the solvent was removed *via* rotary evaporator to yield the product as white crystals (3.97 g, 18.79 mmol, 98% yield).). ^{1}H and ^{13}C NMR spectroscopy data is in accordance with previously reported literature.[44]

N-Allyl-4-methylbenzenesulfonamide

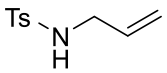

^{1}H NMR (400 MHz, CDCl3) δ 7.78 (dd, J = 8.3, 1.7 Hz, 2H), 7.32 (dd, J = 8.0, 5.6 Hz, 2H), 5.73 (ddd, J = 16.7, 10.6, 5.8 Hz, 1H), 5.17 (dt, J = 17.0, 2.8 Hz, 1H), 5.10 (tt, J = 10.3, 1.4 Hz, 1H), 3.60 (dt, J = 11.4, 3.9 Hz, 2H), 2.44 (d, J = 5.7 Hz, 3H). ^{13}C NMR (101 MHz, CDCl3) δ 143.51, 136.95, 133.01, 129.74, 127.17, 117.65, 45.76, 21.54.

S5.11 Amine acetylation

Under inert conditions, acetic anhydride (0.052 g, 0.51 mmol, 1.1 equiv.) was added to a solution of ethyl (*E*)-3-(1H-indol-2-yl)acrylate (0.100 g, 0.465 mmol, 1.000 equiv.) in EtOAc (2.0 mL). The mixture was stirred under nitrogen overnight. The reaction was quenched by the addition of anhydrous potassium carbonate (200 mg) under stirring. The crude was filtered over celite and concentrated *via* rotary evaporator. The crude was purified via flash column chromatography (silica gel, using a gradient ofpentane/Et_2O 6:4 to 3:7, then EtOAc as eluent) to give **1au** (0.11 g, 0.43 mmol, 92% yield). ^{1}H and ^{13}C NMR spectroscopy data is in accordance with previously reported literature.[46]

Ethyl (*E*)-3-(1-acetyl-1H-indol-2-yl)acrylate (**1au**)

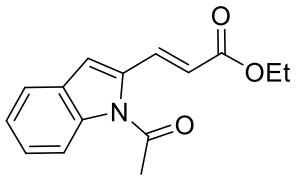

^{1}H NMR (400 MHz, $CDCl_3$) δ 8.56 – 8.39 (m, 1H), 7.87 (dd, J = 8.2, 1.3 Hz, 1H), 7.82 (d, J = 16.2 Hz, 1H), 7.68 (s, 1H), 7.51 – 7.34 (m, 2H), 6.59 (d, J = 16.1 Hz, 1H), 4.31 (q, J = 7.2 Hz, 2H), 2.68 (s, 3H), 1.38 (t, J = 7.1 Hz, 3H). ^{13}C NMR (101 MHz, $CDCl_3$) δ 168.36, 167.21, 136.64, 135.84, 127.81, 127.63, 126.12, 124.51, 120.19, 118.47, 118.37, 116.91, 60.54, 23.98, 14.37.

S5.12 Reductive amination

To a round bottom flask, cinnamaldehyde (0.500 g, 4.0 mmol, 1.0 equiv.) and benzylamine (0.405 g, 4.0 mmol, 1.0 equiv.) were added and dissolved in MeOH (12.4 mL). $NaBH_4$ (0.286 g, 8.0 mmol, 2.000 equiv.) was added to the mixture. The mixture was stirred overnight. The reaction mixture was quenched with sat. aq. $NaHCO_3$ solution and diluted in EtOAc. The aqueous layer

was extractedwith EtOAc (3x20 mL). The combined organic layers were dried over $MgSO_4$, filtered and the solvent was removed using a rotary evaporator. The product **1aw** (0.783 g, 3.5 mmol, 93% yield) was obtained as a pale yellowish oil. ^1H and ^{13}C NMR spectroscopy data is in accordance with previously reported literature.[47]

(*E*)-*N*-Benzyl-3-phenylprop-2-en-1-amine (**1aw**)

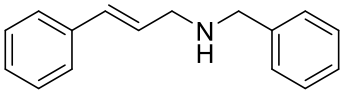

^1H NMR (400 MHz, $CDCl_3$) δ 7.53 – 7.10 (m, 10H), 6.59 (dt, J = 15.8, 1.5 Hz, 1H), 6.37 (dt, J = 15.9, 6.3 Hz, 1H), 3.89 (s, 2H), 3.49 (dd, J = 6.3, 1.5 Hz, 2H). ^{13}C NMR (101 MHz, $CDCl_3$) δ 140.31, 137.19, 131.42, 128.59, 128.51, 128.48, 128.25, 127.39, 127.03, 126.31, 53.40, 51.27.

S5.13 Aldol condensation in acidic media

p-Hydroxybenzaldehyde (0.500 g, 4.1 mmol, 1.0 equiv.) and methyl ethyl ketone (0.734 mL, 8.2 mmol, 2.0 equiv.) were added to a round bottom flask and dissolved in glacial acetic acid (4.1 mL). Sulfuric acid (0.409 mL, 7.37 mmol, 1.8 equiv.) was added dropwise. The reaction was kept under stirring for 1 h. The reaction mixture was quenched *via* dilution in water followed by the addition of aq. 1M NaOH (10 mL) and subsequently extracted with EtOAc (3x20 mL). The combined organic layers were dried over MgSO4, filtered and the solvent was removed *via* rotary evaporator. The crude was purified *via* flash column chromatography (silica gel, using pentane/EtOAc 1:1) to give **1as** (0.706 g, 4.0 mmol, 98% yield).

(*E*)-4-(4-hydroxyphenyl)-3-methylbut-3-en-2-one (**1ay**)

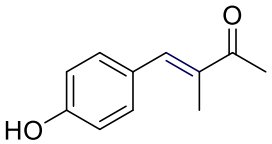

^1H NMR (400 MHz, $CDCl_3$) δ 7.53 (d, J = 1.8 Hz, 1 H), 7.40 (d, J = 8.6 Hz, 2H), 6.96 (d, J = 8.6 Hz, 1H), 2.50 (s, 3H), 2.11 (d, J = 1.4 Hz, 3H). ^{13}C NMR (101 MHz, $CDCl_3$) δ 201.51, 156.96, 140.75, 135.38, 131.95, 128.00, 115.66, 25.78, 12.94. HRMS (ESI): m/z [M+H]+ calcd for $C_{11}H_{12}O_2$, 177.0910; found, 177.0911.

S6. GENERAL PROCEDURE FOR THE ELECTROCHEMICAL HYDROGENATION OF ALKENES

Nickel foam (0.16x1x2 cm) was activated via sonication in a solution of sulfuric acid 3 M for 10 min. The catalyst was then washed with water and used without any further manipulation. The H-cell configuration consists of a nickel foam as working electrode, Ag/AgCl/AgCl 3M as reference electrode, and a Pt wire as counter electrode. The substrate (0.4 mmol) was placed at the working compartment, and both chambers were filled with EtOH (6.25 mL) and aqueous sulfuric acid (0.25 M, 18.75 mL). A chronoamperometry experiment was conducted (– 0.9 V, 18 h). After the reaction was completed, nickel foam was removed from the set-up and washed with 2 mL EtOH under sonication for 5 min. The solution from the working electrode was collected and rinsed with 10 mL EtOAc. Both fractions were combined, phases separated, and the aqueous phase extracted twice with 10 mL EtOAc. The combined organic phases were dried over MgSO4, filtered and the solvent was evaporated *via* rotary evaporator or distillation. The compounds were purified via column chromatography.

For those volatile compounds, CH_2Cl_2 was used in the extraction.

For some samples, other conditions were explored, generally by increasing the $H_2SO_{4(aq)}$ concentration to 0.38 M or switching to a saturated solution of n-BuOH (≈ 7%) in aq. H_2SO_4 (0.25 or 0.5 M).

4-(*p*-Hydroxyphenyl)-2-butanone (**2a**)

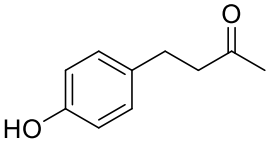

The method was applied using **1a** (0.065 g, 0.4 mmol, 1.0 equiv.). Product **2a** (0.059 g, 0.36 mmol, 89% yield) was purified by column chromatography using pentane/Et_2O (95:5) as eluent. ^1H and ^{13}C NMR spectroscopy data is in accordance with previously reported literature.[25]
^1H NMR (400 MHz, $CDCl_3$) δ 7.07 (d, *J* = 8.5 Hz, 2H), 6.77 (d, *J* = 8.5 Hz, 2H), 4.86 (s, 1H), 2.85 (t, *J* = 7.8 Hz, 2H), 2.79 – 2.66 (m, 2H), 2.16 (s, 3H). ^{13}C NMR (101 MHz, $CDCl_3$) δ 208.61, 153.92, 133.04, 129.43, 115.33, 45.48, 30.17, 28.90.

Cyclohexanone (**2b**)

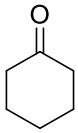

The method was applied using 2-cyclohexenone (0.038 g, 0.4 mmol, 1.0 equiv.) for 5 h. Product **2b** (0.036 g, 0.37 mmol, 90% yield) was determined by GC- FID using a calibration curve.

4-Phenyl-2-butanone (**2c**)

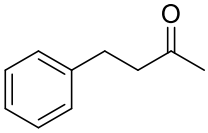

The method was applied using 4-phenyl-3-buten-2-one (0.058 g, 0.4 mmol, 1.0 equiv.). Product **2c** (0.046 g, 0.31 mmol, 77% yield) was purified by column chromatography using pentane/Et_2O (95:5) as eluent. ^1H and ^{13}C NMR spectroscopy data is in accordance with previously reported literature.[25]

^{1}H NMR (400 MHz, $CDCl_3$) δ 7.31 (t, *J* = 7.2 Hz, 2H), 7.22 (t, *J* = 7.5 Hz, 3H), 2.93 (t, *J* = 7.6 Hz, 2H), 2.79 (t, *J* = 7.9 Hz, 2H), 2.17 (s, 3H). ^{13}C NMR (101 MHz, $CDCl_3$) δ 207.95, 141.01, 128.52, 128.31, 126.13, 45.20, 30.09, 29.75.

4-(*p*-Tolyl)-2-butanone (**2d**)

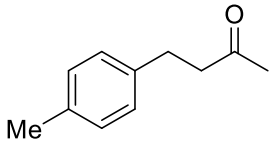

The method was applied using **1d** (0.064 g, 0.4 mmol, 1.0 equiv.). Product **2d** (0.036 g, 0.22 mmol, 55% yield) was purified by column chromatography using pentane/Et_2O (95:5) as eluent. ^{1}H and ^{13}C NMR spectroscopy data is in accordance with previously reported literature.[26]
^{1}H NMR (400 MHz, $CDCl_3$) δ 7.11 (m, 4H), 2.89 (t, *J* = 7.9 Hz, 2H), 2.77 (t, *J* = 7.3 Hz, 2H), 2.34 (s, 3H), 2.16 (s, 3H). ^{13}C NMR (101 MHz, $CDCl_3$) δ 208.10, 137.90, 135.61, 129.19, 128.18, 45.35, 30.09, 29.35, 21.00.

4-(*p*-Methoxyphenyl)-2-butanone (**2e**)

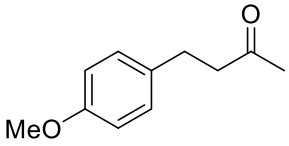

The method was applied using **1e** (0.071 g, 0.4 mmol, 1.0 equiv.). Product **2e** (0.053 g, 0.3 mmol, 75% yield) was purified by column chromatography using pentane/Et_2O (9:1) as eluent. ^{1}H and ^{13}C NMR spectroscopy data is in accordance with previously reported literature.[26]
^{1}H NMR (400 MHz, $CDCl_3$) δ 7.12 (d, *J* = 8.6 Hz, 2H), 6.85 (d, *J* = 8.6 Hz, 2H), 3.80 (s, 3H), 2.92 – 2.83 (m, 2H), 2.79 – 2.71 (m, 2H), 2.15 (s, 3H). ^{13}C NMR (101 MHz, $CDCl_3$) δ 208.16, 157.98, 133.02, 129.23, 113.91, 55.26, 45.46, 30.11, 28.91.

4-(*p*-(Dimethylamino)phenyl)-2-butanone (**2f**)

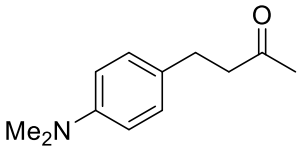

The method was applied using **1f** (0.076 g, 0.4 mmol, 1.0 equiv.). Basification prior to extraction using sat. aq. Na_2CO_3 was carried out. Product **2f** (0.052 g, 0.27 mmol, 68% yield) was purified by column chromatography using pentane/EtOAc (9:1 + 3% Et_3N) as eluent. ^{1}H NMR spectroscopy data is in accordance with previously reported literature.[48]
^{1}H NMR (400 MHz, $CDCl_3$) δ 7.08 (d, J = 8.6 Hz, 2H), 6.71 (d, J = 8.6 Hz, 2H), 2.93 (s, 6H), 2.83 (ddd, J = 9.1, 7.2, 2.0 Hz, 2H), 2.77 – 2.70 (m, 2H), 2.15 (s, 3H). ^{13}C NMR (101 MHz, CDCl3) δ 208.54, 149.24, 128.88, 113.03, 45.67, 40.85, 30.10, 28.88.

4-(*p*-Bromophenyl)-2-butanone (**2g**)

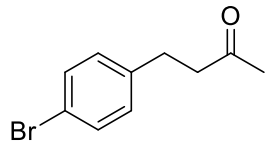

The method was applied using **1g** (0.09 g, 0.4 mmol, 1.0 equiv.). Product **2g** (0.038 g, 0.17 mmol, 42% yield) was purified by column chromatography using pentane/Et_2O (97:3) as eluent. ^{1}H and

^{13}C NMR spectroscopy data is in accordance with previously reported literature.[49] A yield of 59% (0.054 g) was obtained using *n*-BuOH as cosolvent.
^{1}H NMR (400 MHz, $CDCl_3$) δ 7.41 (d, J = 8.4 Hz, 2H), 7.08 (d, J = 8.3 Hz, 2H), 2.91 – 2.82 (m, 2H), 2.79 – 2.72 (m, 2H), 2.16 (s, 3H). ^{13}C NMR (101 MHz, $CDCl_3$) δ 207.51, 140.01, 131.54, 130.14, 119.88, 44.85, 30.14, 29.04.

4-(*m*-Tolyl)-2-butanone (**2h**)

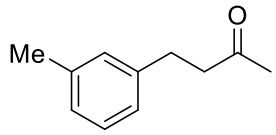

The method was applied using **1h** (0.064 g, 0.4 mmol, 1.0 equiv.). Product **2h** (0.040 g, 0.25 mmol, 61% yield) was purified by column chromatography using pentane/Et_2O (95:5) as eluent. ^1H and ^{13}C NMR spectroscopy data is in accordance with previously reported literature.[50]
^1H NMR (400 MHz, $CDCl_3$) δ 7.20 (t, *J* = 7.9 Hz, 1H), 7.10 – 6.95 (m, 3H), 2.89 (t, *J* = 7.9 Hz, 2H), 2.78 (t, *J* = 7.9 Hz, 2H), 2.35 (s, 3H), 2.17 (s, 3H). ^{13}C NMR (101 MHz, $CDCl_3$) δ 208.06, 140.95, 138.10, 129.13, 128.42, 126.87, 125.27, 45.27, 30.08, 29.68, 21.40.

4-(*m*-Methoxyphenyl)-2-butanone (**2i**)

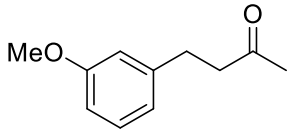

The method was applied using **1i** (0.071 g, 0.4 mmol, 1.0 equiv.) and n-BuOH as cosolvent. Product **2i** (0.051 g, 0.29 mmol, 72% yield) was purified by column chromatography using pentane/Et_2O (95:5) as eluent. ^1H and ^{13}C NMR spectroscopy data is in accordance with previously reported literature.[49]
^1H NMR (400 MHz, $CDCl_3$) δ 7.22 (td, J = 7.9, 7.1, 1.5 Hz, 1H), 6.85 – 6.72 (m, 3H), 3.81 (s, 3H), 2.90 (t, J = 7.6 Hz, 2H), 2.78 (t, J = 7.6 Hz, 2H), 2.16 (s, 3H). ^{13}C NMR (101 MHz, $CDCl_3$) δ 207.91, 159.72, 142.65, 129.50, 120.64, 114.12, 111.40, 55.16, 45.09, 30.09, 29.78.

4-(*m*-Hydroxyphenyl)-2-butanone (**2j**)

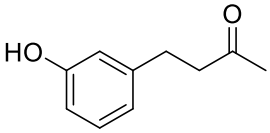

The method was applied using **1j** (0.065 g, 0.4 mmol, 1.0 equiv.) and n-BuOH as cosolvent. Product **2j** (0.054 g, 0.33 mmol, 82% yield) was purified by column chromatography using pentane/EtOAc (9:1) as eluent. ^1H and ^{13}C NMR spectroscopy data is in accordance with previously reported literature.[51]
^1H NMR (400 MHz, $CDCl_3$) δ 7.16 (dd, J = 8.8, 7.6 Hz, 1H), 6.76 (dt, J = 7.6, 1.2 Hz, 1H), 6.73 – 6.68 (m, 2H), 5.63 (s, 1H), 2.96 – 2.84 (m, 2H), 2.78 (ddd, J = 8.5, 6.8, 1.6 Hz, 2H), 2.18 (s, 3H). ^{13}C NMR (101 MHz, $CDCl_3$) δ 208.97, 155.87, 142.76, 129.73, 120.54, 115.35, 113.18, 45.01, 30.18, 29.57.

4-(*m*-Bromophenyl)-2-butanone (**2k**)

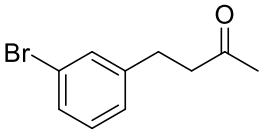

The method was applied using **1k** (0.090 g, 0.4 mmol, 1.0 equiv.). Product **2k** was quantified via ^1H NMR using 1,3,5-trimethoxybenzene as internal standard (21 % yield). ^1H NMR spectroscopy data is in accordance with previously reported literature.[1]

4-(*o*-Hydroxyphenyl)-2-butanone (**2l**)

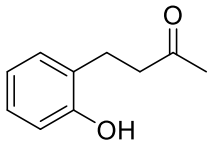

The method was applied using **1l** (0.065 g, 0.4 mmol, 1.0 equiv.). Product **2l** was quantified via ^{1}H NMR using 1,3,5-trimethoxybenzene as internal standard (24 % yield). ^{1}H NMR spectroscopy data is in accordance with previously reported literature.[2]

4-(*o*-(Trifluoromethyl)phenyl)-2-butanone (**2m**)

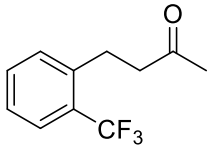

The method was applied using **1m** (0.086 g, 0.4 mmol, 1.0 equiv.). Product **2m** was quantified via ^{1}H NMR using 1,3,5-trimethoxybenzene as internal standard (33 % yield). ^{1}H NMR spectroscopy data is in accordance with previously reported literature.[3]

4,4-Dimethyl-1-phenyl-3-pentanone (**2n**)

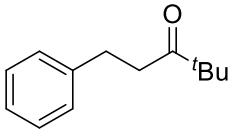

The method was applied using **1n** (0.075 g, 0.4 mmol, 1.0 equiv.). Product **2n** (0.035 g, 0.18 mmol, 46% yield) was purified by column chromatography using pentane/Et_2O (98:2) as eluent. ^{1}H and ^{13}C NMR spectroscopy data is in accordance with previously reported literature.[26]
^{1}H NMR (400 MHz, $CDCl_3$) δ 7.34 – 7.27 (m, 2H), 7.25 – 7.18 (m, 3H), 2.91 (ddd, *J* = 8.1, 6.6, 1.7 Hz, 2H), 2.82 (ddd, *J* = 8.6, 6.7, 1.7 Hz, 2H), 1.13 (s, 9H). ^{13}C NMR (101 MHz, $CDCl_3$) δ 214.97, 141.61, 128.44, 128.41, 126.02, 44.10, 38.50, 30.11, 26.33.

4-(*m*-Aminophenyl)-2-butanone (**2o**)

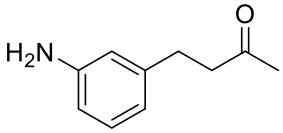

The method was applied using **1o** (0.080 g, 0.4 mmol, 1.0 equiv.) and 0.5 M H_2SO_4 aq. solution. Basification prior to extraction using sat. aq. Na_2CO_3 was carried out. Product **2o** was quantified via ^{1}H NMR using 1,3,5-trimethoxybenzene as internal standard (40 % yield). ^{1}H NMR spectroscopy data is in accordance with previously reported literature.[52]
^{1}H NMR (400 MHz, $CDCl_3$ δ 7.12 – 7.05 (m, 1H), 6.60 (dt, J = 7.6, 1.3 Hz, 1H), 6.54 (dd, J = 6.6, 1.2 Hz, 2H), 3.68 – 3.57 (m, 2H), 2.83 (ddd, J = 7.8, 6.5, 1.8 Hz, 2H), 2.75 (ddd, J = 9.0, 6.4, 1.9 Hz, 2H), 2.16 (s, 3H). ^{13}C NMR (101 MHz, CDCl3) δ 208.17, 146.56, 142.28, 129.45, 118.50, 115.10, 112.97, 45.15, 30.11, 29.76.

Ethyl 3-(*p*-pyridinyl)propanoate (**2p**)

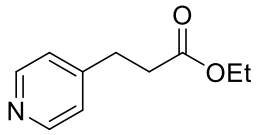

The method was applied using **1p** (0.075 g, 0.4 mmol, 1.0 equiv.). Product **2p** (0.044 g, 0.25 mmol, 62% yield) was purified by column chromatography using pentane/EtOAc (95:5) as eluent. ^{1}H and ^{13}C NMR spectroscopy data is in accordance with previously reported literature.[53]
^{1}H NMR (400 MHz, $CDCl_3$) δ 8.56 – 8.38 (m, 2H), 7.39 – 6.70 (m, 2H), 4.11 (q, *J* = 7.1 Hz, 2H), 2.93 (t, *J* = 7.6 Hz, 2H), 2.62 (t, *J* = 7.6 Hz, 2H), 1.21 (t, *J* = 7.2 Hz, 3H). ^{13}C NMR (101 MHz, $CDCl_3$) δ 172.18, 149.82, 123.68, 60.64, 34.42, 30.06, 14.15.

Ethyl 3-(*m*-pyridinyl)propanoate (**2q**)

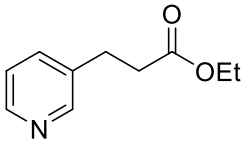

The method was applied using **1q** (0. g, 0. mmol, 1.0 equiv.). Product **2q** was quantified via ^{1}H NMR using 1,3,5-trimethoxybenzene as internal standard (20 % yield). ^{1}H NMR spectroscopy data is in accordance with previously reported literature.[4]

2-Octanone (**2r**)

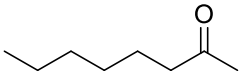

The method was applied using 3-octen-2-one (0.050 g, 0.4 mmol, 1.0 equiv.). Product **2r** (0.029 g, 0.23 mmol, 56% yield) was determined by GC- FID using a calibration curve.

1-(2,6,6-trimethylcyclohex-1-en-1-yl)butan-1-one (**2s**)

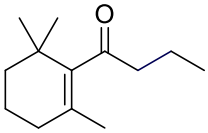

The method was applied using β-damascone (0.077 g, 0.4 mmol, 1.0 equiv.). Product **2s** (0.053 g, 0.27 mmol, 68% yield) was purified by column chromatography using pentane/Et_2O (99:1) as eluent. ^{1}H and ^{13}C NMR spectroscopy data is in accordance with previously reported literature.[54]
^{1}H NMR (400 MHz, $CDCl_3$) δ 2.52 (t, J = 7.4 Hz, 1H), 2.00 – 1.89 (m, 1H), 1.71 – 1.61 (m, 2H), 1.56 (s, 1H), 1.48 – 1.40 (m, 1H), 1.07 (s, 3H), 0.96 (t, J = 7.4 Hz, 2H). ^{13}C NMR (101 MHz, $CDCl_3$) δ 211.82, 143.55, 128.62, 47.67, 38.90, 33.14, 31.12, 28.69, 20.80, 18.88, 16.61, 13.80.

Diethyl succinate (**2t**)

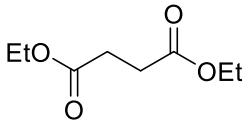

The method was applied using diethyl fumarate or diethyl maleate (0.069 g, 0.4 mmol, 1.0 equiv.). Product **2t** (0.063 g, 0.39 mmol, 90% yield) was purified by column chromatography using pentane/EtOAc (85:15) as eluent. ^{1}H and ^{13}C NMR spectroscopy data is in accordance with previously reported literature.[4]
^{1}H NMR (400 MHz, $CDCl_3$) δ 4.16 (q, J = 7.1 Hz, 4H), 2.63 (s, 4H), 1.27 (t, J = 7.2 Hz, 6H). ^{13}C NMR (101 MHz, $CDCl_3$) δ 172.35, 60.67, 29.19, 14.16.

Diethyl 2-methylsuccinate (**2u**)

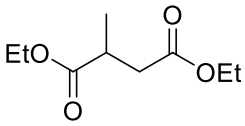

The method was applied using diethyl mesaconate (0.074 g, 0.4 mmol, 1.0 equiv.). Product **2u** (0.028 g, 0.15mmol, 37% yield) was purified by column chromatography using pentane/EtOAc (8:2) as eluent. ^{1}H and ^{13}C NMR spectroscopy data is in accordance with previously reported literature.[4]

^{1}H NMR (400 MHz, $CDCl_3$) δ 4.17 (q, J = 7.2 Hz, 2H), 4.16 (q, J = 7.2 Hz, 2H), 2.92 (dqd, J = 8.2, 7.2, 6.0 Hz, 1H), 2.75 (dd, J = 16.4, 8.1 Hz, 1H), 2.41 (dd, J = 16.4, 6.1 Hz, 1H), 1.28 (t, J = 7.2 Hz, 3H), 1.27 (t, J = 7.2 Hz, 3H). ^{13}C NMR (101 MHz, $CDCl_3$) δ 175.31, 171.88, 60.63, 60.54, 37.73, 35.87, 29.71, 17.02, 14.18, 14.16.

(Ethylsulfonyl)benzene (**2v**)

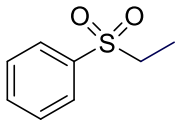

The method was applied using phenyl vinyl sulfone (0.067 g, 0.4 mmol, 1.0 equiv.). Product 2v (0.054 g, 0.32 mmol, 79% yield) was purified by column chromatography using pentane/EtOAc (95:5) as eluent. ^{1}H and ^{13}C NMR spectroscopy data is in accordance with previously reported literature.[55]
^{1}H NMR (400 MHz, $CDCl_3$) δ 7.95 – 7.87 (m, 1H), 7.72 – 7.63 (m, 0H), 7.63 – 7.55 (m, 1H), 3.13 (q, J = 7.4 Hz, 1H), 1.29 (t, J = 7.4 Hz, 2H). ^{13}C NMR (101 MHz, $CDCl_3$) δ 138.53, 133.68, 129.26, 128.20, 50.59, 7.44.

Phenyl-3-pentanol (**2w**)

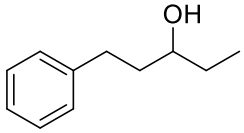

The method was applied using **1w** (0.065 g, 0.4 mmol, 1.0 equiv.). Product **2w** (0.053 g, 0.32 mmol, 80% yield) was purified by column chromatography using pentane/EtOAc (9:1) as eluent. ^{1}H and ^{13}C NMR spectroscopy data is in accordance with previously reported literature.[56]
^{1}H NMR (400 MHz, $CDCl_3$) δ 7.36 – 7.29 (m, 2H), 7.27 – 7.18 (m, 3H), 3.60 (tt, J = 7.6, 4.5 Hz, 1H), 2.84 (ddd, J = 13.6, 9.8, 5.8 Hz, 1H), 2.71 (ddd, J = 13.7, 9.7, 6.7 Hz, 1H), 1.91 – 1.71 (m, 2H), 1.66 – 1.43 (m, 3H), 0.99 (t, J = 7.5 Hz, 3H). ^{13}C NMR (101 MHz, $CDCl_3$) δ 142.27, 128.45, 128.42, 125.82, 72.68, 38.62, 32.11, 30.32, 9.88.

Diethyl 2,2-dipropylmalonate (**2x**)

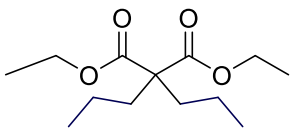

The method was applied using diethyl diallylmalonate (0.096 g, 0.4 mmol, 1 equiv.). A ratio of 1: 1.06: 0.66 between the product (**2x**), the monohydrogenation product and the starting material (**1x**) was determined *via* ^{1}H and ^{13}C NMR, which is in agreement with previously reported literature.[5-7]

Methoxy-*p*-propylbenzene (**2y**)

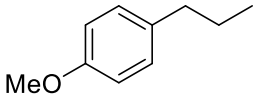

The method was applied using estragole (0.059 g, 0.4 mmol, 1.0 equiv.). Product **2y** (0.052 g, 0.35 mmol, 87% yield) was purified by column chromatography using pentane/Et_2O (98:2) as eluent. ^1H and ^{13}C NMR spectroscopy data is in accordance with previously reported literature.[8]
^1H NMR (400 MHz, $CDCl_3$) δ 7.19 (d, J = 8.6 Hz, 2H), 7.01 – 6.80 (m, 2H), 2.70 – 2.52 (m, 2H), 1.78 – 1.62 (m, 2H), 1.04 (td, J = 7.3, 0.8 Hz, 3H). ^{13}C NMR (101 MHz, $CDCl_3$) δ 157.74, 134.84, 129.38, 113.71, 55.23, 37.23, 24.88, 13.85.

o-Methoxy-*p*-propylphenol (**2z**)

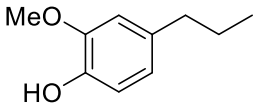

The method was applied using eugenol (0.059 g, 0.4 mmol, 1.0 equiv.). Product **2z** (0.055 g, 0.33 mmol, 83% yield) was purified by column chromatography using pentane/Et_2O (9:1) as eluent. ^1H and ^{13}C NMR spectroscopy data is in accordance with previously reported literature.[1]
^1H NMR (400 MHz, $CDCl_3$) 6.88 (d, *J* = 7.8 Hz, 1H), 6.74 – 6.62 (m, 2H), 3.90 (s, 3H), 3.51 (s, 1H), 2.65 – 2.44 (m, 2H), 1.75 – 1.58 (m, 2H), 0.99 (t, *J* = 7.3 Hz, 3H). ^{13}C NMR (101 MHz, $CDCl_3$) δ 146.42, 143.58, 134.71, 120.99, 114.25, 111.17, 55.85, 37.77, 24.89, 13.81.

Benzyloxy-*o*-methoxy-*p*-propylbenzene (**2aa**)

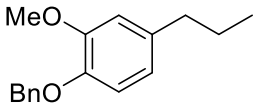

The method was applied using **1aa** (0.102 g, 0.4 mmol, 1.0 equiv.) and n-BuOH as cosolvent. Product **2aa** (0.077 g, 0.30 mmol, 75% yield) was purified by column chromatography using pentane/Et_2O (99:1) as eluent. ^1H and ^{13}C NMR spectroscopy data is in accordance with previously reported literature.[8]
^1H NMR (400 MHz, $CDCl_3$) δ 7.50 – 7.44 (m, 2H), 7.43 – 7.36 (m, 2H), 7.35 – 7.29 (m, 1H), 6.83 (d, J = 8.1 Hz, 1H), 6.76 (d, J = 2.0 Hz, 1H), 6.68 (dd, J = 8.1, 2.0 Hz, 1H), 5.16 (s, 2H), 3.91 (s, 3H), 2.63 – 2.44 (m, 2H), 1.76 – 1.59 (m, 2H), 0.97 (t, J = 7.3 Hz, 3H). ^{13}C NMR (101 MHz, $CDCl_3$) δ 149.49, 146.24, 137.54, 136.11, 128.50, 127.72, 127.29, 120.26, 114.20, 112.43, 71.26, 55.98, 37.72, 24.72, 13.87.

tert-Butyl(2-methoxy-4-propylphenoxy)dimethylsilane (**2ab**)

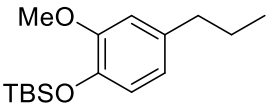

The method was applied using **1ab** (0.111 g, 0.4 mmol, 1.0 equiv.) and n-BuOH as cosolvent. Product **2ab** (60% yield) was quantified *via* ^1H NMR using 1,3,5-trimethoxybenzene as internal standard. ^1H and ^{13}C NMR spectroscopy data is in accordance with previously reported literature.[8]

Decanol (**2ac**)

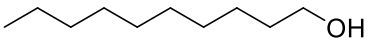

The method was applied using 9-decen-1-ol (0.063 g, 0.4 mmol, 1.0 equiv.). Product **2ac** (0.035 g, 0.22 mmol, 55% yield) was determined by GC-FID using a calibration curve.

p-Propyl toluene (**2ad**)

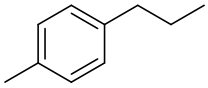

The method was applied using 4-allyltoluene (0.053 g, 0.4 mmol, 1.0 equiv.). Product **2ad** (0.027 g, 0.20 mmol, 50% yield) was determined by GC-FID using a calibration curve.

Benzyl propylcarbamate (**2ae**)

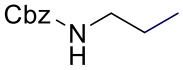

The method was applied using **1ae** (0.076 g, 0,4 mmol, 1 equiv.). Product **2ae** (0.072 g, 0.37 mmol, 93% yield) was obtained without further purification. ^{1}H and ^{13}C NMR spectroscopy data is in accordance with previously reported literature.[57]

^{1}H NMR (400 MHz, $CDCl_3$) δ 7.43 – 7.30 (m, 5H), 5.12 (s, 2H), 4.91 (s, 1H), 3.18 (q, J = 6.7 Hz, 2H), 1.54 (h, J = 7.3 Hz, 2H), 0.94 (t, J = 7.4 Hz, 3H). ^{13}C NMR (101 MHz, $CDCl_3$) δ 156.47, 136.73, 128.55, 128.51, 128.11, 128.07, 66.55, 42.82, 23.19, 11.21.

Tosyl propylamine (**2af**)

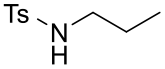

The method was applied using *N*-allyl tosylamide (0.085 g, 0,4 mmol, 1 equiv.). Product **2af** (0.081 g, 0.37 mmol, 95% yield) was obtained without further purification. ^{1}H and ^{13}C NMR spectroscopy data is in accordance with previously reported literature.[58]

^{1}H NMR (400 MHz, CDCl3) δ 7.77 (d, J = 8.3 Hz, 2H), 7.38 – 7.20 (m, 2H), 4.67 (t, J = 6.1 Hz, 1H), 2.91 (td, J = 7.2, 6.2 Hz, 2H), 2.44 (s, 3H), 1.58 – 1.33 (m, 2H), 0.88 (t, J = 7.4 Hz, 3H). ^{13}C NMR (101 MHz, CDCl3) δ 143.33, 137.04, 129.69, 127.10, 44.96, 22.92, 21.52, 11.11.

*n*Propanol (**2ai**)

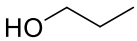

The method was applied using allyl alcohol (0.053 g, 0.4 mmol, 1.0 equiv.). Product **2ai** (0.009 g, 0.14 mmol, 36% yield) was determined by GC-FID using a calibration curve.

N-Butyl phtalamide (**2ai**)

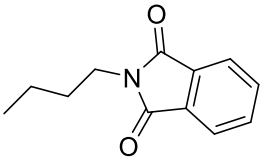

The method was applied using *N*-(3-Butynyl)phthalimide (0.080 g, 0.4 mmol, 1.0 equiv.). Product **2ai** (0.035 g, 0.17 mmol, 43% yield) was purified by column chromatography using pentane/Et_2O (9:1) as eluent. ^{1}H and ^{13}C NMR spectroscopy data is in accordance with previously reported literature.[59]

^{1}H NMR (400 MHz, $CDCl_3$) δ 7.86 (dd, J = 5.5, 3.0 Hz, 2H), 7.73 (dd, J = 5.4, 3.1 Hz, 2H), 3.71 (t, J = 7.3 Hz, 2H), 1.79 – 1.59 (m, 2H), 1.39 (dq, J = 14.7, 7.4 Hz, 2H), 0.97 (t, J = 7.3 Hz, 3H). ^{13}C NMR (101 MHz, $CDCl_3$) δ 168.49, 133.83, 132.20, 123.14, 37.81, 30.65, 20.09, 13.64.

S7. OTHER SYNTHETIC PROCEDURES

S7.1 Ketal synthesis

In a round-bottom flask, cyclohexanone (1.1 mL, 10.2 mmol, 1.0 equiv.), triethyl orthoformate (2.0 mL, 12.23 mmol, 1.2 eq) and hydrochloric acid in EtOH (0.037 g, 1.02 mmol, 0.10 equiv.) were stirred at room temperature overnight. The crude reaction mixture was treated with $NaHCO_3$ 0.15 M (20 mL) and stirred for 10 minutes. The aqueous phase was extracted 3 times with EtOAc. The combined organic layers were dried over $MgSO_4$, filtered and concentrated. Product **4** (0.260 g, 1.51 mmol, 18% yield) was purified by column chromatography using petroleum ether/EtOAc (95:5) + 3% Et_3N. ^1H and ^{13}C NMR spectroscopy data is in accordance with previously reported literature.[60]

1,1-Diethoxycyclohexane (**4**)

^1H NMR (400 MHz, $CDCl_3$) δ 3.46 (q, J = 7.1 Hz, 1H), 1.69 – 1.60 (m, 1H), 1.51 (p, J = 5.8 Hz, 1H), 1.40 (q, J = 5.8 Hz, 1H), 1.18 (t, J = 7.1 Hz, 1H). ^{13}C NMR (101 MHz, $CDCl_3$) δ 99.92, 54.76, 33.81, 25.69, 23.00, 15.57.

S7.2 Ether synthesis

A round bottom flask was loaded with NaH (0.741 mL, 13.3 mmol, 3.3 equiv.), sealed with septum and purged with N_2, followed by the addition of THF (30 mL) and substrate (0.414 mL, 4.0 mmol, 1.0 equiv.). After 1 h reaction, EtI (1.560 g, 10.0 mmol, 2.5 equiv.) was added dropwise to the reaction mixture and let to react overnight. The reaction mixture was quenched by the addition of EtOH (10 mL) and then water (100 mL). The solution was extracted with EtOAc (3x20 mL), dried over MgSO4 and concentrated via distillation to give the desired product.

Ethoxycyclohexane (**3b**)

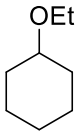

The method was applied using cyclohexanol (0.401 g, 4.0 mmol, 1.0 equiv.). Product **3b** (0.170 g, 33% yield) was purified by column chromatography using pentane/Et2O (99:1) as eluent. The product yield was determined by GC- FID. ^1H and ^{13}C NMR spectroscopy data is in accordance with previously reported literature.[61]

^1H NMR (400 MHz, $CDCl_3$) δ 3.51 (q, J = 7.0 Hz, 2H), 3.23 (dp, J = 9.0, 3.9 Hz, 1H), 1.93 (dtd, J = 8.8, 4.8, 4.3, 1.9 Hz, 2H), 1.82 – 1.67 (m, 2H), 1.63 – 1.51 (m, 1H), 1.36 – 1.26 (m, 4H), 1.20 (t, J = 7.0 Hz, 3H). ^{13}C NMR (101 MHz, $CDCl_3$) δ 62.85, 34.12, 32.38, 25.84, 24.21, 15.55.

Ethoxy-2-cyclohexene (**6b**)

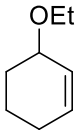

The method was applied using 2-cyclohexenol (0.393 g, 4.0 mmol, 1.0 equiv.). Product **6b** (0.230 g, 1.82 mmol, 46% yield) was purified by column chromatography using pentane/Et2O (99:1) as eluent. The product was determined by GC- FID. ^{1}H and ^{13}C NMR spectroscopy data is in accordance with previously reported literature.[62]

^{1}H NMR (400 MHz, $CDCl_3$) δ 5.86 (dtd, J = 10.1, 3.5, 1.3 Hz, 1H), 5.82 – 5.72 (m, 1H), 3.87 (ddt, J = 6.1, 4.6, 1.9 Hz, 1H), 3.65 – 3.47 (m, 2H), 2.07 (ddtd, J = 16.1, 7.3, 3.4, 1.8 Hz, 1H), 1.97 (dtdd, J = 12.5, 6.3, 2.6, 1.5 Hz, 1H), 1.90 – 1.74 (m, 2H), 1.73 – 1.64 (m, 1H), 1.61 – 1.50 (m, 1H), 1.23 (t, J = 7.0 Hz, 3H). ^{13}C NMR (101 MHz, $CDCl_3$) δ 130.60, 128.07, 72.64, 63.40, 28.45, 25.24, 19.33, 15.76.

S8. DETERMINATION OF IMPURITIES

The following compounds were used as sample or employed in calibration curves for a qualitative and quantitative analysis *via* GC–MS–FID of the upscaled ECH of **1b** to **2b** (scheme S14).

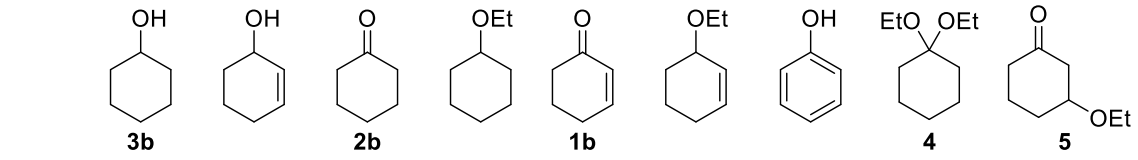

Scheme S14 Retention times (RT) for a variety of compounds which presence could be possible in the reaction crude of the large scale reaction for the ECH of **1b** to **2b** (Table 2, entry 5).

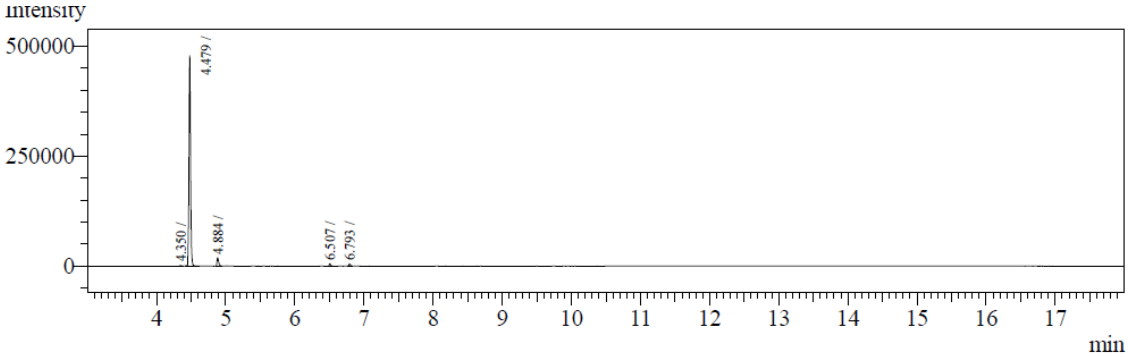

Calibration curves

Cyclohexanol

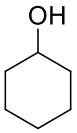

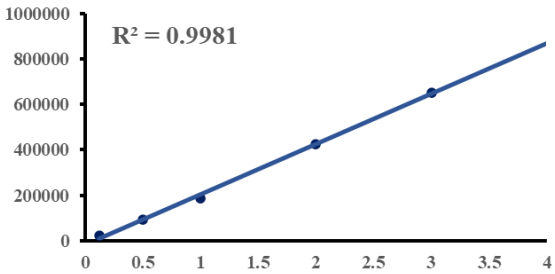

mg/ml	3	2	1	0.5	0.125
Area	650744	426226	184916	91830	21415

2-Cyclohexenol

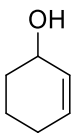

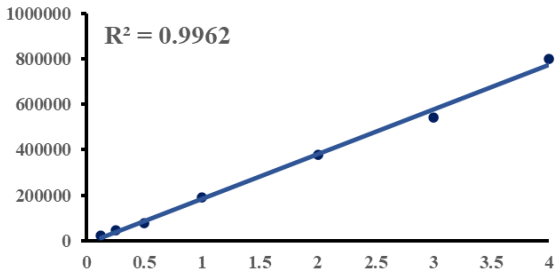

mg/ml	4	3	2	1	0.5	0.25	0.125
Area	799348	543879	380085	189591	78955	45990	20726

Cyclohexanone

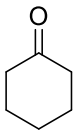

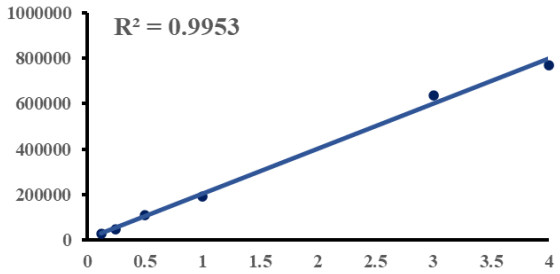

mg/ml	4	3	1	0.5	0.25	0.125
Area	771414	638855	193276	109411	45444	26188

2-Cyclohexenone

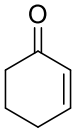

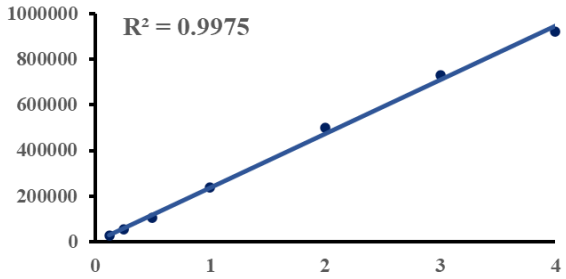

mg/ml	4	3	2	1	0.5	0.25	0.125
Area	923759	731448	499922	239274	104657	54756	26237

Ethoxy-2-cyclohexene

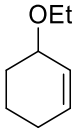

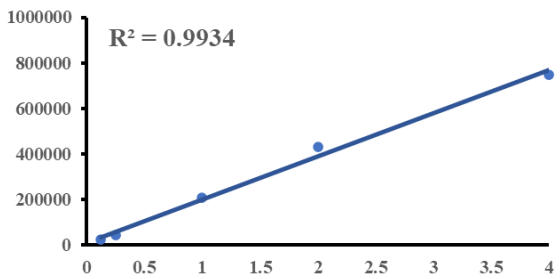

mg/ml	4	2	1	0.25	0.125
Area	749881	432137	208370	46486	24564

Phenol

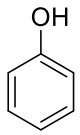

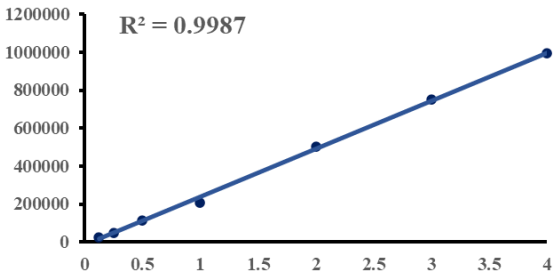

mg/ml	4	3	2	1	0.5	0.25	0.125
Area	994663	748719	503207	209011	114282	46103	25630

1,1-Diethoxycyclohexane

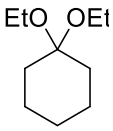

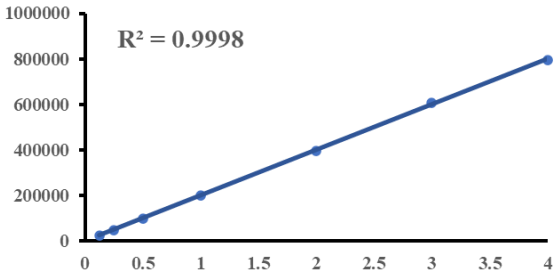

mg/ml	4	3	2	1	0.5	0.25	0.125
Area	795151	607552	395607	201488	98696	50298	25993

3-Ethoxycyclohexanone

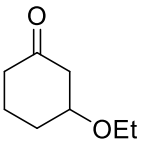

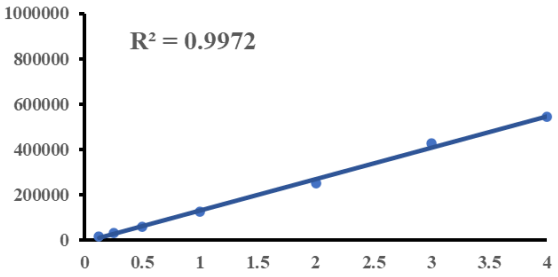

mg/ml	4	3	2	1	0.5	0.25	0.125
Area	543223	426853	252358	128328	61442	32259	16231

2-Octanone

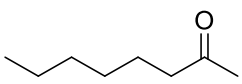

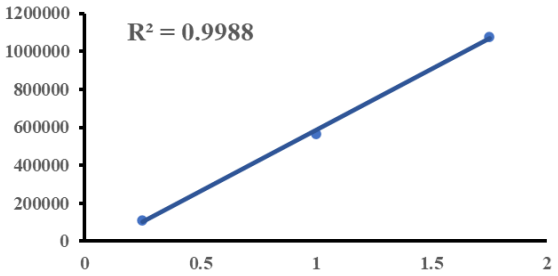

mg/ml	1.75	1	0.25
Area	1076658	565626	111671

Decanol

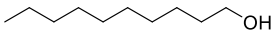

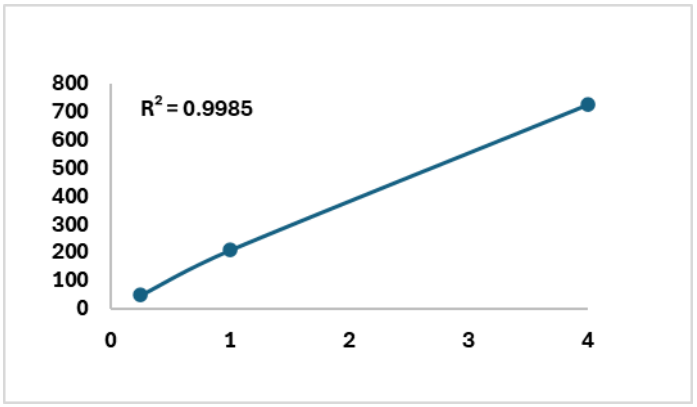

mg/ml	4	1	0.25
Area	48.73	208.53	724.39

9-Decen-1-ol

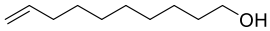

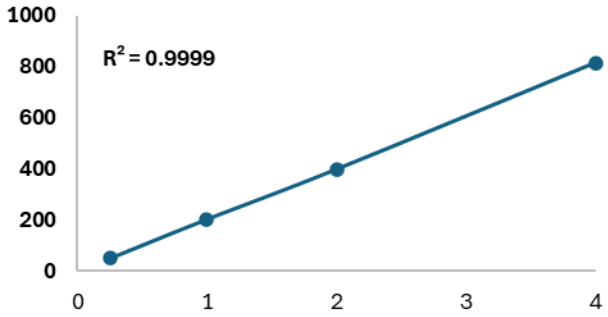

mg/ml	4	2	1	0.25
Area	814.95	398.91	202.97	50.05

p-Propyl toluene

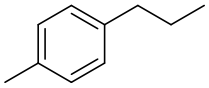

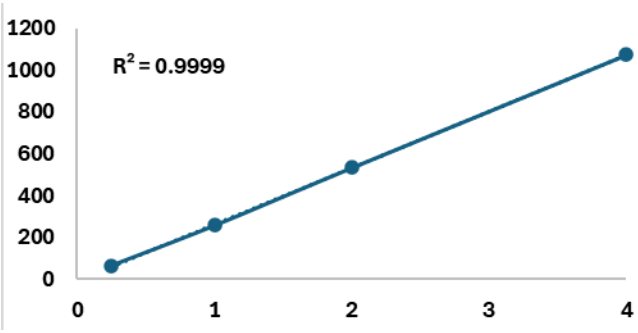

mg/ml	4	2	1	0.25
Area	1072.6	532.33	257.15	65.21

p-Allyl toluene

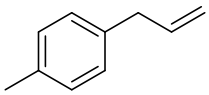

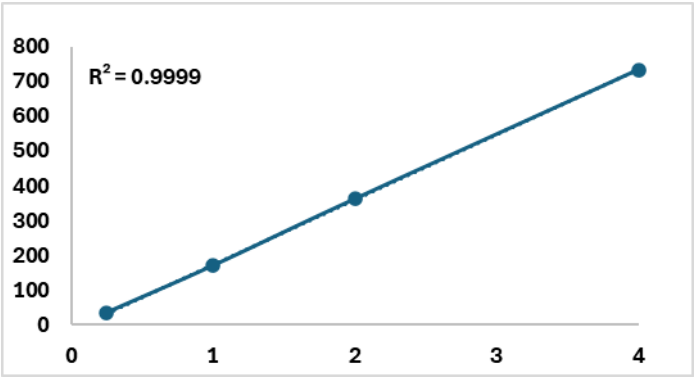

mg/ml	4	2	1	0.25
Area	732.48	361.69	170.3	35.31

S9. NMR SPECTRA

(*E*)-4-(*p*-Hydroxyphenyl)-3-buten-2-one (**1a**)

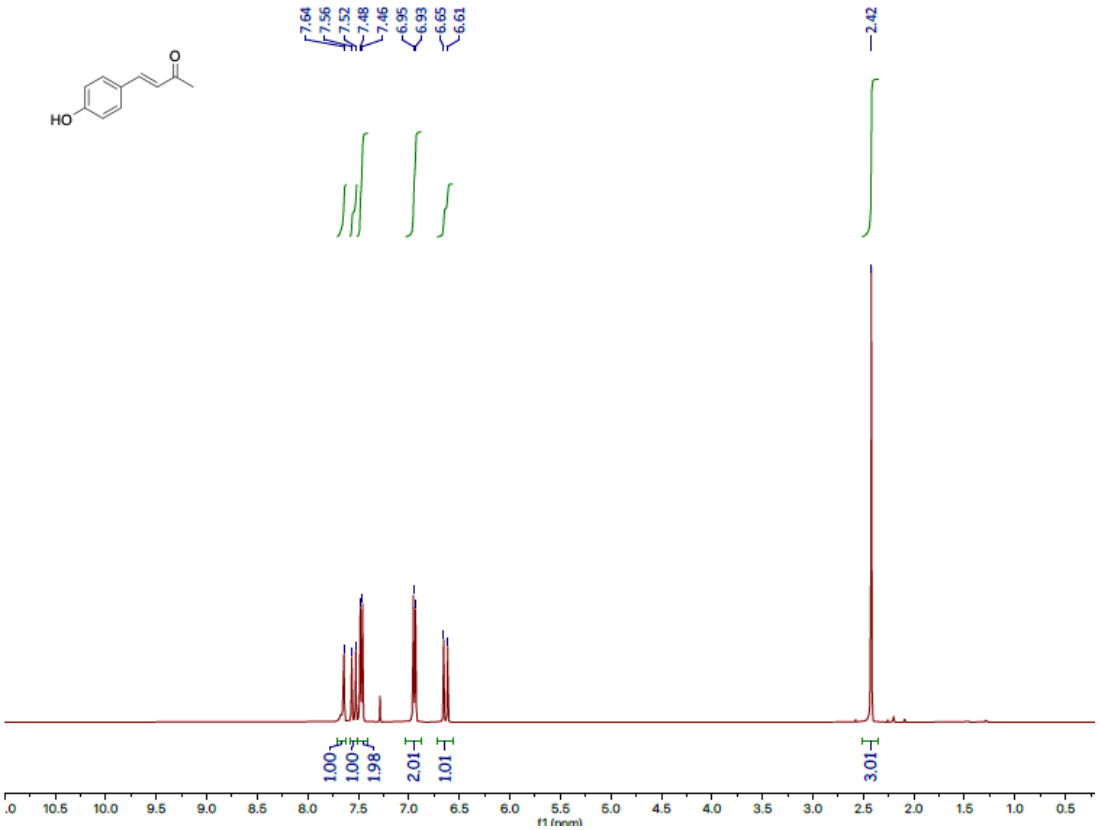

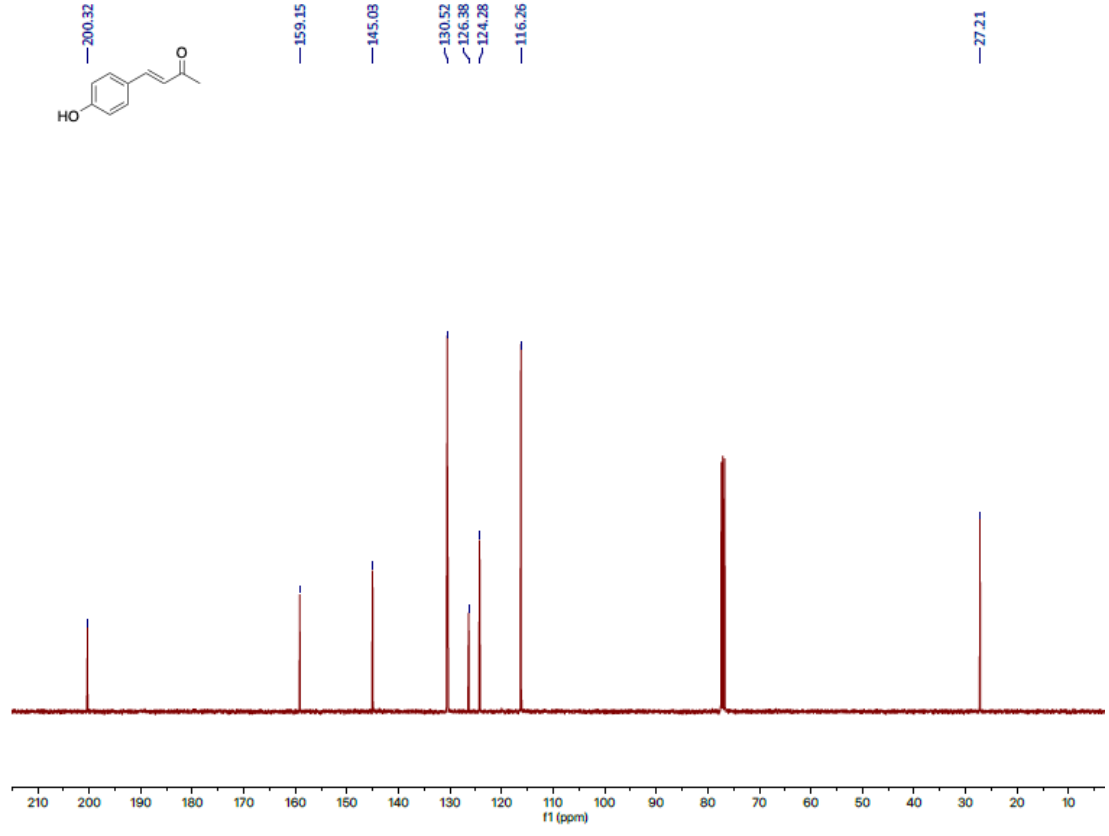

(*E*)-4-(*p*-Tolyl)-3-buten-2-one (**1d**)

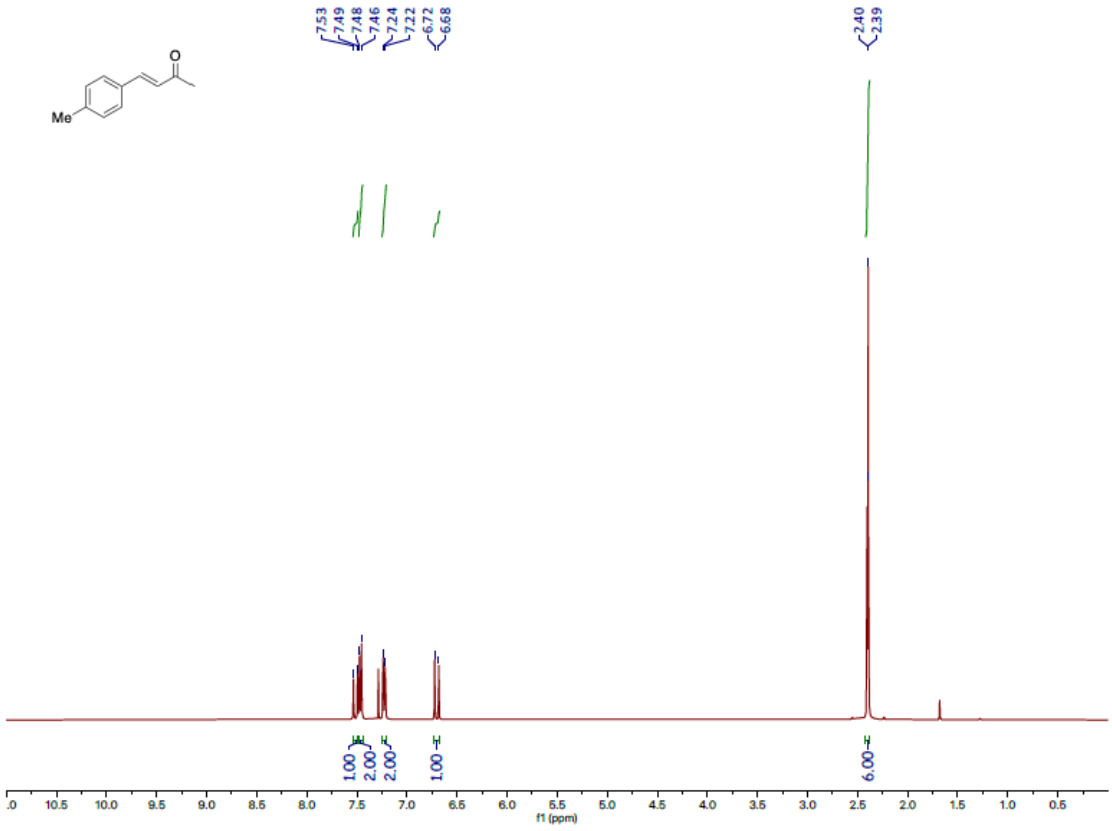

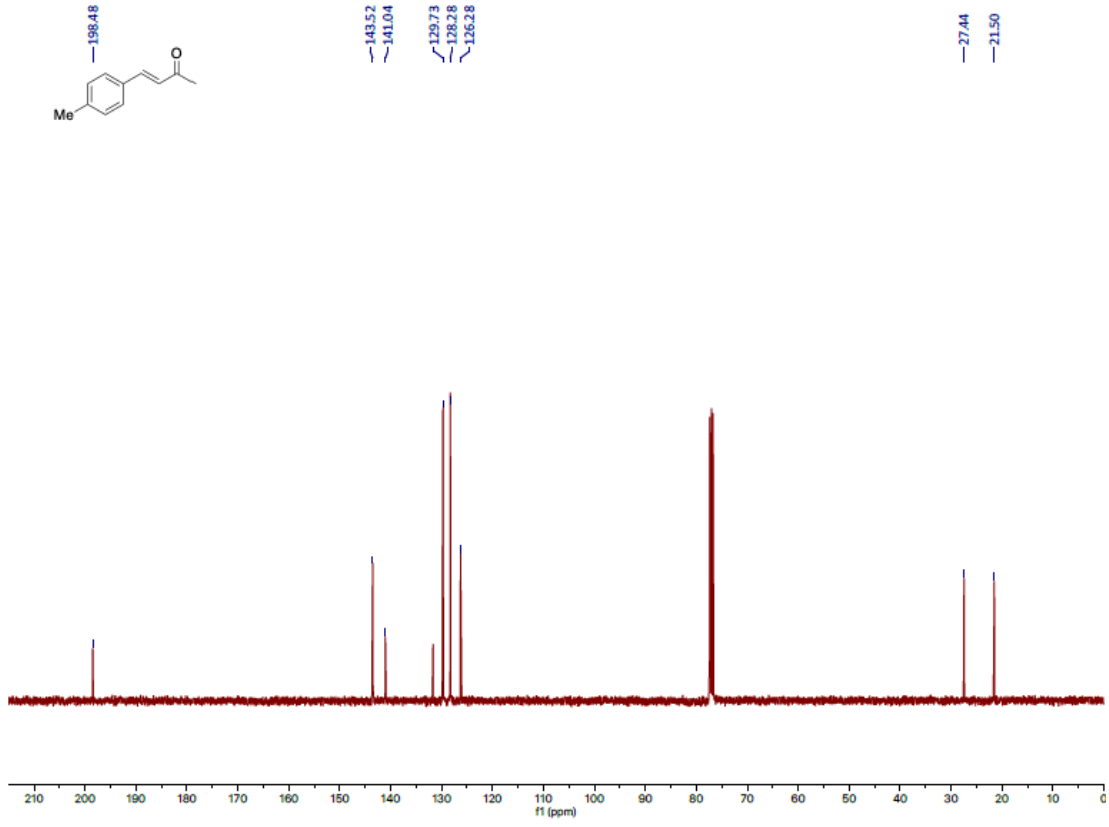

(*E*)-4-(*p*-Methoxyphenyl)-3-buten-2-one (**1e**)

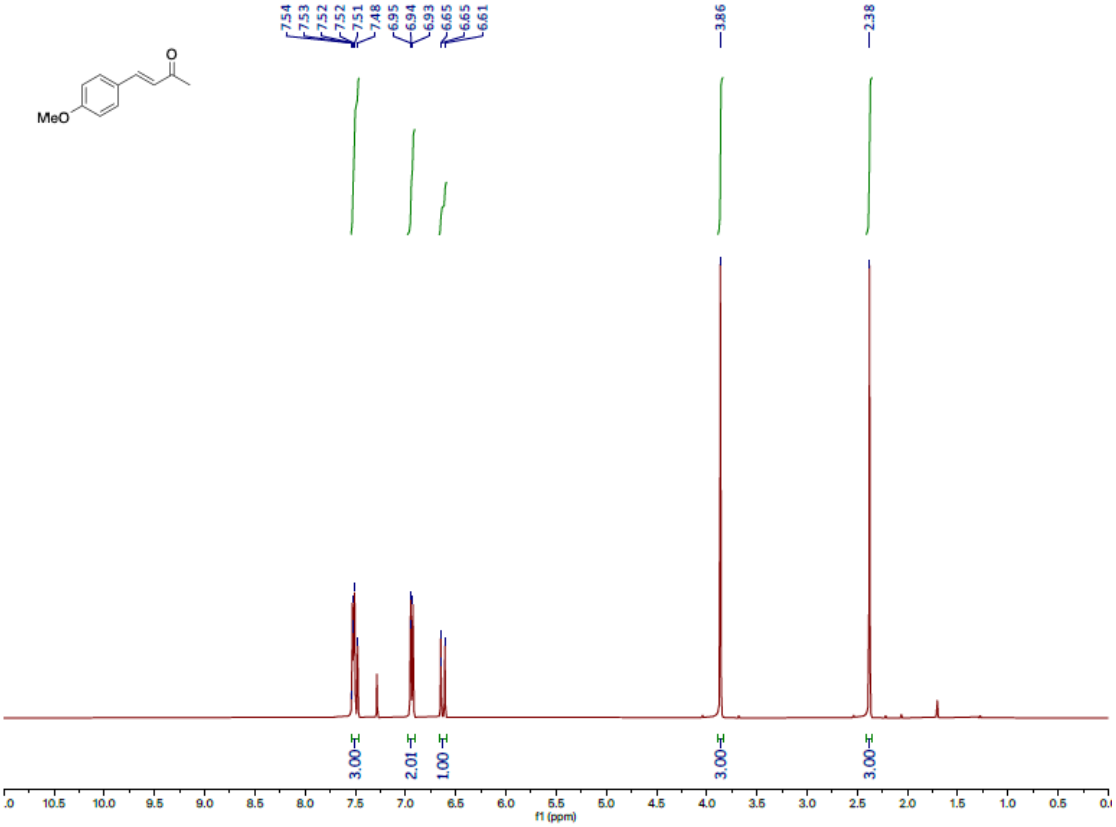

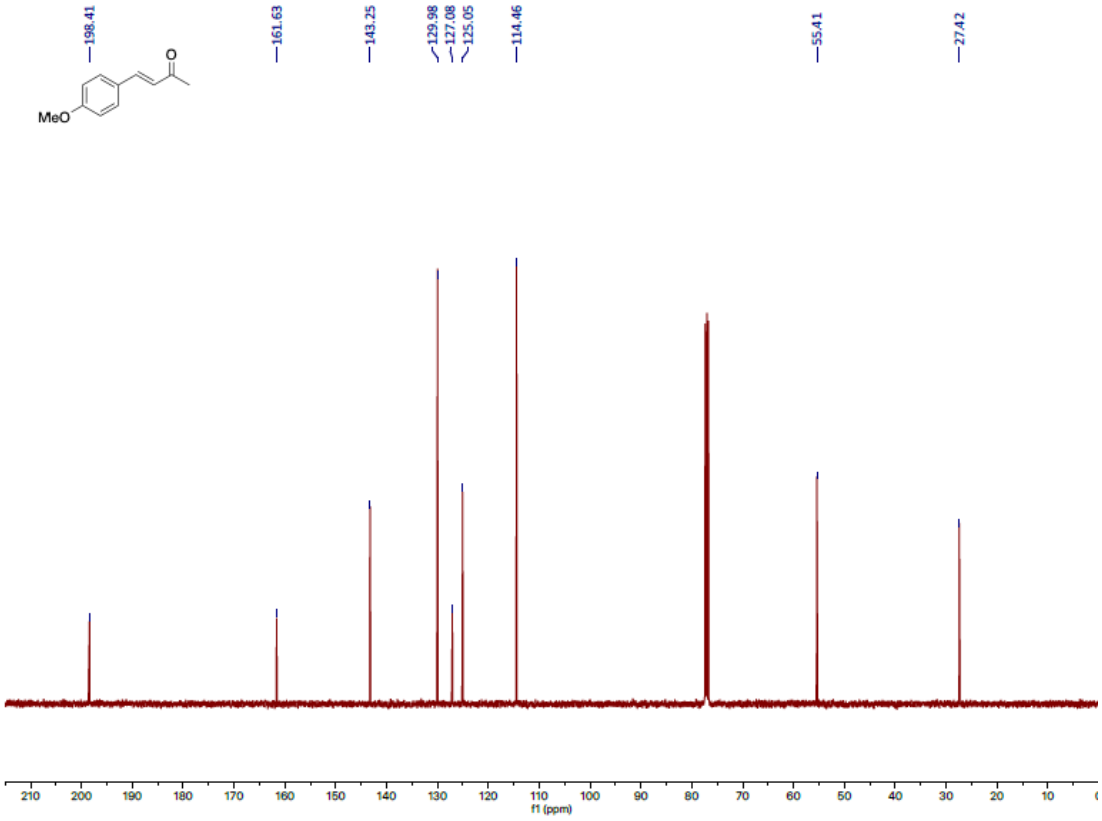

(*E*)-4-(4-(Dimethylamino)phenyl)-3-buten-2-one (**1f**)

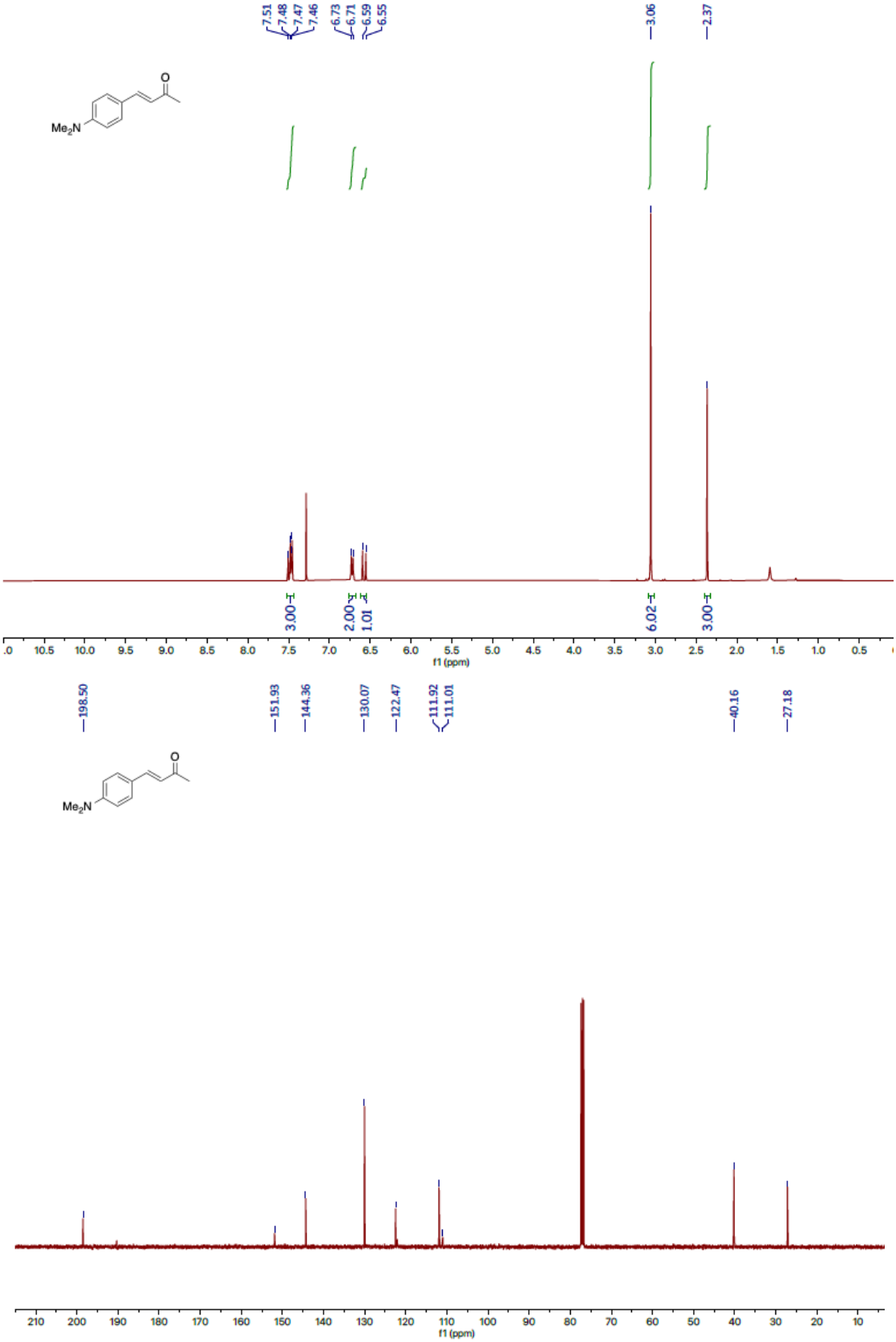

(*E*)-4-(*p*-Bromophenyl)-3-buten-2-one (**1g**)

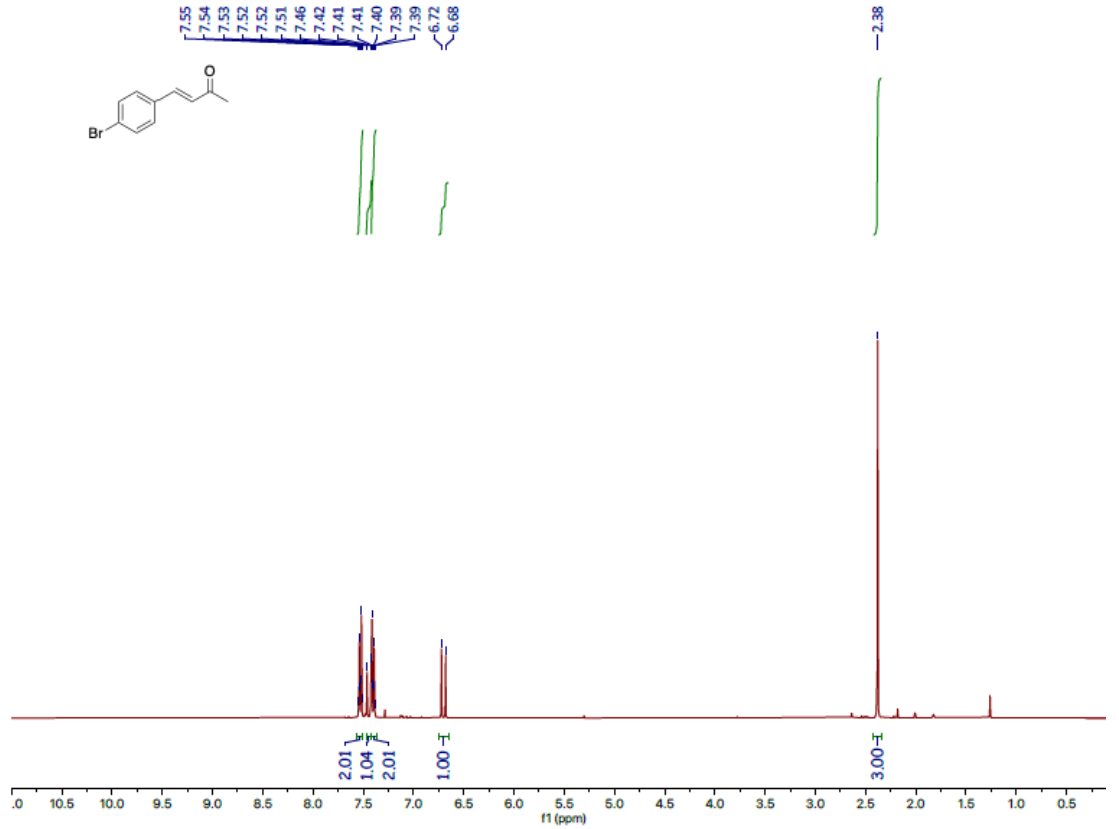

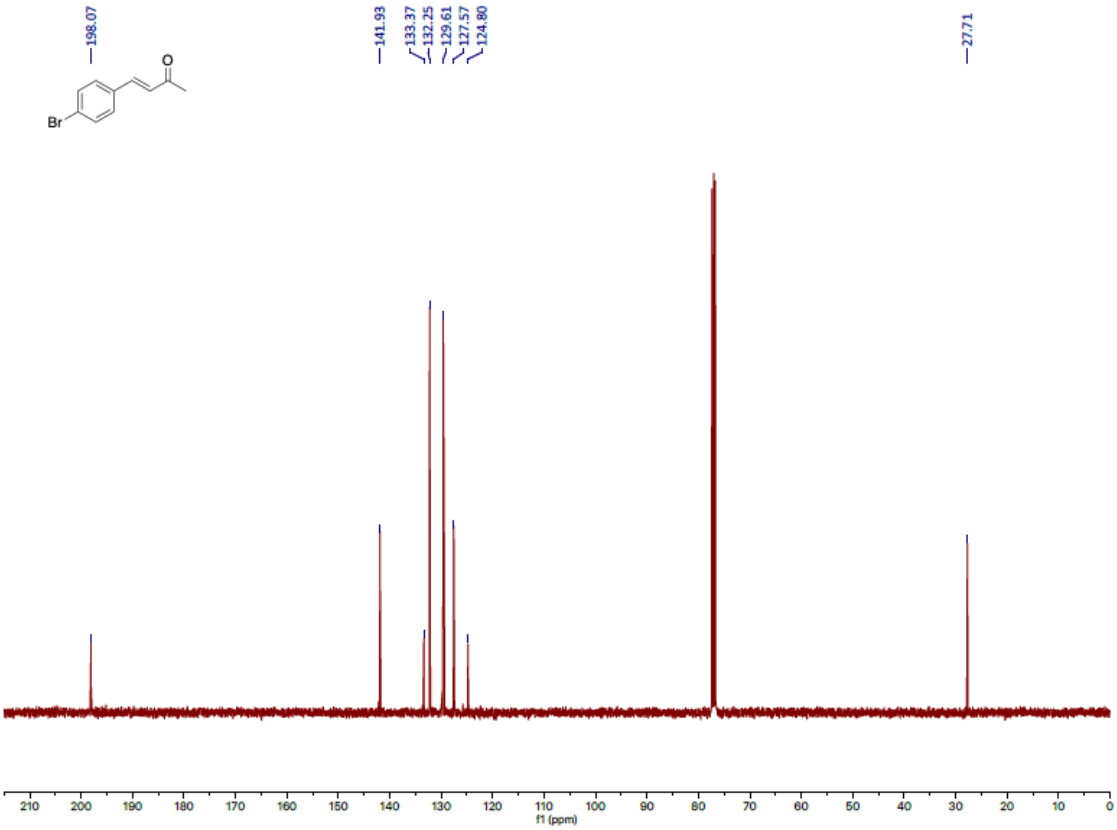

(*E*)-4-(*m*-Tolyl)-3-buten-2-one (**1h**)

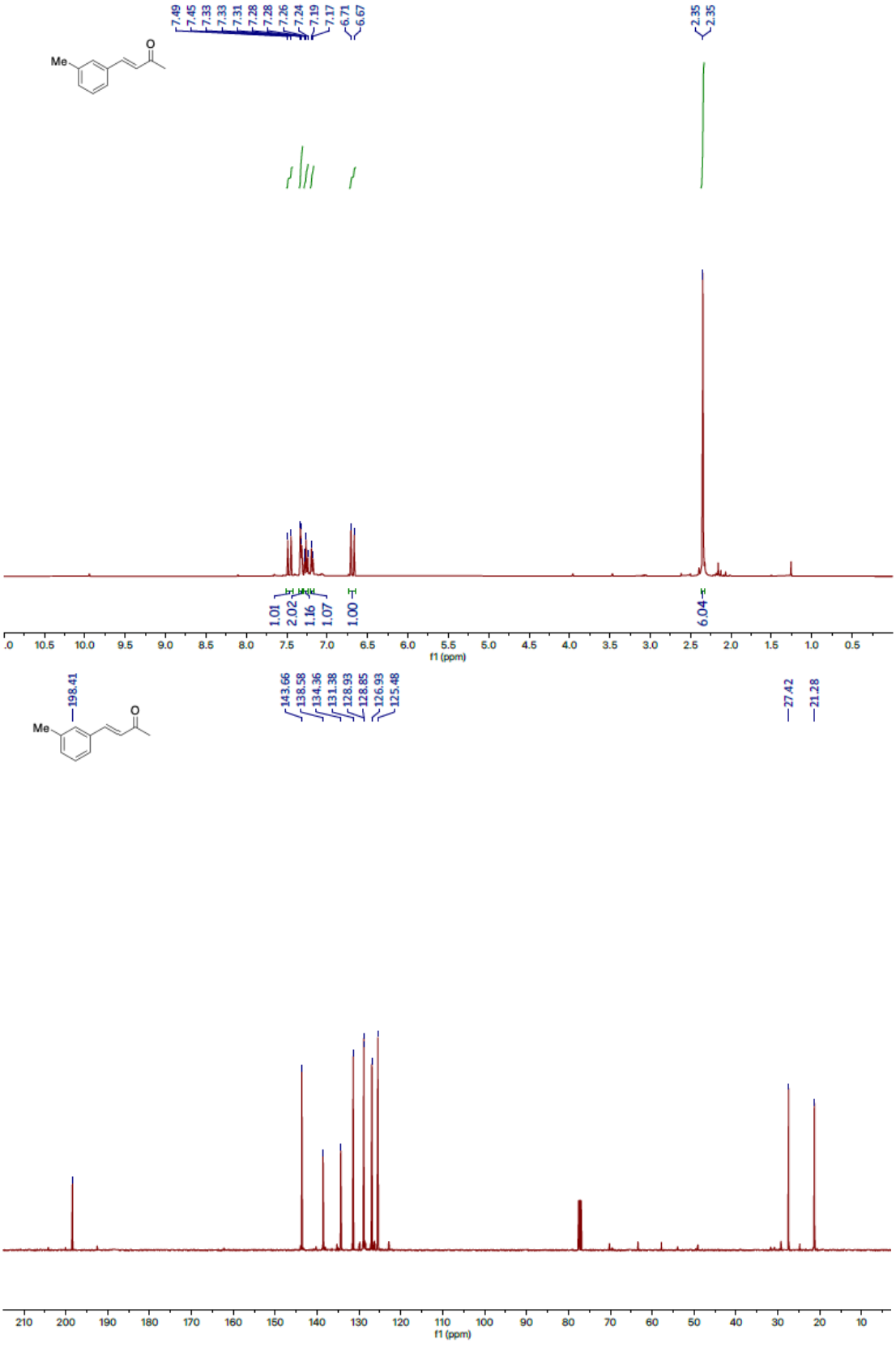

(*E*)-4-(3-Methoxyphenyl)-3-buten-2-one (**1i**)

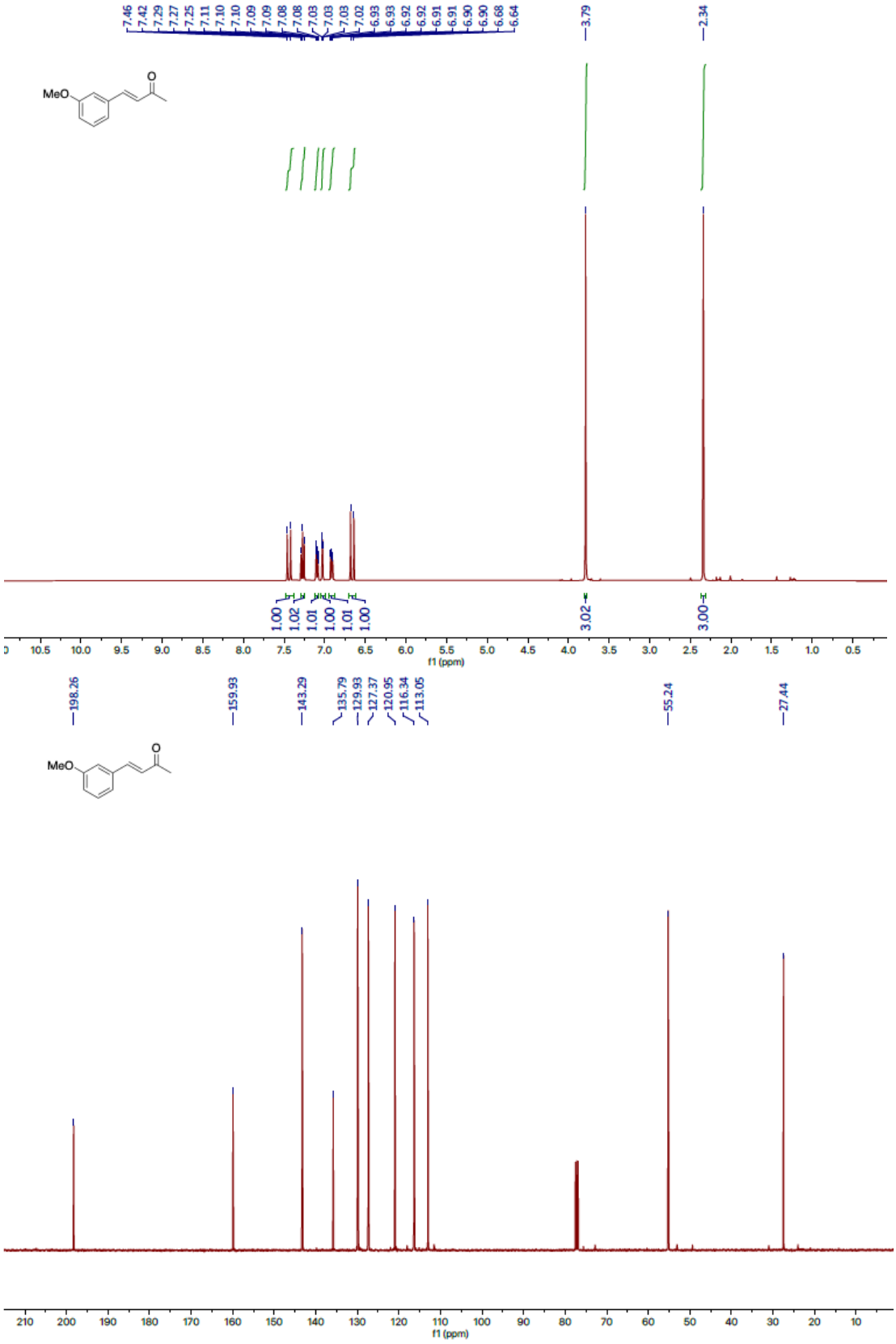

(*E*)-4-(3-Hydroxyphenyl)-3-buten-2-one (**1j**)

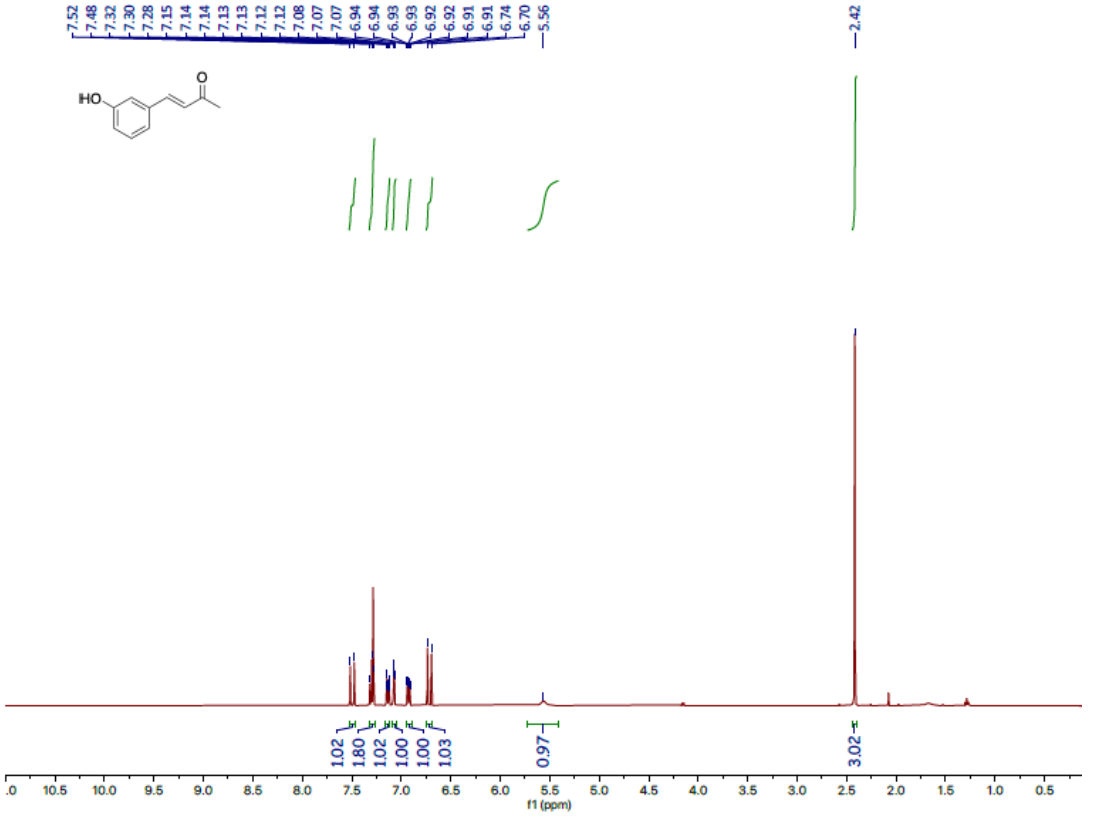

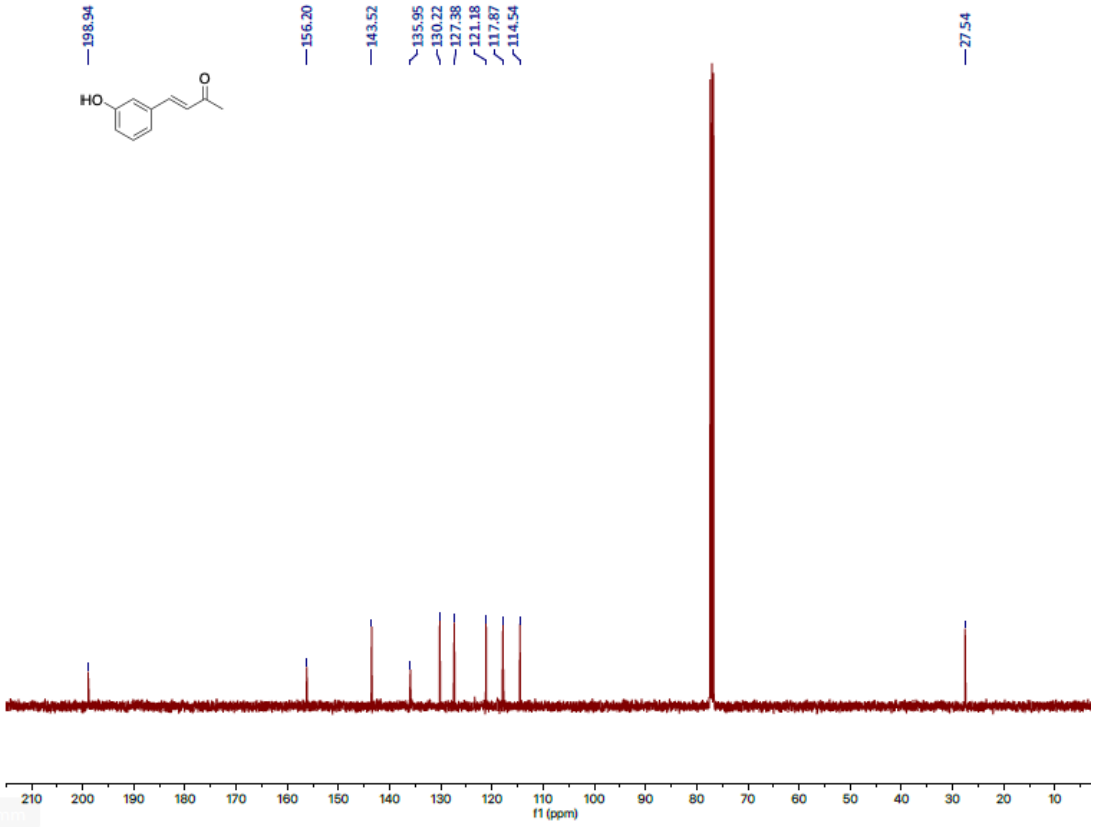

(*E*)-4-(*m*-Bromophenyl)-3-buten-2-one (**1k**)

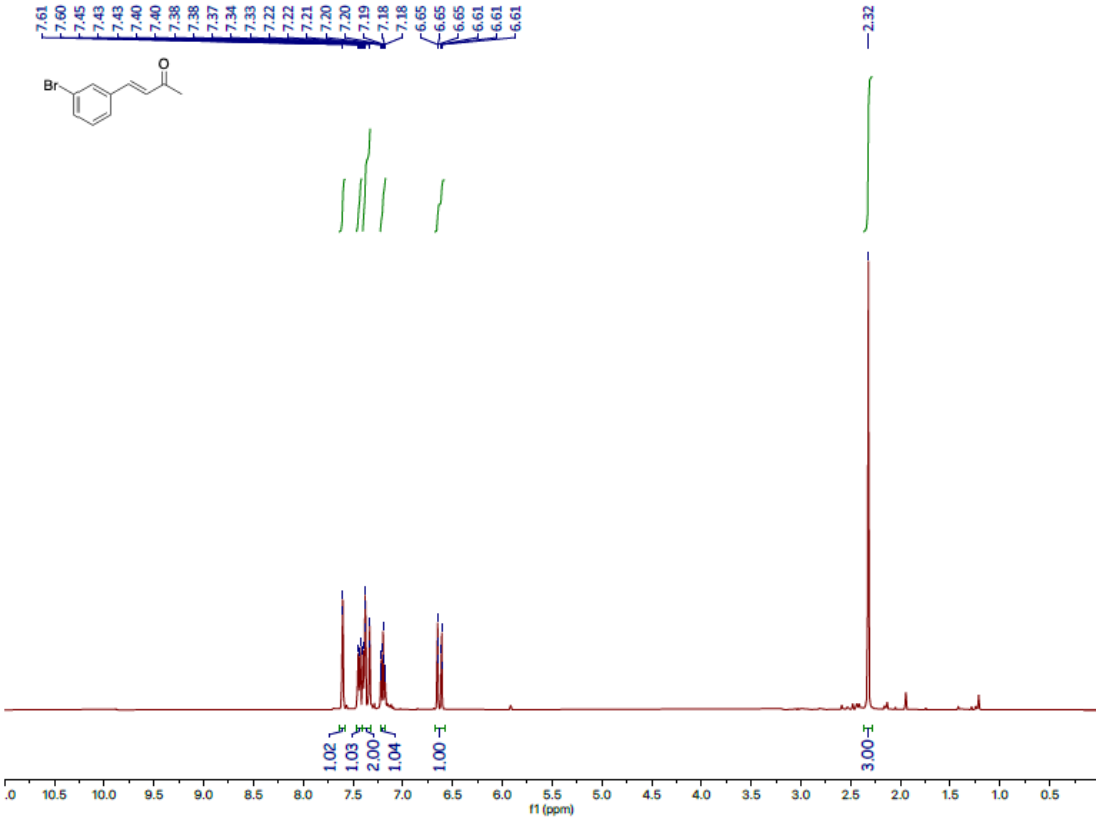

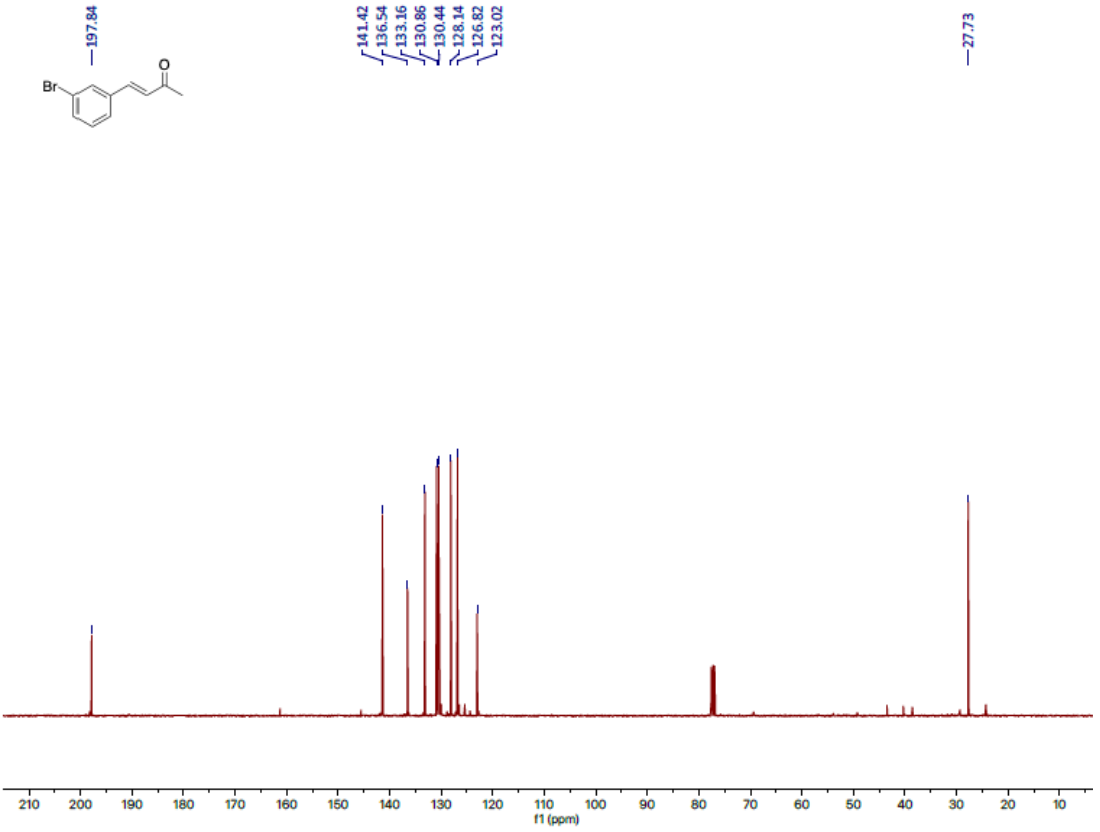

(*E*)-4-(*o*-Hydroxyphenyl)but-3-en-2-one (**1l**)

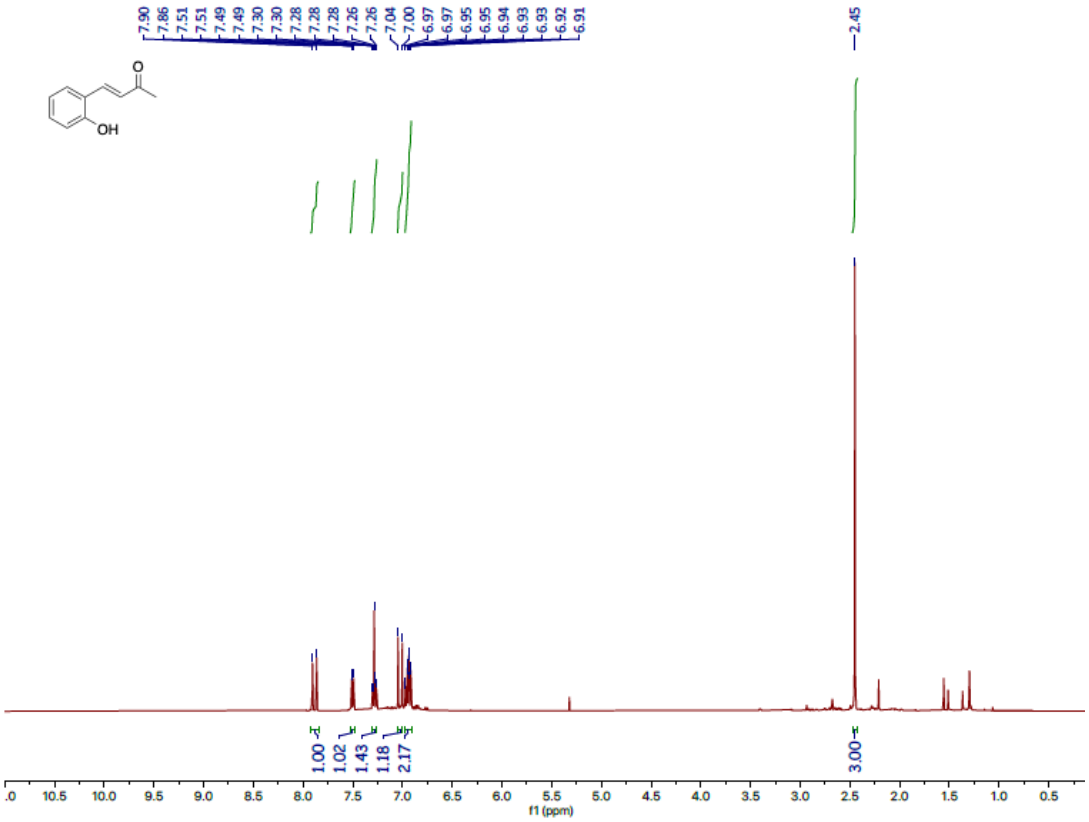

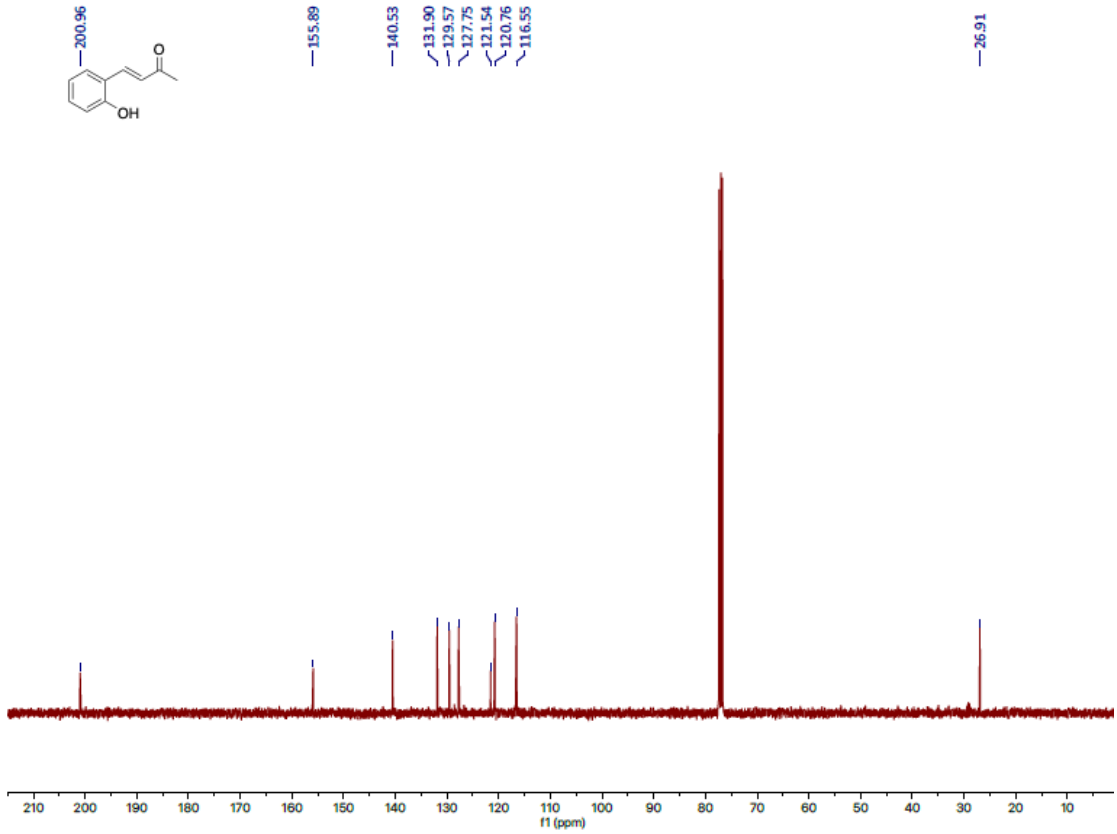

(*E*)-4-(*o*-(trifluoromethyl)phenyl)-3-buten-2-one (**1m**)

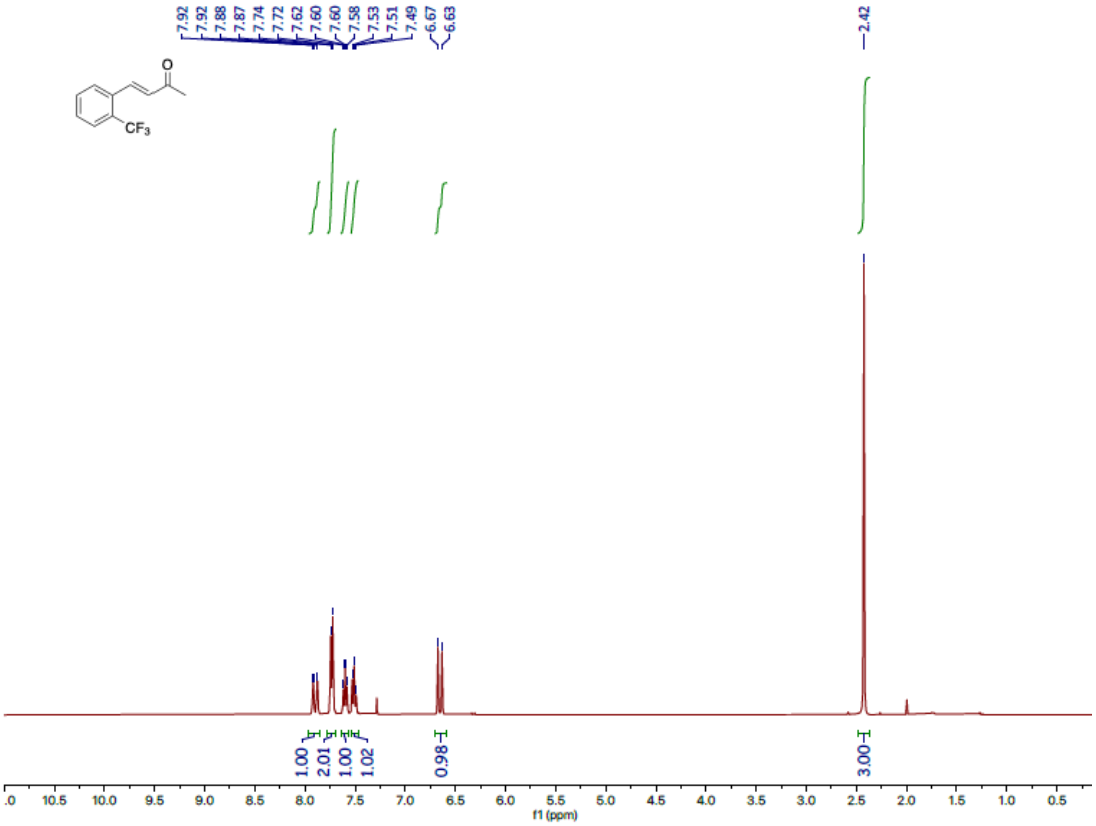

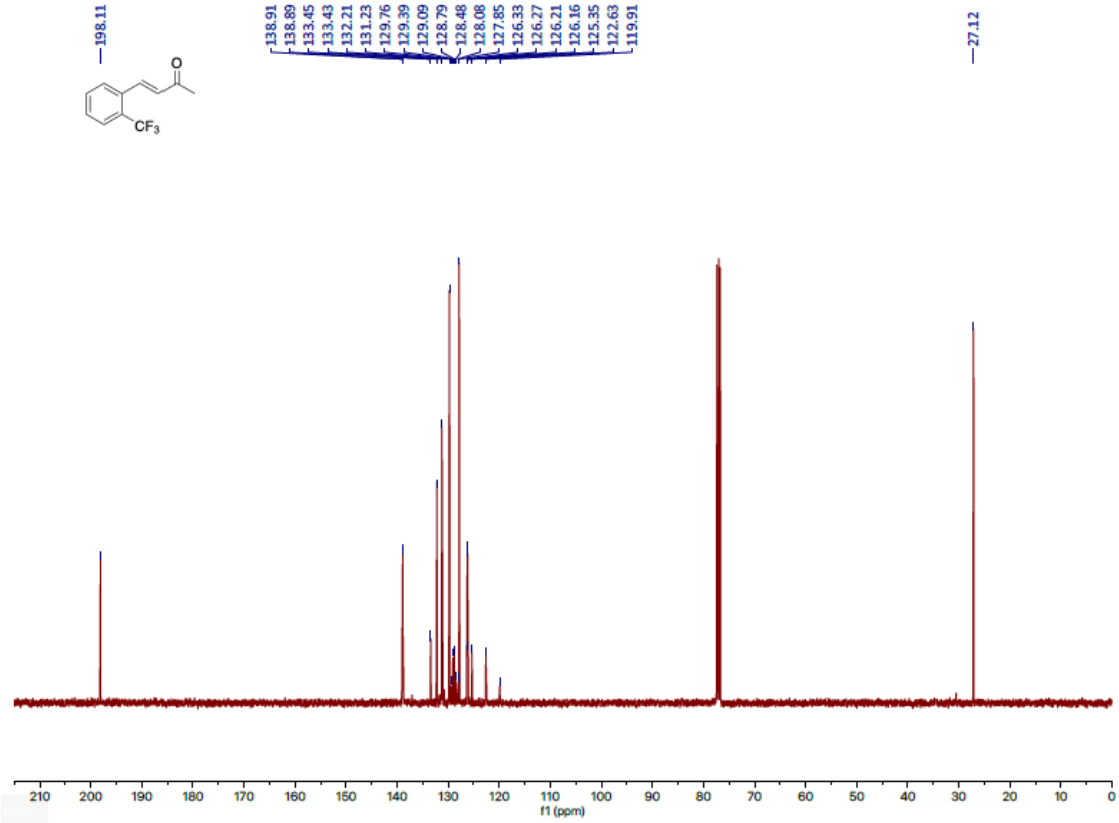

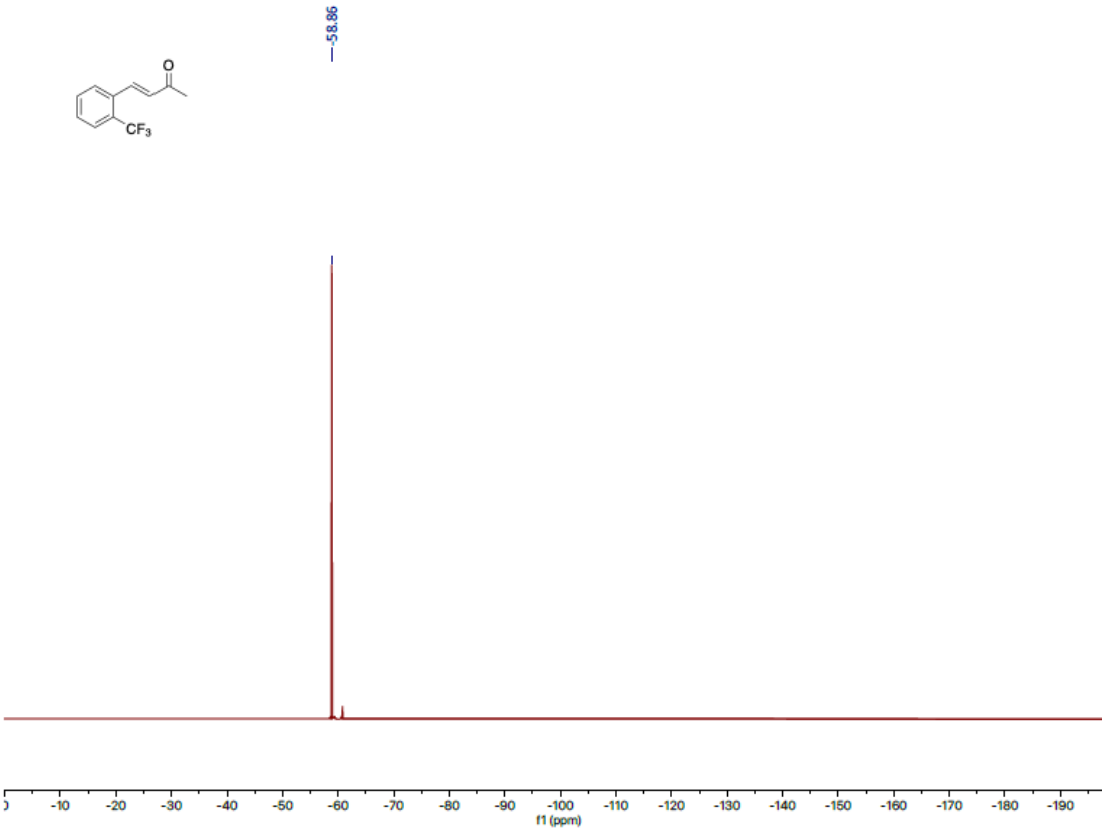
-58.86
O
CF3
0
-10
-20
-30
-40
-50
-60
-70
-80
-90
-100
-110
-120
-130
-140
-150
-160
-170
-180
-190
f1 (ppm)

(*E*)-4,4-Dimethyl-1-phenyl-3-penten-3-one (**1n**)

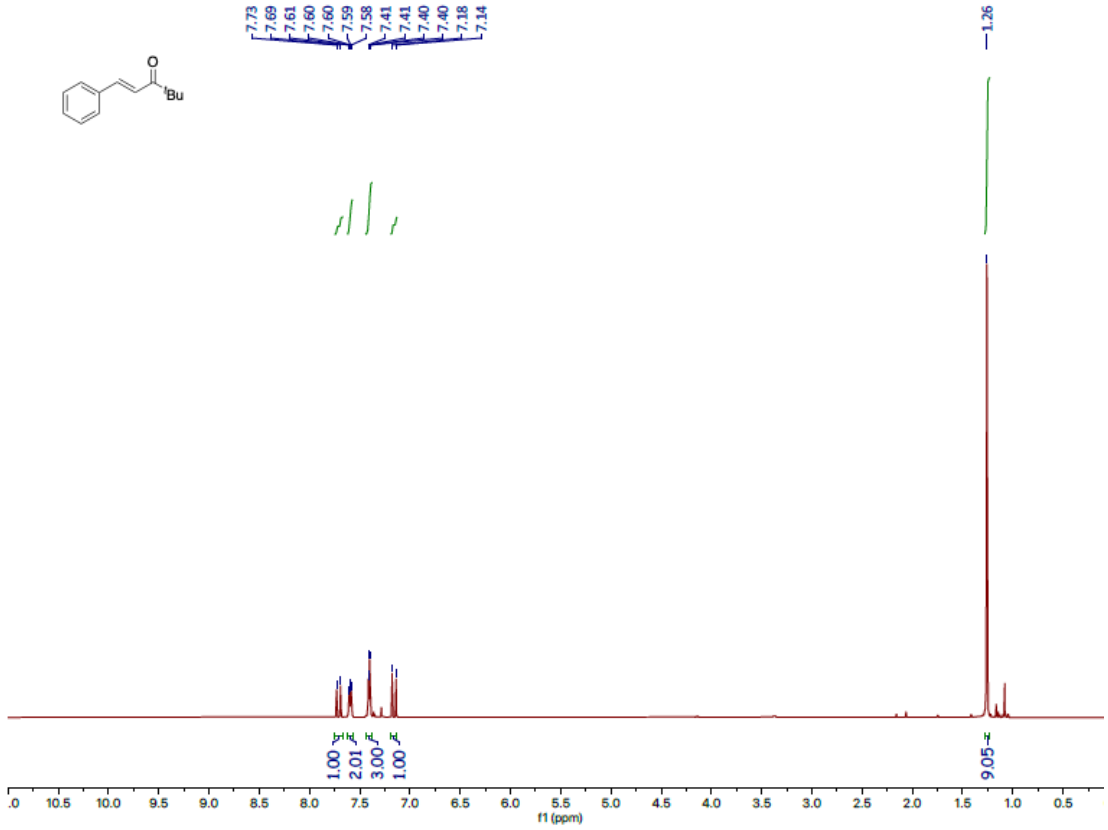

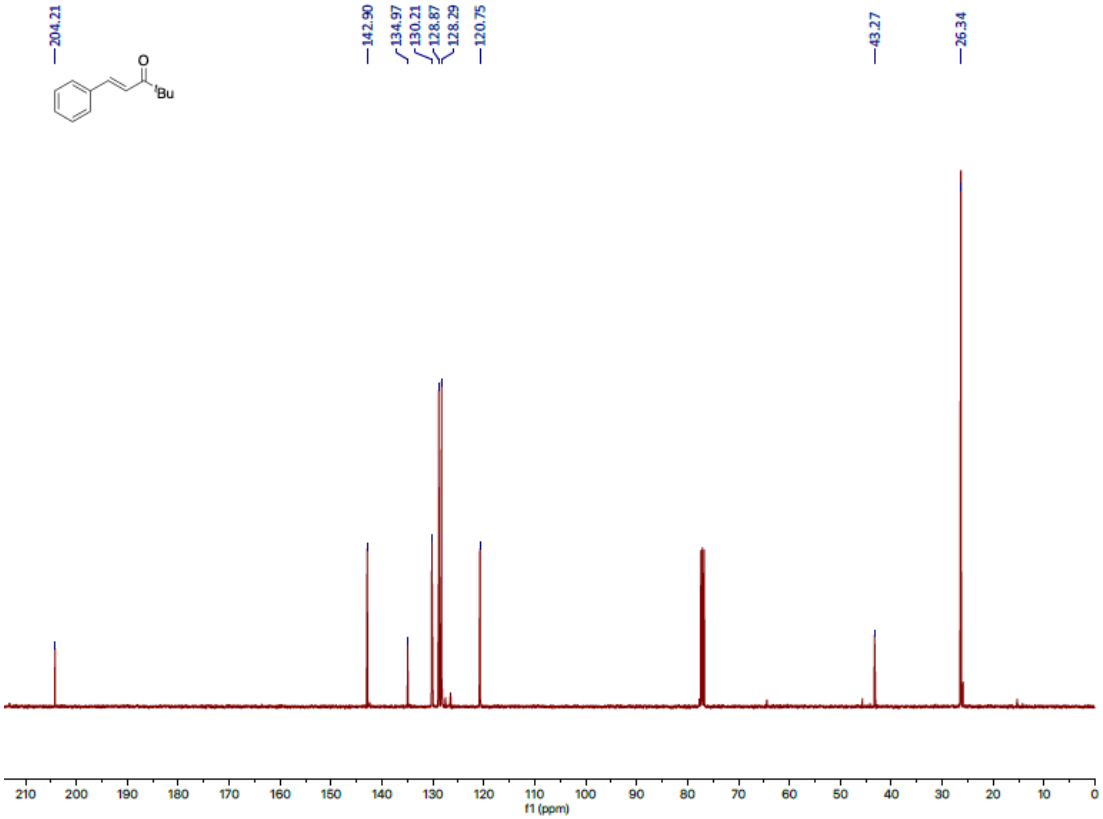

(*E*)-4-(3-nitrophenyl)-3-buten-2-one (**1o**)

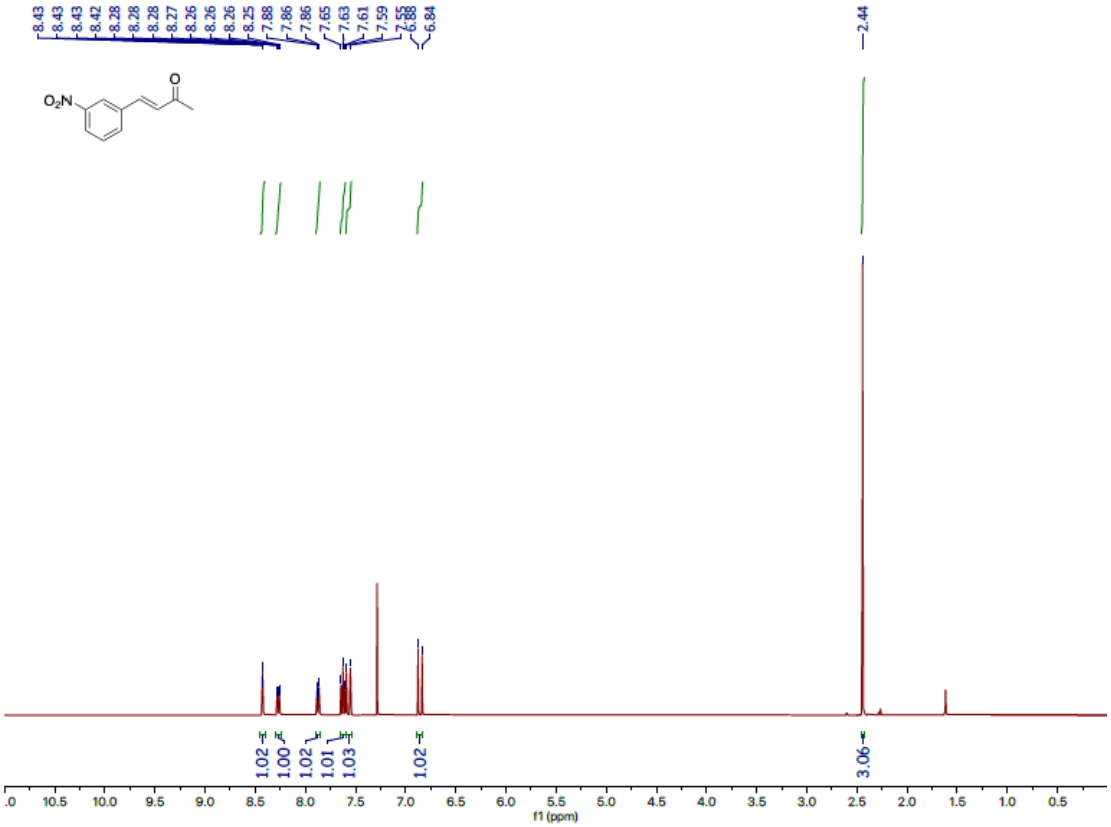

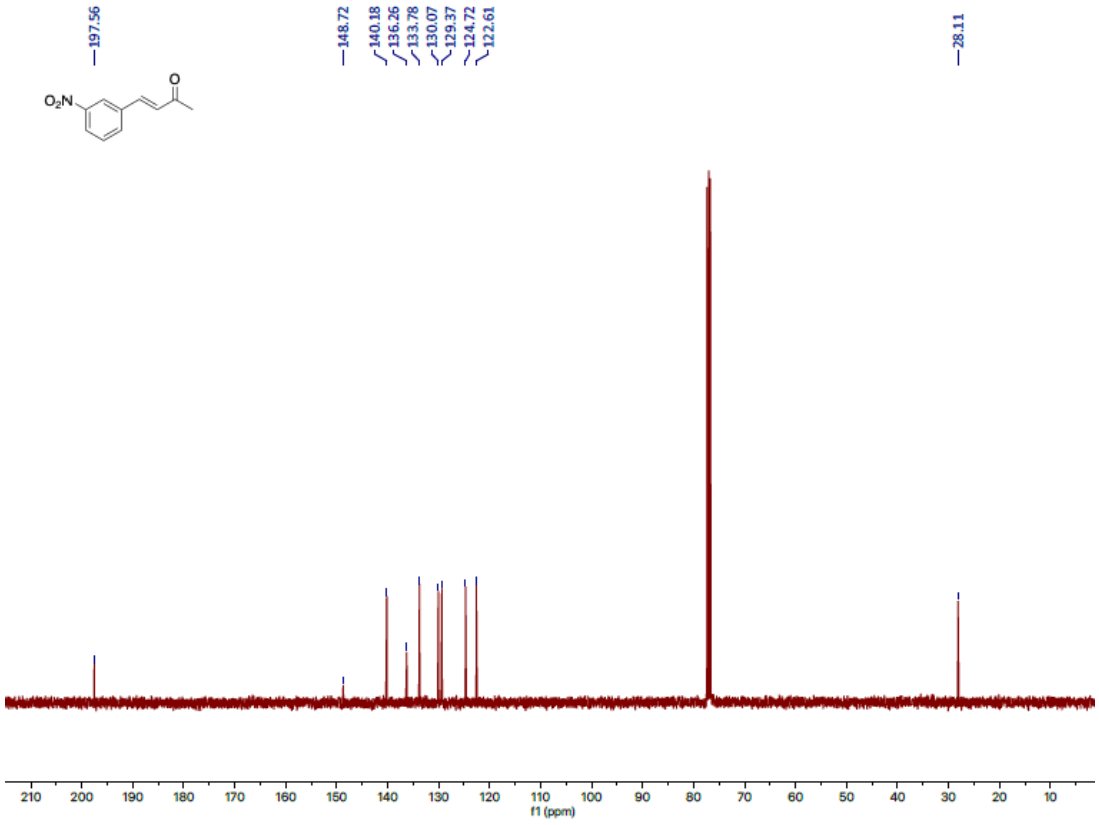

Ethyl (*E*)-3-(pyridin-4-yl)acrylate (**1p**)

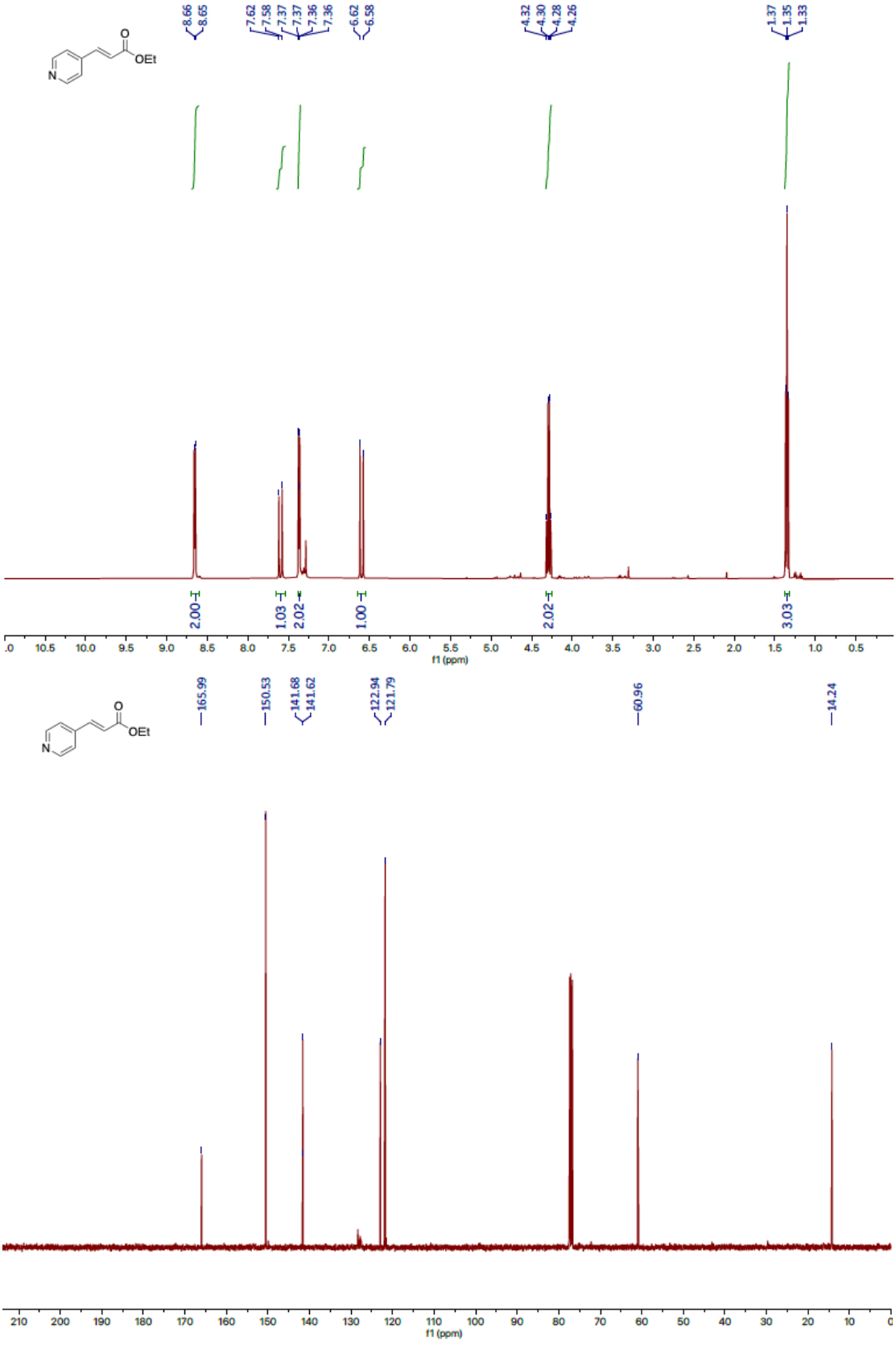

Ethyl (*E*)-3-(pyridin-3-yl)acrylate (**1q**)

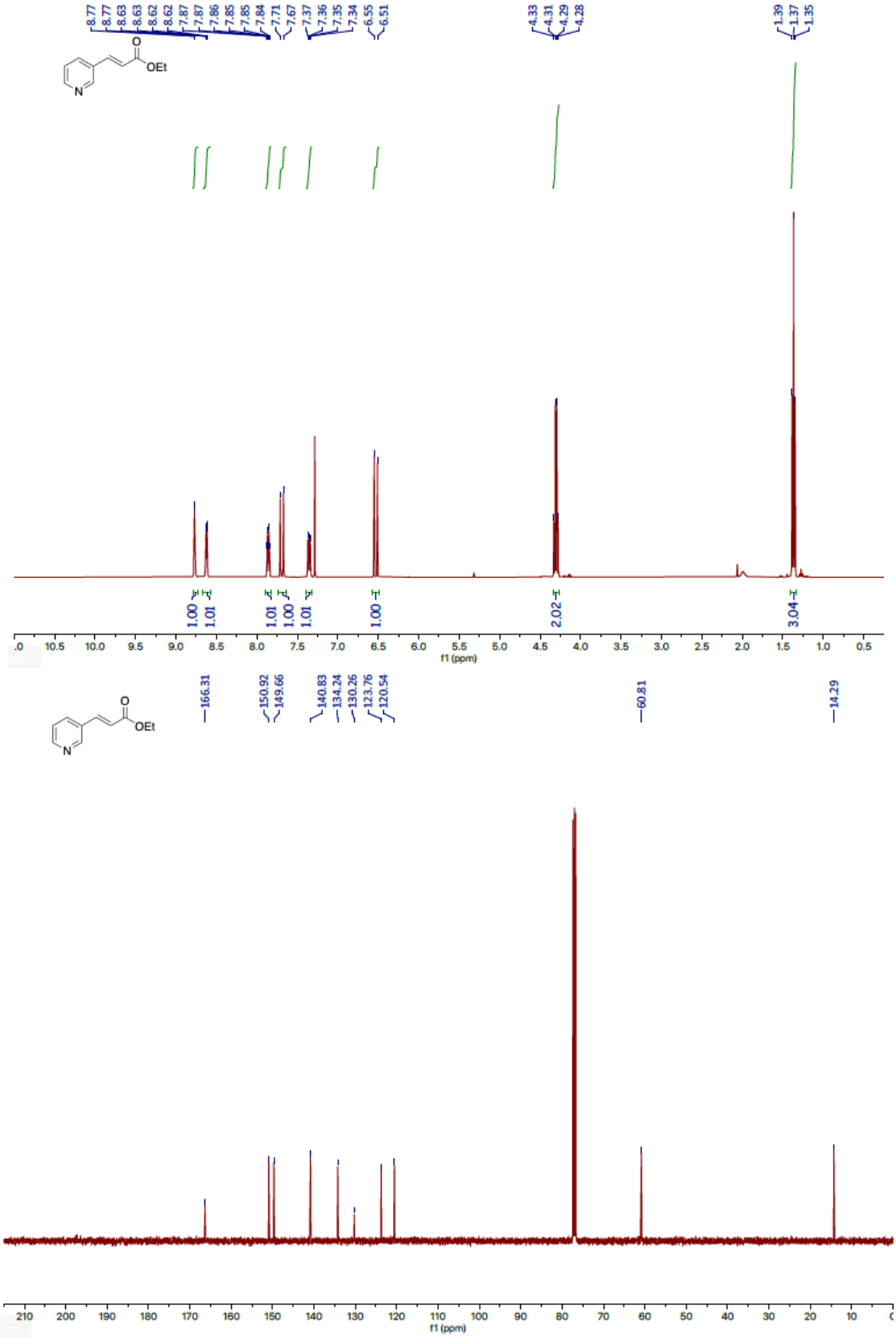

Diethyl mesaconate (**1u**)

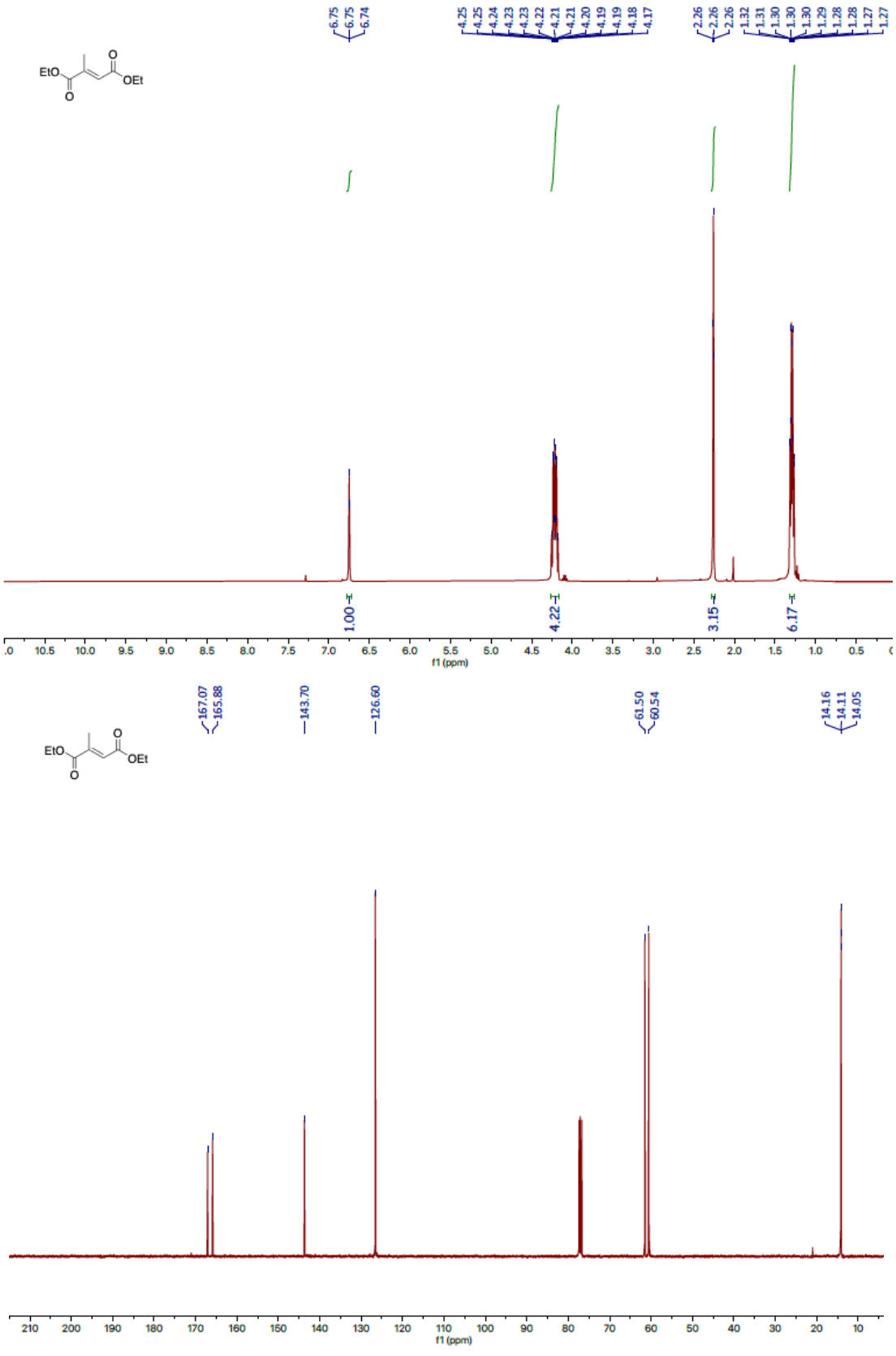

5-Phenyl-1-penten-3-ol (**1w**)

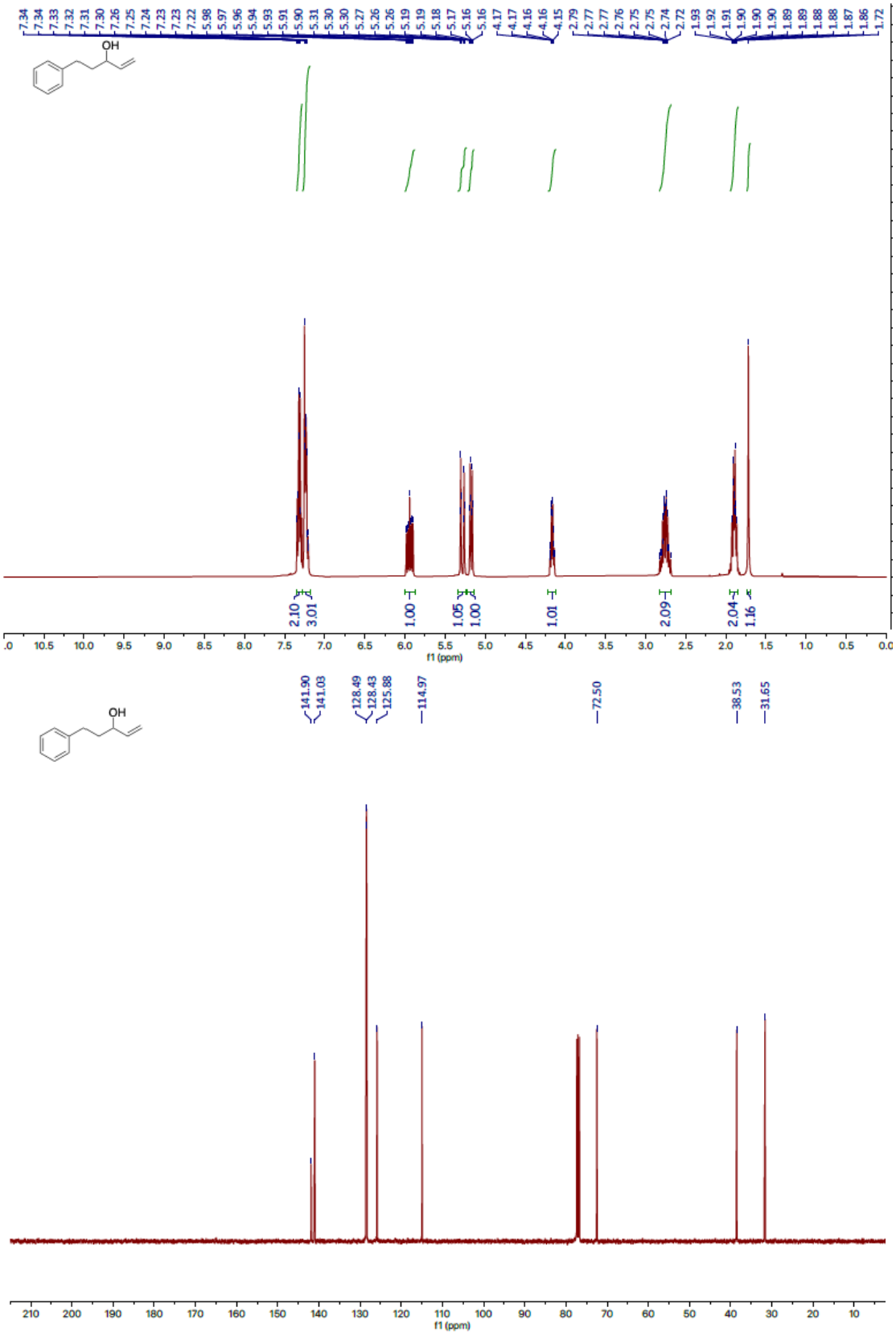

4-Allyl-1-(benzyloxy)-2-methoxybenzene (**1aa**)

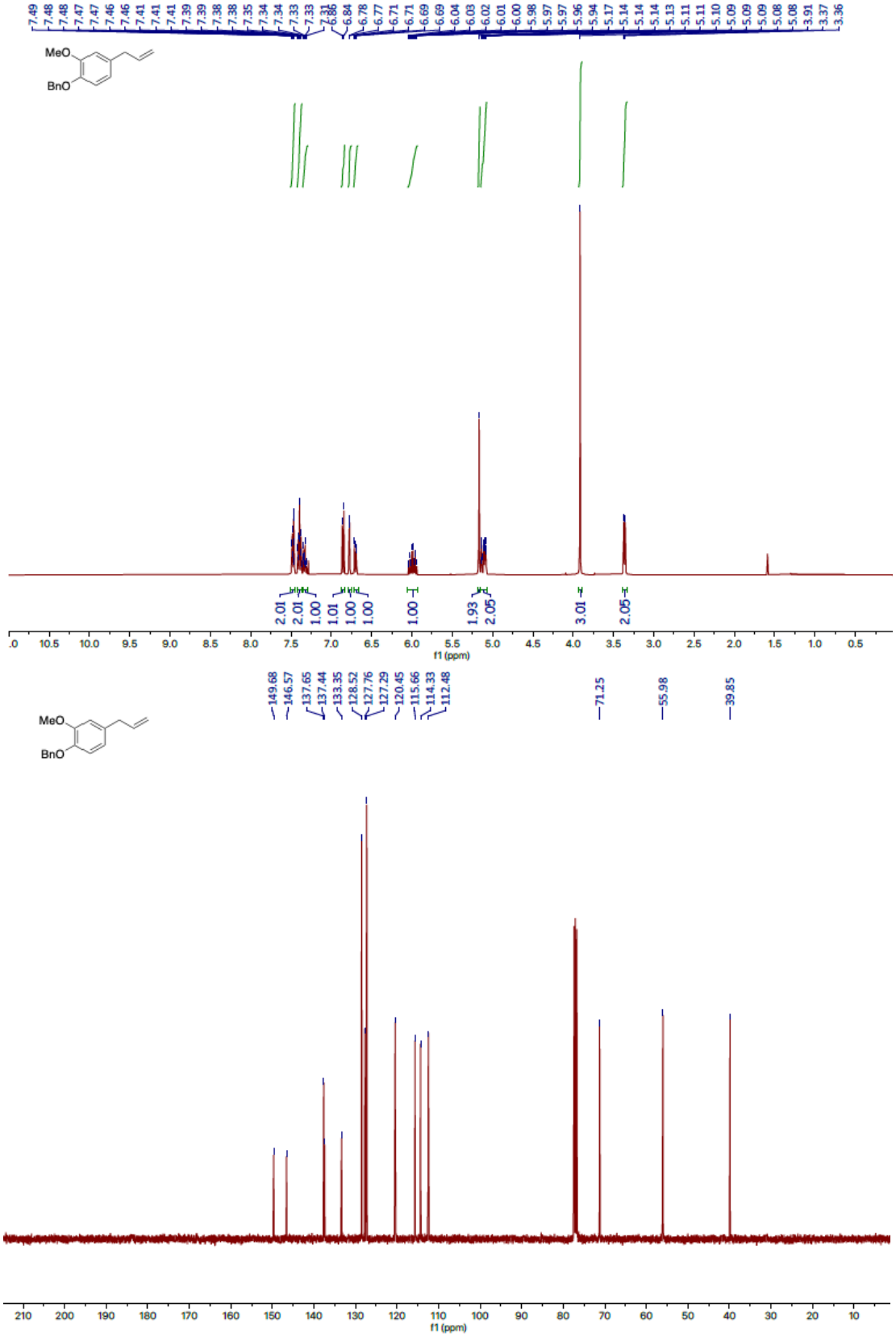

(4-allyl-2-methoxyphenoxy)(tert-butyl)dimethylsilane (**1ab**)

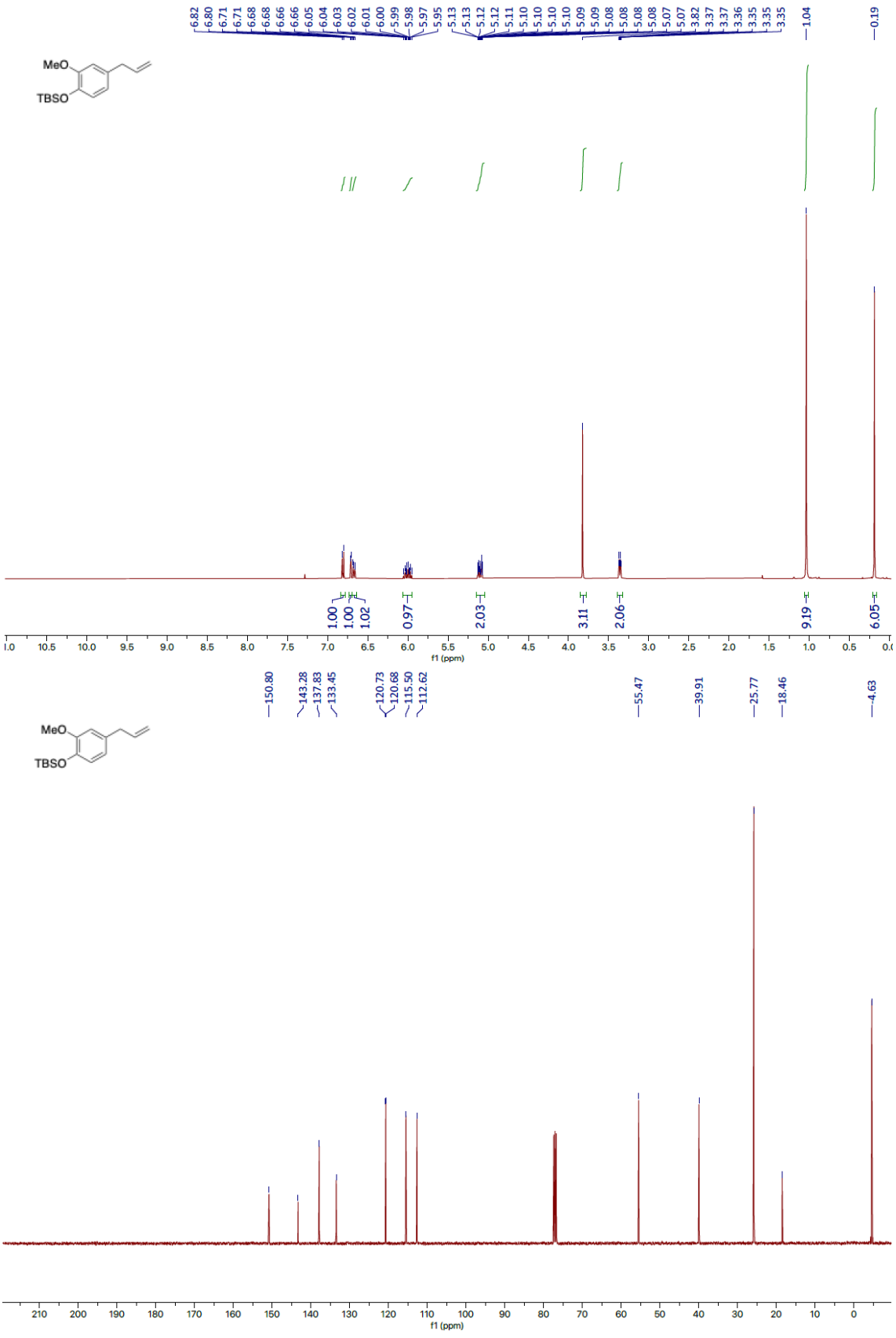

Benzyl allylcarbamate (**1ae**)

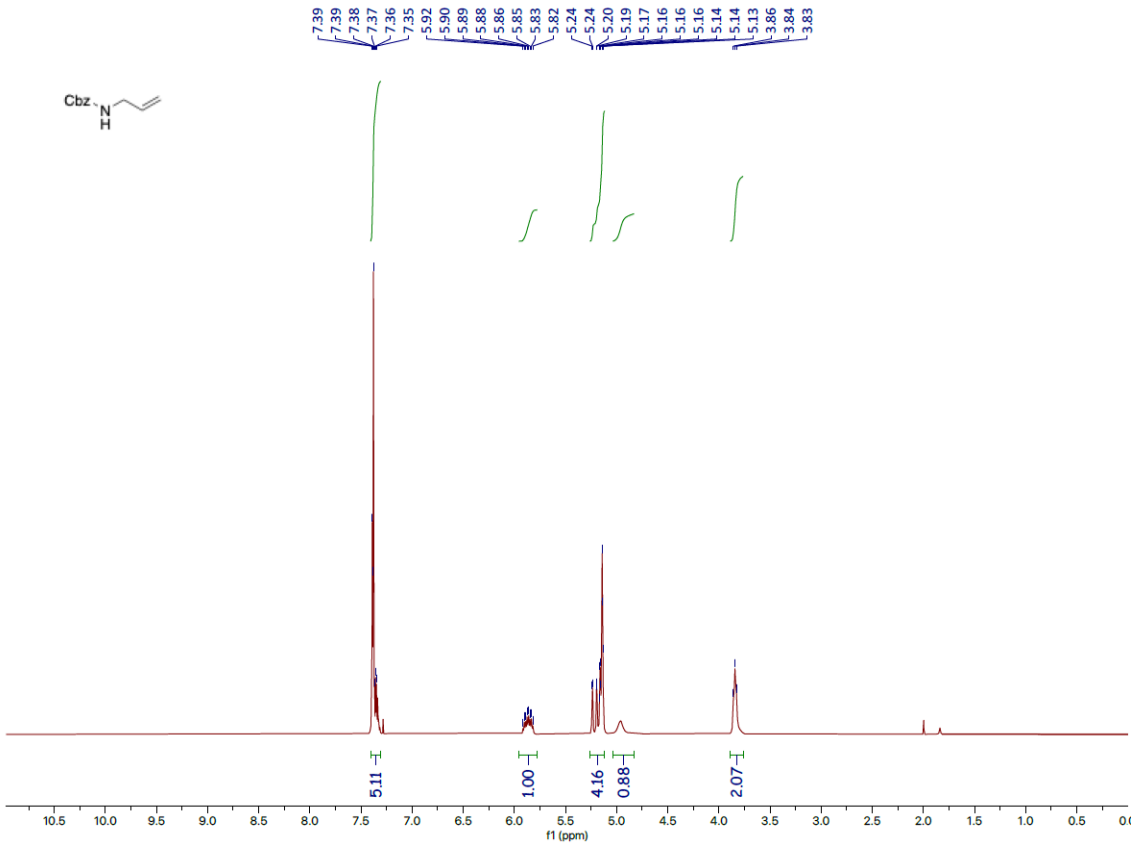

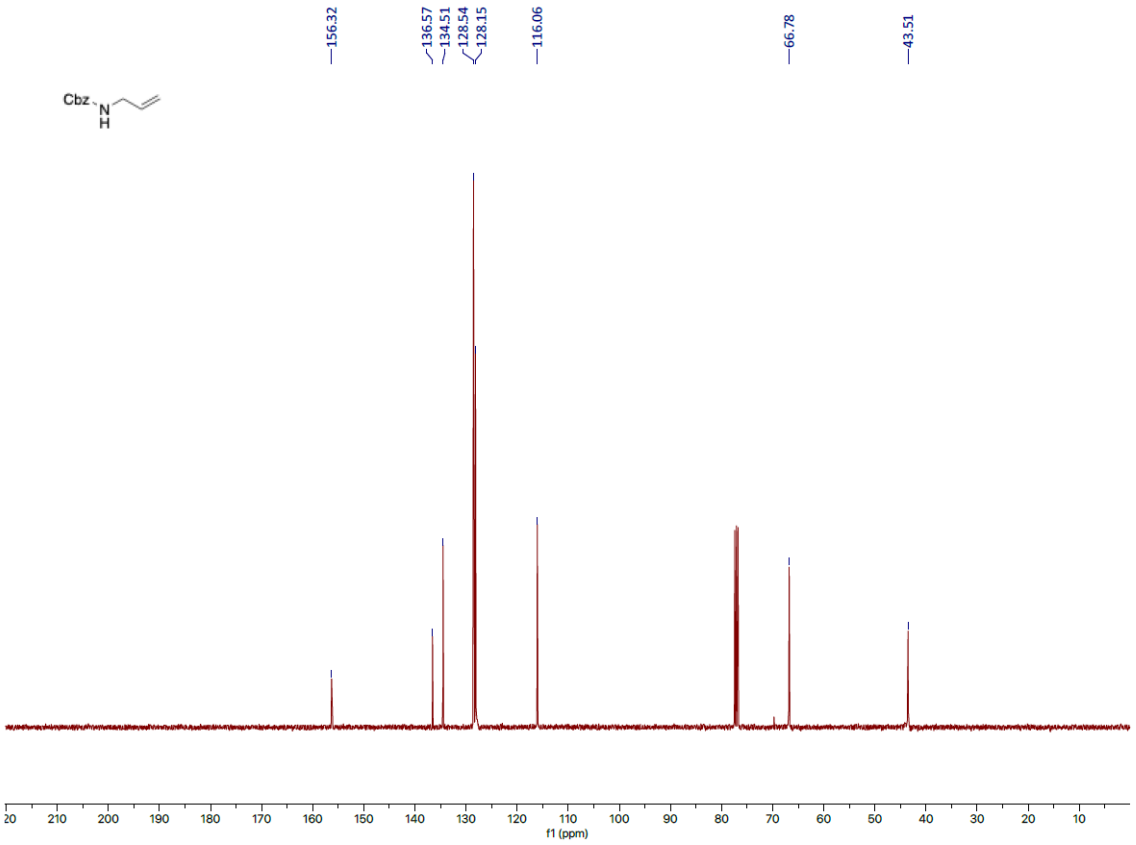

4-Methyl-*N*-propylbenzenesulfonamide (**1af**)

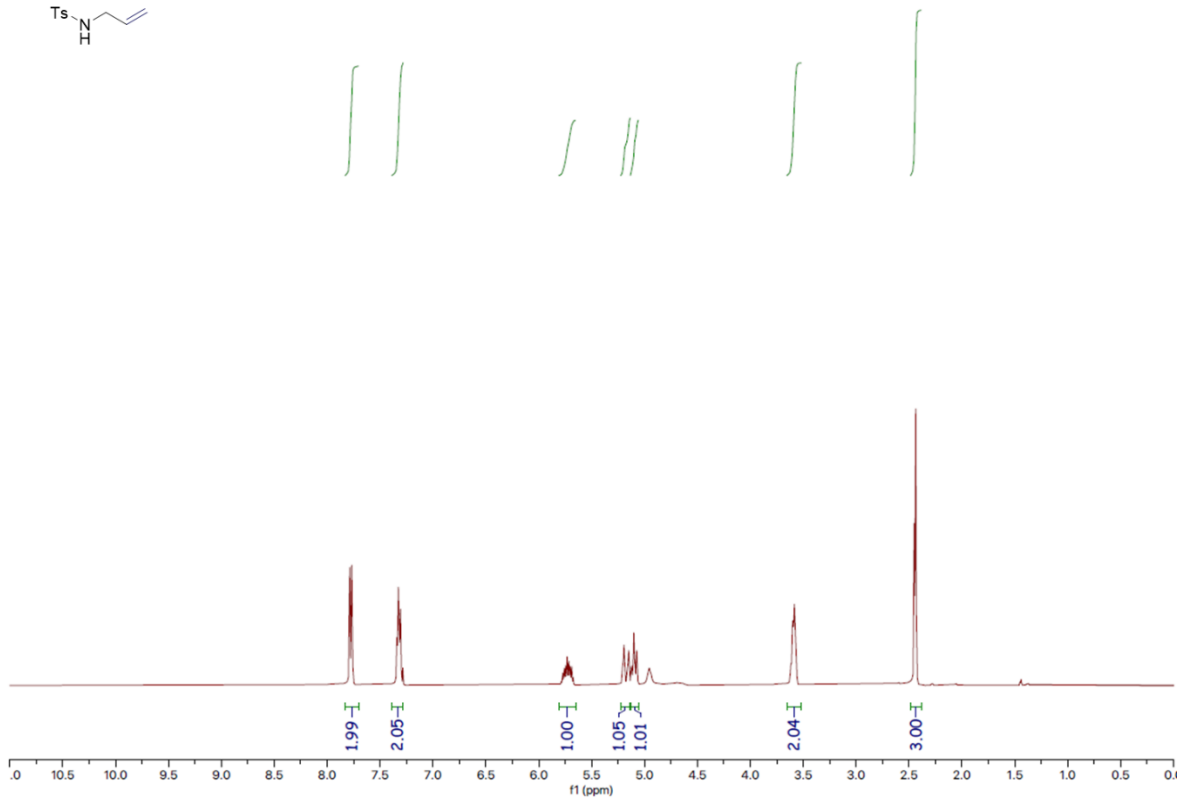

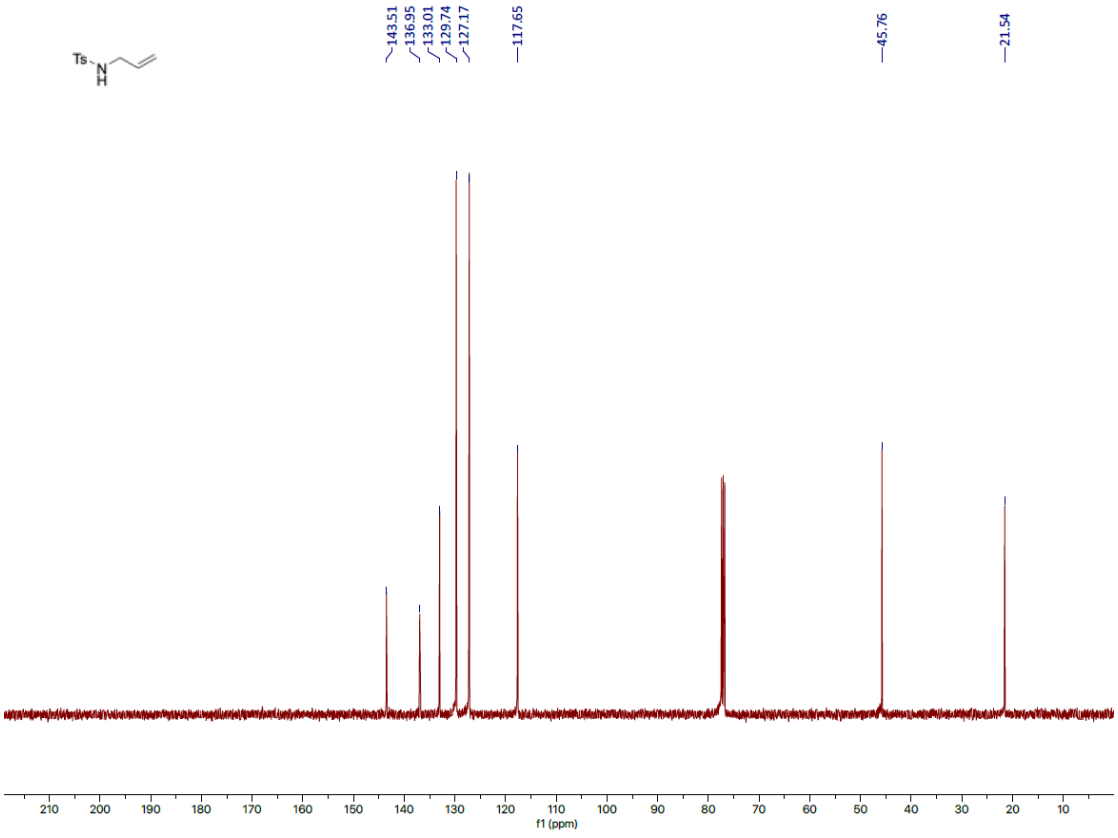

(9H-Fluoren-9-yl)methyl allylcarbamate (**1ag**)

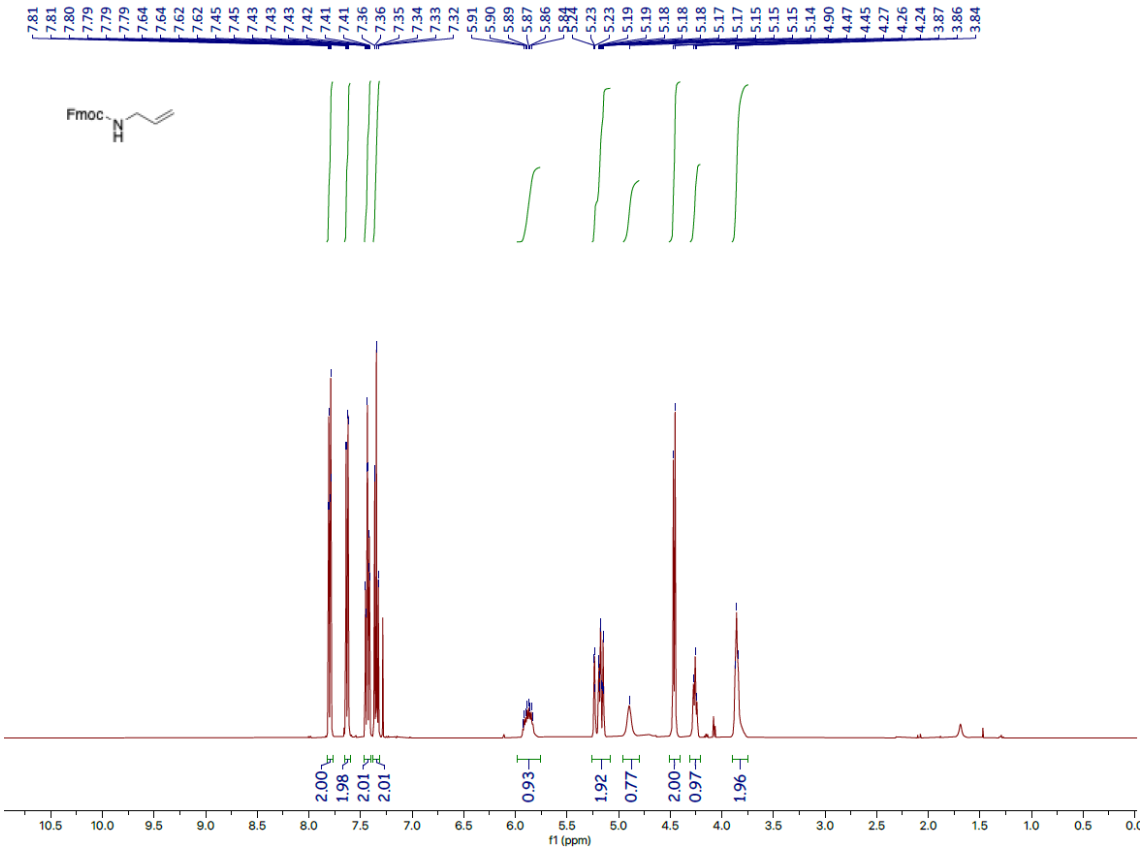

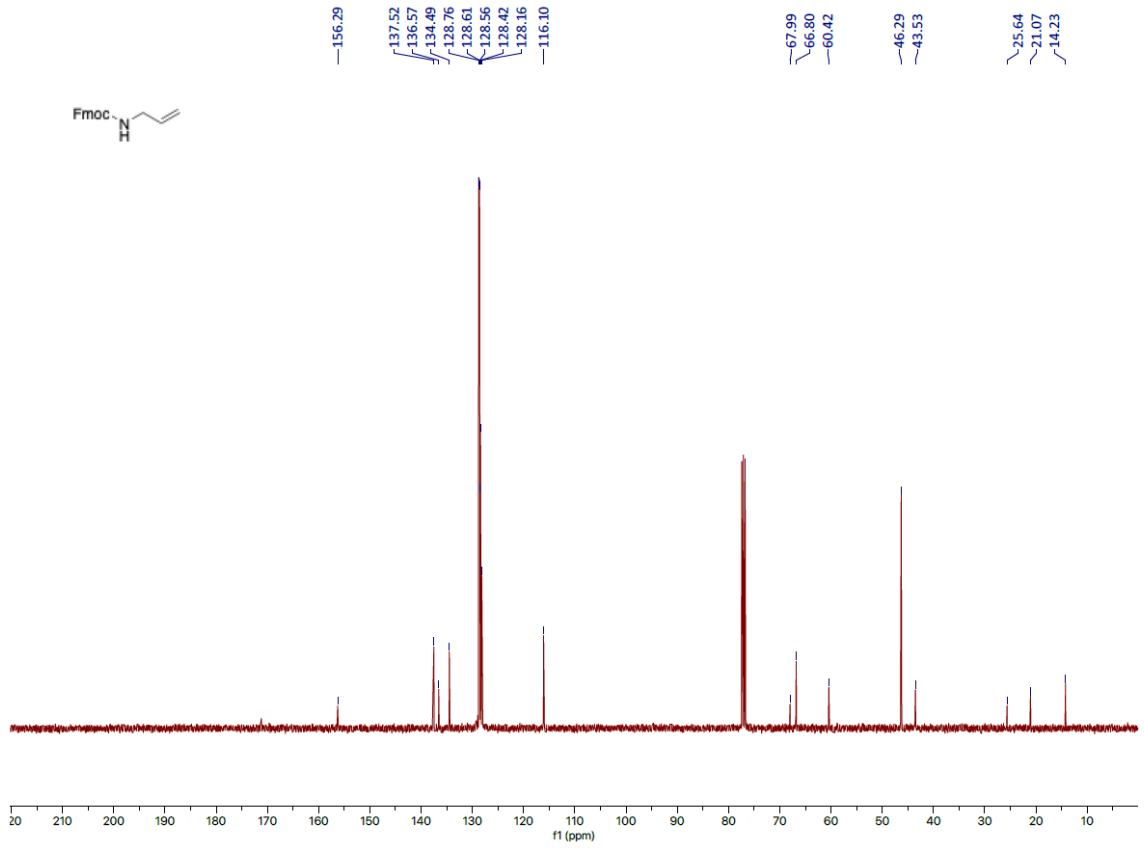

tert-Butyl allylcarbamate (**1ah**)

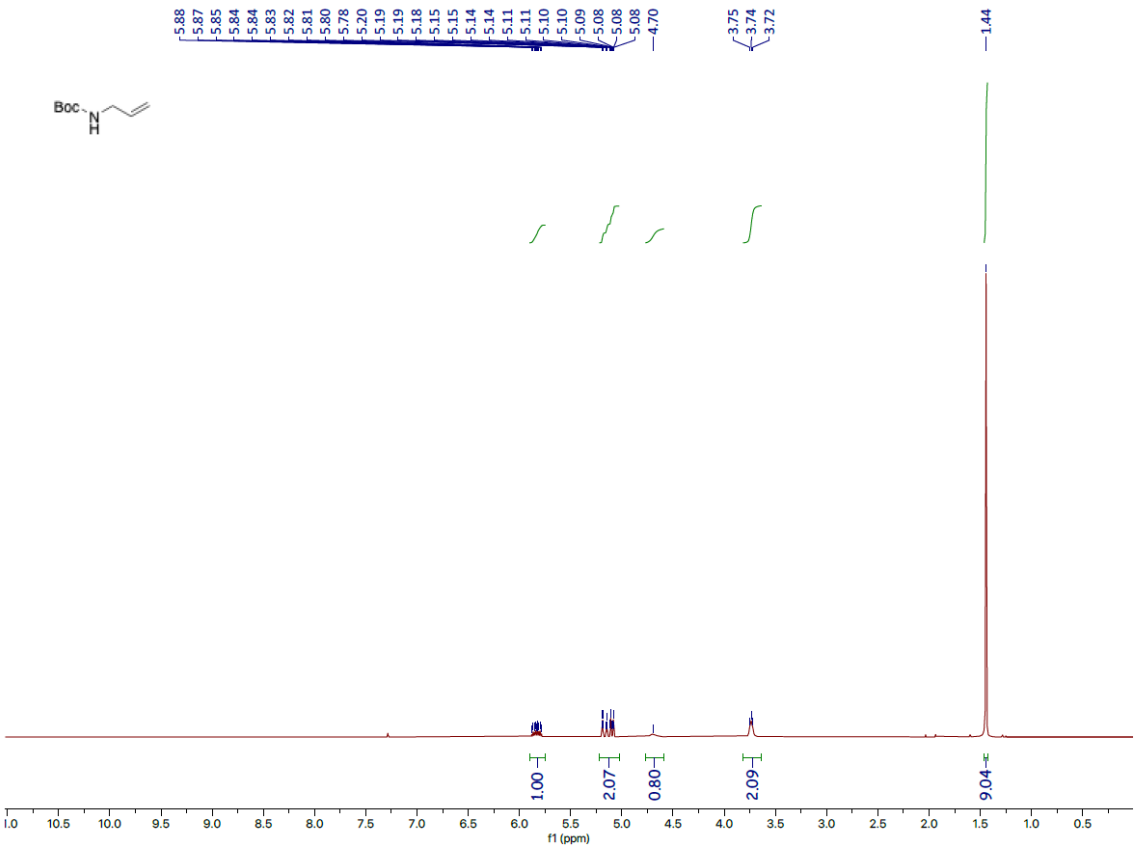

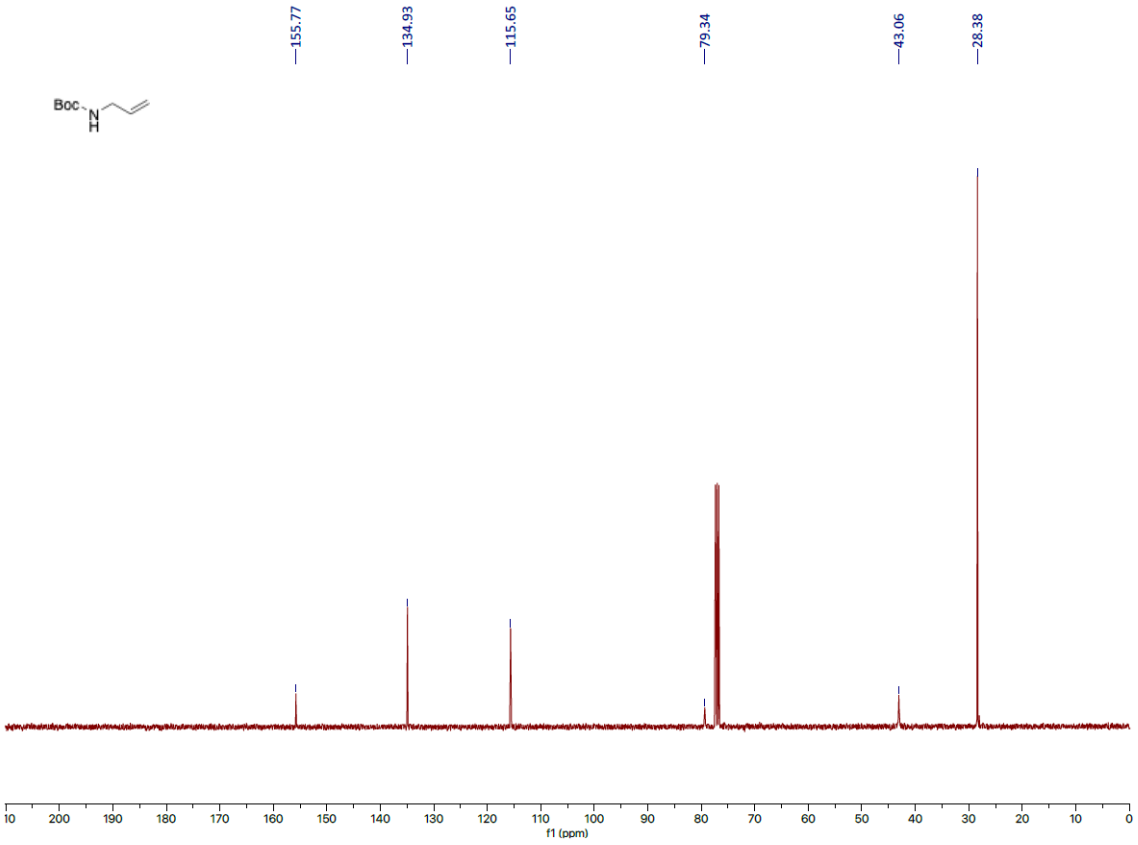

Benzyl prop-2-yn-1-ylcarbamate (**1aj**)

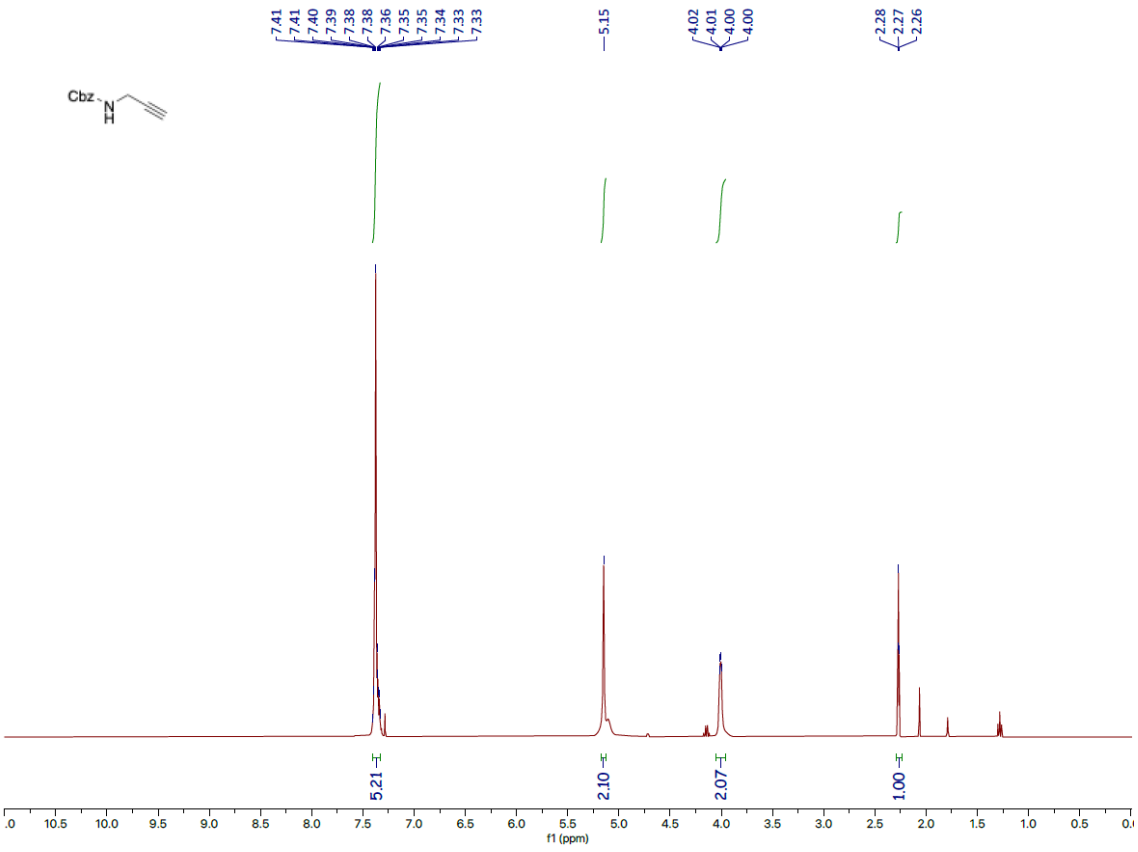

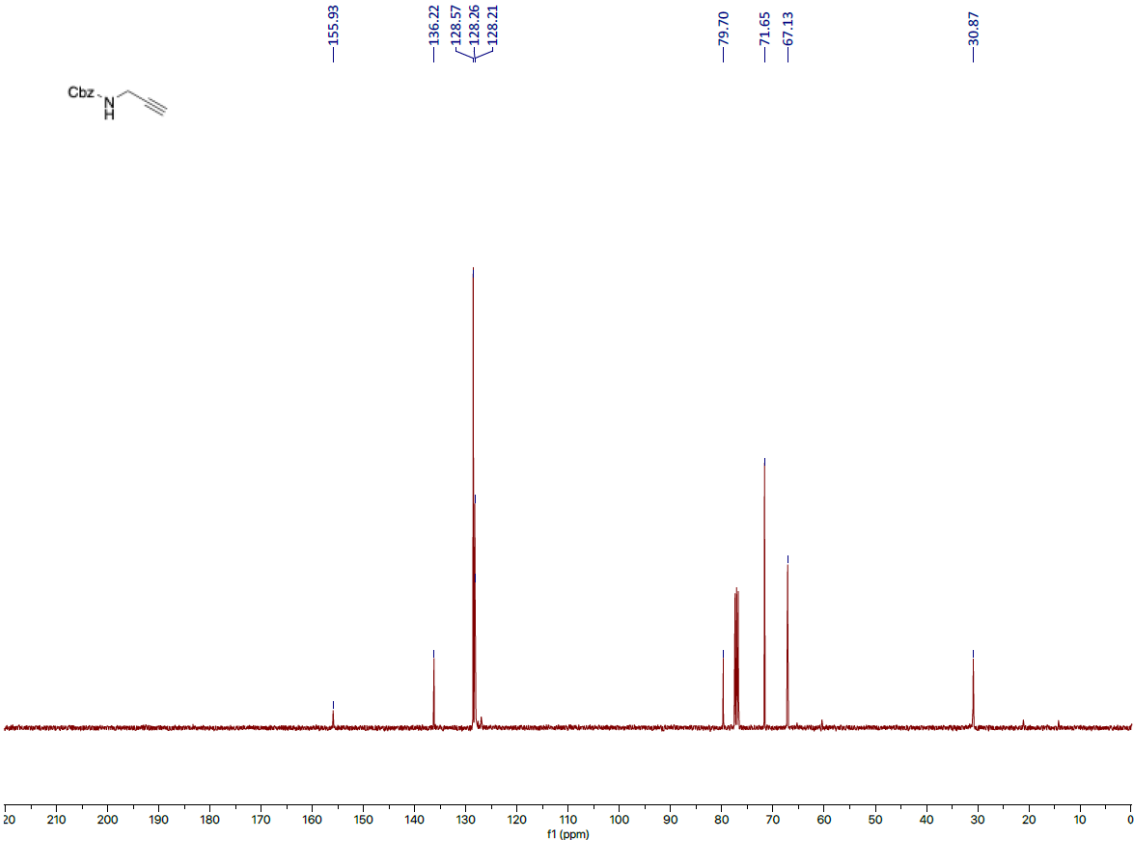

(*E*)-4-(3-iodophenyl)but-3-en-2-one (**1ak**)

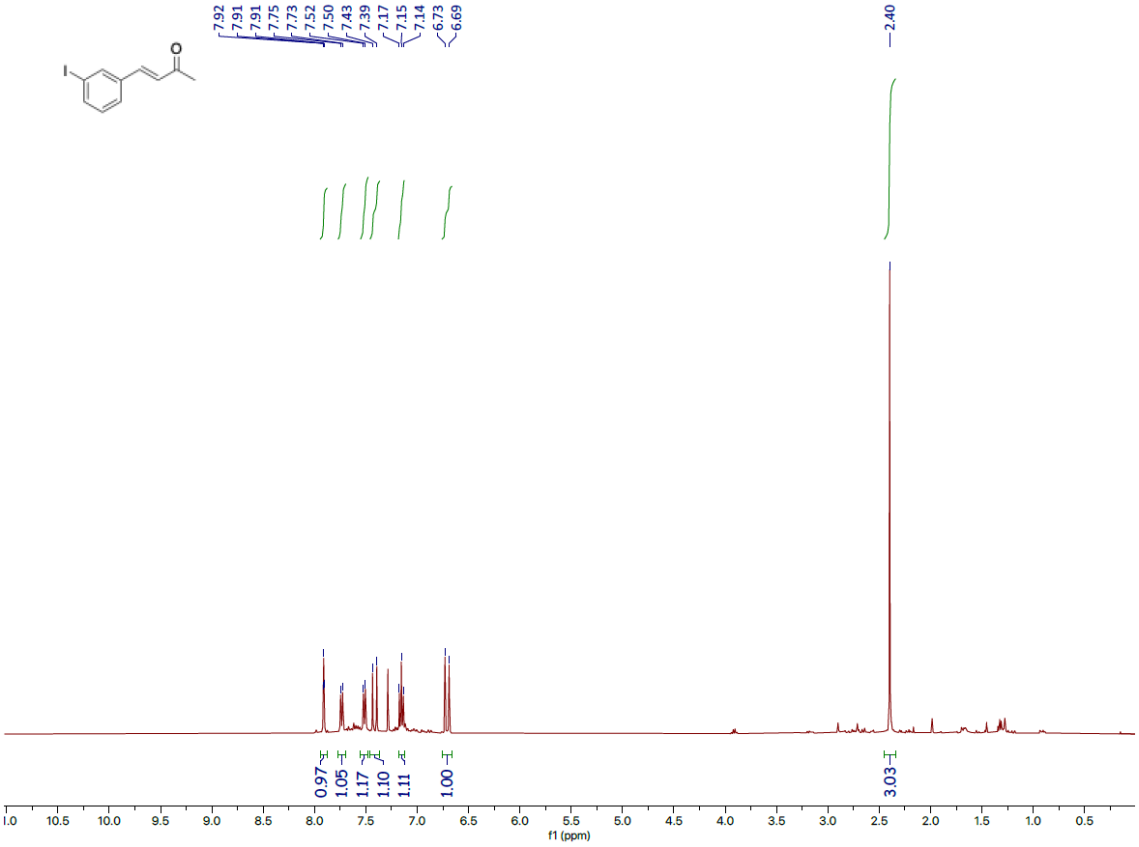

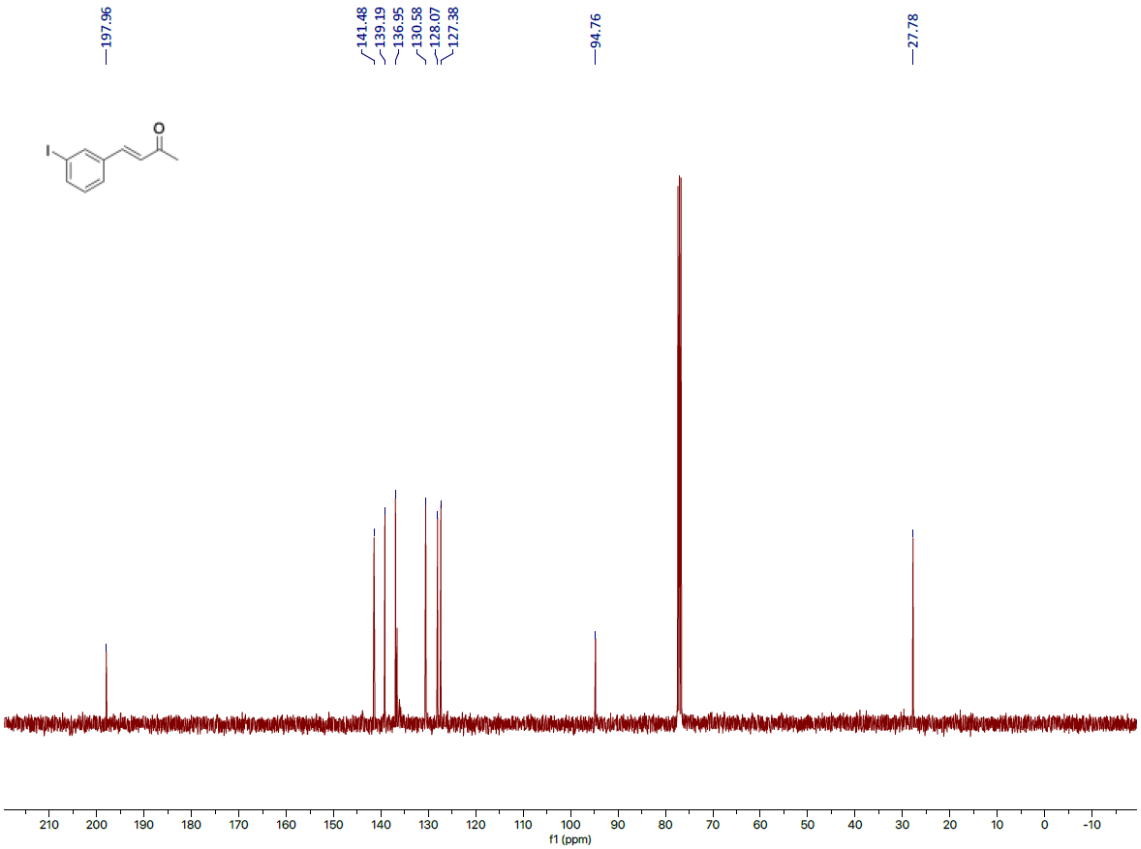

(*E*)-4-(furan-2-yl)but-3-en-2-one (**1al**)

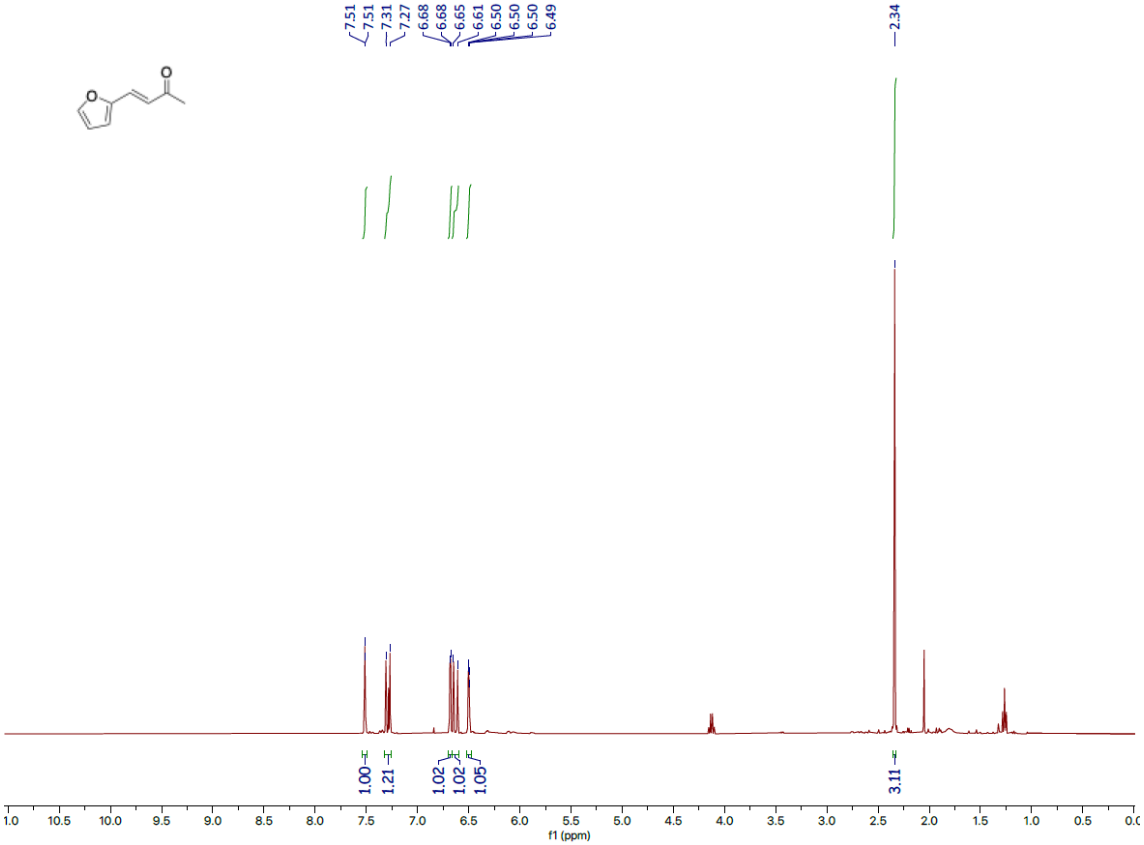

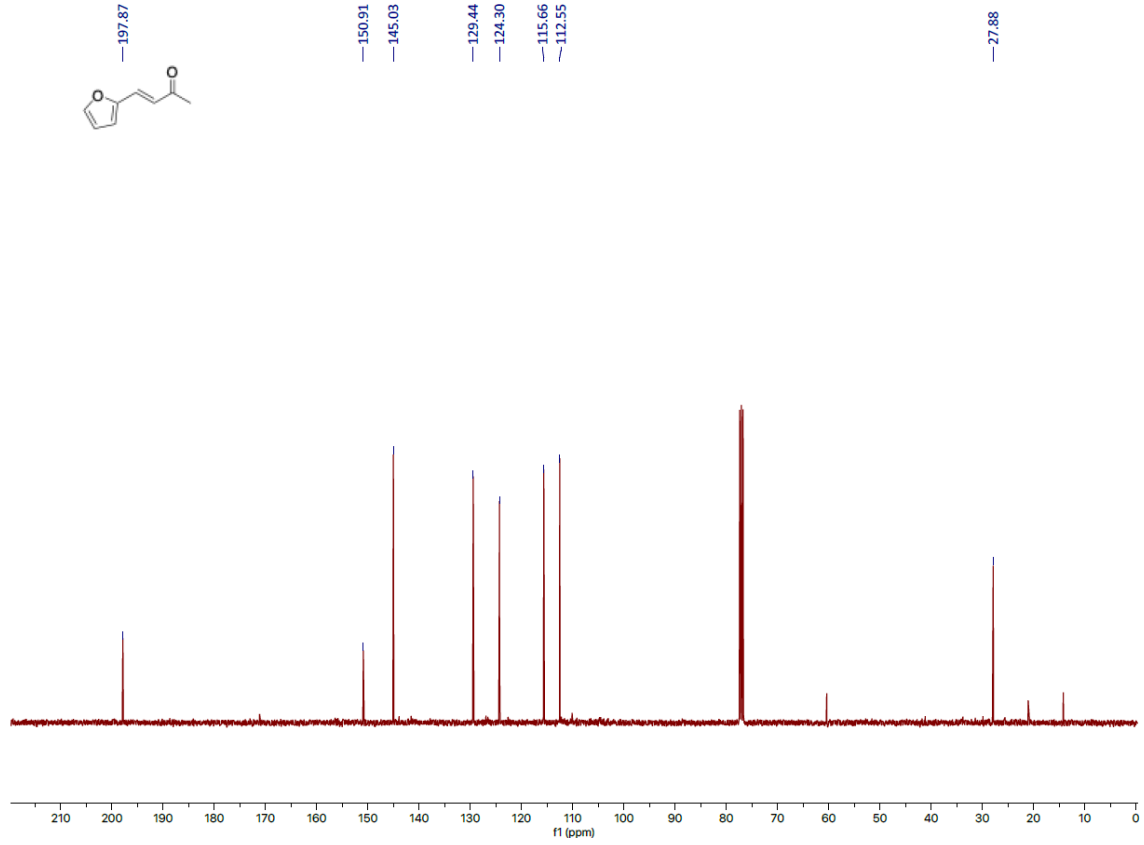

(*E*)-4-(4-hydroxy-3-iodo-5-methoxyphenyl)but-3-en-2-one (**1am**)

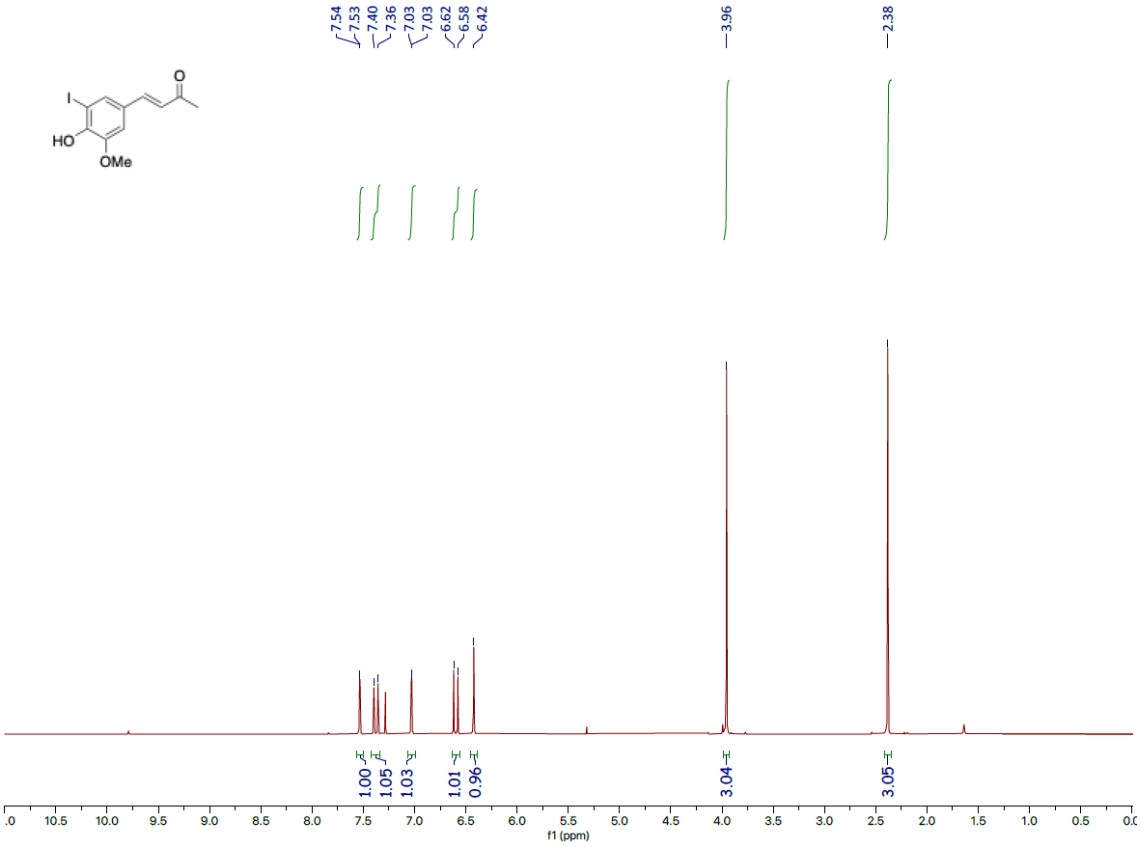

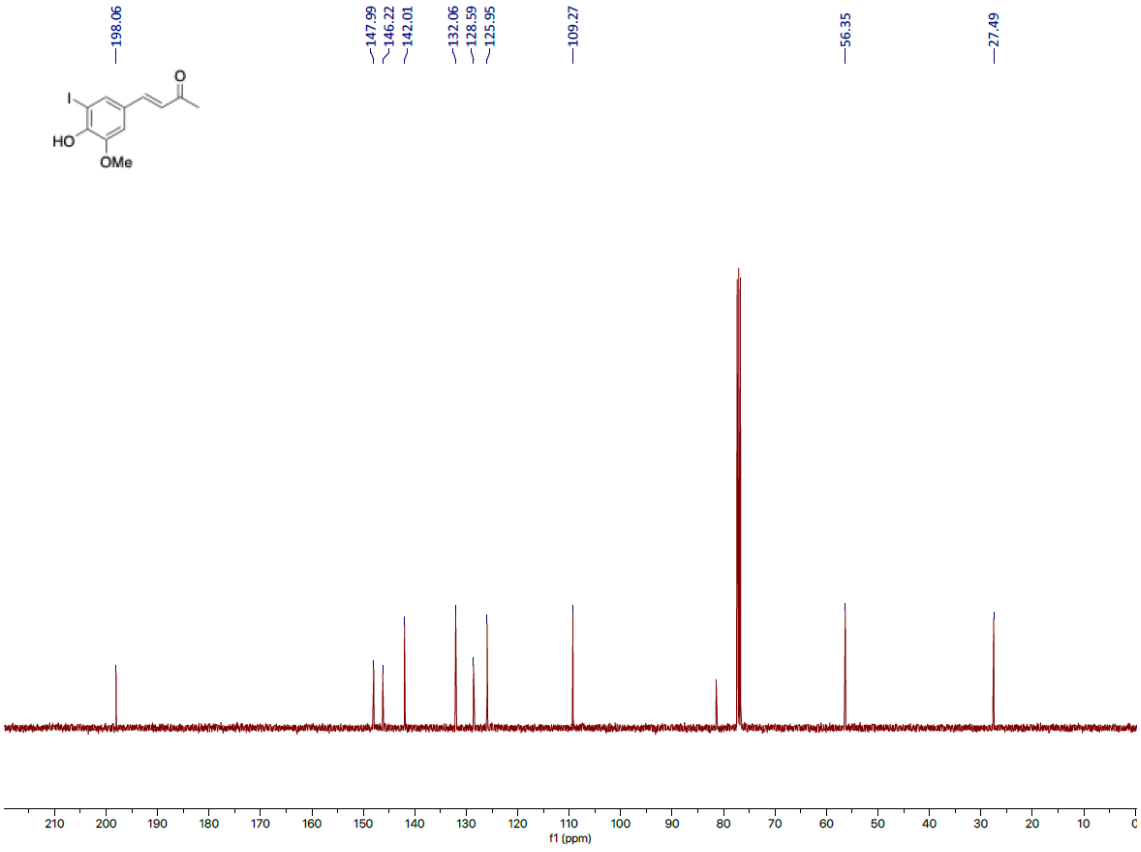

(3*E*,5*E*)-6-phenylhexa-3,5-dien-2-one (**1aq**)

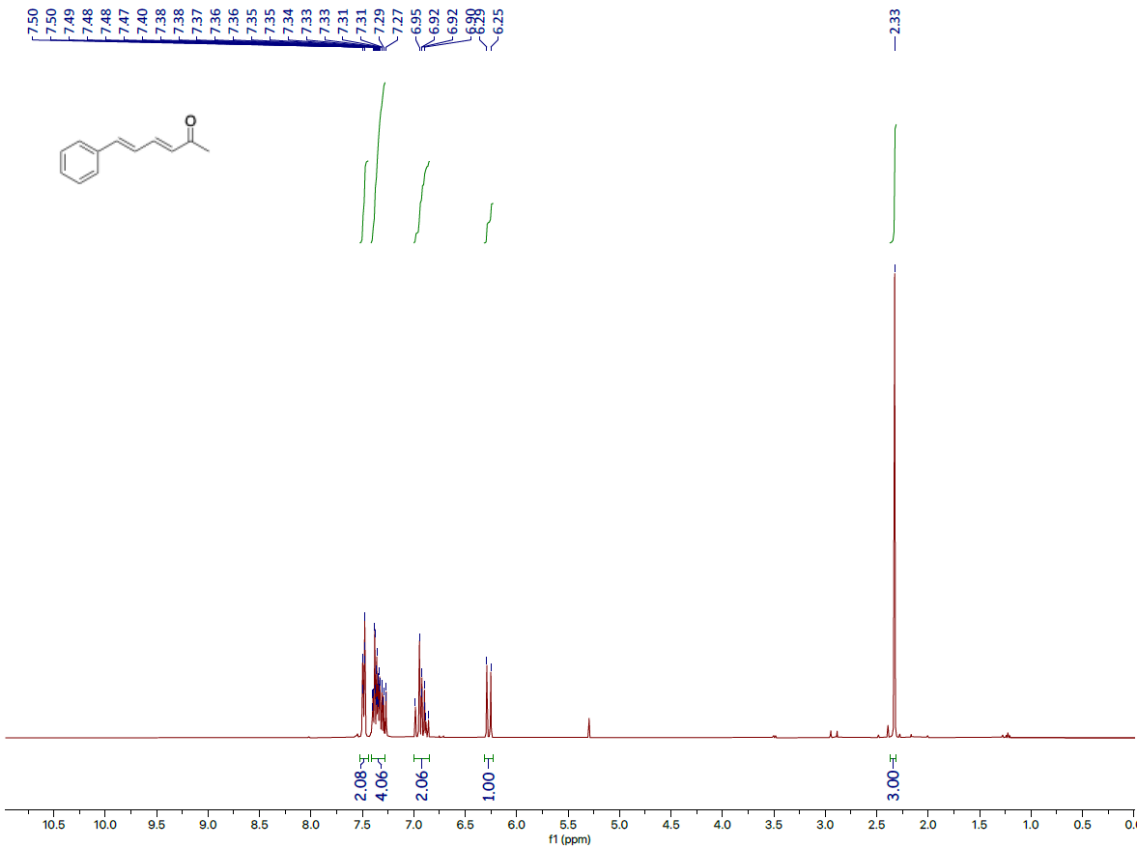

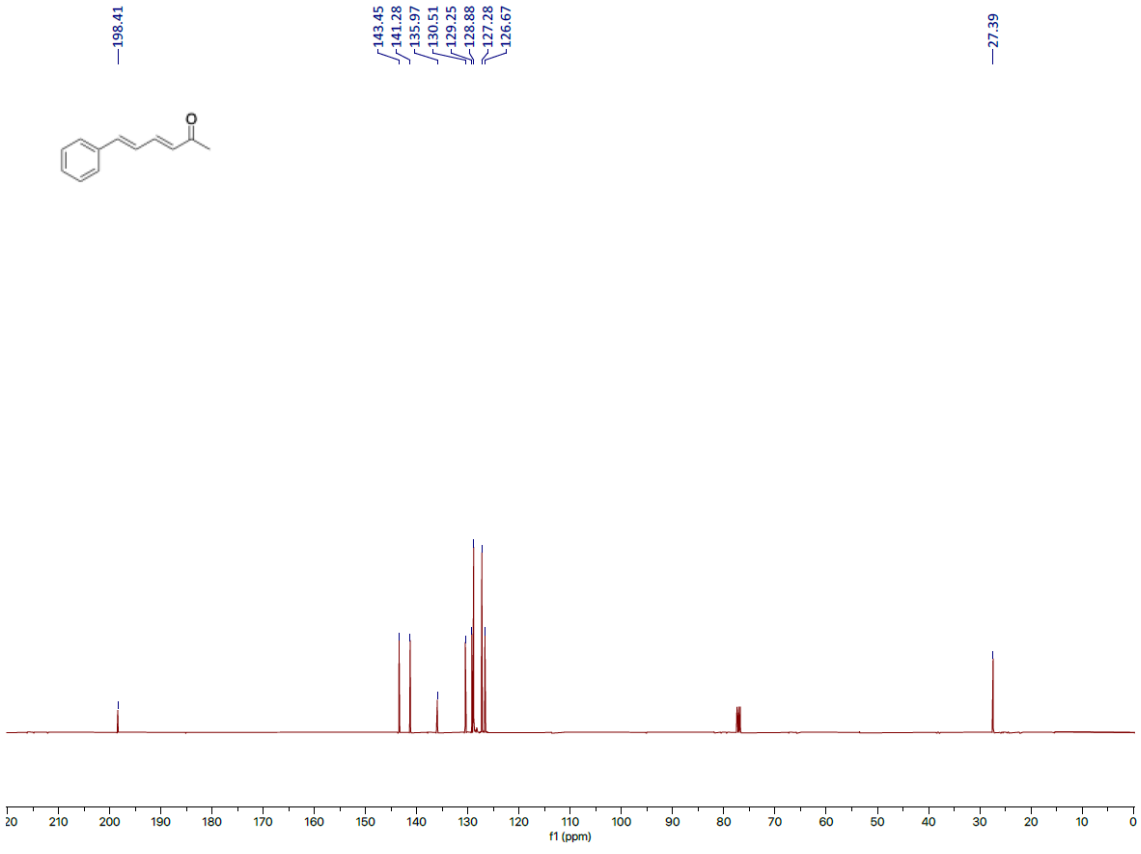

Ethyl (*E*)-3-(1-acetyl-1H-indol-2-yl)acrylate (**1au**)

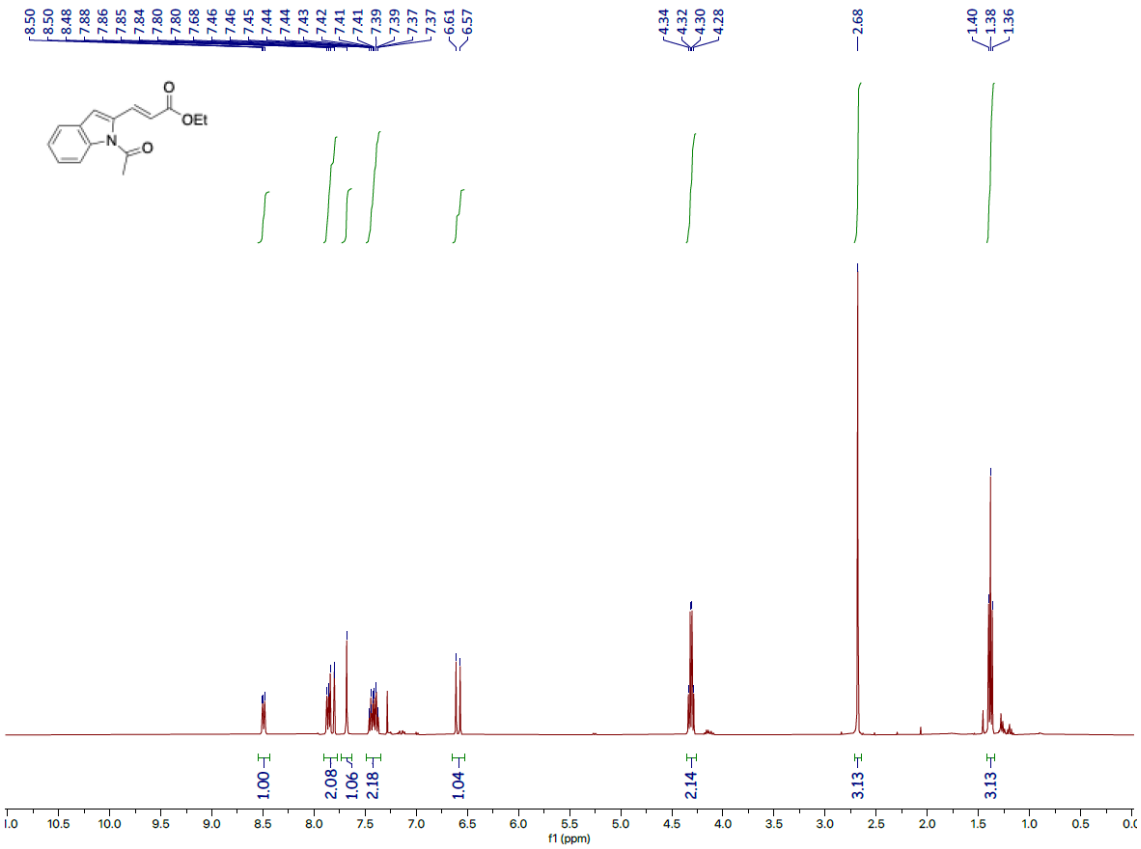

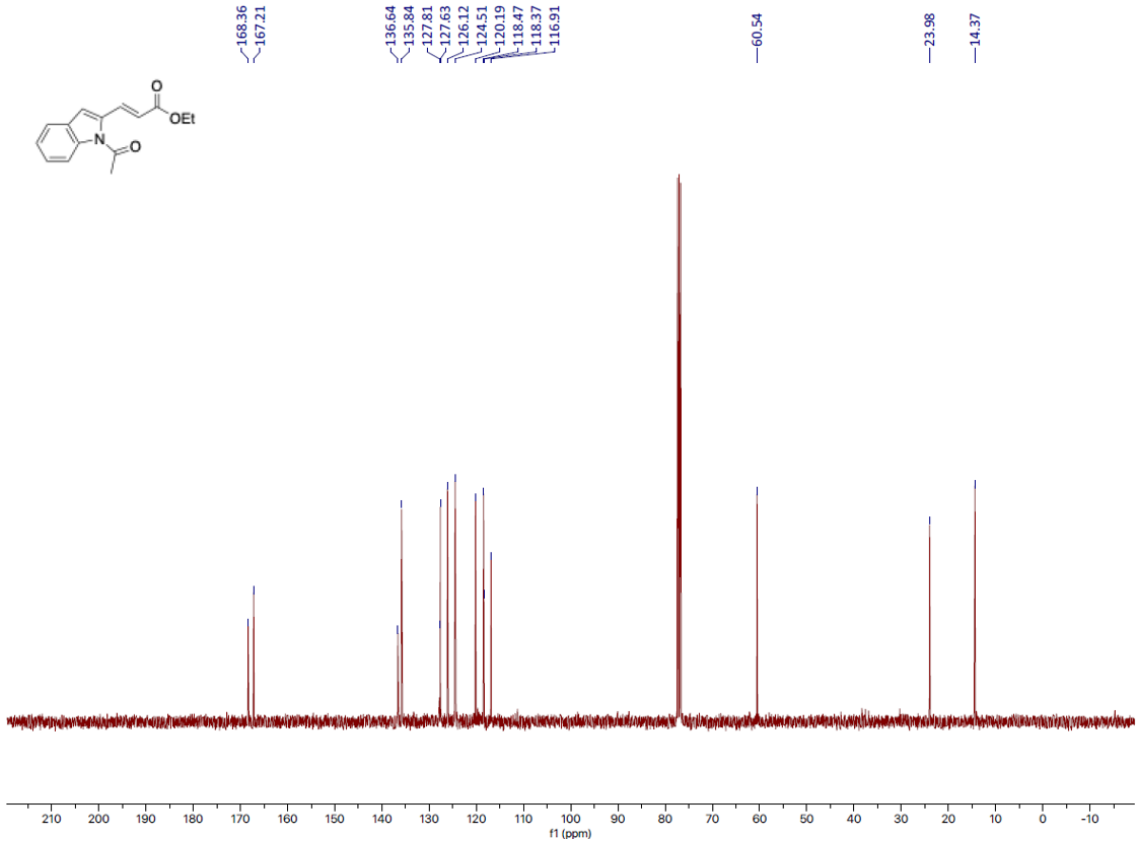

(*E*)-4-(1H-indol-4-yl)but-3-en-2-one (**1av**)

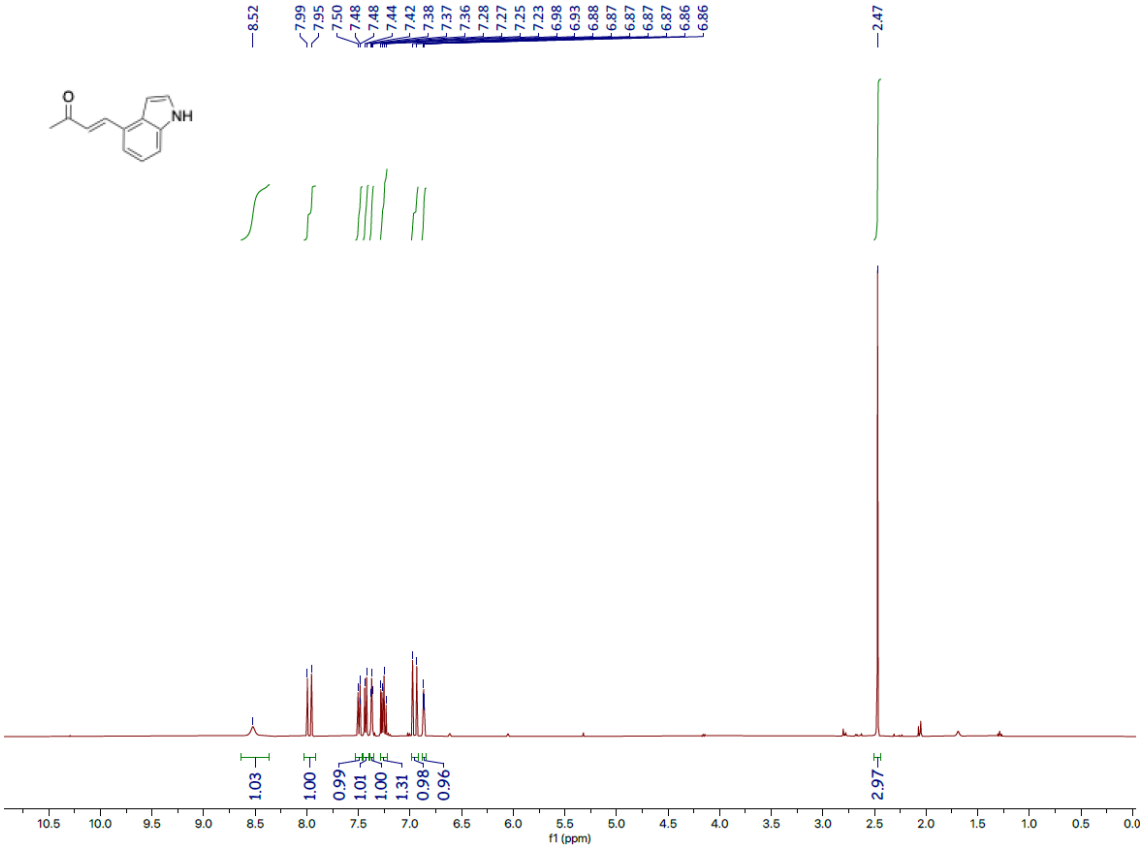

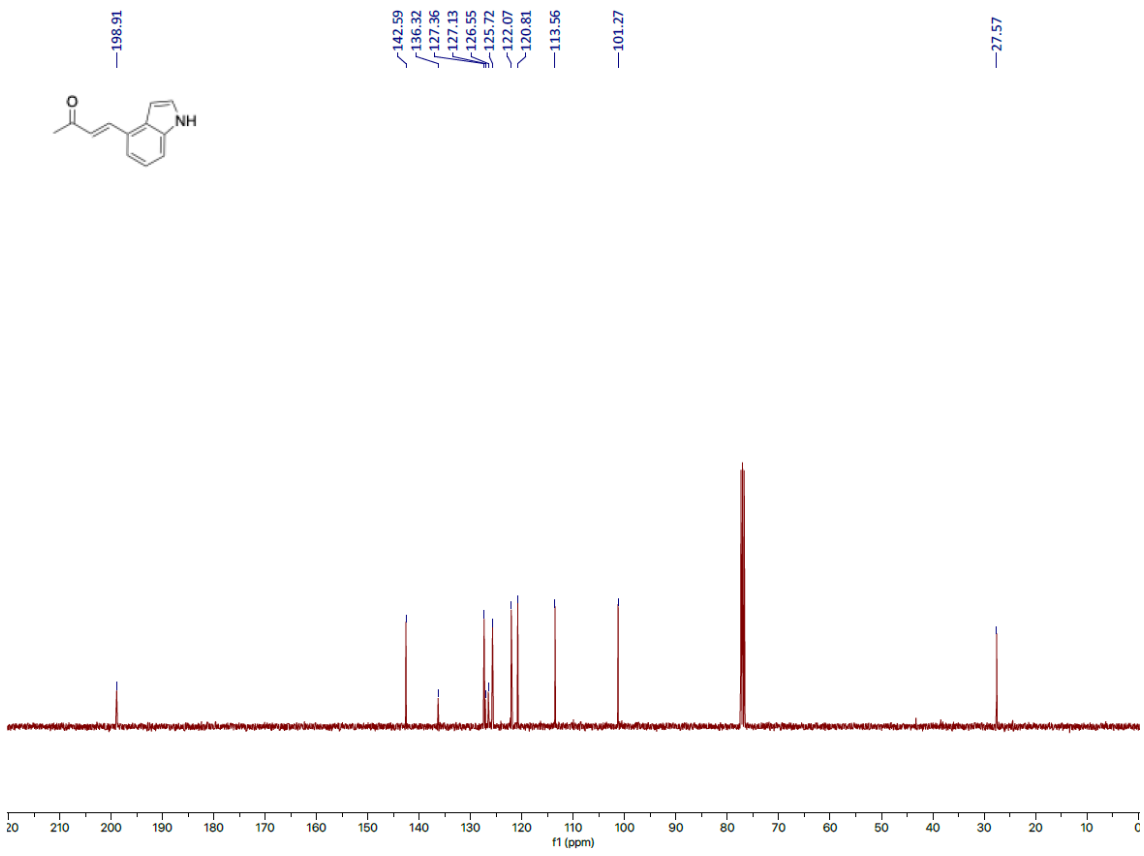

(*E*)-*N*-Benzyl-3-phenylprop-2-en-1-amine (**1aw**)

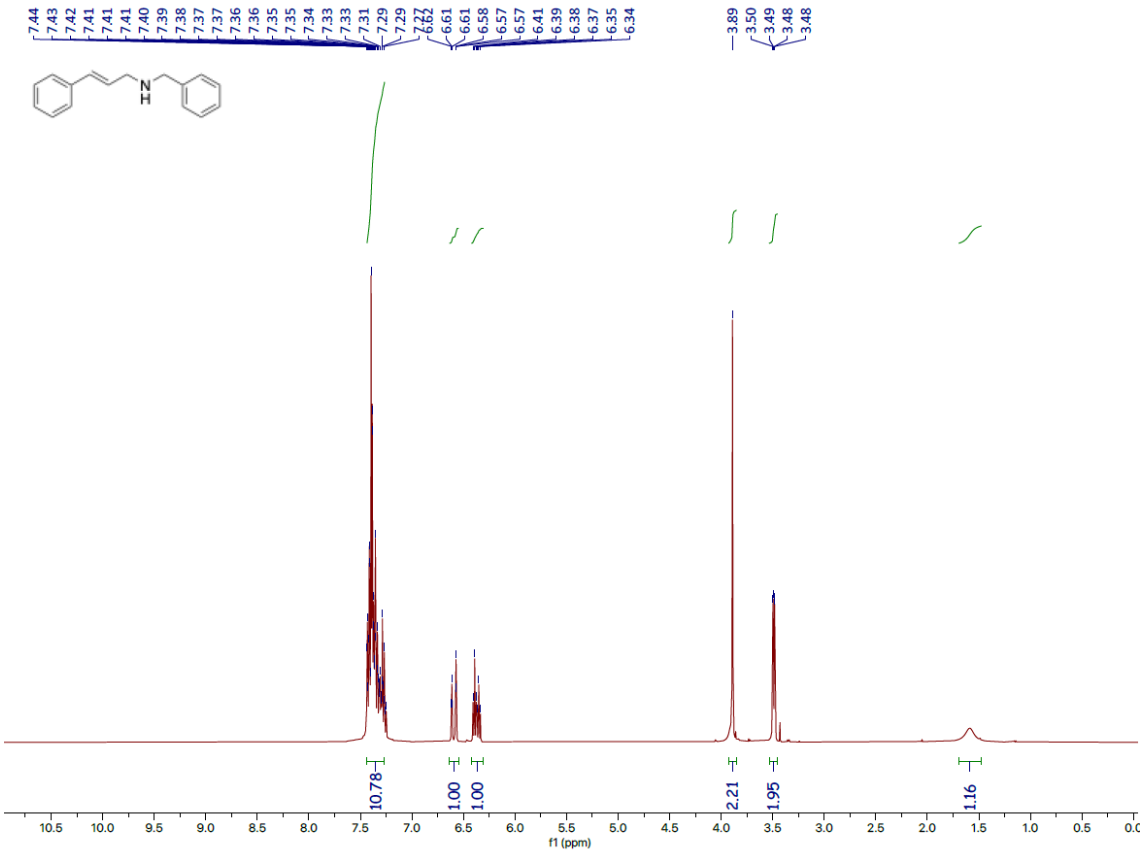

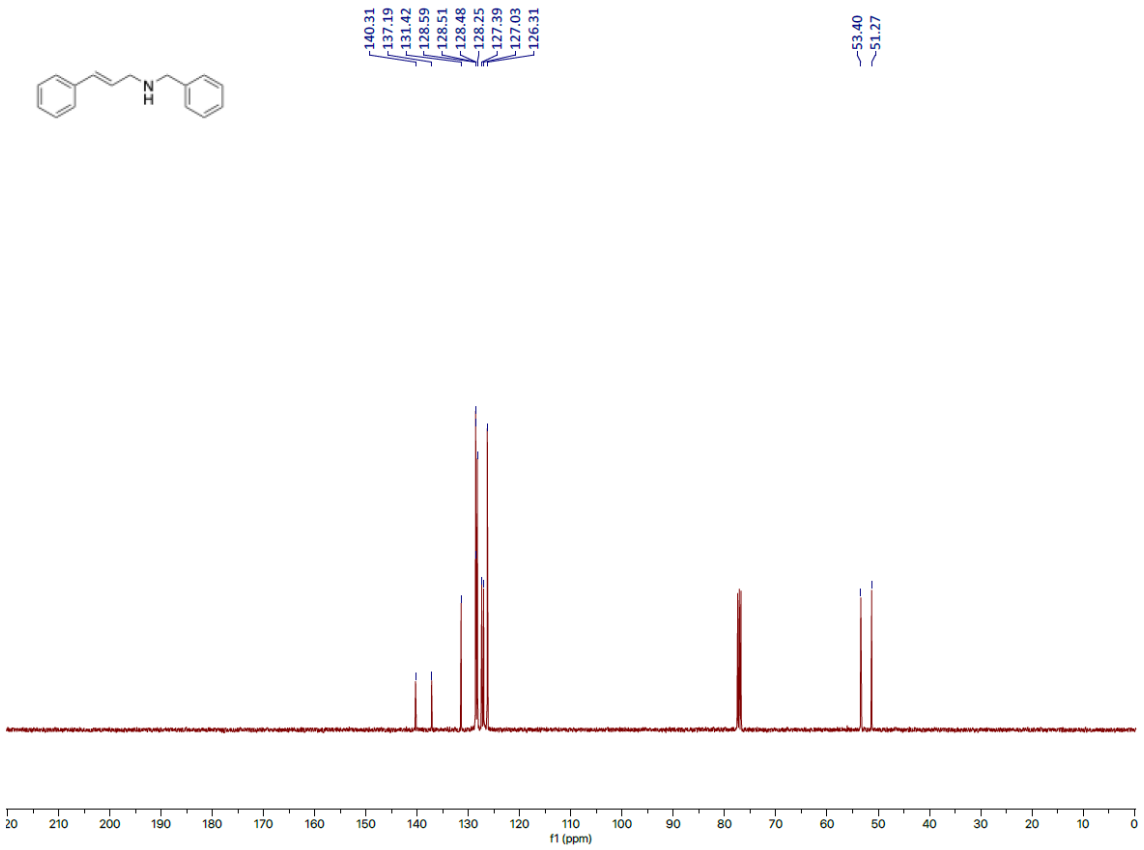

Ethyl (E)-3-(4-methoxyphenyl)-2-methylacrylate (**1ax**)

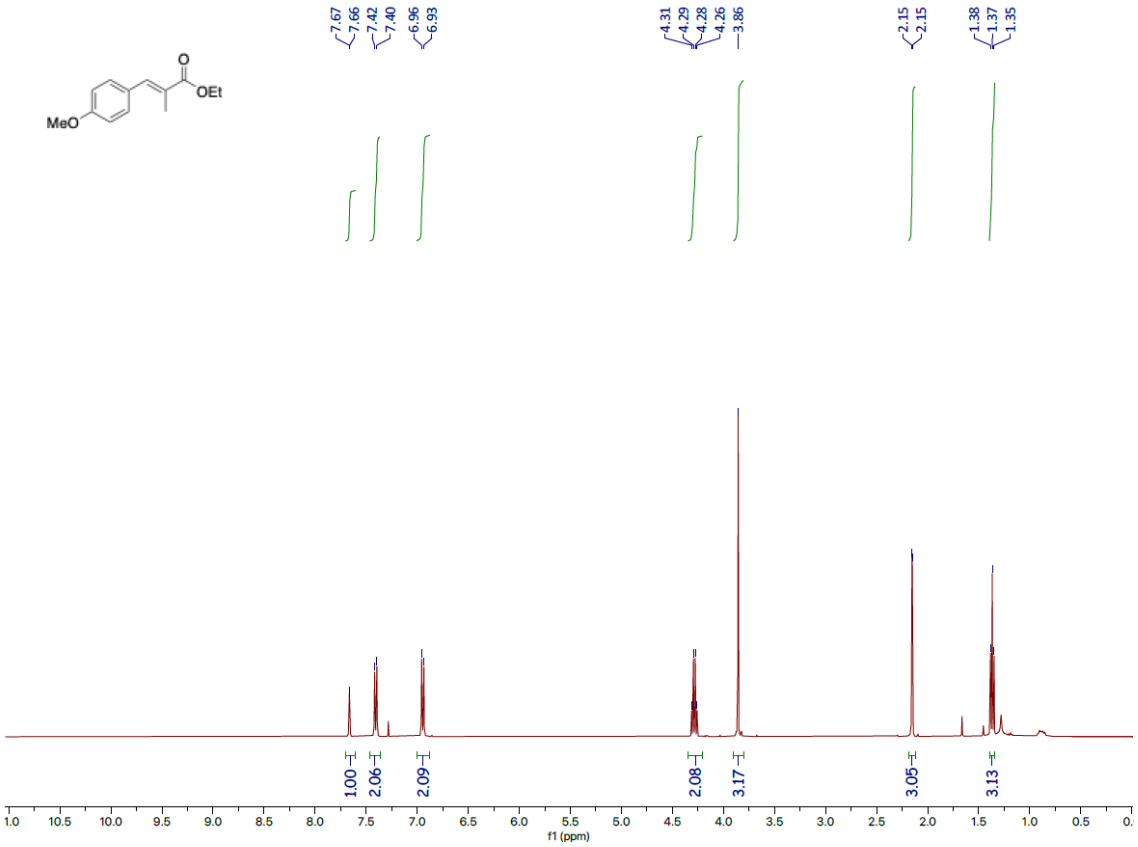

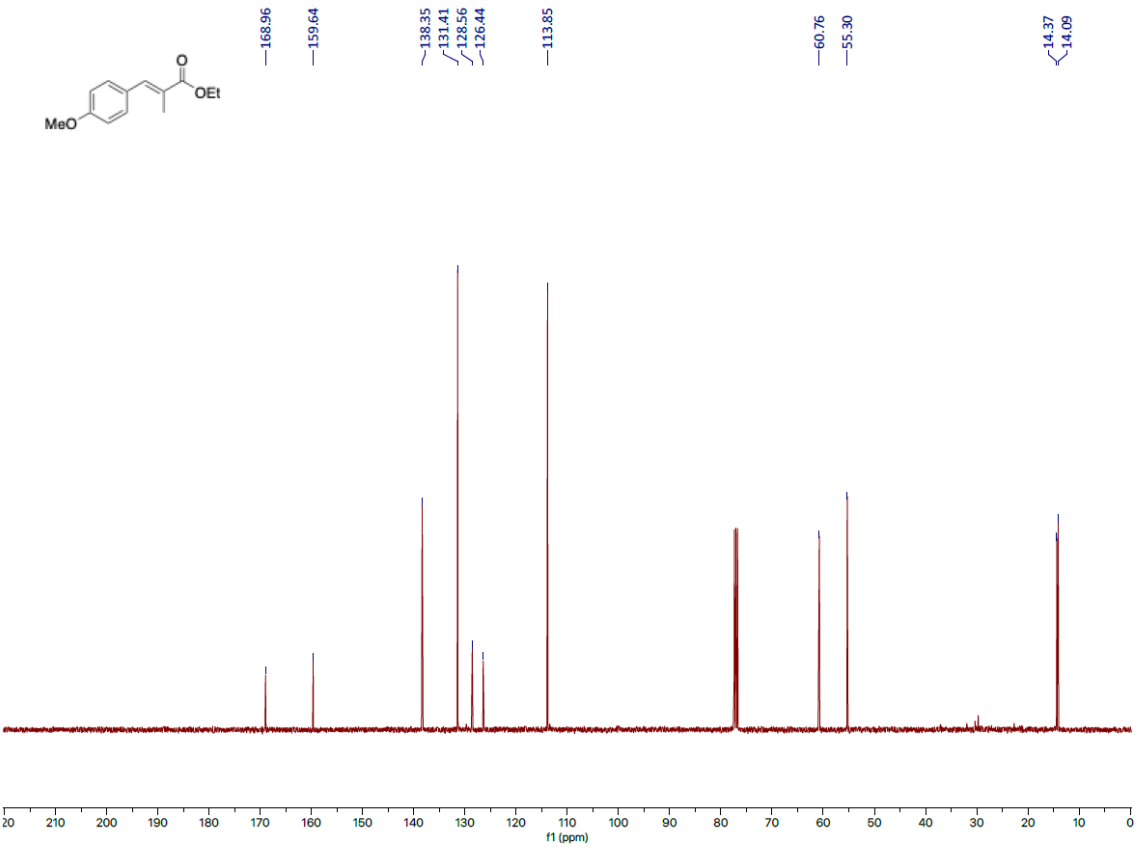

(E)-4-(4-Hydroxyphenyl)-3-methylbut-3-en-2-one (**1ay**)

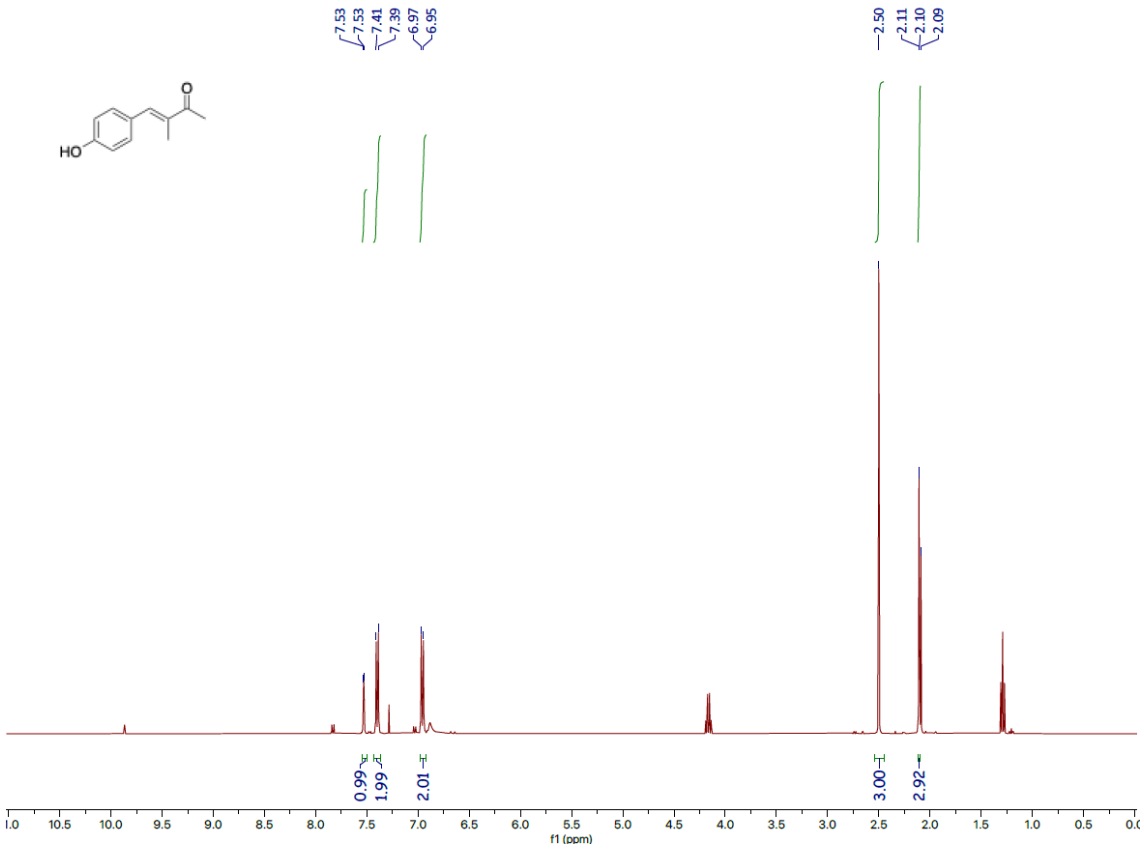

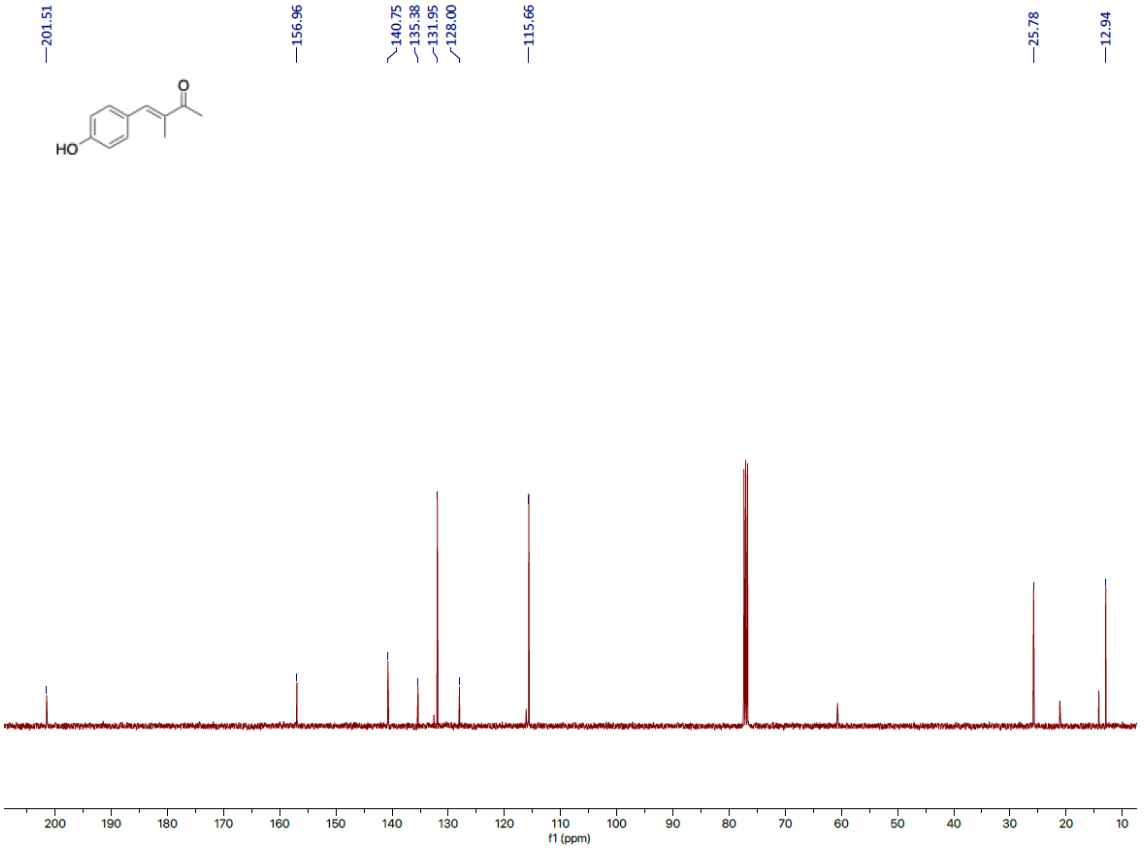

4-(*p*-Hydroxyphenyl)-2-butanone (**2a**)

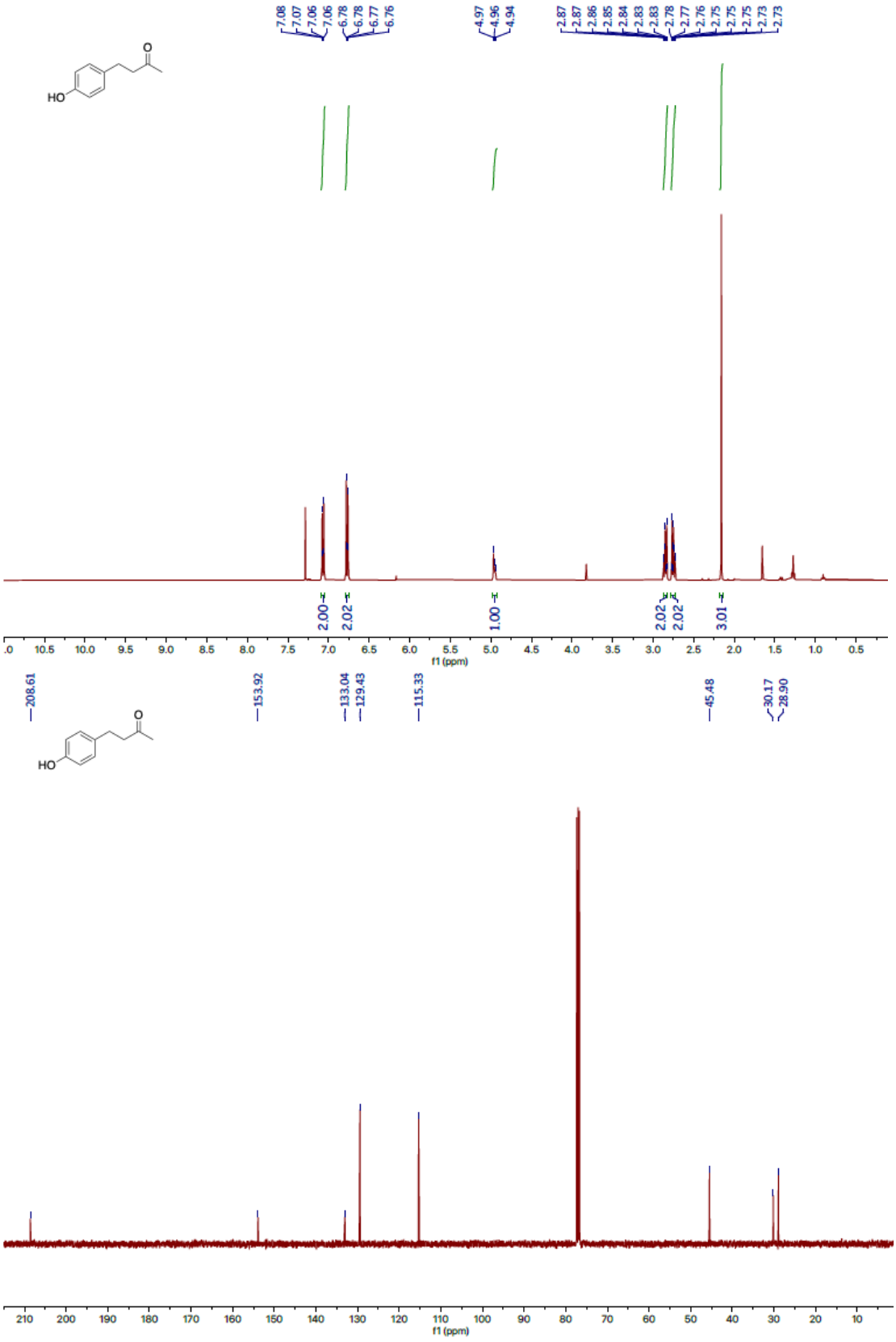

4-Phenyl-2-butanone (**2c**)

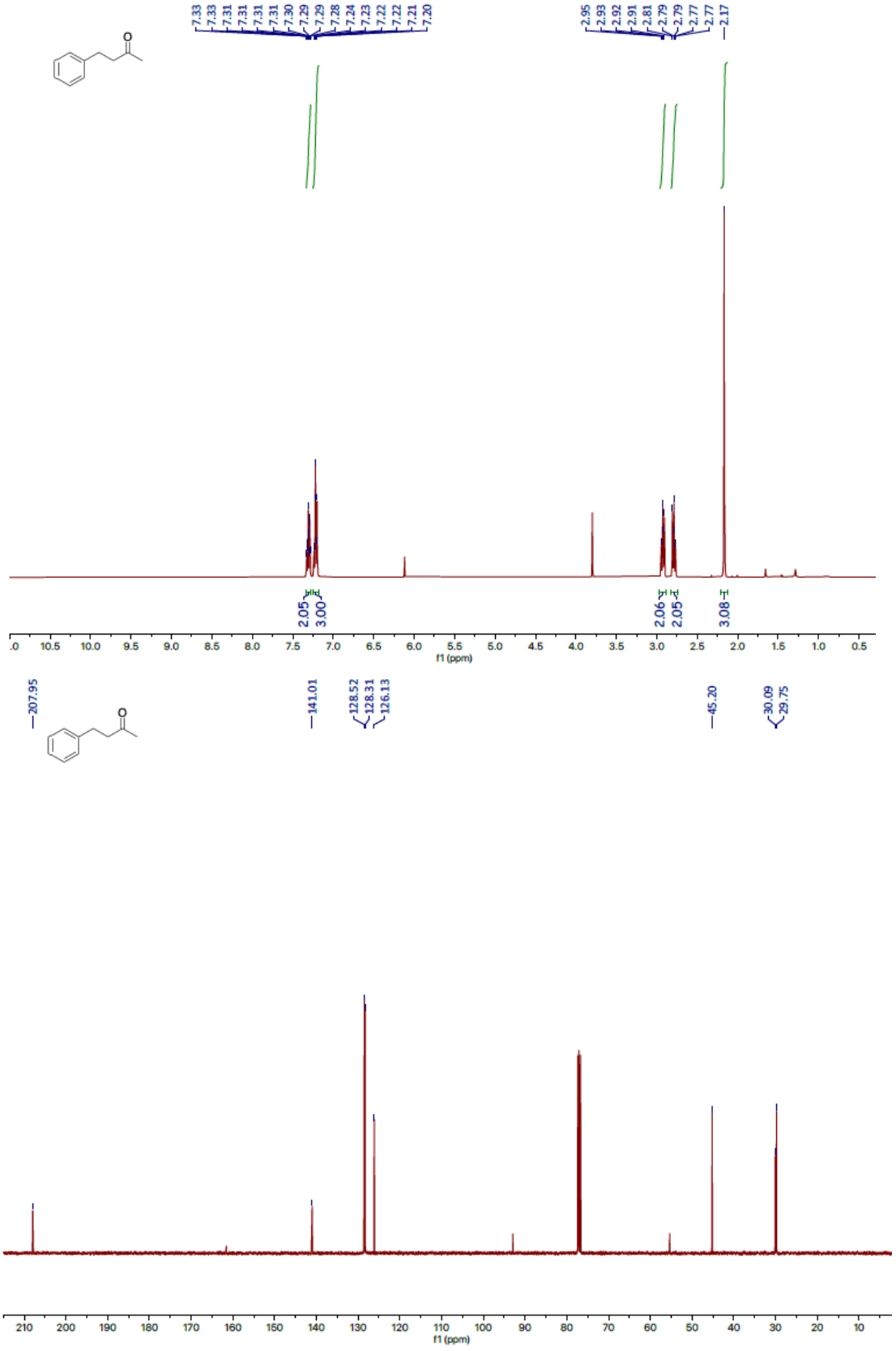

4-(*p*-Tolyl)-2-butanone (**2d**)

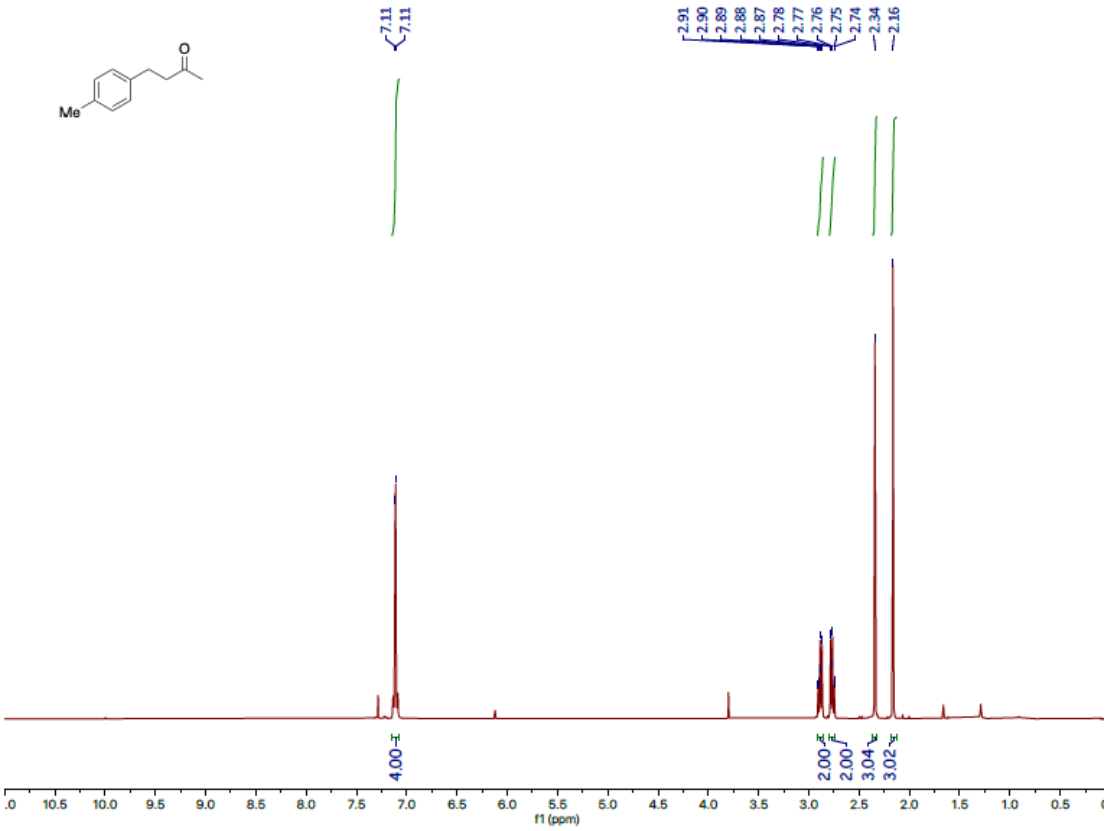

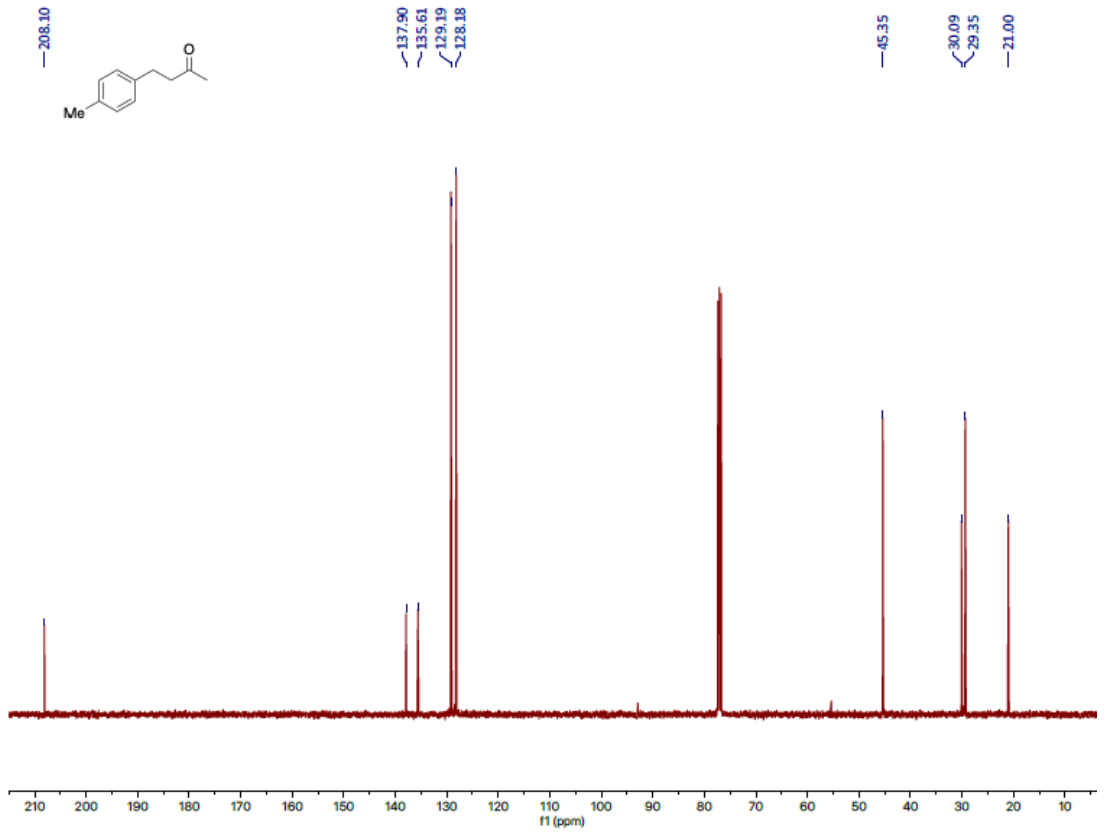

4-(*p*-Methoxyphenyl)-2-butanone (**2e**)

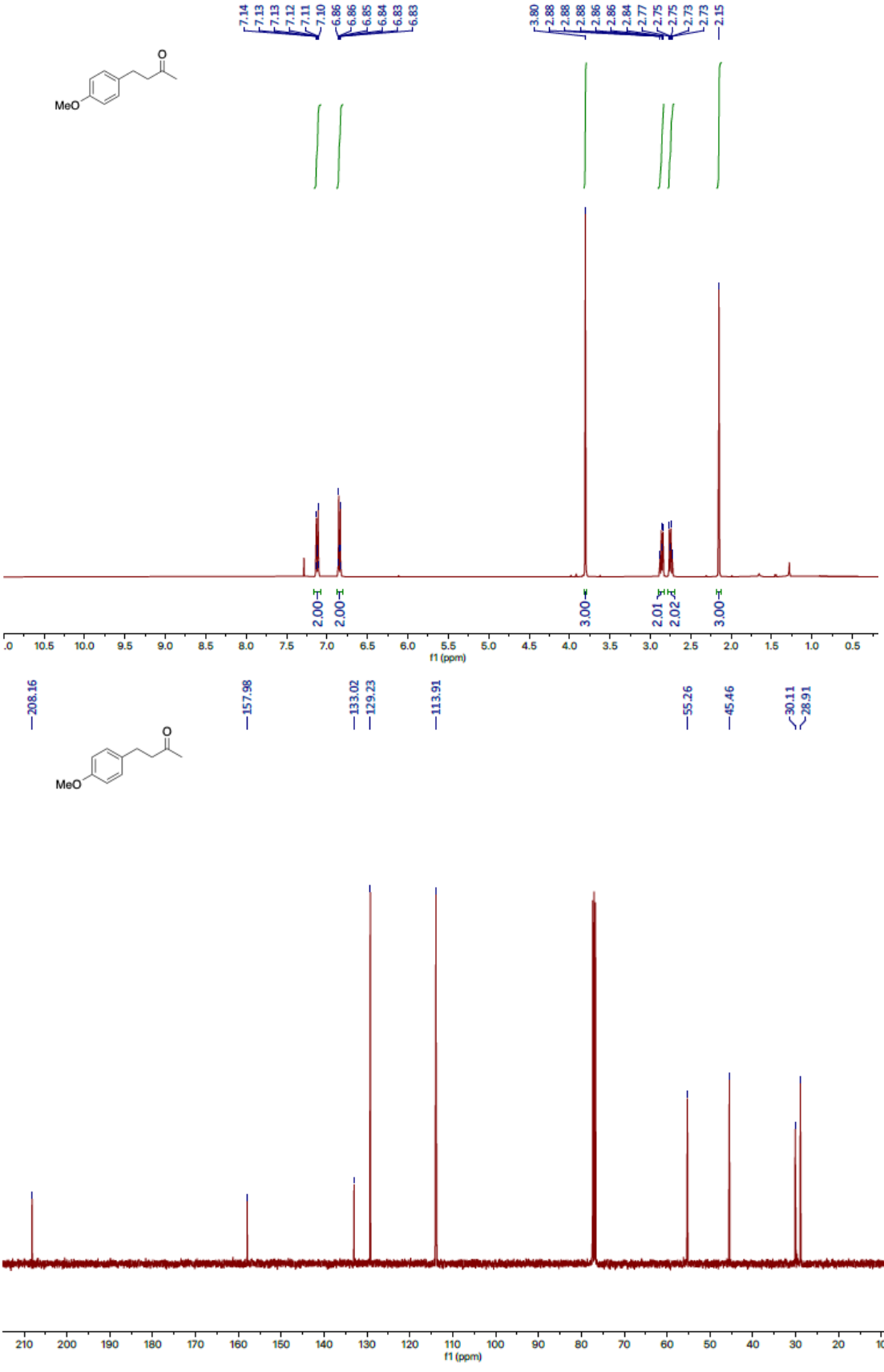

4-(*p*-(Dimethylamino)phenyl)-2-butanone (**2f**)

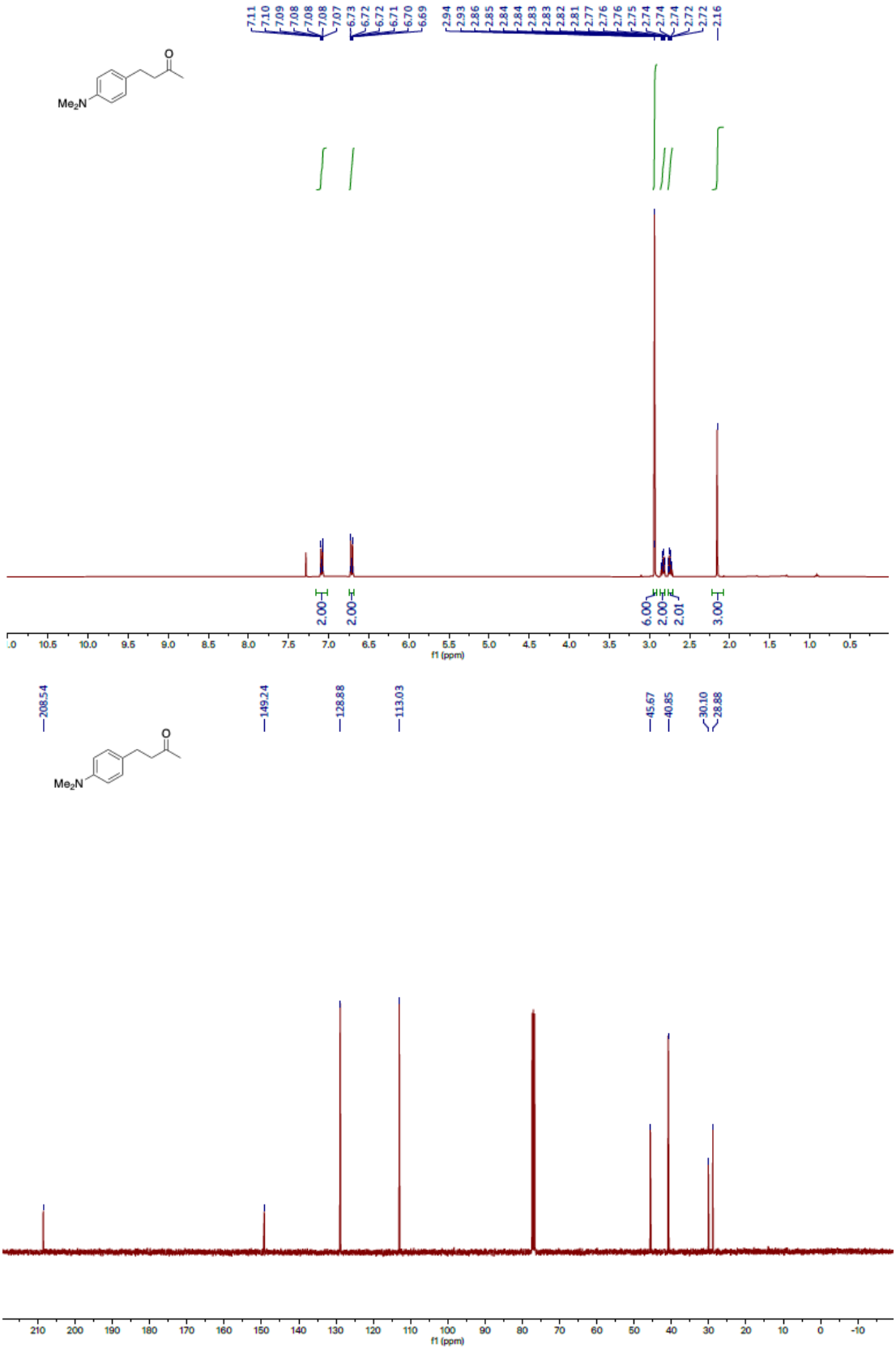

4-(*p*-Bromophenyl)-2-butanone (**2g**)

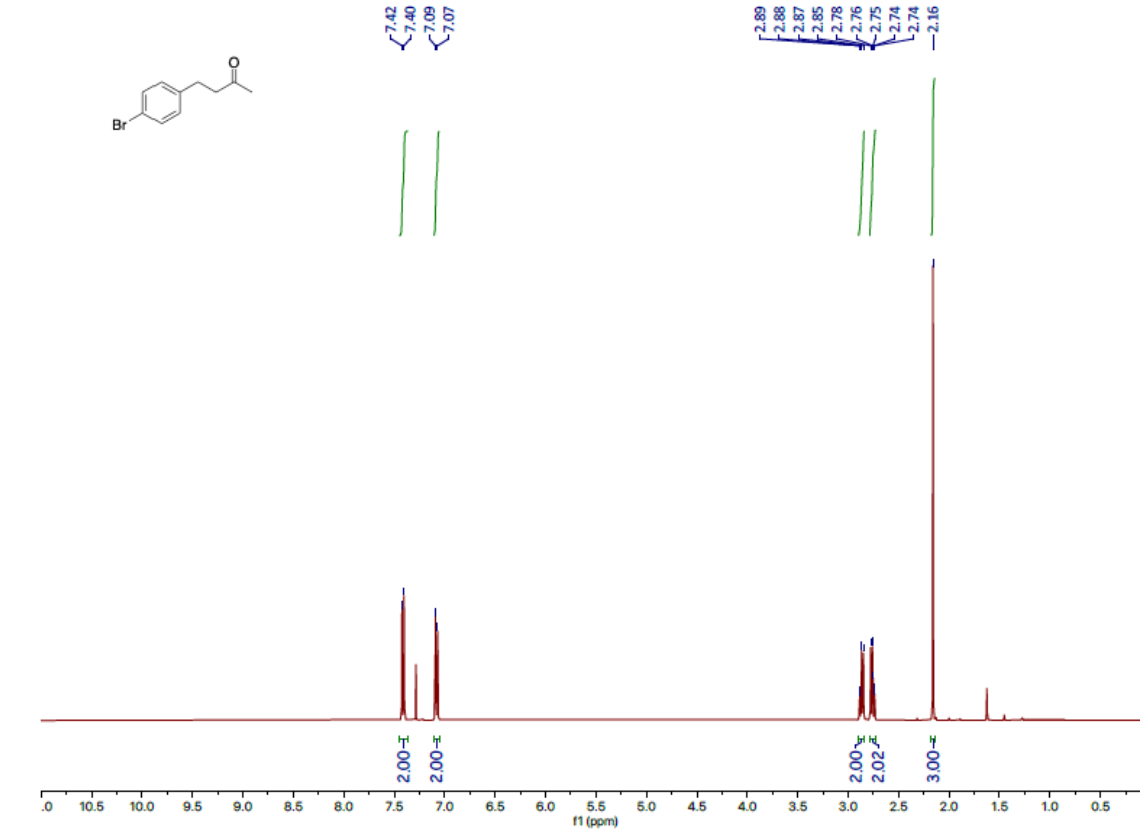

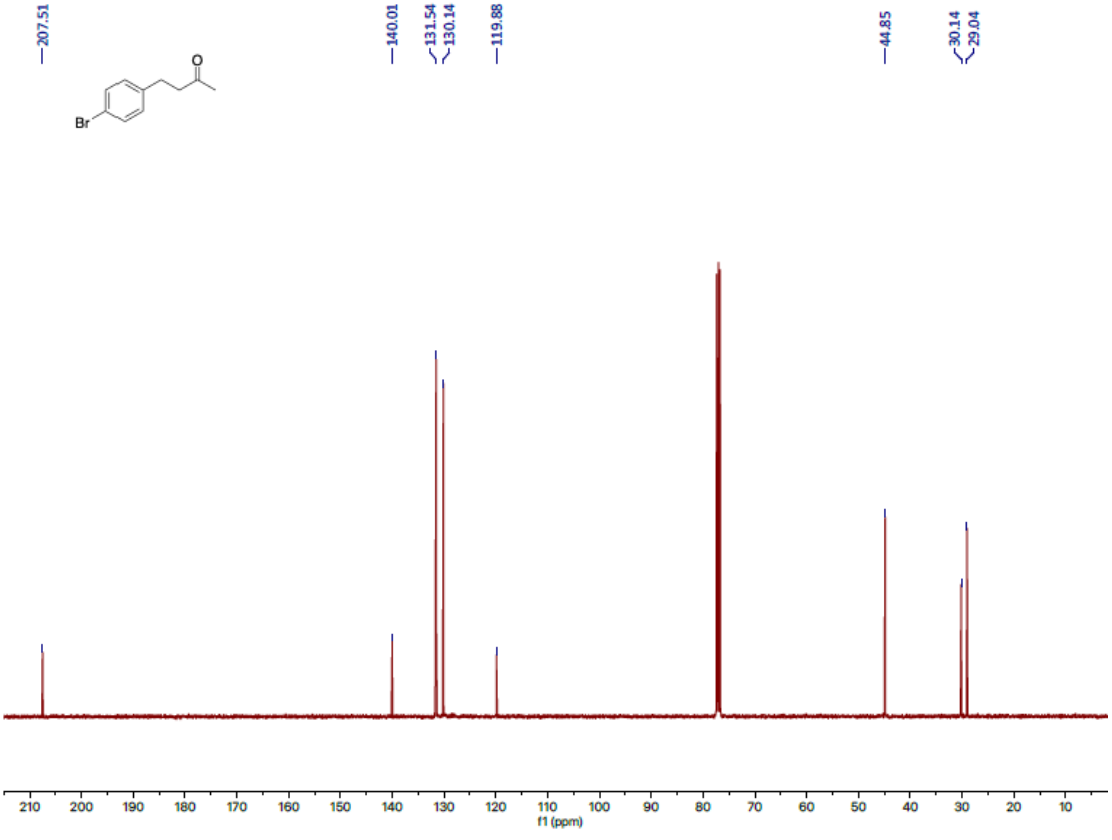

4-(*m*-Tolyl)-2-butanone (**2h**)

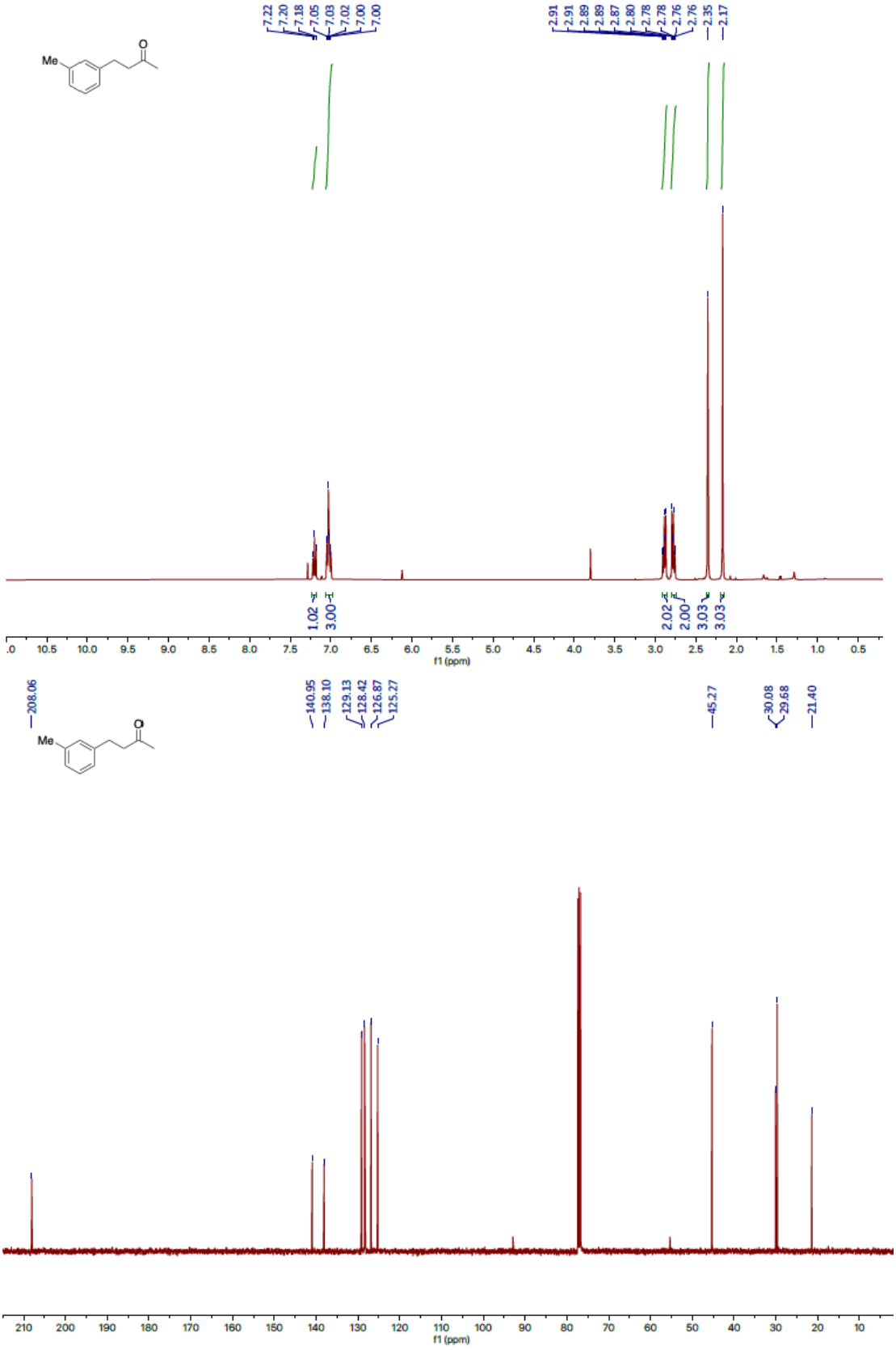

4-(*m*-Methoxyphenyl)-2-butanone (**2i**)

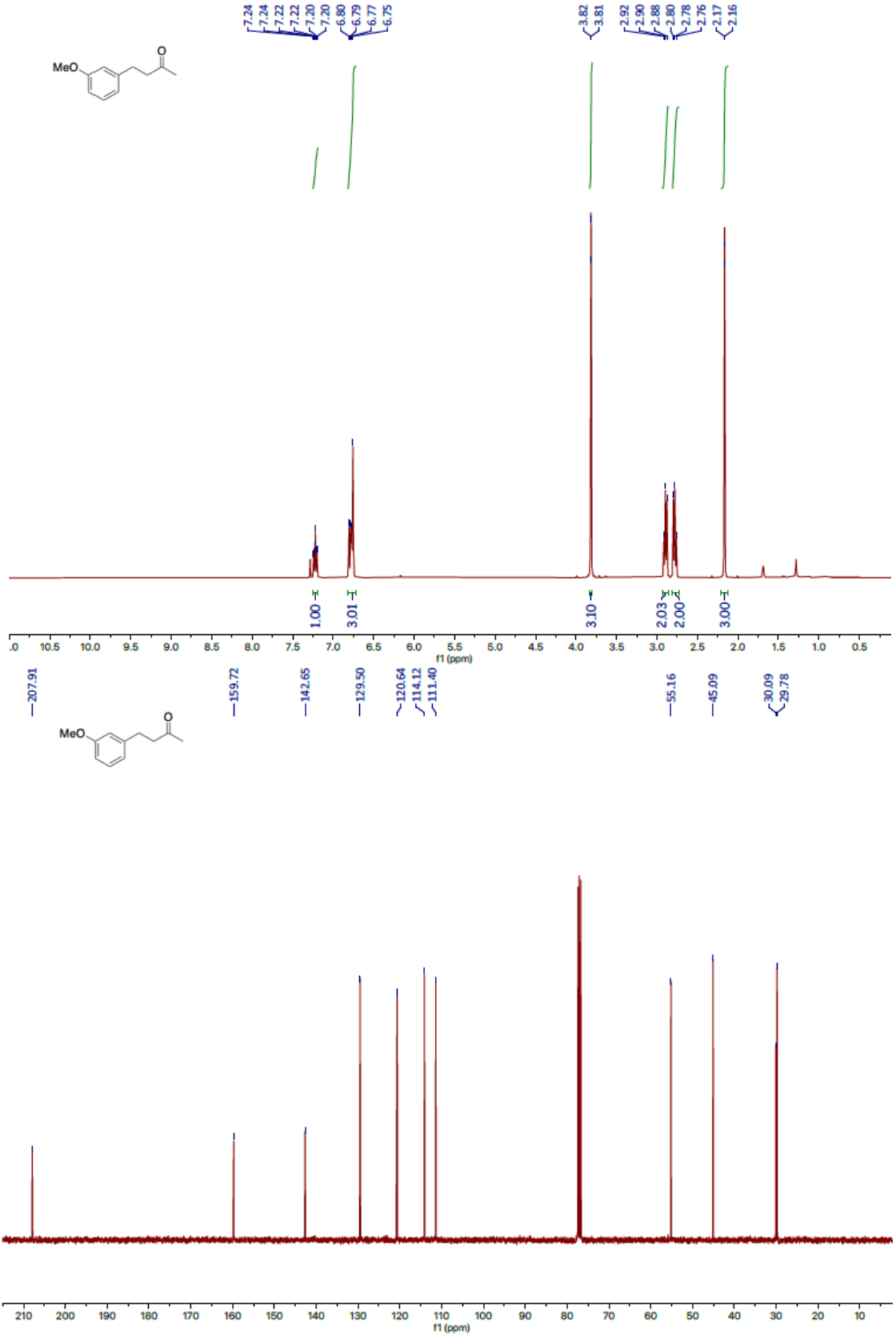

4-(*m*-Hydroxyphenyl)-2-butanone (**2j**)

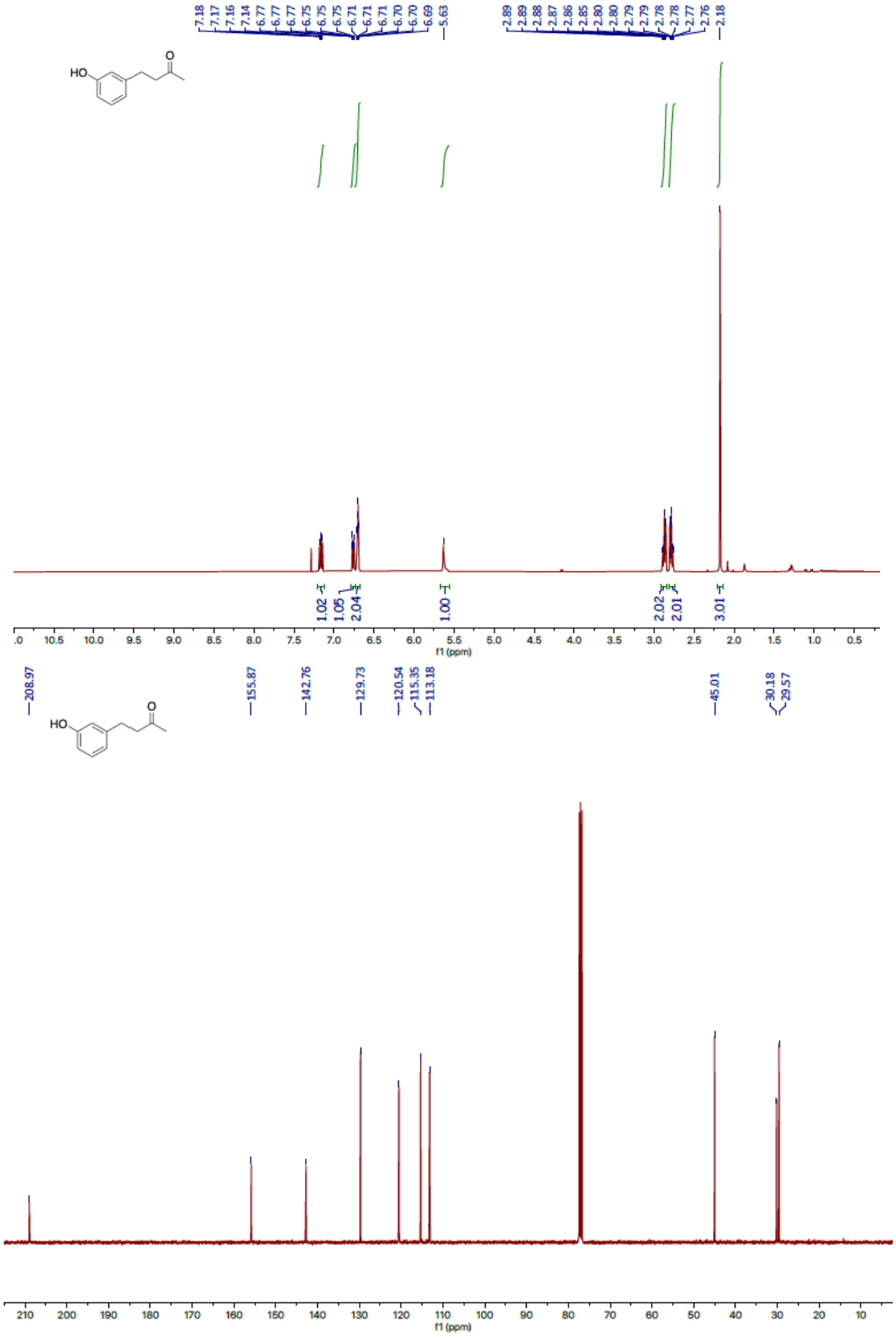

4,4-Dimethyl-1-phenyl-3-pentanone (**2n**)

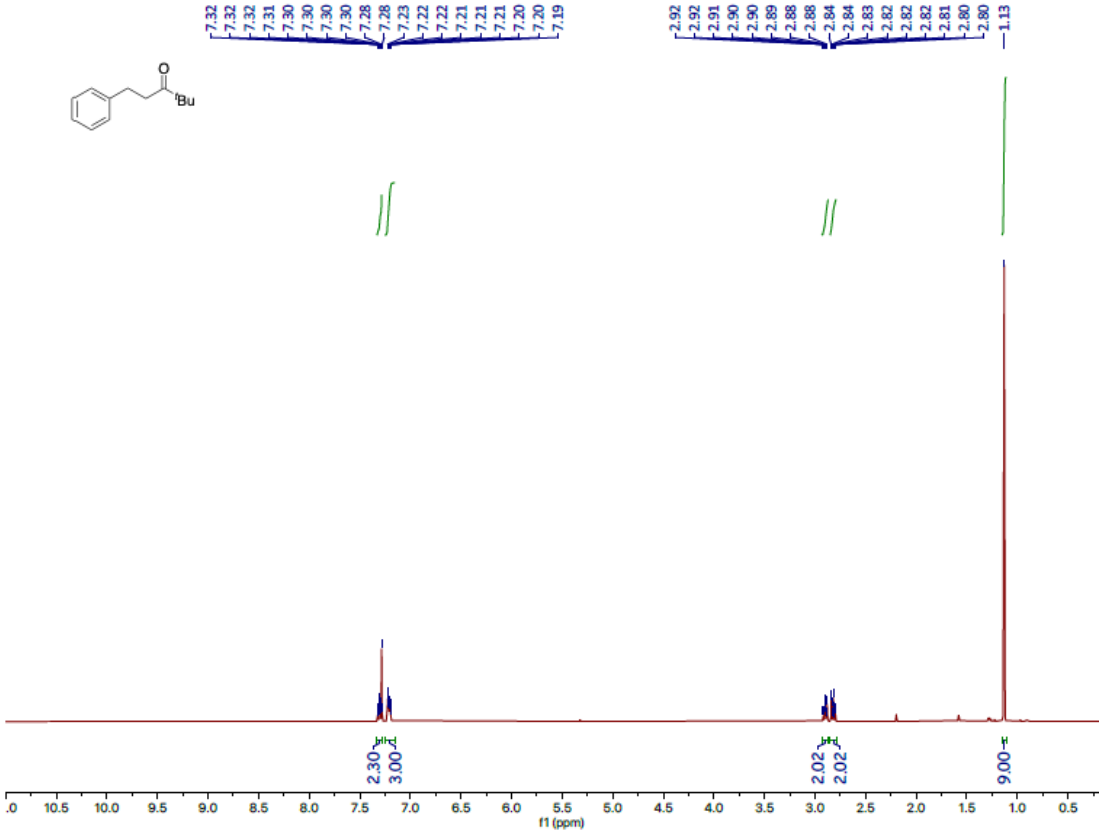

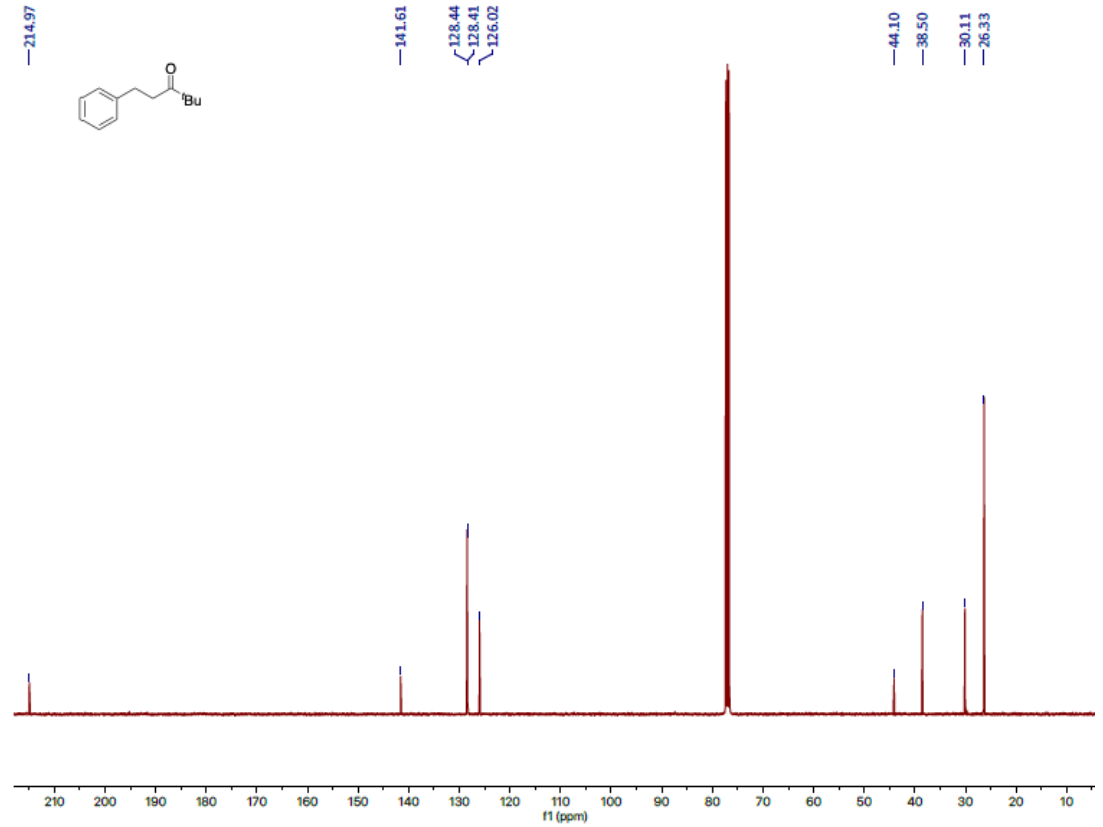

4-(*m*-Aminophenyl)-2-butanone (**2o**)

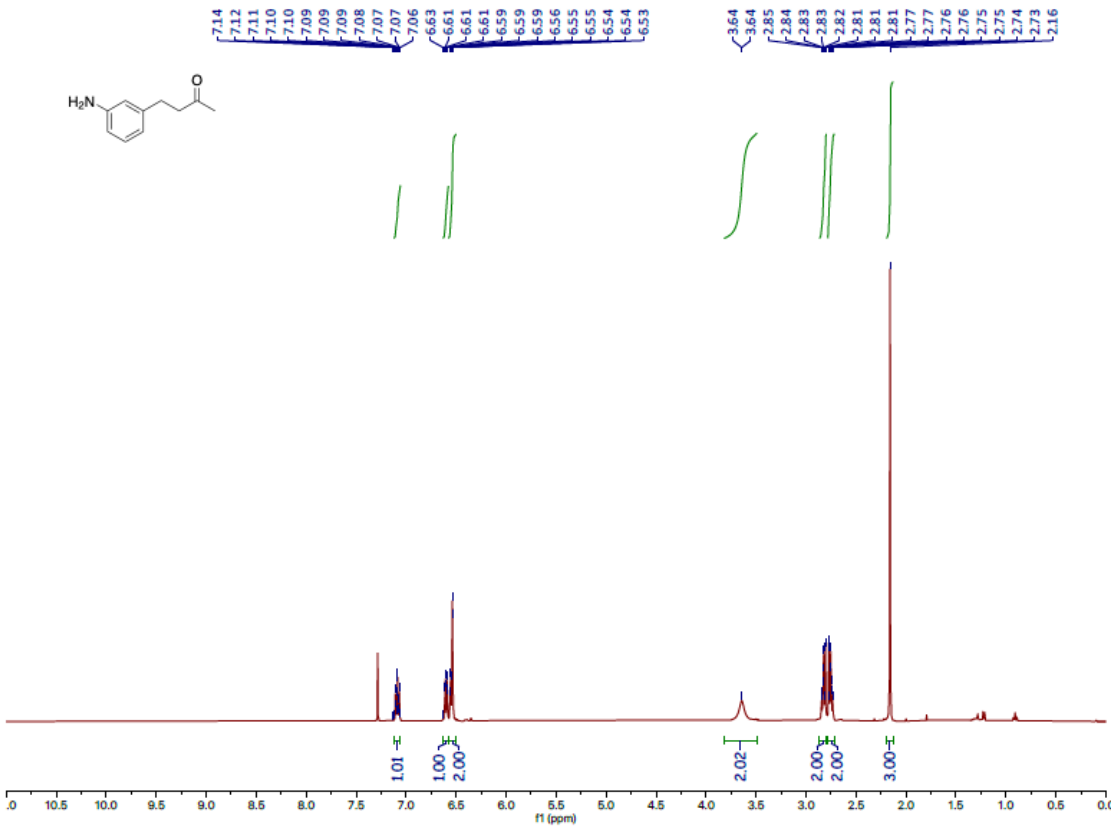

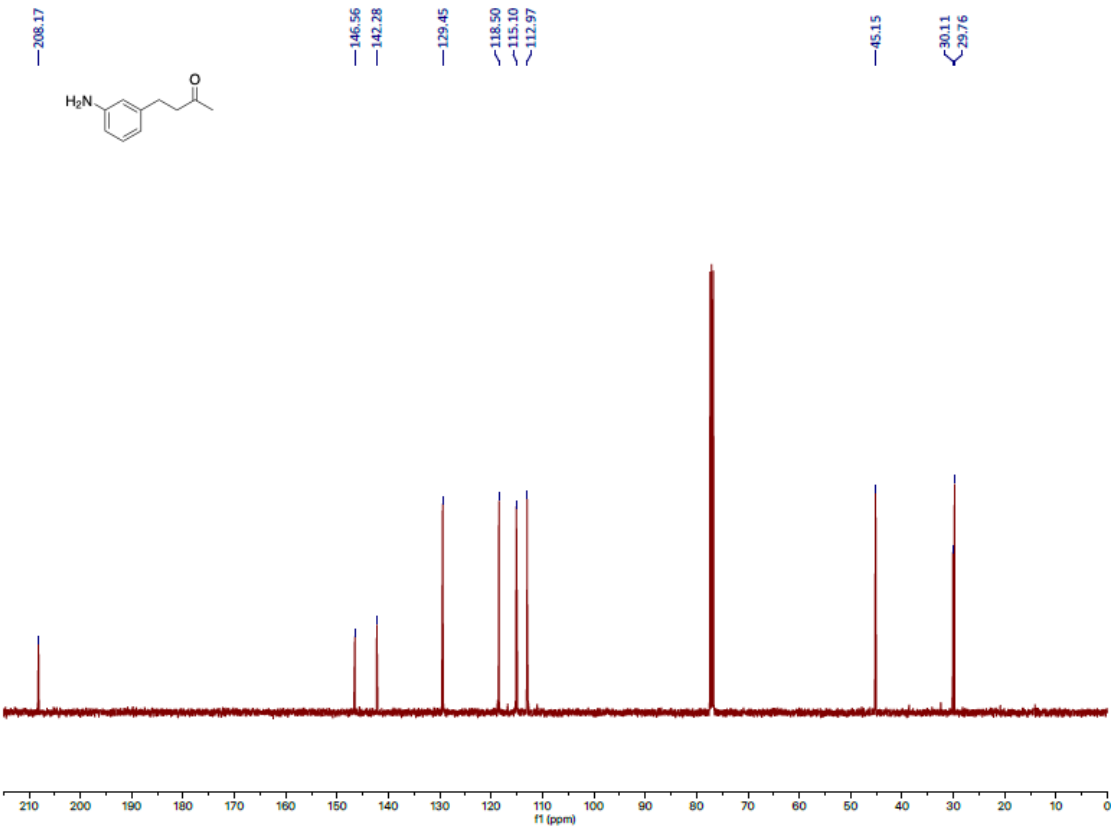

Ethyl 3-(*p*-pyridinyl)propanoate (**2p**)

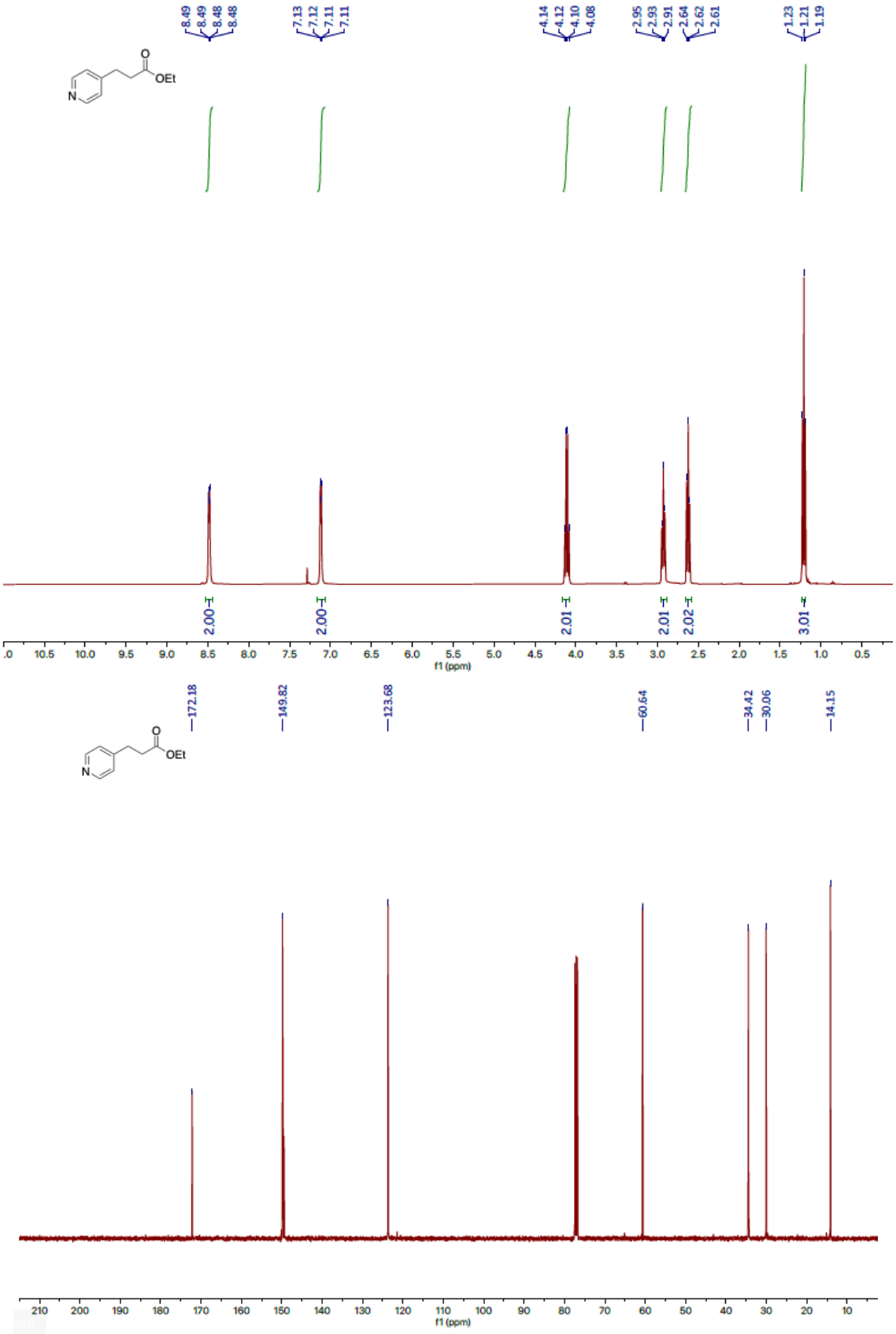

1-(2,6,6-Trimethylcyclohex-1-en-1-yl)butan-1-one (**2s**)

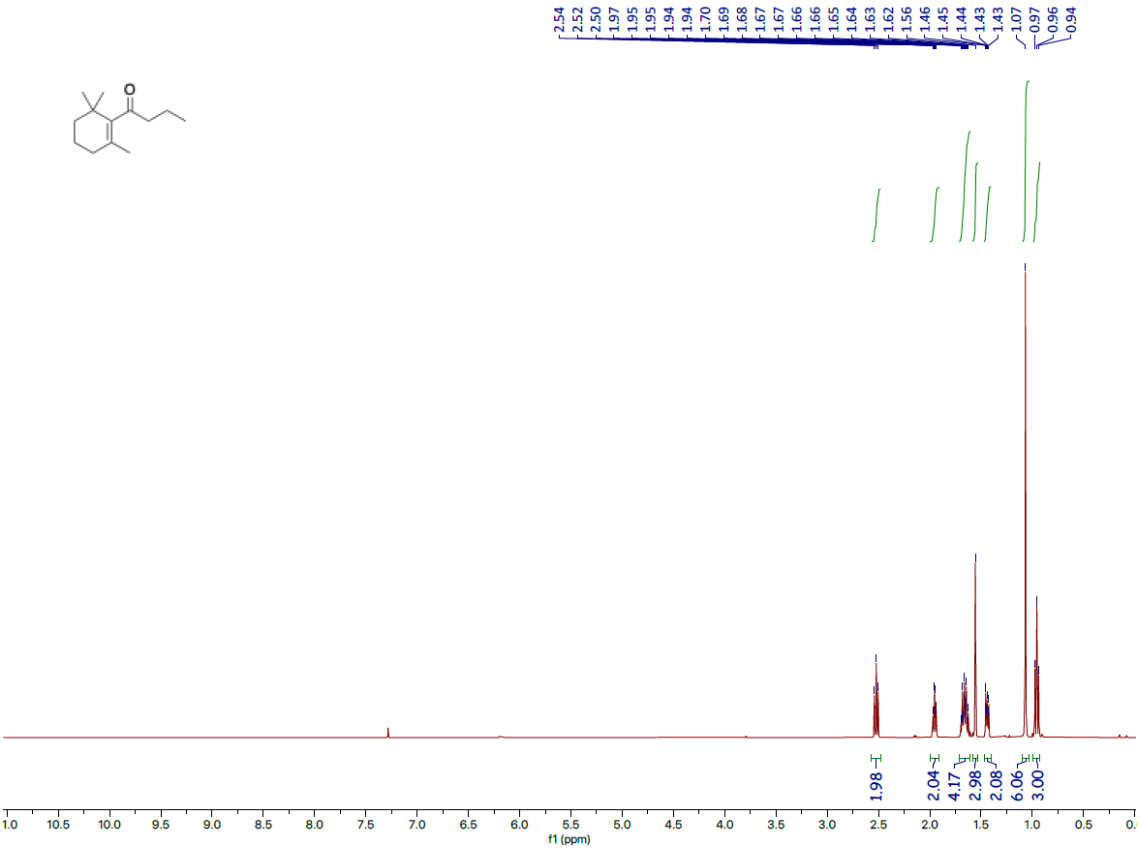

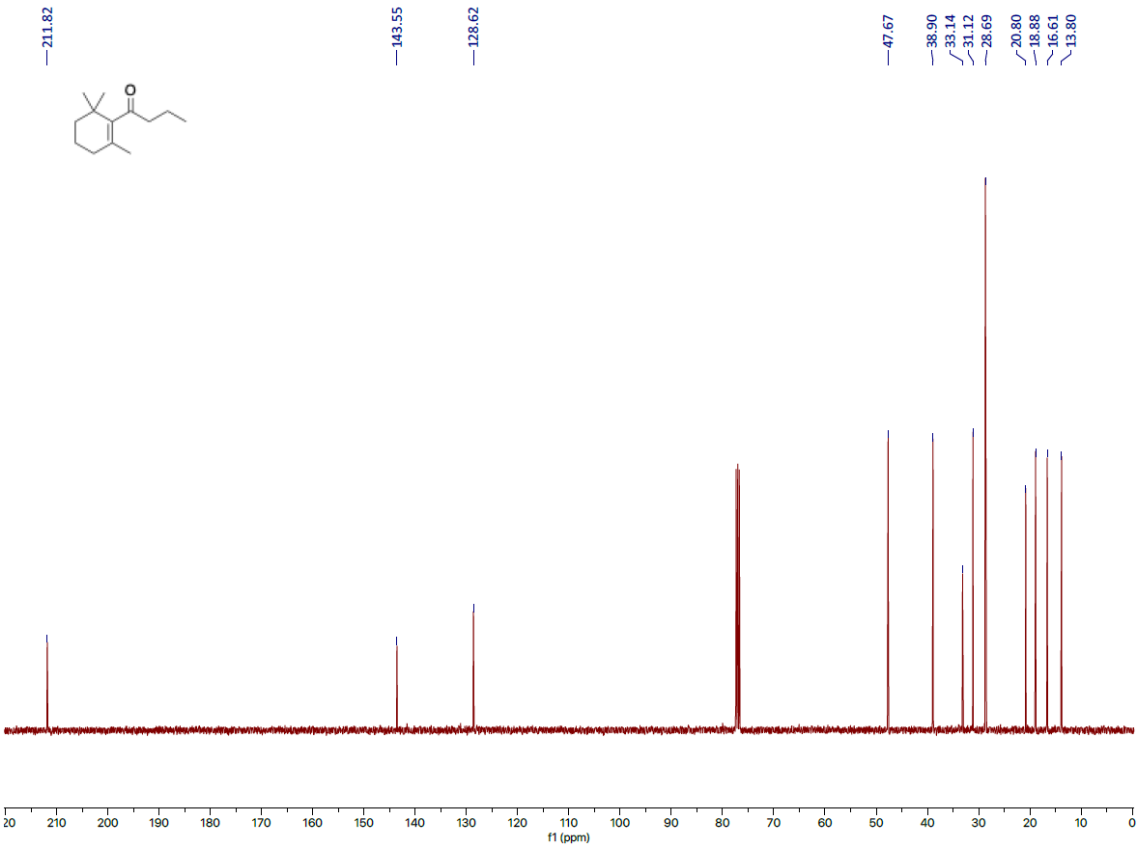

Diethyl succinate (**2t**)

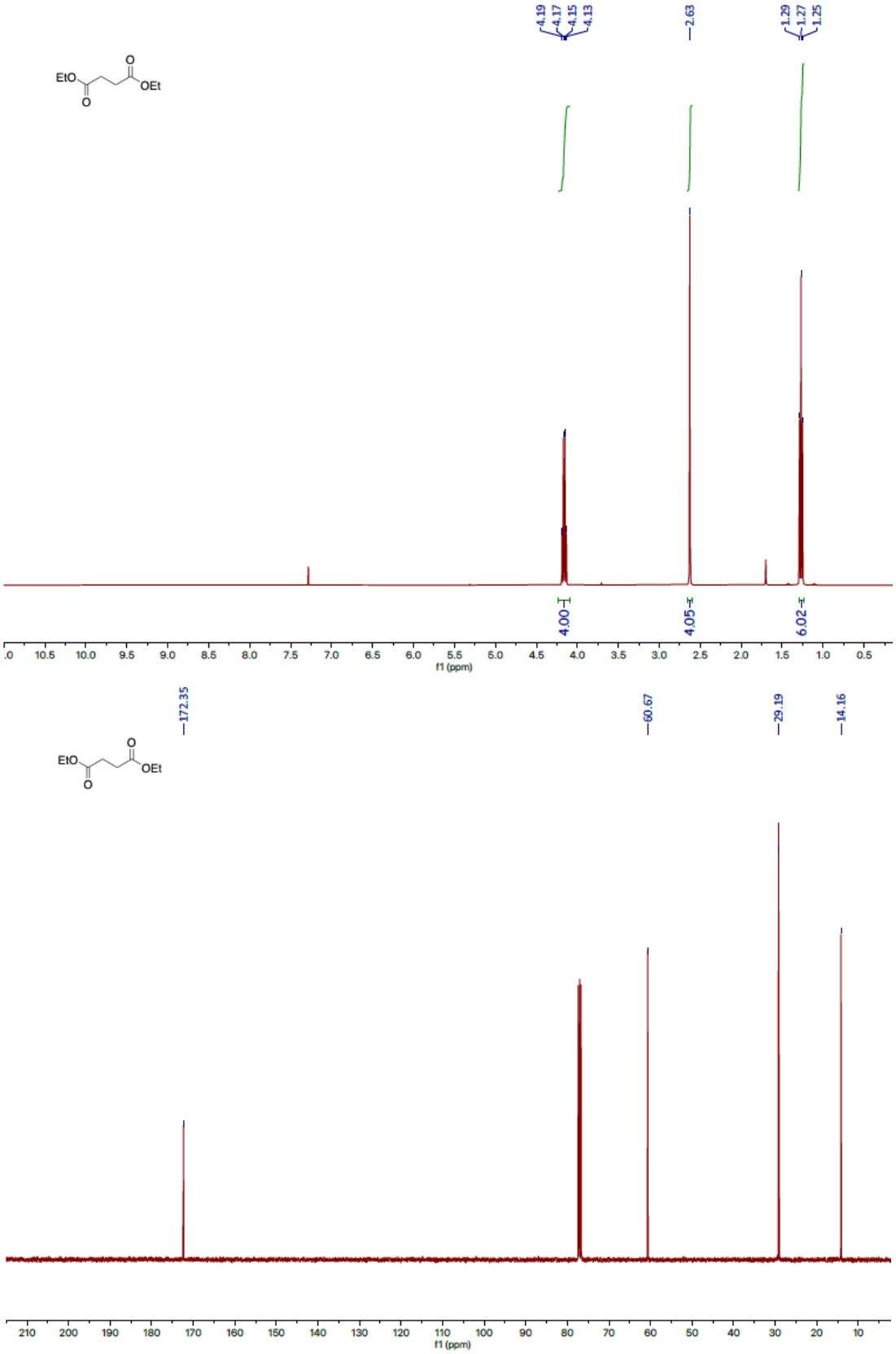

Diethyl 2-methylsuccinate (**2u**)

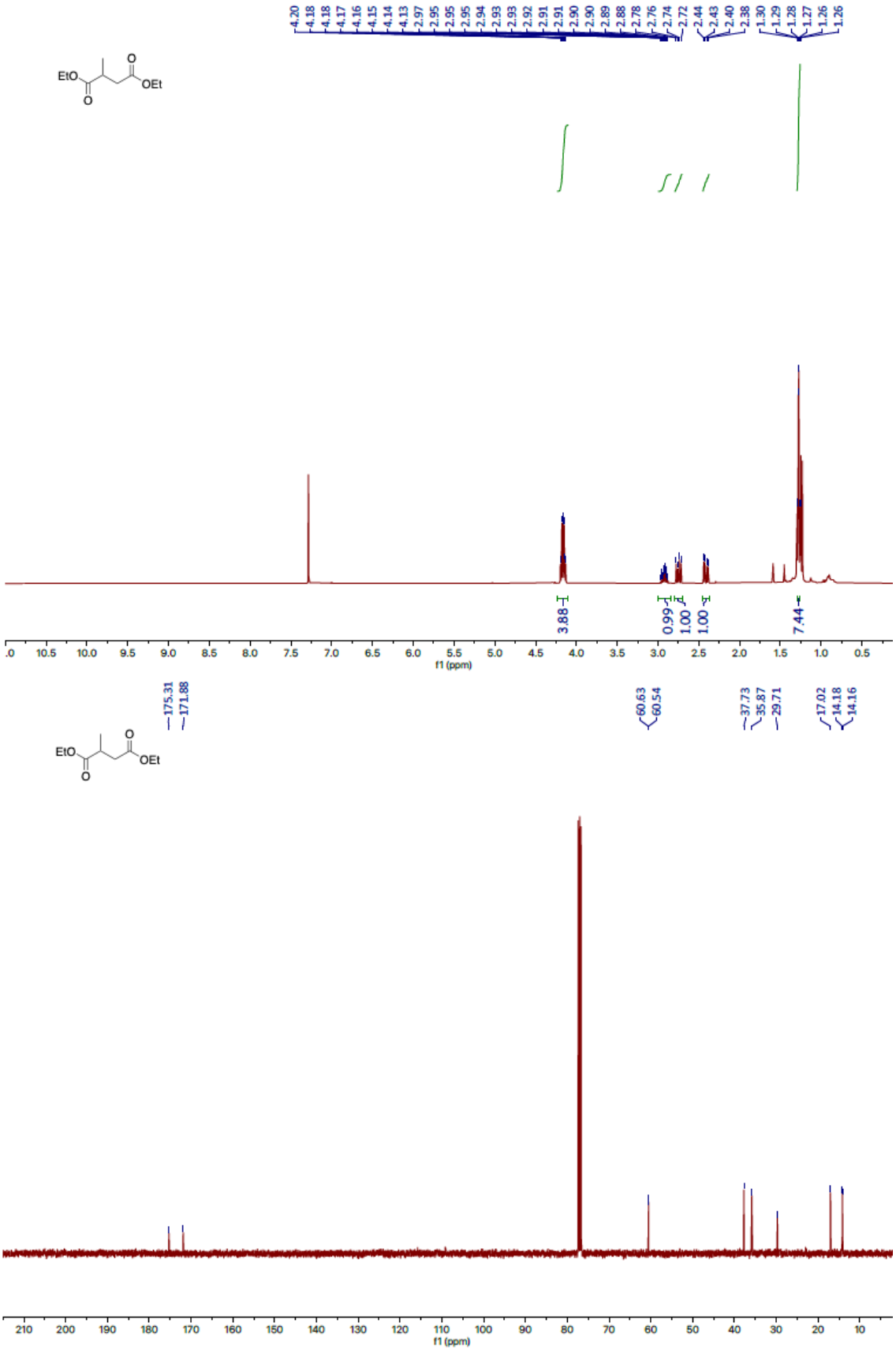

(Ethylsulfonyl)benzene (**2v**)

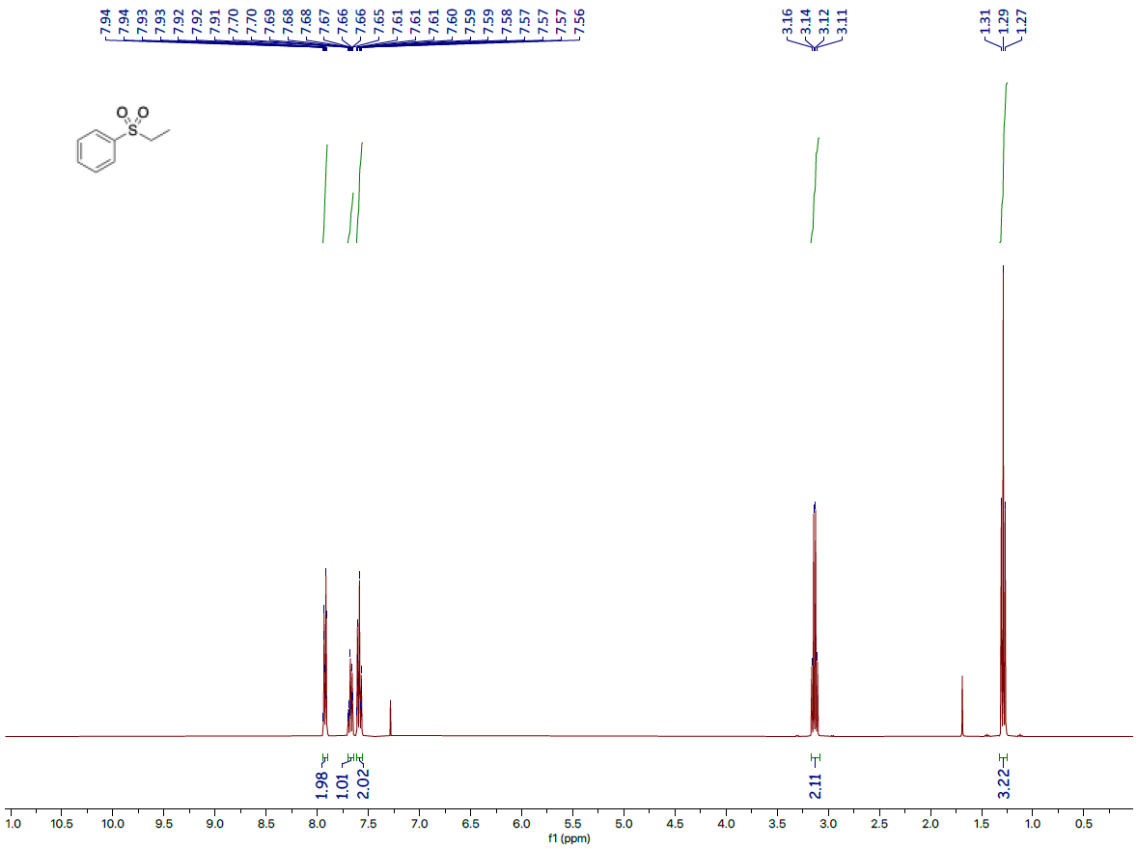

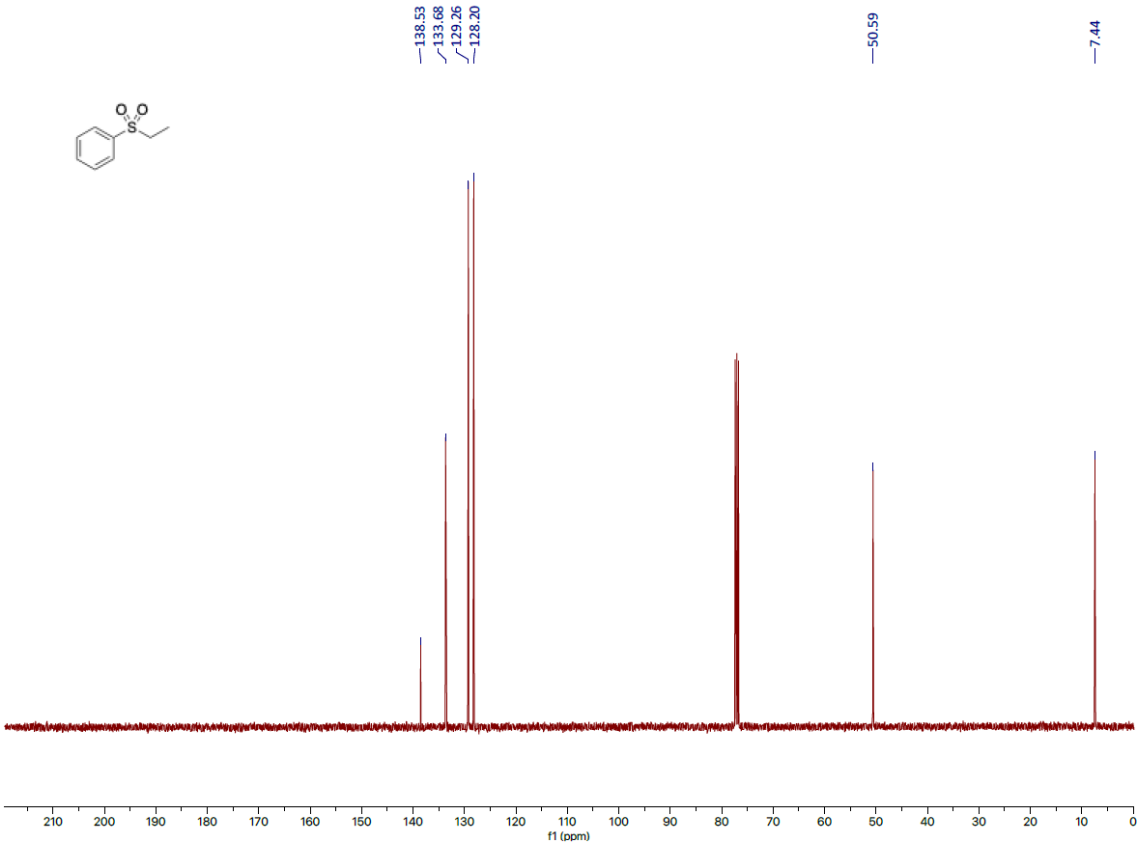

Phenyl-3-pentanol (**2w**)

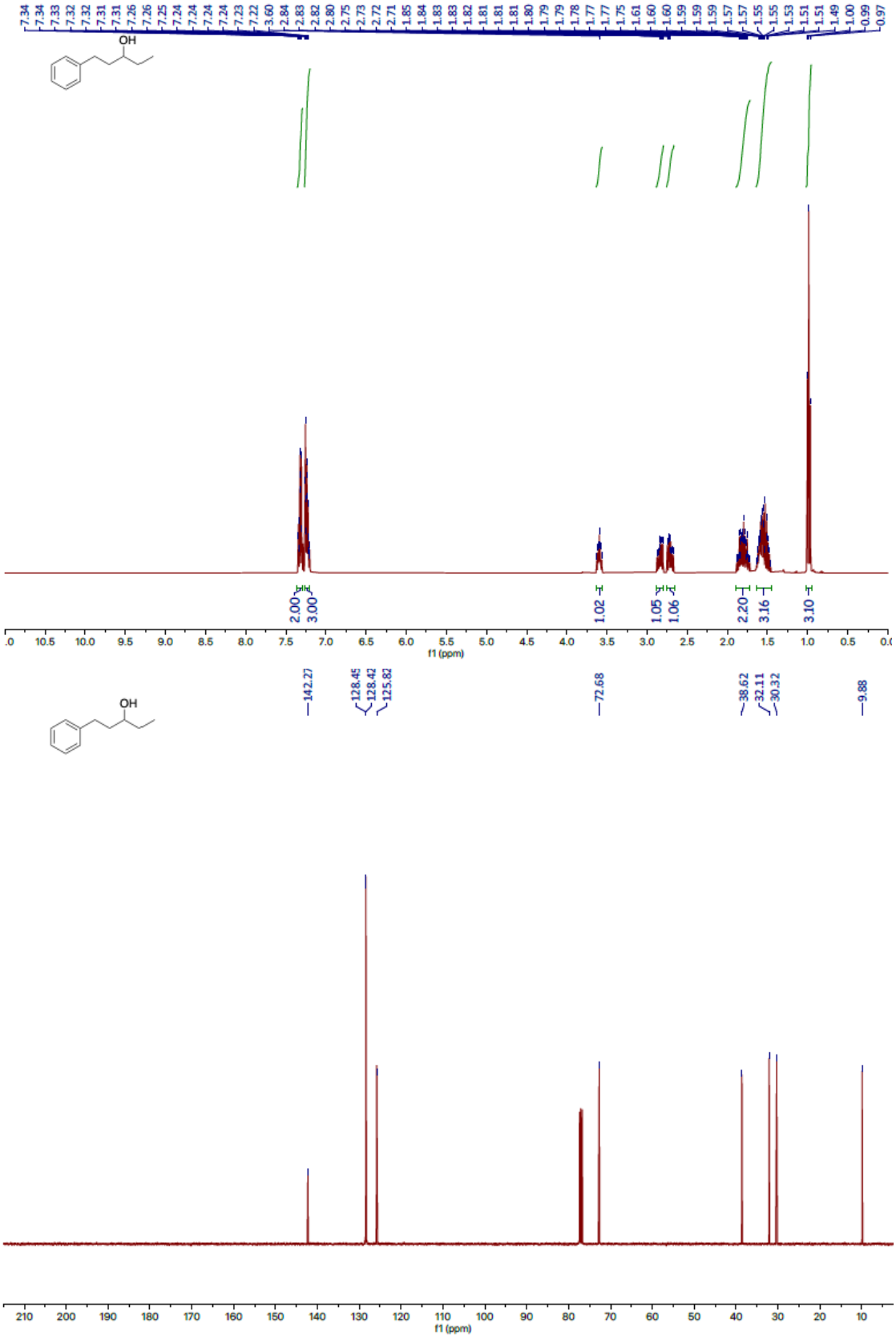

Methoxy-*p*-propylbenzene (**2y**)

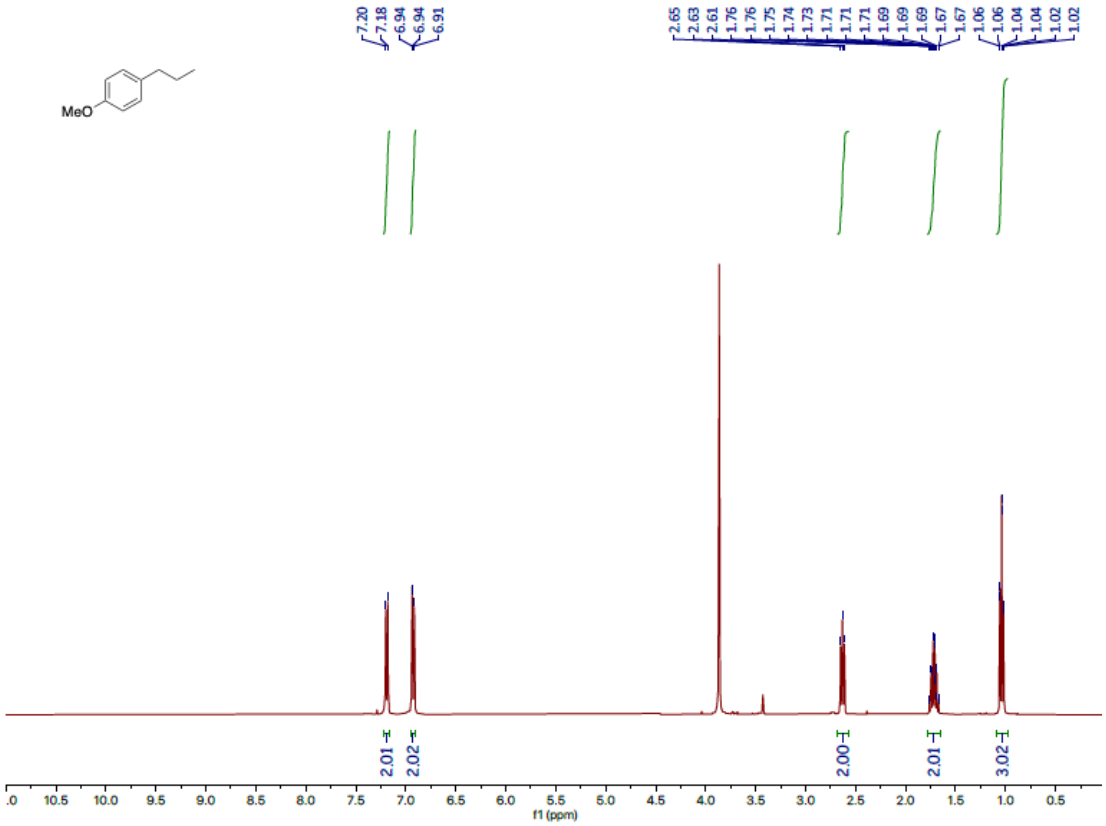

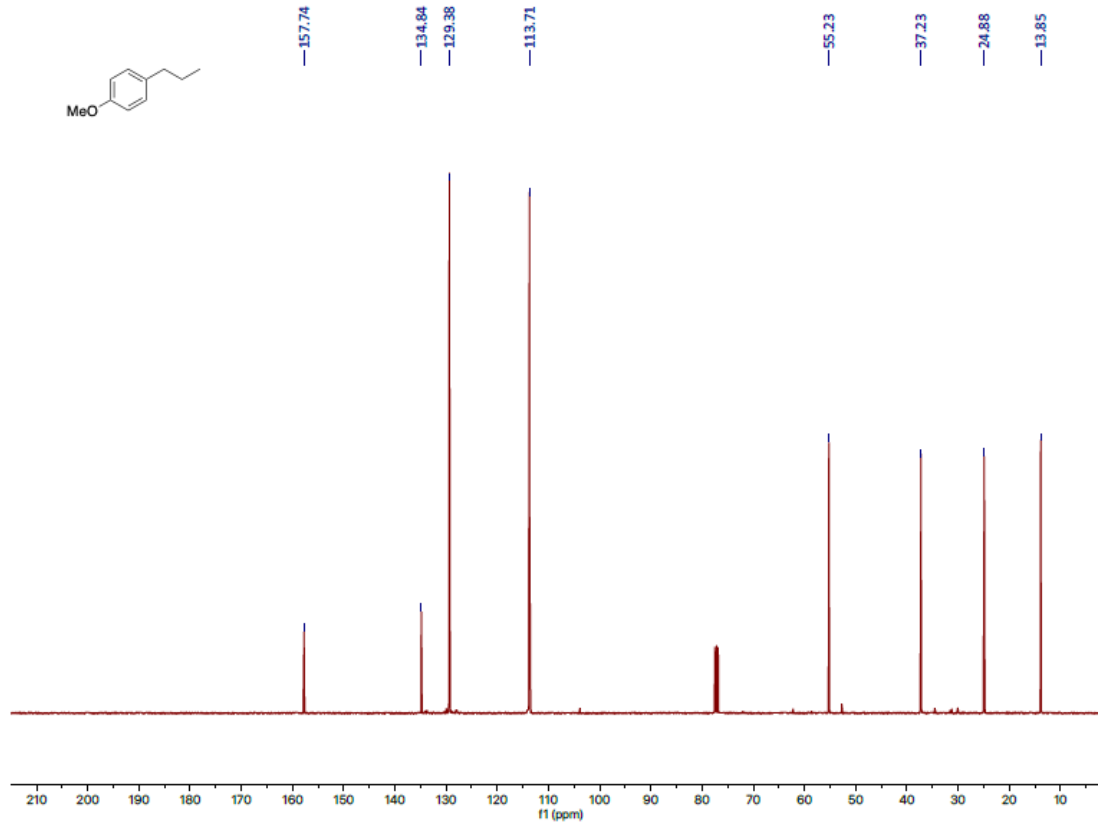

o-Methoxy-*p*-propylphenol (**2z**)

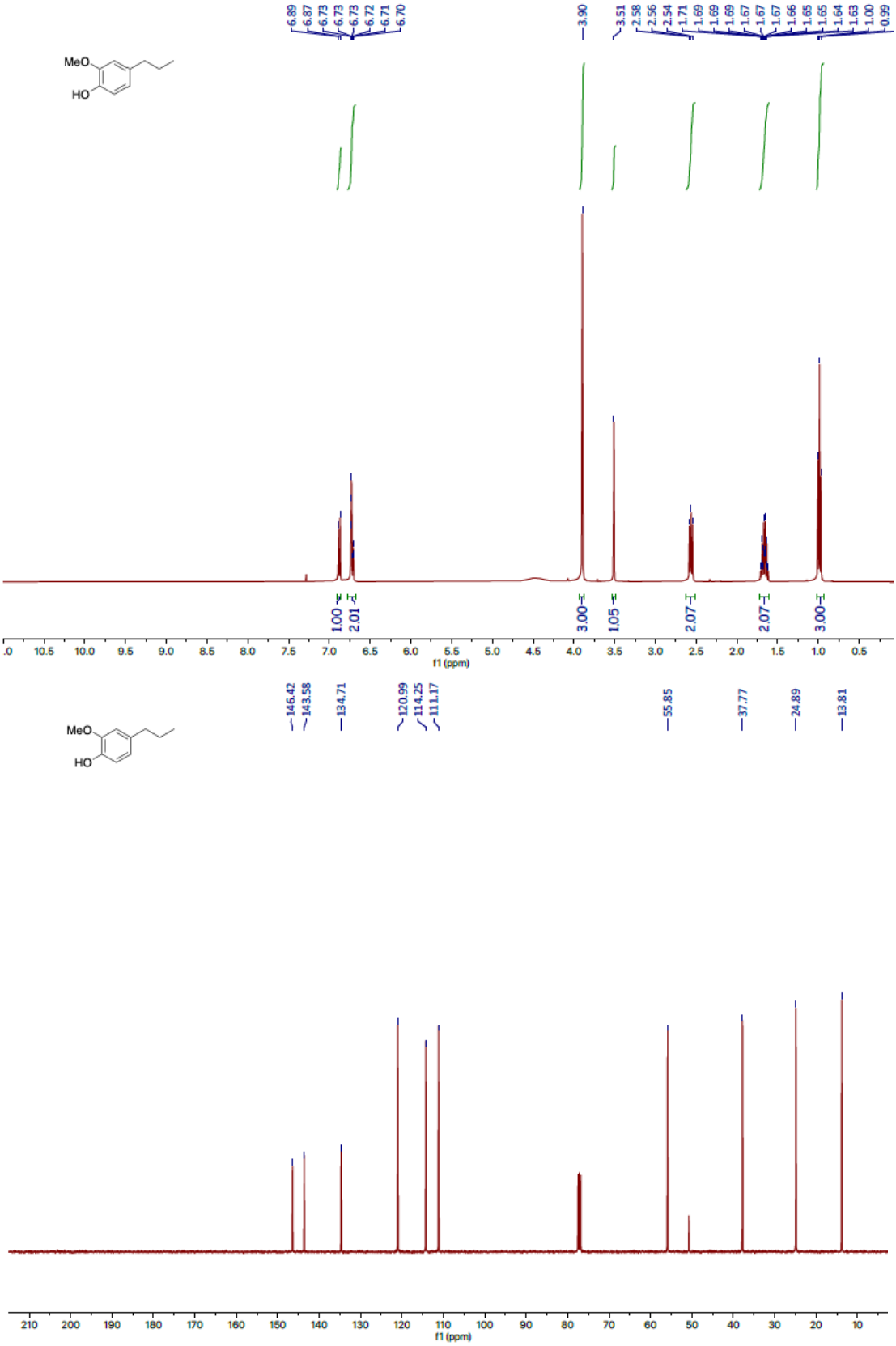

Benzyloxy-*o*-methoxy-*p*-propylbenzene (**2aa**)

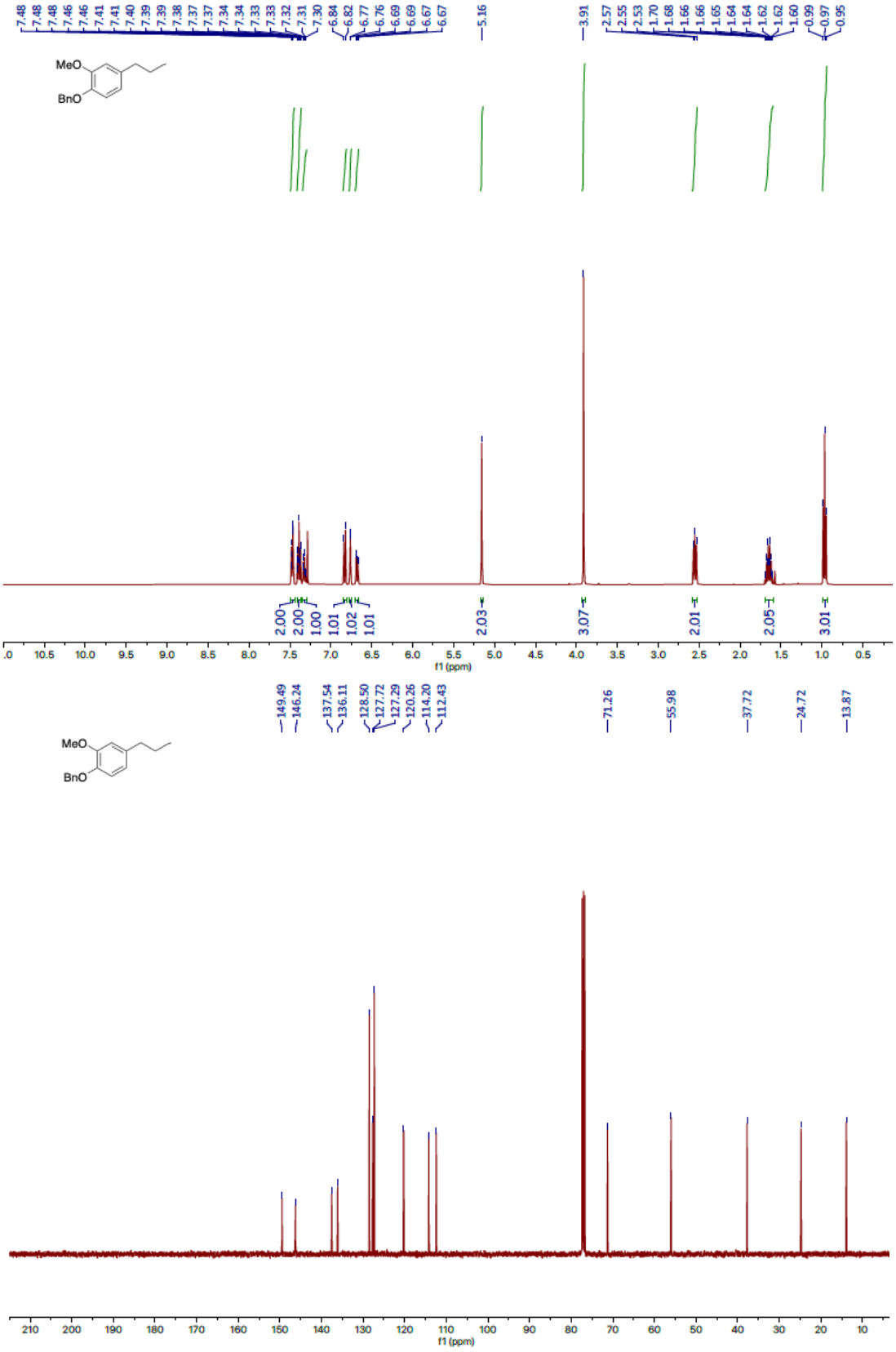

Benzyl propylcarbamate (**2ae**)

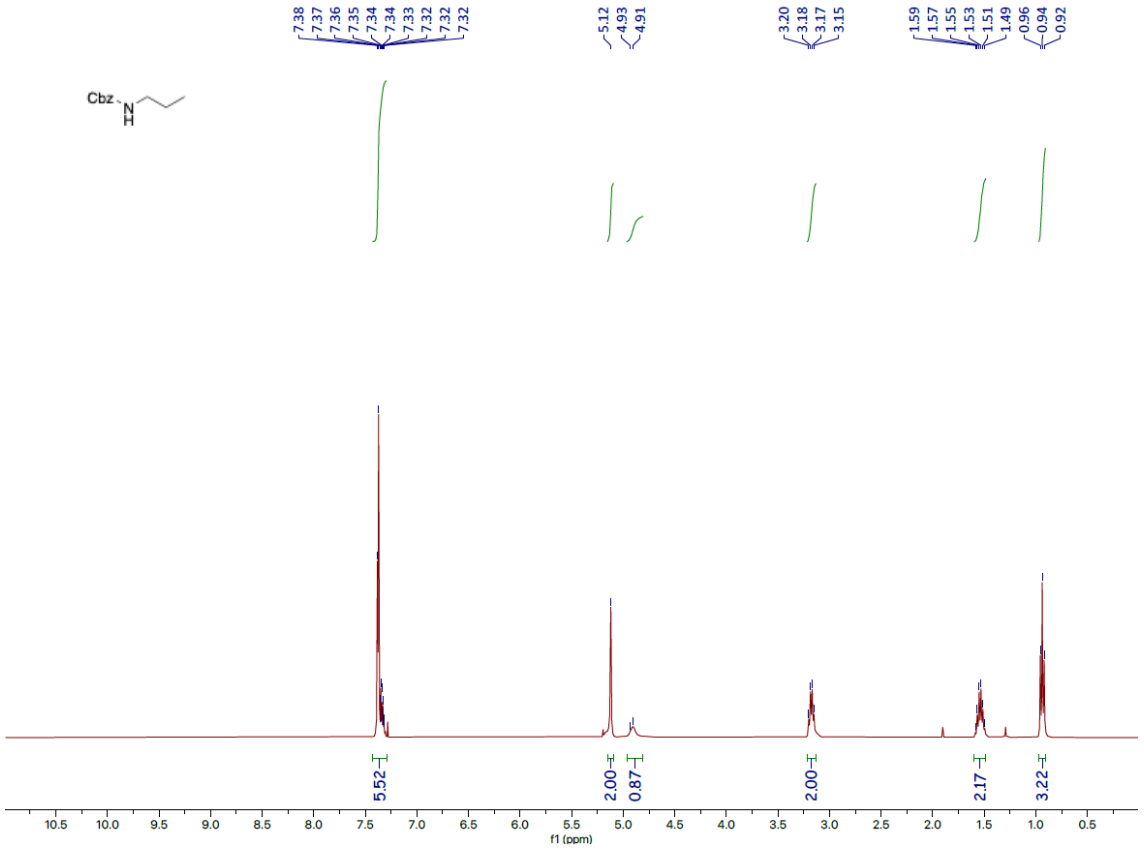

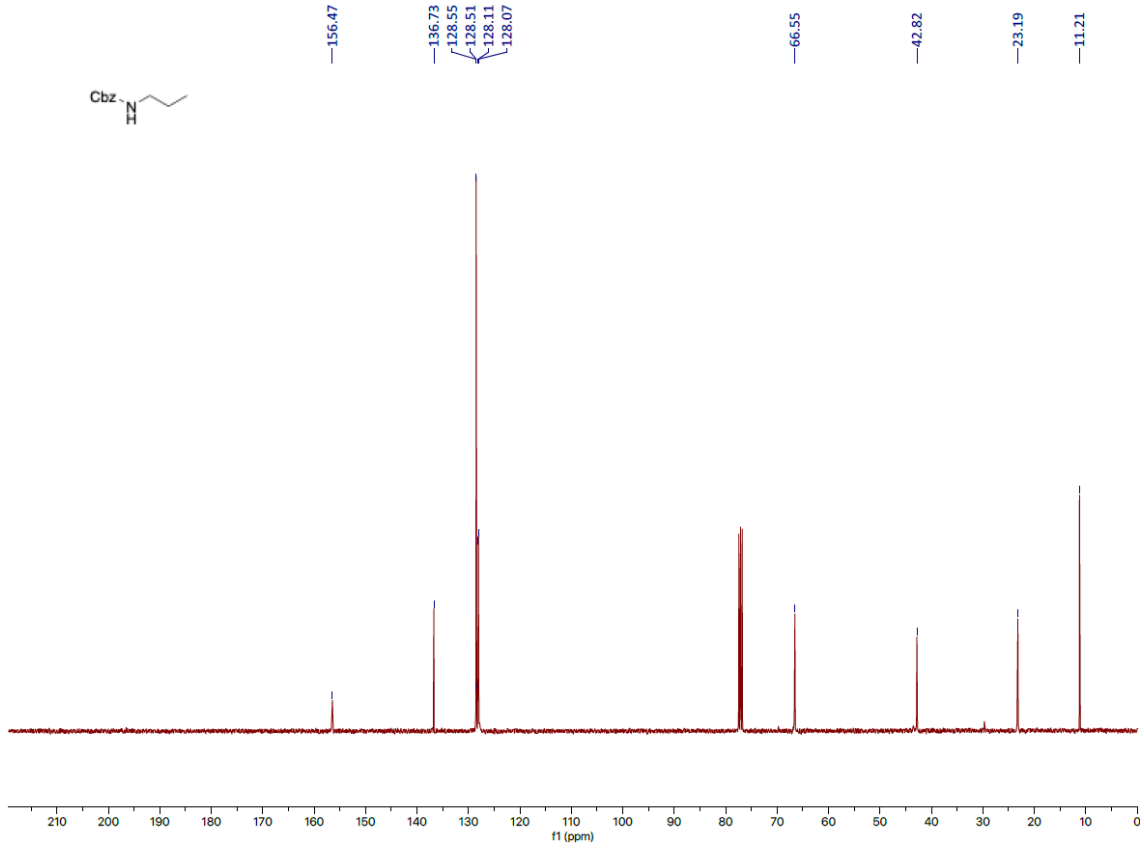

4-Methyl-N-propylbenzenesulfonamide (**2af**)

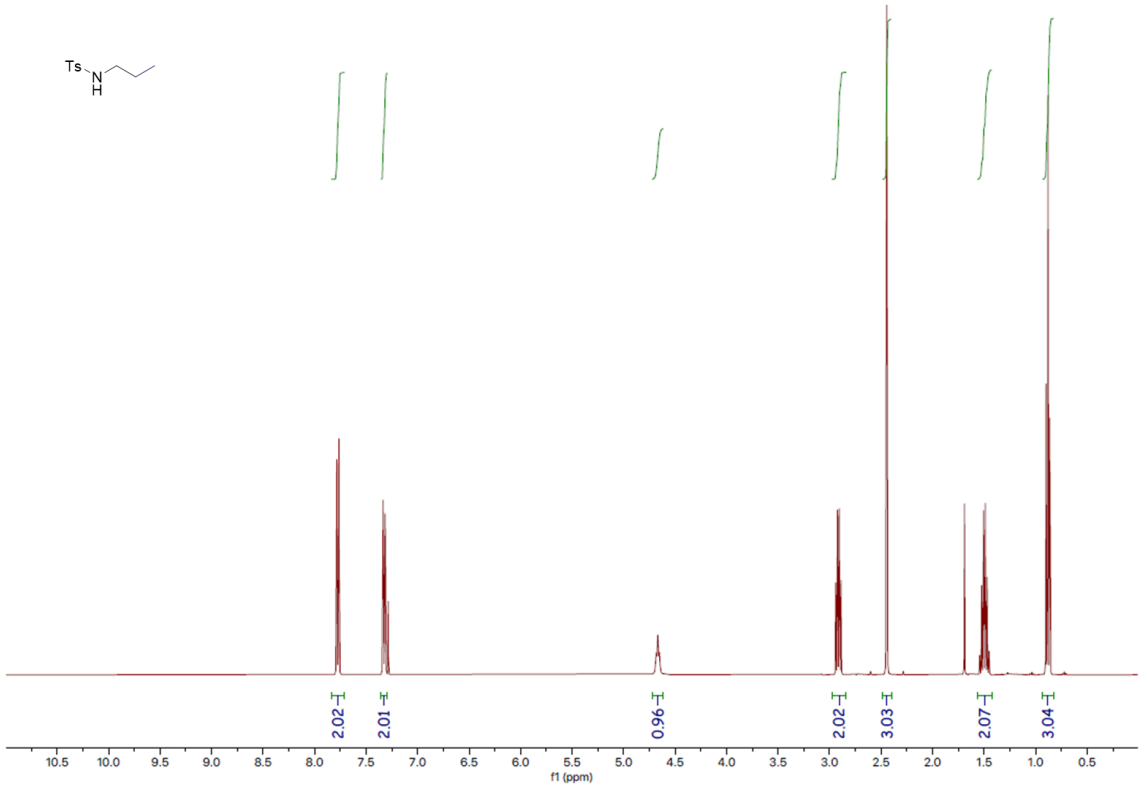

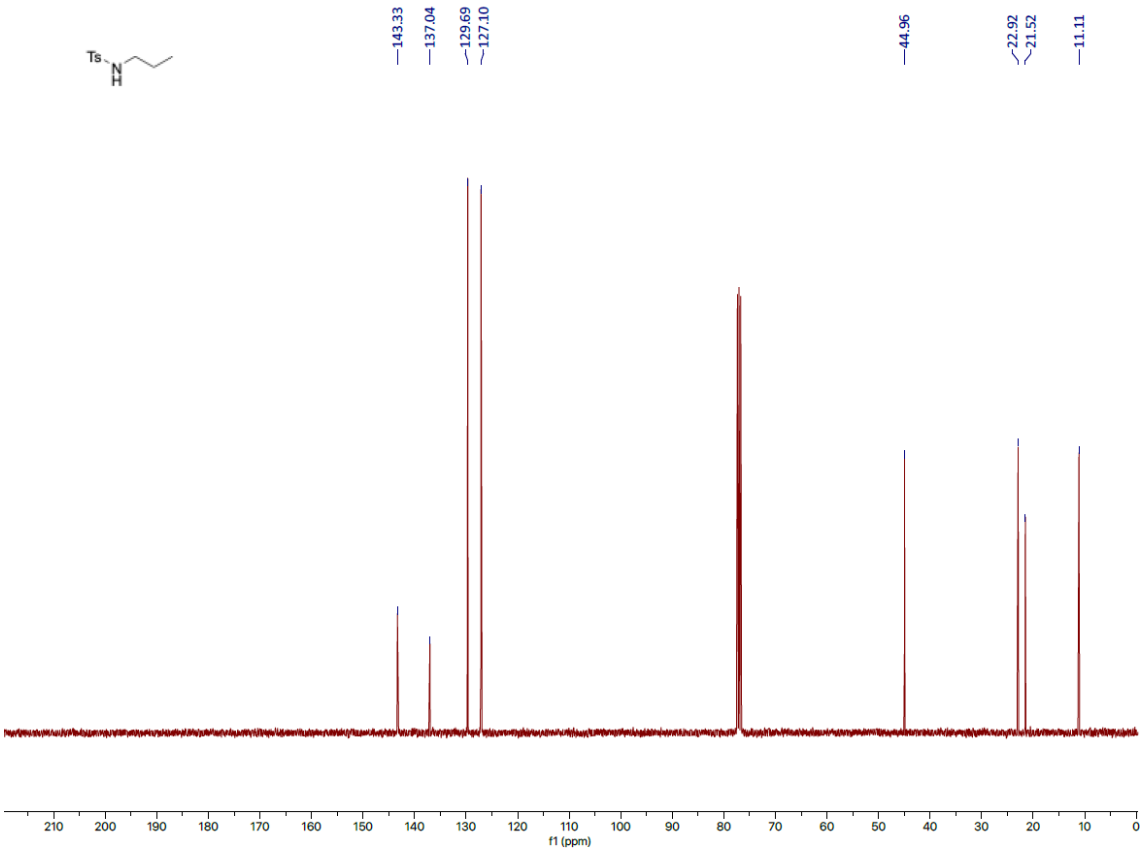

N-butyl phtalamide (**2ai**)

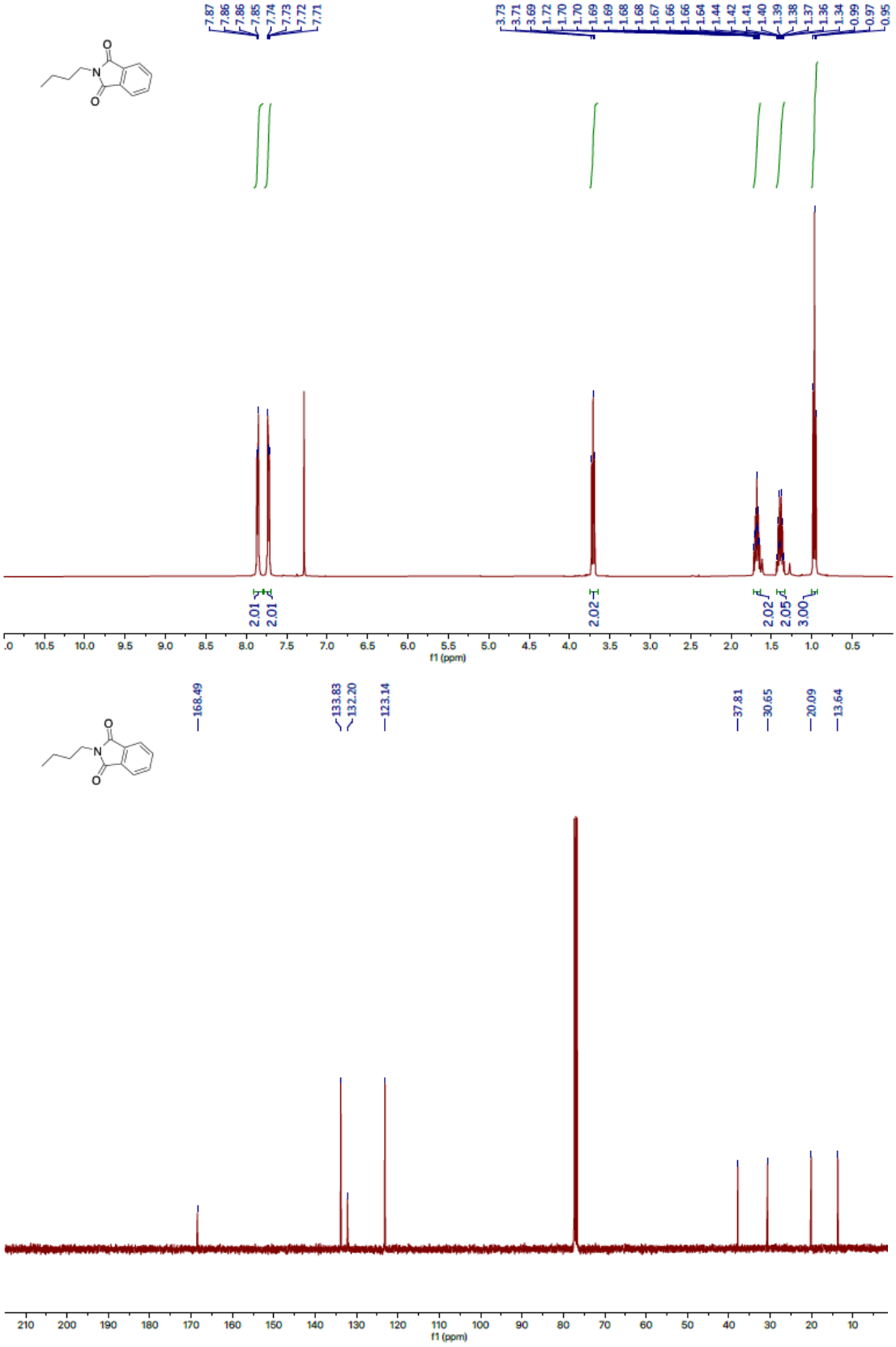

1,1-Diethoxycyclohexane (**4**)

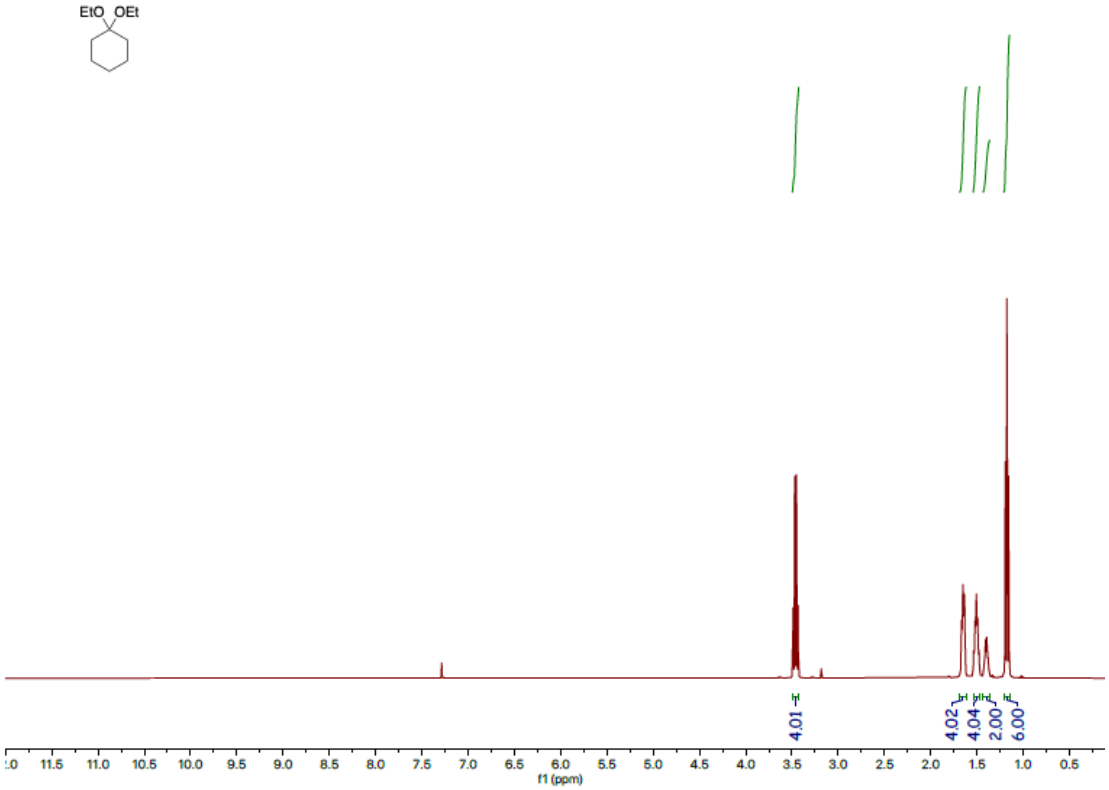

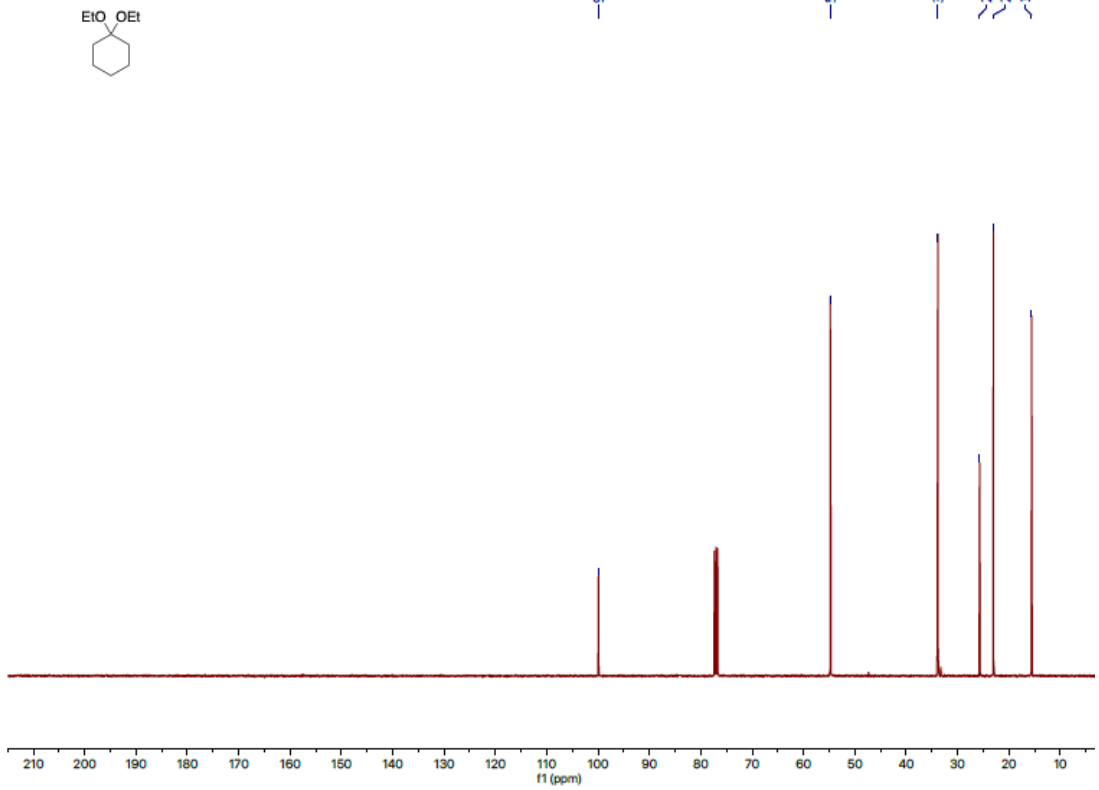

Ethoxycyclohexane (**3b**)

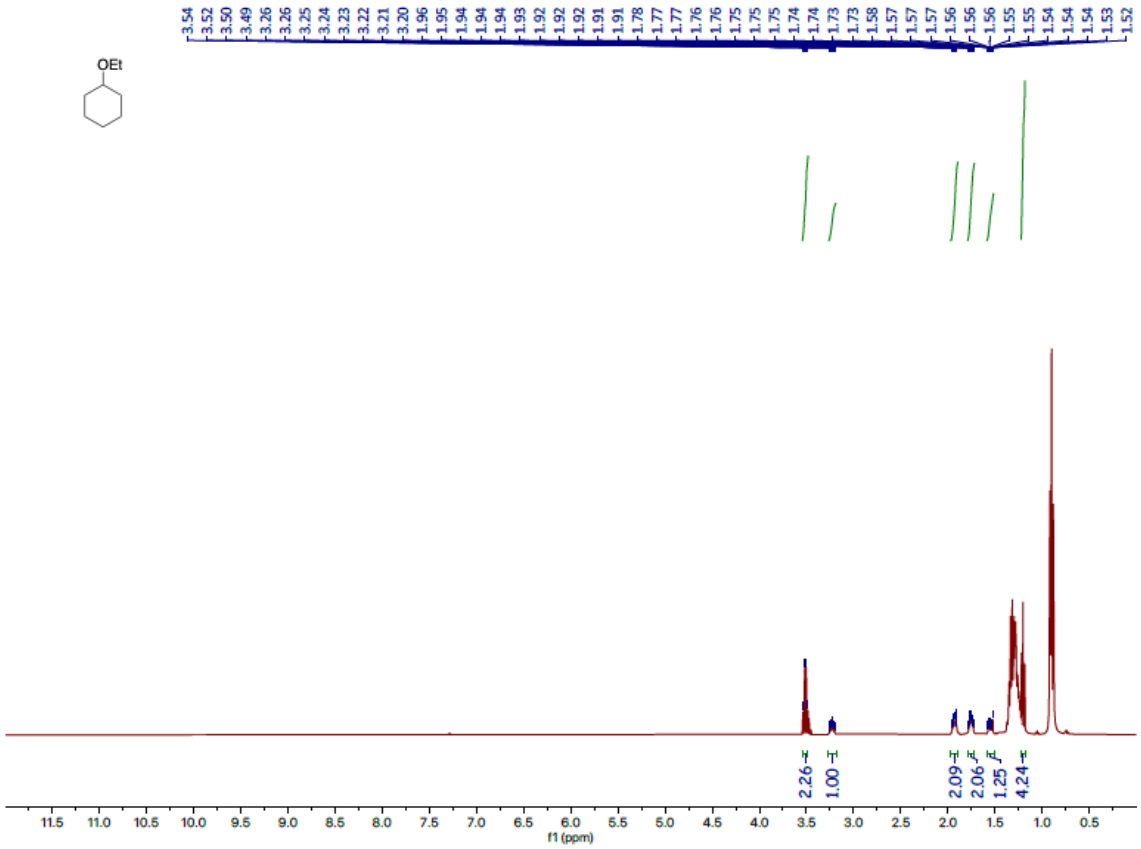

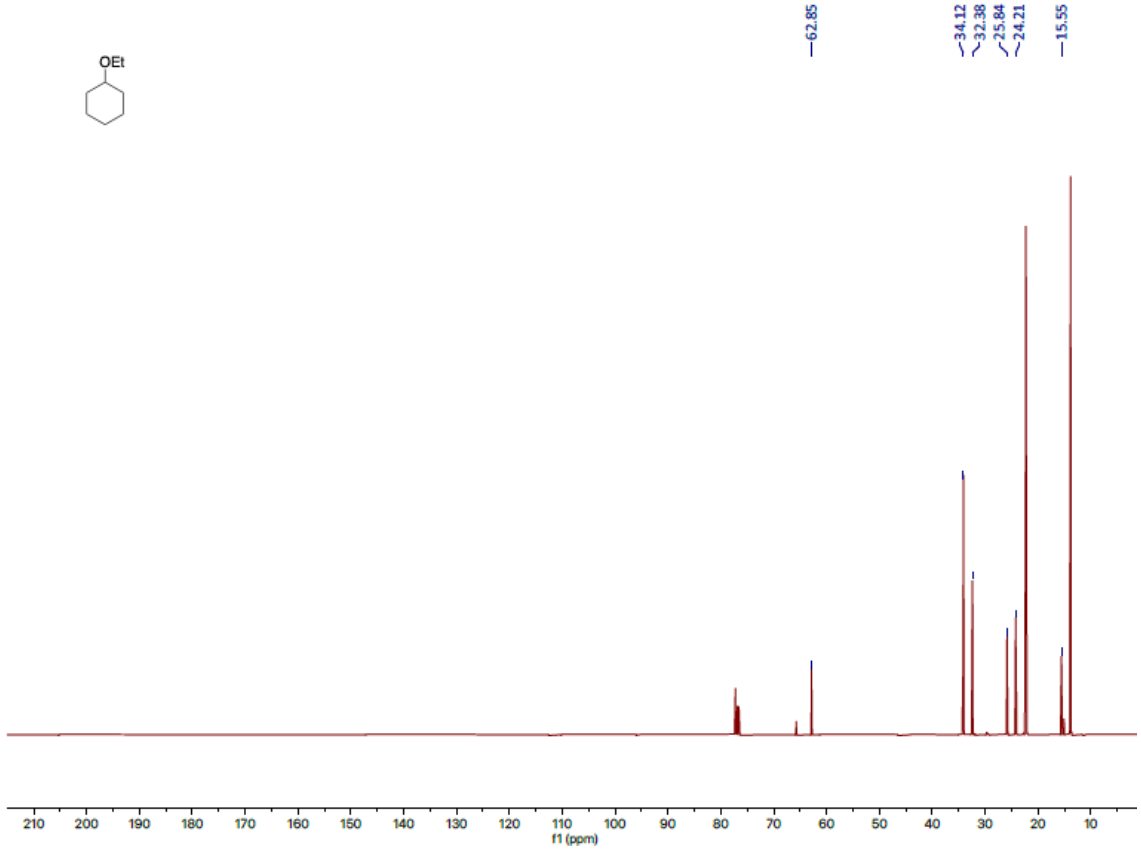

Ethoxy-2-cyclohexene (**6b**)

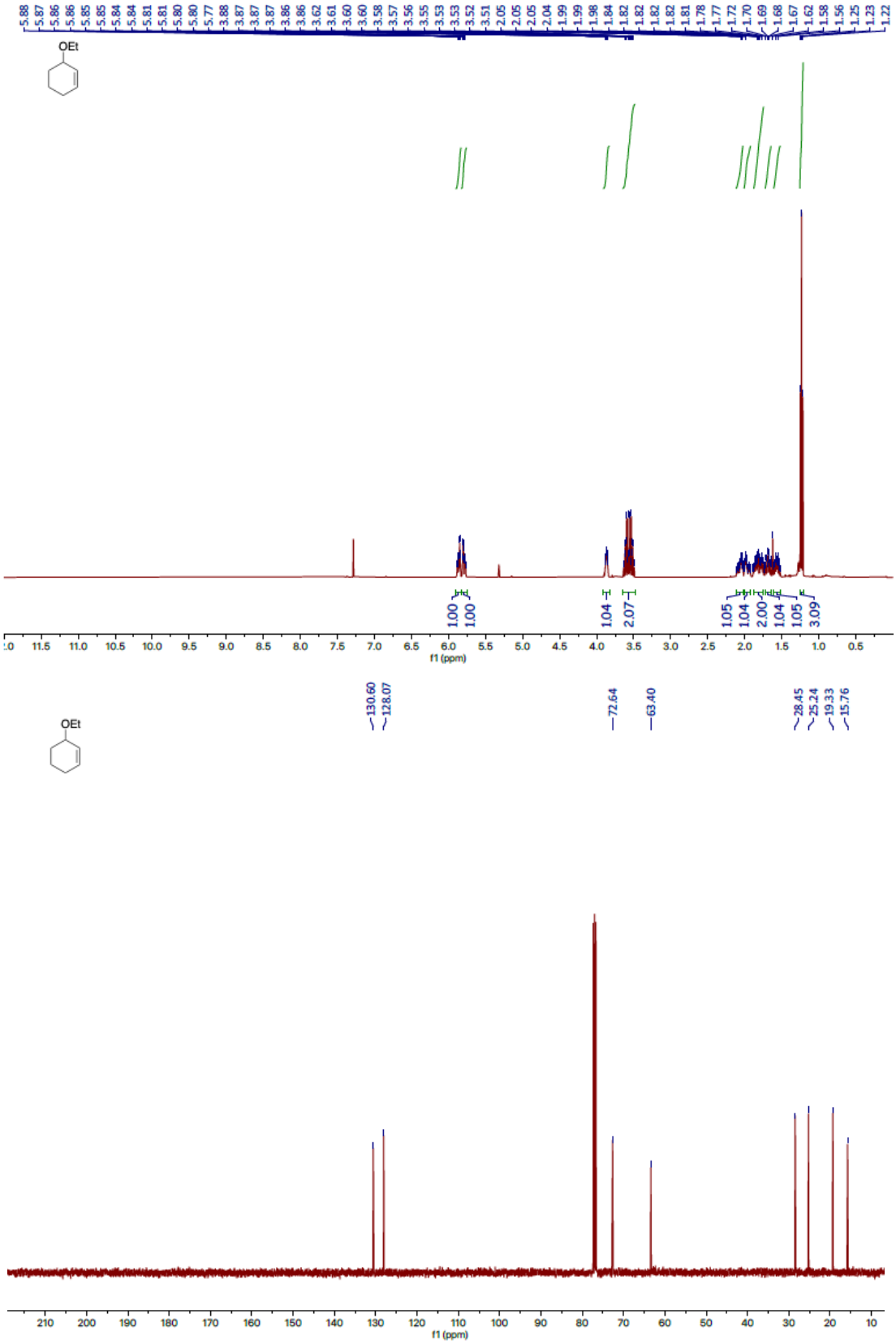

S10. REFERENCES

1. X. Zhou, Y. Xu, G. Dong, *Journal of the American Chemical Society* 2021, *143*, **48**, 20042 – 20048.
2. R. S. Lewis, C. J. Garza, A. T. Dang, T.K.A. Pedro, W. J. Chain, *Organic Letters* 2015, **17**, 9, 2278 – 2281.
3. Y. Huang, P. Wang, J. Liu, M. Cai, *Journal of Chemical Research* 2013, **37**, 6, 333 – 336.
4. L. Longwitz, T. Werner, *Angewandte Chemie International Edition* 2020, **59**, 7, 2760 – 2763.
5. A. Pews-Davtyan, F.K. Scharnagl, M.F. Hertrich, C. Kreyenschulte, S. Bartling, H. Lund, R. Jackstell, M. Beller, *Green Chemistry* 2019, **21**, 18, 5104-5112.
6. I. Tellitu, I. Beitia, M. Diaz, A. Alonso, I. Moreno, E. Dominguez, *Tetrahedron 2015*, **71**, 8251 – 8255.
7. J. Escudero, V. Bellosta, J. Cossy, *Angewandte Chemie International Edition* 2018, **57**, 574 – 578.
8. D. P. Ojha, K. Gadde, K.R. Prabhu, *Organic Letters* 2016, **18**, 5062 – 5065
9. D. Bao, B. Millare, W. Xia, B.G. Steyer, A.A. Gerasimenko, A. Ferreira, A. Contreras, V.I. Vullev, *The Journal of Physical Chemistry A* 2009, **113**, 7, 1259 – 1267.
10. M.A. Stoffels, F.J.R. Klauck, T. Hamadi, F. Glorius, J. Leker, *Advanced Synthesis & Catalysis* 2020, **362**, 6, 1258-1274.
11. X. Liu, D. Astruc, *Advanced Synthesis & Catalysis* 2018, **360**, 18, 3426 – 3459.
12. T. Maegawa, Y. Kitamura, S. Sako, T. Udzu, A. Sakurai, A. Tanaka, Y. Kobayashi, K. Endo, U. Bora, T. Kurita, A. Kozaki, Y. Monguchi, H. Sajiki, *Chemistry – A European Journal* 2007, **13**, 20, 5937 – 5943.
13. Á. Molnár, *Chemical Reviews* 2011, **111**, 3, 2251 – 2320.
14. F.-X. Felpin, *The Journal of Organic Chemistry* 2005, **70**, 21, 8575 – 8578.
15. J. Babjak, V.A. Ettel, V. Paserin, METHOD OF FORMING NICKEL FOAM. 1990/09/18, 1990.
16. European Chemicals Agency. http://echa.europa.eu/information-on-chemicals/registeredsubstances.
17. P. Nuss, M.J. Eckelman, *PLOS ONE* 2014, **9**, 7, e101298.
18. P. Engels, F. Cerdas, T. Dettmer, C. Frey, J. Hentschel, C. Herrmann, T. Mirfabrikikar, M. Schuler, Journal of Cleaner Production, 2022, **336**, 130474.
19. M. Cossutta, J. McKechnie, S.J. Pickering, *Green Chemistry* 2017, **19**, 24, 5874 – 5884.
20. *Mineral commodity summaries 2021*; Reston, VA, 2021; p 200.
21. P.P. Lopes, D. Tripkovic, P.F.B.D. Martins, D. Strmcnik, E.A. Ticianelli, V.R. Stamenkovic, N.M. Markovic, *Journal of Electroanalytical Chemistry* 2018, **819**, 123 – 129.
22. W. Wei, P.B. Samuelsson, A. Tilliander, R. Gyllenram, P.G. Jönsson, Energy Consumption and Greenhouse Gas Emissions of Nickel Products, *Energies* [Online], 2020.
23. IEA Energy Statistics Data Browser. https://www.iea.org/data-and-statistics/data-tools/energy-statistics-data-browser (accessed 2022).
24. R. Mozingo, Palladium Catalysts Organic Syntheses, Coll. Vol. 3, p.685 (1955); Vol. 26, p.77 (1946) DOI:10.15227/orgsyn.026.0077.
25. S. Rojas-Buzo, P. García-García, A. Corma, *Green Chemistry* 2018, **20**, 13, 3081 – 3091.
26. X. Li, L. Li, Y. Tang, L. Zhong, L. Cun, J. Zhu, J. Liao, J. Deng, *The Journal of Organic Chemistry* 2010, **75**, 9, 2981 – 2988.
27. S.-L. Zhang, Z.-Q. Deng, *Organic & Biomolecular Chemistry* 2016, *14*, 30, 7282 – 7294.
28. L. Martínez-Montero, V. Gotor, V. Gotor-Fernández, I. Lavandera, *ACS Catalysis* 2018, **8**, 3, 2413 – 2419.
29. J. Xiao, G.-W. Li, W.-Q. Zhang, *Chemical Research in Chinese Universities* 2013, **29**, 2, 256 – 262.
30. R. Gomes, A.M. Diniz, A. Jesus, A.J. Parola, F. Pina, *Dyes and Pigments* 2009, **81**, 1, 69 – 79.
31. W. Yufeng, G. Zhou, Q. Meng, X. Tang, G. Liu, H. Yin, J. Zhao, F. Yang, Z. Yu, Y. Luo, *Journal of Organic Chemistry* 2018, **83**, 13051 – 13062.

32. M. Bakos, Z. Dobi, D. Fegyverneki, Á. Gyömöre, I. Fernández, T. Soós, *ACS sustainable chemistry and engineering* 2018, **6**, 10869 – 10875.
33. E.K. Ryu, Y.S. Choe, K.-H. Lee, Y. Choi, B.-T. Kim, *Journal of Medicinal Chemistry* 2006, **49**, 20, 6111 – 6119.
34. Z. Gao, S.P. Fletcher, *Chemical Communications* 2018, **54**, 3601 – 3604.
35. A. Nonnenmacher, R. Mayer, H. Plieninger, *Liebigs Annalen der Chemie* 1983, **12**, 2135 – 2140.
36. N. Wasfy, F. Rasheed, R. Robidas, I. Hunter, J. Shi, B. Doan, C.Y. Legault, D. Fishlock, A. Orellana, *Chemical Science* 2021, **12**, 4, 1503 – 1512.
37. J. Lu, P.H. Toy, *Synlett* 2011, **12**, 1723 – 1726.
38. J.C. Tripp, C.H. Schiesser, D.P. Curran, *Journal of the American Chemical Society* 2005, **127**, 15, 5518 – 5527.
39. M. van Gemmeren, M. Börjesson, A. Tortajada, S.-Z. Sun, K. Okura, R. Martin, *Angewandte Chemie International Edition* 2017, **56**, 23, 6558 – 6562.
40. S.T.C. Eey, M.J. Lear, *Organic Letters* 2010, **12**, 23, 5510 – 5513.
41. H. Iwamoto, T. Tsuruta, S. Ogoshi, *ACS catalysis* 2021, **11**, 6741 – 6749.
42. E. Richmond, I.U. Khan, J. Moran, *Chemistry – A European Journal* 2016, **22**, 12274 – 12277.
43. H. Teller, M. Corbet, L. Mantilli, G. Gopakumar, R. Goddard, W. Thiel, A. Fürstner, *Journal of the American Chemical Society* 2012, **134**, 15331 – 15342.
44. H. D. Pickford, J. Nugent, B. Owen, J.J. Mousseau, R.C. Smith, E.A. Anderson, *Journal of the American Chemical Society* 2021, **143**, 9729 – 9736.
45. K. Eto, M. Yoshino, K. Takahashi, J. Ishihara, S. Hatakeyama, *Organic Letters* 2011, **13**, 5398 – 5401.
46. Y. Kim, Y. Park, S. Chang, *ACS Central Science* 2018, *4*, 768 – 775.
47. F. Xu, S.A. Shuler, D.A. Watson, *Angewandte Chemie International Edition* 2018, **57**, 12081 –12085
48. X. Hu, D. Martin, M. Melaimi, G. Bertrand, *Journal of the American Chemical Society* 2014, **136**, 39, 13594 – 13597.
49. W.J. Kerr, R.J. Mudd, L.C. Paterson, J.A. Brown, *Chemistry – A European Journal* 2014, **20**, 45, 14604 – 14607.
50. L. Huang, J. Qi, X. Wu, W. Wu, H. Jiang, *Chemistry – A European Journal* 2013, **19**, 46, 15462 – 15466.
51. H.-C. Huang, M. Ramanathan, Y.-H. Liu, S.-M. Peng, S.-T. Liu, *Applied Organometallic Chemistry* 2017, **31**, 8, e3673.
52. G. Shtacher, S. Dayagi, *Journal of Medicinal Chemistry* 1972, **15**, 11, 1174 – 1177.
53. S. Zhang, L. Li, X. Li, J. Zhang, K. Xu, G. Li, M. Findlater, *Organic Letters* 2020, ***22***, 9, 3570 – 3575.
54. G.K. Zielinski, C. Samojlowicz, T. Wdowik, K. Grela, *Organic & Biomolecular Chemistry* 2015, **13**, 2684 – 2688.
55. E. Voutyritsa, I. Triandafillidi, C.G. Kokotos, *Synthesis* 2017, **49**, 917 – 924.
56. R.C. Mykura, S. Veth, A. Varela, L. Dewis, J.J. Farndon, E.L. Myers, V.K. Aggarwal, *Journal of the American Chemical Society* 2018, *140*, **44**, 14677 – 14686.
57. D. Leow, Y.-H. Chen, T.-H. Hung, Y. Su, Y.-Z. Lin, *European Journal of Organic Chemistry* 2014, 7347 – 7352
58. J. K. Laha, S. Sharma, N. Dayal, *European Journal of Organic Chemistry*, 2015, 7885 – 7891.
59. S. Khamarui, R. Maiti, R.R. Mondal, D.K. Maiti, *RSC Advances* 2015, ***5***, 129, 106633 – 106643.
60. E. Pérez-Mayoral, R.M. Martín-Aranda, A.J. López-Peinado, P. Ballesteros, A. Zukal, J. Čejka, *Topics in Catalysis* 2009, ***52***, 1, 148 – 152.
61. X. Cui, A.-E. Surkus, K. Junge, C. Topf, J. Radnik, C. Kreyenschulte, M. Beller, *Nature Communications* 2016, ***7***, 1, 11326.

62. W.B. Motherwell, G. Bégis, D.E. Cladingboel, L. Jerome, T.D. Sheppard, *Tetrahedron* 2007, ***63***, 28, 6462 – 6476.